

PB 212 805

A Computer Based Mathematical Method for Predicting the Braking Performance of Trucks and Tractor-Trailers

PHASE I REPORT

Motor Truck Braking and Handling Performance Study

by

Ray W. Murphy

James E. Bernard

Christopher B. Winkler

September 15, 1972

Highway Safety
Research Institute

Reproduced by

NATIONAL TECHNICAL
INFORMATION SERVICE

U S Department of Commerce
Springfield VA 22151

Highway Safety Research Institute / University of Michigan

216
1

N O T I C E

**THIS DOCUMENT HAS BEEN REPRODUCED FROM THE
BEST COPY FURNISHED US BY THE SPONSORING
AGENCY. ALTHOUGH IT IS RECOGNIZED THAT CER-
TAIN PORTIONS ARE ILLEGIBLE, IT IS BEING RE-
LEASED IN THE INTEREST OF MAKING AVAILABLE
AS MUCH INFORMATION AS POSSIBLE.**

1. Report No. UM-HSRI-PF-72-1	2. Government Accession No.	3. Recipient's Catalog No. <i>PB-212805</i>	
4. Title and Subtitle A computer based mathematical method for predicting the braking performance of trucks and tractor-trailers. Phase I report: Motor truck braking and handling performance study.		5. Report Date September 15, 1972	
		6. Performing Organization Code	
7. Author(s) R.W. Murphy, J.E. Bernard and C.B. Winkler		8. Performing Organization Report No. UM-HSRI-PF-72-1	
9. Performing Organization Name and Address Highway Safety Research Institute University of Michigan Huron Parkway and Baxter Road Ann Arbor, Michigan 48105		10. Work Unit No.	
		11. Contract or Grant No.	
12. Sponsoring Agency Name and Address Motor Vehicle Manufacturers Association 320 New Center Building Detroit, Michigan 48202		13. Type of Report and Period Covered Phase I report	
		14. Sponsoring Agency Code	
15. Supplementary Notes			
16. Abstract The purpose of the study was to establish a digital computer based mathematical method for predicting the braking performance of trucks and tractor-trailers. Two simulation programs were developed, each based on a two-dimensional (vertical plane) mathematical model, one of which can represent a two- or three-axle truck, the other a three-, four-, or five-axle tractor-trailer combination. In each case the user may specify the vehicle geometry, brakes, suspension, tire and tire-road interface characteristics, weight, and payload distribution. The user can also introduce road roughness into the program in order to study its effect on braking performance. Detailed descriptions of the mathematical models of the vehicles, suspension systems, tires, brakes, and brake systems are given in section 2. In sec. 3, the digital computer programs for simulating vehicle braking performance are described. Sec. 4 treats vehicle parameters and their measurement. The dynamic tests on the full scale vehicles are reported in sec. 5. Comparison of the results from vehicle simulation and vehicle tests are made in sec. 6, along with a discussion of these results. The details involved with the descriptions of the mathematical models and computer programs are included in appendices A through F.			
17. Key Words Trucks Tractor-trailers Braking performance Mathematical models		18. Distribution Statement Unlimited	
19. Security Classif. (of this report) Unclassified		20. Security Classif. (of this page) Unclassified	
21. No. of Pages 216		22. Price <i>3.00-0.95</i>	

Highway Safety Research Institute

A Computer Based Mathematical Method for Predicting the Braking Performance of Trucks and Tractor-Trailers

PHASE I REPORT:

Motor Truck Braking and Handling Performance Study

by

Ray W. Murphy

James E. Bernard

Christopher B. Winkler

September 15, 1972

Highway Safety Research Institute / University of Michigan

Tb

HORI

19389

cap 2

CONTENTS

Acknowledgements.....xiii

Conspectus..... xv

1.0 Introduction..... 1

2.0 The Mathematical Models..... 3

 2.1 Introduction..... 3

 2.2 Static Considerations..... 3

 2.3 Suspension Systems..... 12

 2.3.1 Assumptions..... 12

 2.3.2 Coulomb Friction..... 12

 2.3.3 Viscous Friction..... 16

 2.3.4 Spring Forces..... 17

 2.3.5 Single Axle Suspension Model..... 17

 2.3.6 Walking Beam Suspension Model..... 19

 2.3.7 Four Spring Suspension Model..... 26

 2.4 The Tire Model..... 30

 2.4.1 Wheel Rotational Dynamics..... 31

 2.4.2 Shear Forces at the Tire/Road Interface..... 33

 2.4.3 Normal Forces at the Tire/Road Interface..... 34

 2.4.4 Rough Road Simulation..... 34

 2.5 Brakes and Brake Systems..... 34

 2.5.1 Delays and Lags in Brake System Response..... 35

 2.5.2 Calculation of Brake Torque..... 36

 2.5.3 Brake Factor Calculations..... 38

 2.5.4 Brake Fade..... 42

 2.5.5 Mechanical Actuation of Parking Brakes..... 46

 2.5.6 Brake Torque Applied to the Drive Shaft..... 46

 2.5.7 Use of Proportioning Valves..... 46

 2.5.8 Spring Actuation of Foundation Brakes..... 48

 2.5.9 Antilock System Simulation--A Suggested Approach..... 48

3.0 The Simulation Programs..... 51

 3.1 Program Specifications..... 51

 3.2 Program Structure..... 51

 3.3 Simulation Costs..... 51

4.0 Measurement of Vehicle Parameters..... 53

 4.1 Suspensions..... 53

 4.1.1 Rear Suspension Parameters..... 53

 4.1.2 Front Suspension Parameters..... 66

 4.1.3 Trailer Suspension Parameters..... 67

 4.2 Inertial Properties..... 67

 4.2.1 Weights..... 73

 4.2.2 Center of Gravity Position..... 73

 4.2.3 Pitch Moment of Inertia..... 77

Preceding page blank

4.2.4	Rolling Inertia of Wheels.....	82
4.2.5	Summary of Inertial Parameter Measurements....	82
4.3	Tire Parameters.....	82
5.0	Vehicle Braking Tests.....	89
5.1	Introduction.....	89
5.2	Test Procedures.....	103
5.2.1	Brake Effectiveness Test.....	103
5.2.2	Parking Brake Test.....	103
5.2.3	Brake Balance Test.....	103
5.2.4	Brake Response Time Tests.....	103
5.3	Test Results.....	103
5.3.1	Effectiveness Tests.....	103
5.3.2	Parking Brake Test.....	119
5.3.3	Brake Balance Test.....	121
5.3.4	Brake Response Time Tests.....	122
6.0	Results and Conclusions.....	127
6.1	Correlation of Results From Tests and Simulation: Program Validation.....	127
6.1.1	Validation Procedure.....	127
6.1.2	Validation Results--Effectiveness Test.....	128
6.1.3	Validation Results--Pitch Angle.....	141
6.1.4	Validation Results--Parking Brake Test.....	143
6.2	Conclusions.....	146
6.3	Recommendations for Further Work.....	146
Appendices		
A.	List of Symbols.....	149
B.	Equations on Motion.....	157
C.	Flow Charts.....	165
D.	Program Manipulation.....	171
E.	A Short Algorithm for the Choice of Tire Parameters.....	189
F.	Validation Data.....	199
References.....		209

FIGURES

2-1.	Straight truck, braking performance model.....	4
2-2.	Articulated vehicle, braking performance model.....	5
2-3.	Walking beam suspension.....	6
2-4.	Four spring suspension.....	6
2-5.	Sprung weight and payload.....	7
2-6.	Combined sprung weight and payload.....	8
2-7.	Static loading of a trailer equipped with a walking beam suspension.....	9
2-8.	Static loading of a trailer equipped with a four spring suspension.....	9
2-9.	Static loading of a tractor with a walking beam suspension.....	11
2-10.	Static loading of a tractor with a four spring suspension.....	11
2-11.	Mass spring system with viscous damping and coulomb friction.....	13
2-12.	Coulomb friction with dead zone.....	14
2-13.	Coulomb friction represented by limiting (saturation) functions.....	15
2-14.	System used in sample calculations of δ	15
2-15.	Force-velocity characteristic of shock absorbers at suspension I.....	17
2-16.	Nonlinear spring force-deflection characteristics.....	18
2-17.	Single axle suspension model.....	18
2-18.	Walking beam suspension model.....	20
2-19.	Free body diagrams: walking beam suspension.....	23
2-20.	Free body diagrams: frame with walking beam suspension.....	24
2-21.	Free body diagram: four spring suspension.....	27
2-22.	Four spring suspension model.....	29
2-23.	Free body diagram: unsprung masses of the four spring suspension model.....	29
2-24.	Free body diagram: frame with four spring suspension.....	30
2-25.	Free body diagram: wheel with braking.....	31
2-26.	A typical μ -slip curve.....	32
2-27.	μ -slip curves generated using the tire model.....	34
2-28.	Typical empirical brake pressure response curves.....	36
2-29.	Simulated brake pressure response curves.....	37
2-30.	Brake factor-lining friction curves for typical drum brakes.....	39
2-31.	Leading shoe-trailing shoe brake.....	40

FIGURES (Continued)

2-32.	Two leading shoe brake.....	40
2-33.	Effect of brake fade on brake factor.....	43
2-34.	Procedure for determination of engine rate sensitive brake torque.....	47
2-35.	Proportioning valve-line pressure characteristics.....	47
3-1.	Simplified flow diagram, braking performance program.....	52
4-1.	Loading scheme for rear axle suspension measurements.....	54
4-2.	Measurement scheme for walking beam suspension.....	54
4-3.	Vertical force-deflection characteristics measured at each wheel center, four spring suspension.....	55
4-4.	Vertical force-deflection characteristics, averaged for each side, four spring suspension.....	56
4-5.	Vertical force-deflection characteristics, averaged for all four wheels, four spring suspension.....	57
4-6.	Vertical force-deflection characteristics measured at each wheel center, walking beam suspension.....	58
4-7.	Vertical force-deflection characteristics, averaged for each side, walking beam suspension.....	59
4-8.	Vertical force-deflection characteristics, averaged for all four wheels, walking beam suspension.....	60
4-9.	Vertical force-deflection characteristics for rubber springs on walking beam suspension, averaged for each side.....	61
4-10.	Averaged vertical force-deflection characteristics for rubber springs, walking beam suspension.....	62
4-11.	Averaged vertical force-deflection characteristics for bushings and structural members only, walking beam suspension.....	63
4-12.	Measurement scheme, four spring suspension.....	64
4-13.	Detailed measurement scheme for walking beam suspension.....	65
4-14.	Scheme for loading front suspension.....	66
4-15.	Spindle center deflections from tests of straight truck front suspension.....	68
4-16.	Averaged spindle center deflections from tests of straight truck front suspension.....	69
4-17.	Spindle center deflection from tests of tractor front suspension.....	70

FIGURES (Continued)

4-18.	Averaged spindle center deflection from tests of tractor front suspension.....	71
4-19.	Averaged force deflection characteristics for the four spring suspension of the trailer.....	72
4-20.	Scheme for determining center of gravity height.....	74
4-21.	Weights and c.g. locations of truck and tractor.....	75
4-22.	Weights and c.g. locations for truck in three load conditions.....	76
4-23.	Weights and c.g. locations for the empty trailer.....	77
4-24.	Weights and c.g. locations for tractor-trailer, in the empty and the loaded condition.....	78
4-25.	Pitch moment of inertia measurement.....	79
4-26.	Apparatus for measuring polar moment of inertia of wheels and rotating assemblies.....	83
5-1.	Test vehicle, straight truck.....	90
5-2.	Test vehicle, tractor-trailer.....	91
5-3.	High c.g. load configuration.....	92
5-4.	Articulation angle limiter.....	93
5-5.	Brake pedal stop.....	94
5-6.	Signal processing equipment installed in truck.....	95
5-7.	Signal processing equipment installed in tractor cab.....	96
5-8.	Stabilized platform unit mounted on tractor frame.....	97
5-9.	Results from effectiveness tests on straight truck from 30 mph, empty and loaded on dry surface.....	107
5-10.	Results from effectiveness tests on straight truck from 50 mph, empty and loaded on dry surface.....	108
5-11.	Results from effectiveness tests on straight truck from 30 mph, with high c.g. load.....	109
5-12.	Results from effectiveness tests on straight truck from 30 mph, empty and loaded, on wet surface.....	110
5-13.	Pitch-deceleration data for the empty straight truck.....	111
5-14.	Pitch-deceleration data for the loaded (low c.g.) straight truck.....	112
5-15.	Pitch-deceleration data for the loaded (high c.g.) straight truck.....	113
5-16.	Results from effectiveness tests on tractor-trailer from 30 mph, empty and loaded, on dry surface.....	114
5-17.	Results from effectiveness tests on tractor-trailer from 60 mph, empty and loaded, on dry surface.....	115

FIGURES (Continued)

5-18. Results from effectiveness tests on tractor-trailer from 30 mph, empty and loaded, on wet surface..... 116

5-19. Jackknifing of tractor-trailer in brake effectiveness test..... 117

5-20. Tractor pitch-deceleration characteristic, in combination with trailer; empty and loaded..... 118

5-21. Results from brake response time tests on the straight truck..... 123

5-22. Results from brake response time tests on tractor-trailer..... 124

6-1. Straight truck brake timing..... 129

6-2. Tractor-trailer brake timing..... 129

6-3. Effectiveness test validation: straight truck, empty, 30 mph, dry surface..... 130

6-4. Effectiveness test validation: straight truck, empty, 50 mph, dry surface..... 131

6-5. Effectiveness test validation: straight truck, low c.g. load, 30 mph, dry surface..... 131

6-6. Effectiveness test validation: straight truck, low c.g. load, 50 mph, dry surface..... 132

6-7. Effectiveness test validation: straight truck, high c.g. load, 30 mph, dry surface..... 132

6-8. Effectiveness test validation: straight truck, low c.g. load, 50 mph, dry surface..... 133

6-9. Effectiveness test validation: straight truck, empty, 30 mph, wet surface..... 134

6-10. Effectiveness test validation: straight truck, low c.g. load, 30 mph, wet surface..... 134

6-11. Effectiveness test validation: tractor-trailer, empty, 30 mph, dry surface..... 135

6-12. Effectiveness test validation: tractor-trailer, empty, 60 mph, dry surface..... 136

6-13. Effectiveness test validation: tractor-trailer, loaded, 30 mph, dry surface..... 136

6-14. Effectiveness test validation: tractor-trailer, loaded, 60 mph, dry surface..... 137

6-15. Effectiveness test validation: tractor-trailer, empty, 30 mph, wet surface..... 137

6-16. Effectiveness test validation: tractor-trailer, loaded, 30 mph, wet surface..... 138

6-17. Pitch angle validation: straight truck, empty..... 141

6-18. Pitch angle validation: straight truck, low c.g. load..... 142

FIGURES (Continued)

6-19.	Pitch angle validation: straight truck, high c.g. load.....	142
6-20.	Pitch angle validation: tractor-trailer.....	143
6-21.	Parking brake air pressure behavior.....	144

TABLES

2.1	Variables in the equations for the single axle suspension.....	19
2.2	Nomenclature for the walking beam suspension.....	21
2.3	Nomenclature for the four spring suspension.....	26
2.4	Typical parameters for brake factor and brake effectiveness calculations.....	45
4.1	Inertial properties of test vehicles.....	84
4.2	Polar moments of inertia for rotating assemblies.....	85
4.3	Vertical spring rate of truck tires.....	85
4.4	Longitudinal stiffness of truck tires.....	86
5.1	Vehicle specifications, straight truck.....	98
5.2	Vehicle specifications, tractor-trailer.....	99
5.3	Loading conditions for test vehicles.....	100
5.4	Instrumentation, straight truck.....	101
5.5	Instrumentation, tractor-trailer.....	102
5.6	Test condition matrix.....	104
5.7	Test measurements.....	105
5.8	Maximum performance, straight truck.....	106
5.9	Maximum performance, tractor-trailer.....	120
5.10	Parking brake tests.....	121
5.11	Brake balance test results, tractor-trailer.....	121
5.12	Brake response and release times.....	125
6.1	Key for Figures 6-3 through 6-8.....	130
6.2	Key for Figures 6-9 and 6-10.....	133
6.3	Key for Figures 6-11 through 6-16.....	135
6.4	Tabulated stopping distances.....	139
6.5	Parking brake modal data.....	145
6.6	Parking brake tests validation.....	145

Preceding page blank

ACKNOWLEDGEMENTS

The work described in this report was conducted at the Highway Safety Research Institute (HSRI) of the University of Michigan, under contract to the Motor Vehicle Manufacturers Association of the United States, Inc. (MVMA).

The authors wish to acknowledge that many individuals and organizations made significant contributions to the program, not only by supplying vehicles, but also by providing technical assistance. These include: Mr. P. Terrano, White Motors, Chairman of the Ad Hoc Advisory Panel of the MVMA Motor Truck Research Committee, and Panel members M.A. Bowen, Chrysler Corporation; J.W. Gurney, Ford Motor Company; E. Ottenhoff, Chrysler Corporation; T.E. Price, Diamond Reo Trucks; R.E. Rassmussen, General Motors Corporation; H. Western, G.M. Truck and Coach; and G. Whitcomb, International Harvester Company. Further technical assistance was provided by Mr. J.W. Marshall of Uniroyal and Mr. J.E. Getz of Fruehauf.

Vehicles were supplied for use in this program by White Motors, Diamond Reo Trucks, and the Fruehauf Corporation. Tires were supplied by Uniroyal.

Special credit is surely due to Mr. Jerome J. Boron, Manager, Motor Truck Technical Services Department of MVMA, for his patient and constant guidance in the administrative matters.

The extensive computer models were programmed by Ms. Linda Howe and Mr. Garrick Hu of HSRI.

Preceding page blank

CONSPECTUS

The Motor Vehicle Manufacturers Association Truck and Tractor-Trailer Braking and Handling Project was begun at HSRI in mid-1971 with the expressed purpose of establishing a digital computer-based mathematical method for predicting the longitudinal and directional response of trucks and tractor-trailers. The work included conversion of existing HSRI programs to digital computer format and the extension of these programs to include various problems unique to trucks and articulated vehicles. In addition, key parameters, including tire parameters, were measured by HSRI for use in the simulation, and extensive vehicle testing was done to validate the simulation. A flow chart of the project is given in Figure A.

The work has been divided into three segments:

- a) Phase I. Empirical and analytical work resulting in a validated digital computer program to predict braking performance of trucks and articulated vehicles. The Phase I work is complete, and the subject of this report.
- b) Phase II. Empirical and analytical work resulting in a validated digital computer program to predict the directional response of trucks and articulated vehicles. The empirical work is complete, and the analytical work is currently in progress.
- c) Phase III. Refinement and extension of the previous work including consideration of:
 - 1) development of a digital computer-based method for predicting the moments of inertia and center of gravity locations along the principal axes for various truck, tractor, and trailer configurations;
 - 2) refinement of tandem suspension models already developed and formulation of models for three additional suspension types;
 - 3) determination of the longitudinal slip characteristics of truck tires;
 - 4) development of models for typical truck antilock systems to be used with Phase I (Braking Performance) and Phase II (Braking and Handling Performance) simulation programs;
 - 5) extension of the Phase I (Braking Performance) Program to include provision for simulating a doubles (tractor-semitrailer-full trailer) combination;
 - 6) development of more complete models of mechanical friction brakes, which will more accurately predict the decrease in brake effectiveness as a result of fade;
 - 7) development of a computer-based mathematical model for evaluating the acceleration and handling performance of trucks and tractor-trailer combinations;
 - 8) development of a computer-based mathematical method to study the dynamics of automotive air brake systems.

Many previous investigators have considered truck and articulated vehicle braking. (An extensive list of references is given in [1].) The effect of brake force distribution on braking performance of trucks and articulated vehicles has been thoroughly investigated analytically [2-5]. In these investigations, steady-state deceleration levels were assumed and quasi static relations were used to determine the load transfer from the rear axles onto the front axle, and, in [4], to determine the inter-axle load transfer for the tandem axles.

Preceding page blank

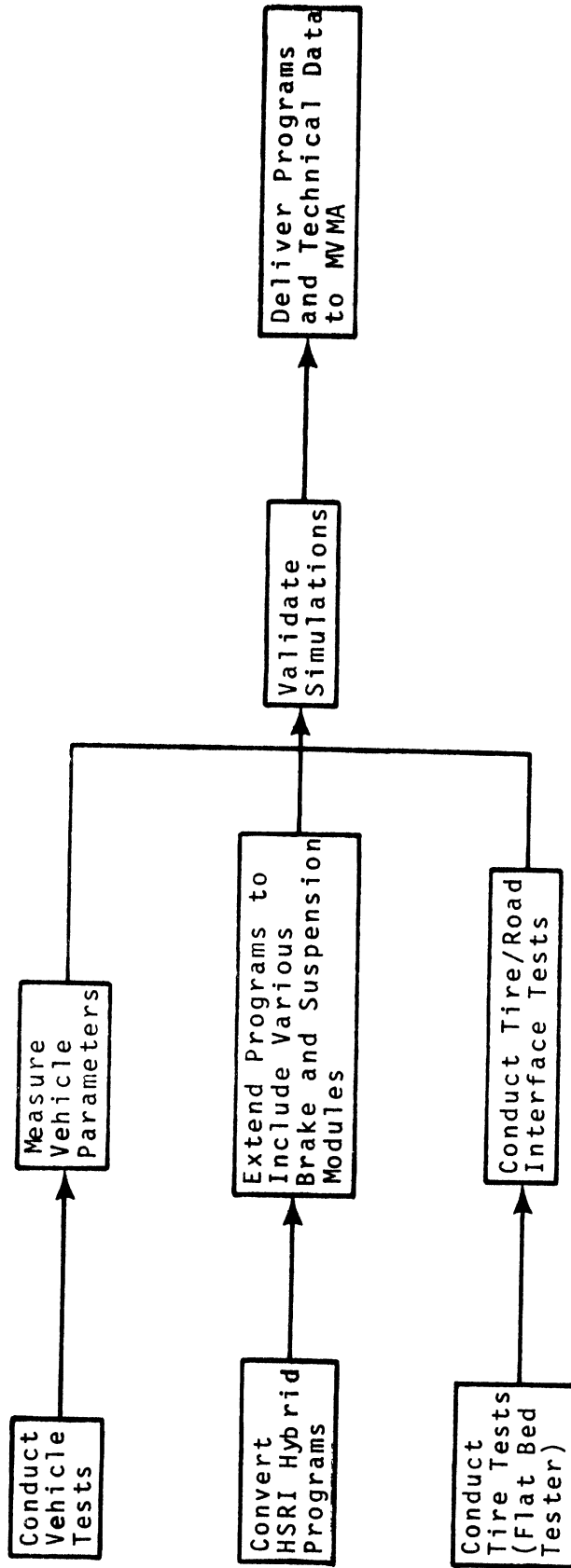


Figure A. Truck braking and handling project plan.

Many important effects which may be observed empirically may only be modeled by nonlinear equations, and thus do not facilitate analytical solution. To consider these effects, and, hopefully, to improve insight into the overall braking problem, computer simulations have been developed in varying degrees of sophistication [6, 7].

In the simulation of trucks and articulated vehicles, however, only moderate success has been obtained because one or more of the following factors has, for one reason or another, been subject to serious compromise in the modeling:

- a) tandem axle dynamics
- b) the tire model
- c) the brake system model

In Phase I, each of these problems has been considered in detail. However, as is shown in the block diagram in Figure B, the modular structure of the program allows convenient modification and extension of the Phase I work.

TANDEM AXLE DYNAMICS

To allow large payloads without unduly large axle loads, many trucks and articulated vehicles make use of tandem axle suspensions. These suspensions commonly have a mechanism for "load levelling," i.e., to attempt to maintain equal loading on each of the tandem axles in the presence of road irregularities. This mechanism may also cause unequal load distribution during braking, which may, in fact, result in so-called "brake hop." Thus, a careful analysis of tandem suspensions is in order if wheel lockup is to be simulated accurately.

In the Phase I work, two very common tandem suspensions have been modeled: the four spring with load leveler and the walking beam. Experimental results suggest that the four spring suspension tends to transfer load from the leading tandem to the trailing tandem, while the walking beam tends to transfer load from the trailing tandem to the leading tandem. This phenomenon is also predicted by the computer simulation, as may be seen from the results in Chapter 6 of this report.

The program structure will allow convenient addition of other suspension models and refinement of the present models; thus future work may easily be incorporated into the present program.

THE TIRE MODEL

In general, the shear force generated at the tire/road interface is a function of a multiplicity of variables describing (1) the geometric and material properties of the road surface, (2) the state of interface contamination, (3) the mechanical properties of the tire, and (4) the kinematics of the tire's rolling/sliding motion. In the present analysis, the effects of road variables and interface contamination are not considered. The tire/road shear force potential is described in terms of a speed-dependent "friction coefficient." To simulate a particular road surface it is necessary to empirically determine the tire/road "friction coefficient" for that surface. The model formulated to characterize the tire traction mechanics accordingly represents the shear force components as functions of (1) friction coefficient, (2) various parameters describing the relevant mechanical properties of the tire, and (3) the dynamical variables describing the tire contact patch kinematics.

BRAKE SYSTEM MODEL

Previous truck and articulated vehicle simulations have required user input of brake forces as a function of time, with the restriction that the brake force be limited to values less than some percentage of the normal force at the tire/road interface. In the present analysis, pressure at the treadle valve versus time is input by the user;

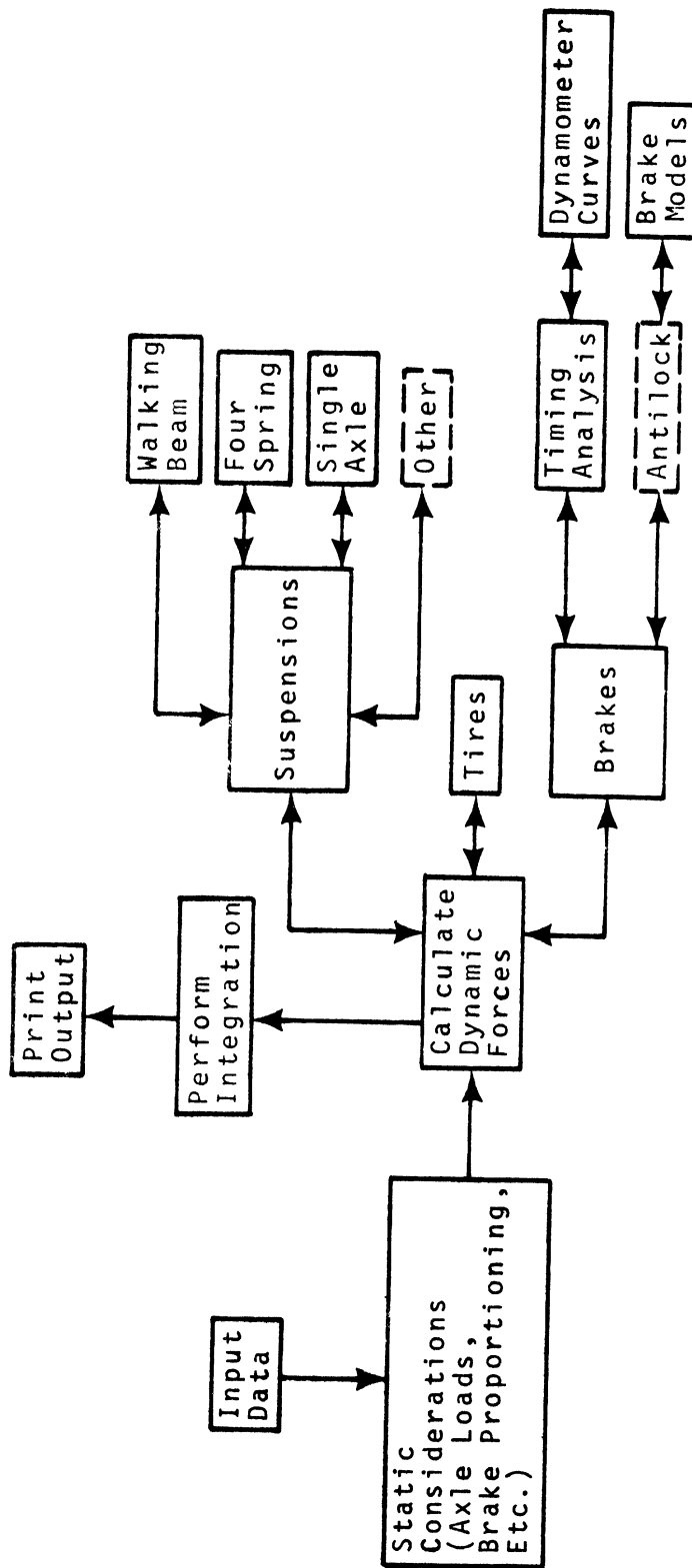


Figure B. Structure of the Phase I simulation program. The dashed line indicates future work.

the resulting line pressure and brake torque at each axle will then be computed. These computations depend on user input parameters descriptive of brake response time and dynamometer curves (line pressure-brake torque relationships) or on user input brake parameters chosen to simulate the appropriate brakes at each axle. This system may be used in the simplified manner of previous systems by choosing step pressure rise at the treadle valve and linear dynamometer curves. But the program also facilitates study of the dynamic effects of brake timing and a variety of separate braking devices. In addition, it is anticipated that simulation of commonly available antilock devices will soon be added as program options.

Brake fade is modeled to account for its averaged effect over the length of the stop, even though experimental results indicate that brake fade varies with time. A more sophisticated approach to this problem will be developed in Phase III.

Difficulties have, of course, been encountered. Where quick resolution has been impossible (as in the case of the modeling of brake fade), the work has been scheduled for further attention in Phase III. It must, however, be concluded from the validation results in Chapter 6 that meaningful results may be obtained through the use of the present model.

SIMULATION APPLICATIONS

The simulation exercises which have been presented in this report were undertaken to verify the computer model used and, of course, were designed to parallel the experimental work performed. However, they in no way constitute a limit of uses to which the program may be applied.

For example, a variety of parameter studies are possible through the use of the program. These include, along with many others:

- the effect of brake response time on stopping distance;
- maximum vehicle deceleration with or without wheel lock as a function of wheelbase, center of gravity position, gross vehicle weight, tire/road friction, suspension geometry, etc.;
- effect of brake proportioning on wheels unlocked stopping distance;
- vehicle pitch angle as a function of deceleration under the effect of changes in wheelbase, center of gravity position, gross vehicle weight, etc.;
- axle loads as a function of wheelbase, center of gravity position, or gross vehicle weight at various levels of deceleration (Note that rough road analysis may be conveniently included.);
- loading at the fifth wheel as a result of articulated vehicle braking;
- effects of the variation of tire characteristics from axle to axle.

Since the program is quite economical to use (details are in Chapter 3), it is expected that a properly chosen array of runs may be used in a cost effective manner to gain insight into a wide range of truck and articulated vehicle braking problems.

1.0 INTRODUCTION

The purpose of the research study reported herein was to establish a digital computer based mathematical method for predicting the braking performance of trucks and tractor-trailers. To this end, the study was directed toward accomplishing the following tasks:

1. Develop mathematical models of trucks and tractor-trailers which include detailed descriptions of the vehicle dynamics, brakes and braking systems, suspension systems, and the tire-road interface.
2. Construct programs for the digital computer, utilizing the mathematical models developed, in order to simulate the dynamic response of trucks and tractor-trailers to braking control inputs.
3. Measure the necessary inertial, suspension, tire and brake system parameters of a typical heavy truck and tractor-trailer for use in the computer simulation program.
4. Conduct a series of braking tests using the same truck and tractor-trailer to provide the test data necessary to validate the computer based simulation programs.

In accordance with the objectives of the study, two simulation programs were developed, each based on a two-dimensional (vertical plane) mathematical model, one of which can represent a two- or three-axle truck, the other a three-, four-, or five-axle tractor-trailer combination. In each case, the user may specify the vehicle geometry, brakes, suspension, tire and tire-road interface characteristics, weight, and payload distribution. The user can also introduce road roughness into the program in order to study its effect on braking performance.

In the next section of this report, detailed descriptions of the mathematical models of the vehicles, suspension systems, tires, brakes, and brake systems are given. In Section 3, the digital computer programs for simulating vehicle braking performance are described. Section 4 treats vehicle parameters and their measurement. The dynamic tests on the full scale vehicles are reported in Section 5. Comparison of the results from vehicle simulation and vehicle tests are made in Section 6, along with a discussion of these results.

Many of the tedious details involved with the descriptions of the mathematical models and computer programs have been relegated to the appendices. A table of symbols used in the programs and the report is given in Appendix A. Appendix B contains the equations of motion for the mathematical models. Appendix C contains the flow diagrams for the computer programs, while Appendix D contains a list of detailed instructions for using the computer programs, along with examples of typical input and output data. A short program to facilitate determination of certain tire parameters from test data is given in Appendix E. Test vehicle data is contained in Appendix F.

2.0 THE MATHEMATICAL MODELS

2.1. INTRODUCTION

Two mathematical models are described herein: one for a two- or three-axle straight truck and the other for a three-, four-, or five-axle articulated vehicle. The straight truck model is applicable to both light and heavy trucks, and bobtailed tractors. The articulated vehicle model is applicable to any combination having a two- or three-axle tractor and a semi-trailer with one or two axles.

Brakes in both models may be selected on an axle by axle basis. For vehicles equipped with hydraulic brakes, "duo servo" drum, two leading shoe drum, or disc brakes can be specified. Single or double wedge, or S-cam brakes can be specified for vehicles equipped with air systems. Provision is made for time delays and lags in brake response, as well as a gross representation of the effects of brake fade. Various miscellaneous brake modules can be specified, including spring brakes, engine and exhaust brakes, auxiliary retarders, and load sensing brake proportioning systems. Provision is also made for use of tabular "dynamometer curves", and for the inclusion of a user written subroutine for representing a wheel antilock system.

For suspension systems, spring rate, viscous damping, and coulomb friction may be specified. The viscous damping may have different characteristics in jounce and rebound, and the spring rate may be non-linear. Either walking beam or four elliptic leaf spring tandem axle suspension types may be used.

Tire-road interface characteristics are very carefully modeled, with the brake force produced at the wheel being a function of wheel slip, vehicle velocity, vertical load on the tire, tire longitudinal stiffness, and pavement surface characteristics.


Diagrams showing the essential features of the model of the two-axle straight truck and the three-axle tractor-trailer are given in Figures 2-1 and 2-2.** The equations of motion, based upon the coordinate systems given in these figures, are detailed in Appendix B. Equations describing the tandem suspensions shown in Figures 2-3 and 2-4, however, are given in Section 2.3.

The remainder of this section is devoted to detailed descriptions of the various components and modules of the mathematical models.

2.2. STATIC CONSIDERATIONS

The calculation of frequently used constants, including the static loadings, the effects of added payload, and certain others, must be accomplished before the actual simulation process begins.* The characteristics of the empty vehicle may be specified separately from those of the payload, in which case the program calculates the proper combined loads, the C.G. locations, and moment of inertia of the loaded vehicle. For this discussion an empty straight truck configuration is used as an example; the mathematics for the articulated vehicle are analogous. The empty truck and the payload to be added are shown in Figure 2-5. The empty truck has sprung weight W positioned at a point A_1 inches behind the front axle as shown, and pitch moment of inertia J about that point. The payload has weight PW and moment of inertia PJ about its center of gravity. If the combined weight and C.G. locations are designated with barred variables:

*The bulk of these calculations are in the initial stages of subroutine FCT1.

**Note  indicates center of gravity location.

X, Z, θ , ZS1 and ZS2 are displacements measured from the static equilibrium position. The dimensions are measured at static equilibrium.

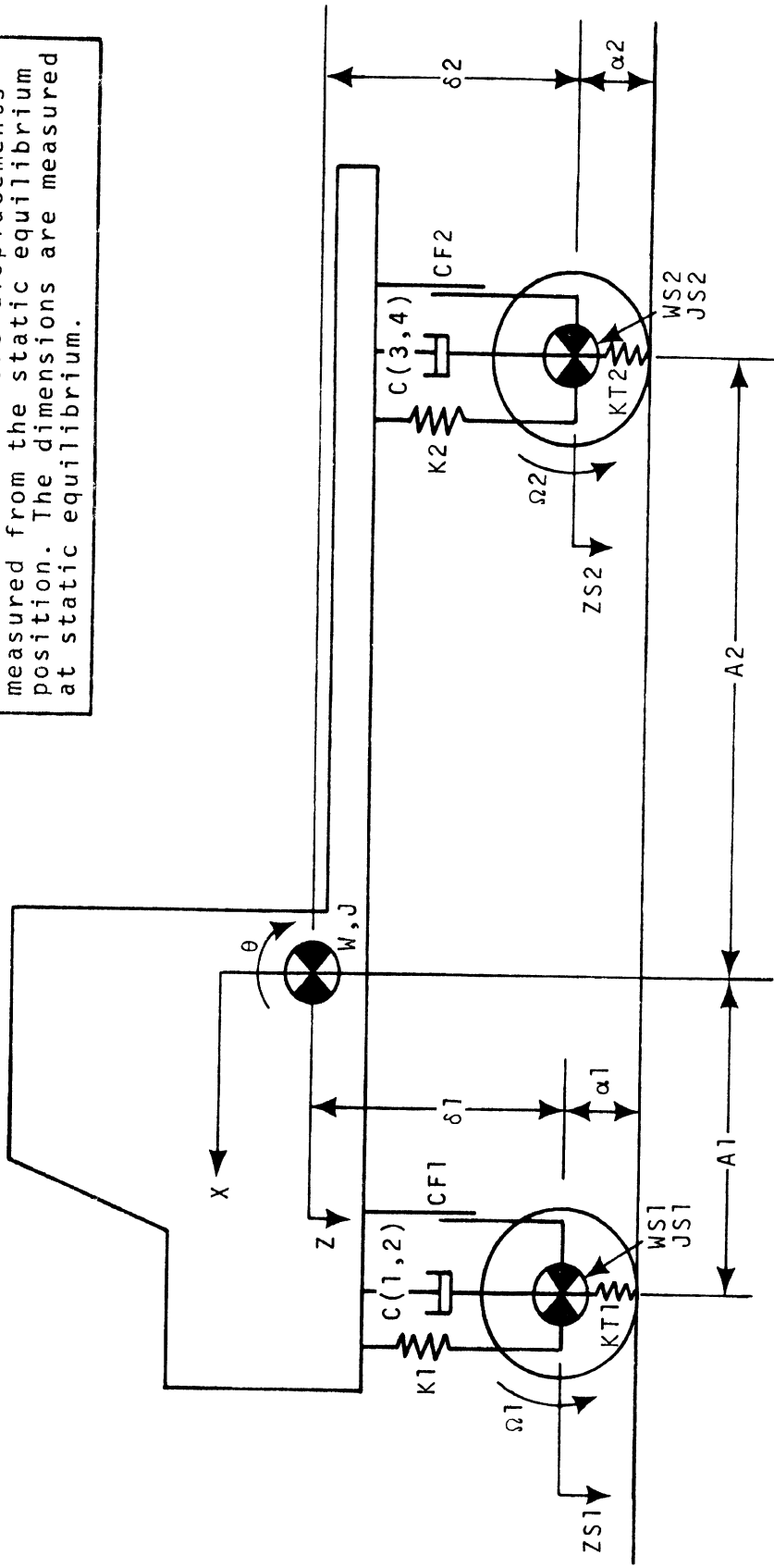


Figure 2-1. Straight truck, braking performance model

$X, Z, \theta, ZS1$ and $ZS2$ are displacements measured from the static equilibrium position. The dimensions are measured at static equilibrium.

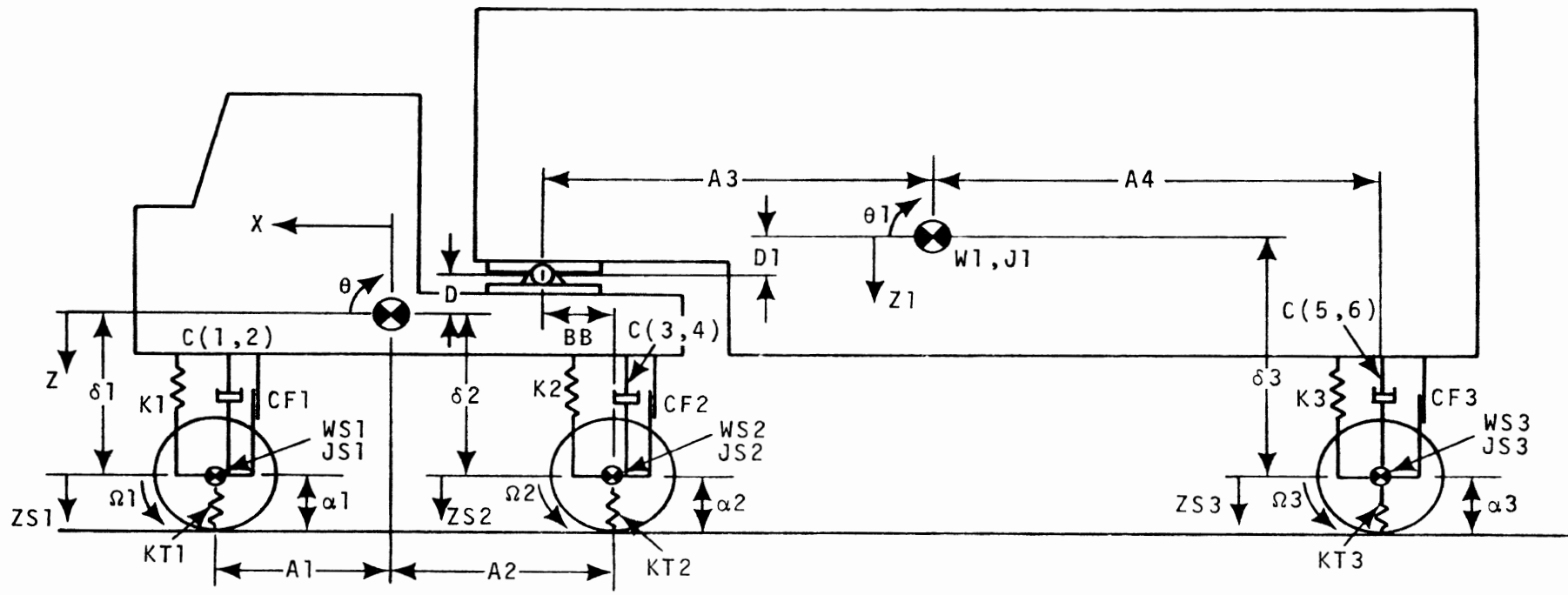


Figure 2-2. Articulated vehicle, braking performance model

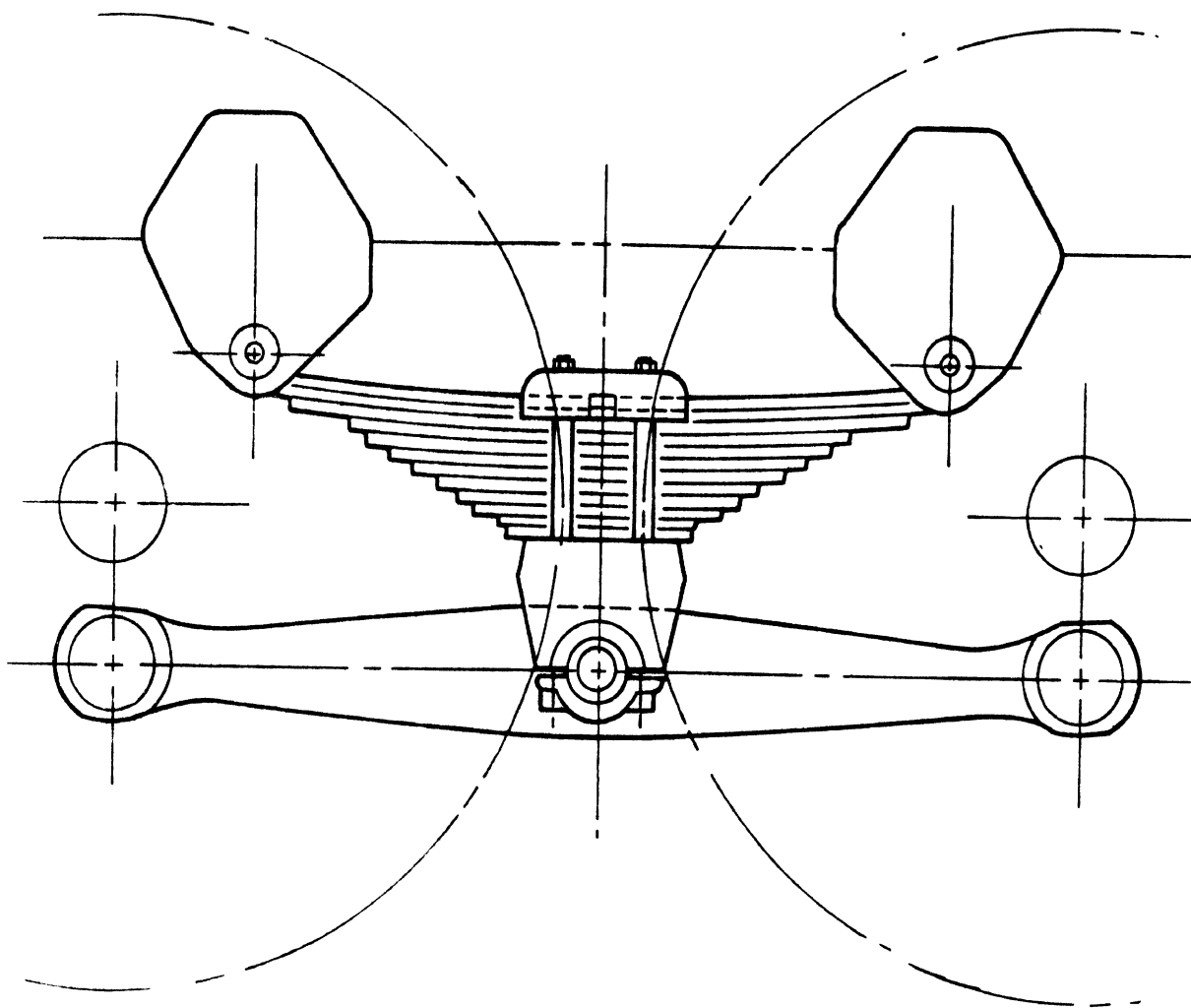


Figure 2-3. Walking beam suspension

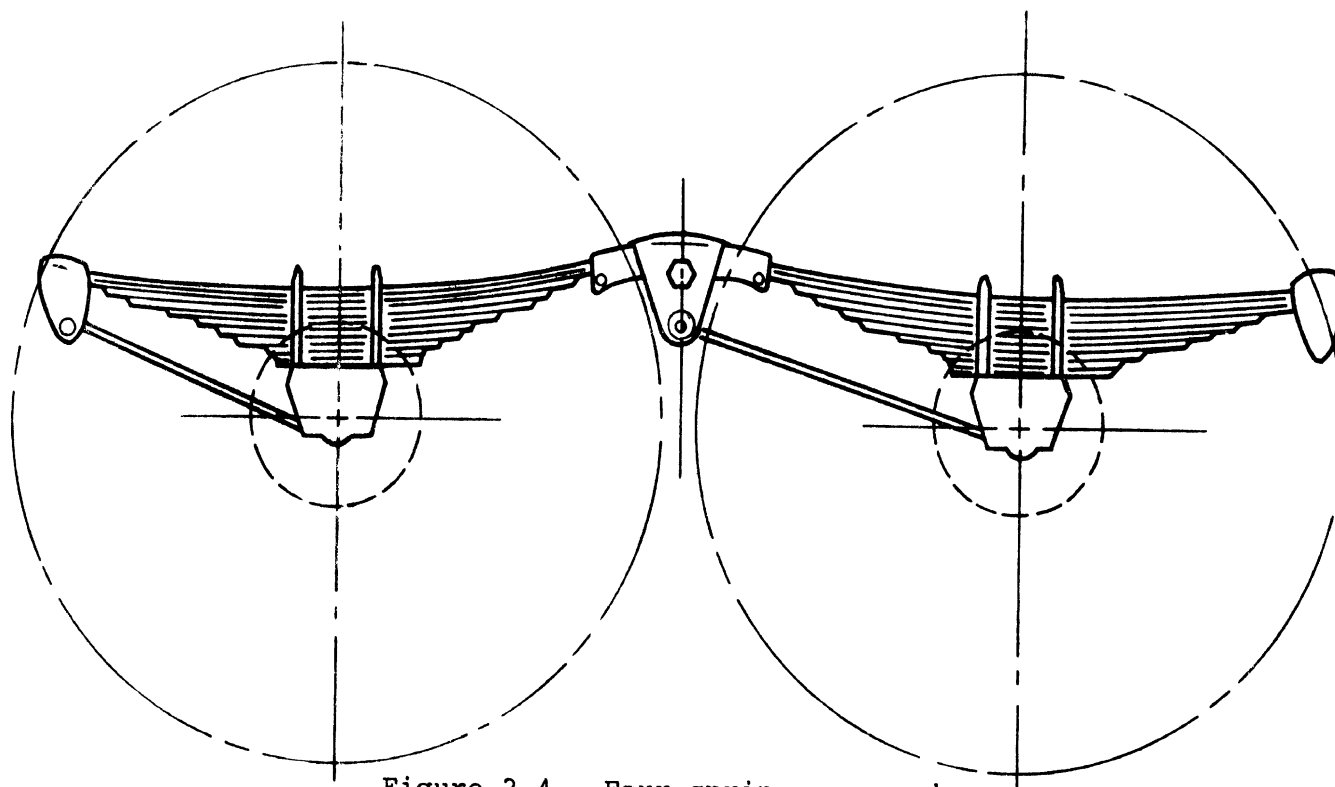


Figure 2-4. Four spring suspension

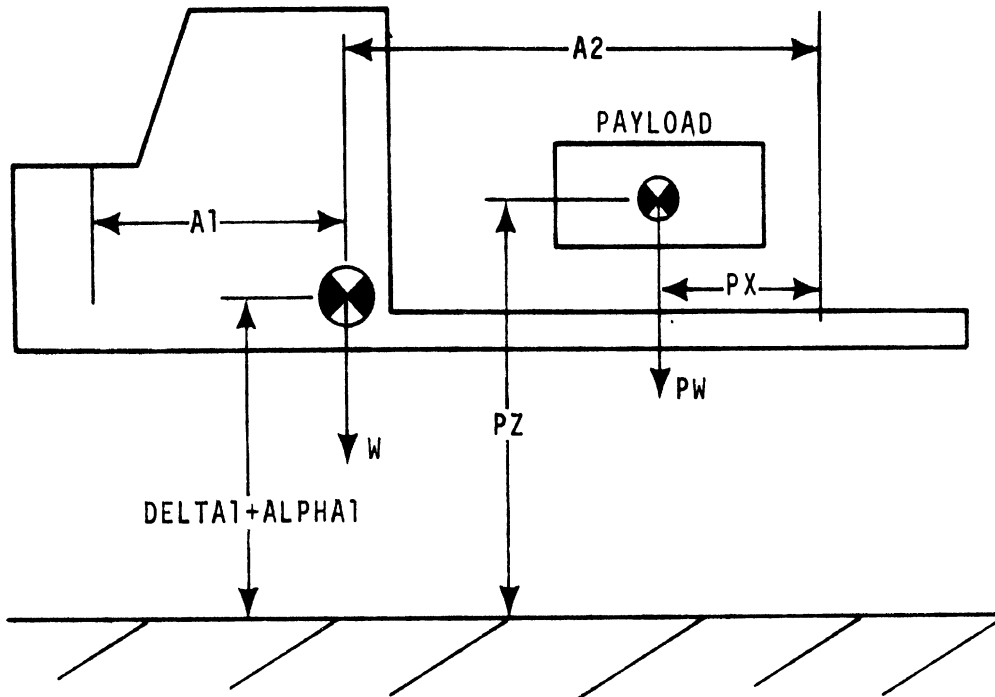


Figure 2-5. Sprung weight and payload

$$\bar{W} = W + PW \quad (2-1)$$

The summation of moments yields

$$\bar{A2} = \frac{(PW)(PX) + W(A2)}{\bar{W}} \quad (2-2)$$

$$\bar{DELTA1} = \frac{W(DELTA1 + ALPHA1) + PW(PZ)}{\bar{W}} - ALPHA1 \quad (2-3)$$

The new configuration is shown in Figure 2-6.

The distances a, b, c, and d are found using the empty vehicle information and equations 2-2 and 2-3.

$$a = \bar{A1} - A1 \quad (2-4a)$$

$$b = A2 - PX \quad (2-4b)$$

$$c = \bar{DELTA1} - DELTA1 \quad (2-4c)$$

$$d = PZ - ALPHA1 - \bar{DELTA1} \quad (2-4d)$$

The parallel axis theorem is applied to find the pitch moment of inertia of the combination of the empty truck plus the payload:

$$\bar{J} = J + \frac{W}{g}(a^2+c^2) + PJ + \frac{WP}{g}(b^2+d^2) \quad (2-5)$$

For the remainder of this report, the moment of inertia and mass center location parameters will appear without bars, with the understanding that the calculations given in Equations 2-1 through 2-5 have been completed, and the unbarred variables now refer to the loaded vehicle.

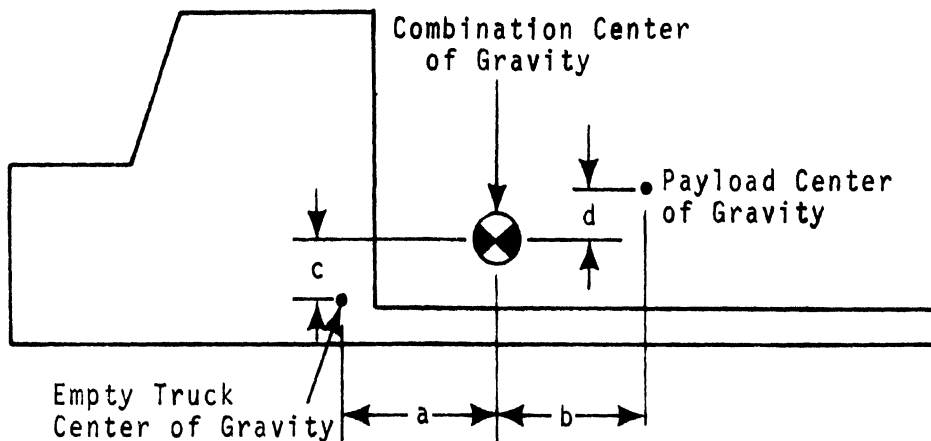


Figure 2-6. Combined sprung weight and payload

The calculation of the static load is, like the calculations given above, straightforward. The calculations become more complicated, however, with the introduction of tandem suspensions. In the following example, calculations to determine the static loads at various points on an articulated vehicle are shown. The calculations for the straight truck can be accomplished using the same equations by simply setting the term VS, which represents the vertical force at the fifth wheel, to zero. For this example, we have assumed tandem axles on the tractor and trailer; the static loading for a single axle tractor can be determined by using the walking beam suspension with the appropriate dimensions set to zero.

The trailer shown in Figure 2-7 is equipped with a walking beam suspension. Summing moments at the sprung mass connection to the suspension yields

$$VS = \frac{W1(A4)}{A3+A4} \quad (2-6)$$

and

$$TXX = W1 - VS \quad (2-7)$$

For the walking beam:

$$NS4 = WS4 + \frac{TXX(AA10)}{AA9 + AA10} \quad (2-8a)$$

$$NS5 = WS4 + WS5 + TXXX - NS4 \quad (2-8b)$$

The calculations for the trailer equipped with four spring suspension, shown in Figure 2-8, are more complicated.

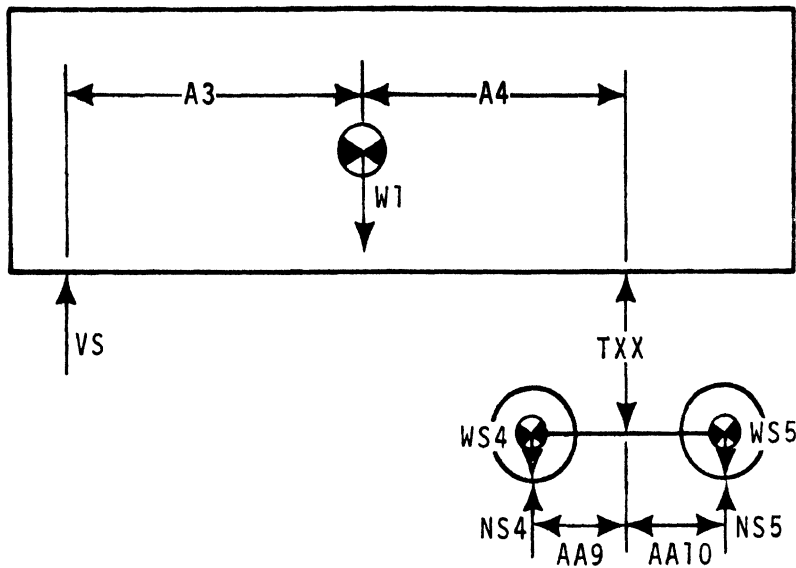


Figure 2-7. Static loading of a trailer equipped with a walking beam suspension

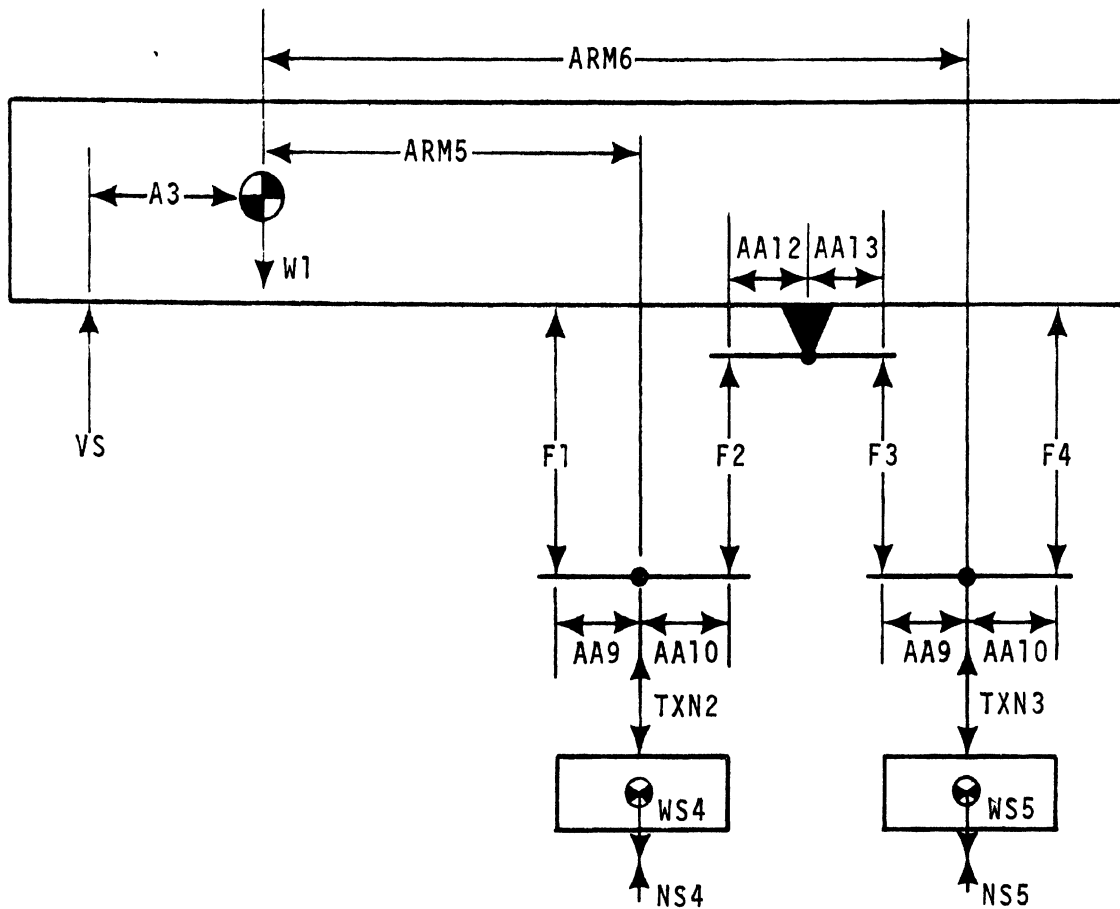


Figure 2-8. Static loading of a trailer equipped with a four spring suspension

By summing moments about the axles and the load leveler:

$$F1 = F2(AA10)/AA9 \quad (2-9a)$$

$$F3 = F2(AA12)/AA13 \quad (2-9b)$$

$$F4 = \frac{F2(AA9)(AA12)}{(AA10)(AA13)} \quad (2-9c)$$

The static axle loads are given by:

$$TXN2 = F1 + F2 = F2(1 + \frac{AA10}{AA9}) \quad (2-10a)$$

$$TXN3 = F3 + F4 = F2(\frac{AA12}{AA13})(1 + \frac{AA9}{AA10}) \quad (2-10b)$$

Summing moments about the kingpin then yields

$$W1(A3) = TXN2(ARM5 + A3) + TXN3(ARM6 + A3) \quad (2-11)$$

Substitution of equation 2-10 in equation 2-11 gives:

$$TXN3 = \frac{(W1)(A3)}{A3 + ARM6 + (\frac{AA13}{AA12})(\frac{1 + AA10/AA9}{1 + AA9/AA10})(A3 + ARM5)} \quad (2-12a)$$

$$TXN2 = \frac{TXN3(1 + \frac{AA10}{AA9})}{\frac{AA12}{AA13}(1 + \frac{AA9}{AA10})} \quad (2-12b)$$

The static loads NS and the king pin force VS are given by:

$$NS4 = TXN2 + WS4 \quad (2-13a)$$

$$NS5 = TXN3 + WS5 \quad (2-13b)$$

$$VS = W1 - TXN2 - TXN3 \quad (2-13c)$$

Calculation of the static loads on the tractor is considered next. The tractor shown in Figure 2-9 is equipped with walking beam rear suspension. Summing moments about the front suspension, the load on the walking beam is given by:

$$XXX = \frac{W(A1) + VS(A1+A2-BB)}{A1 + A2} \quad (2-14)$$

For the static loads:

$$NS2 = \frac{(XXX)(AA2)}{AA1 + AA2} + WS2 \quad (2-15a)$$

$$NS3 = XXX + WS2 + WS3 - NS2 \quad (2-15b)$$

$$NS1 = W + VS + WS1 - XXX \quad (2-15c)$$

The tractor equipped with a four spring configuration is shown in Figure 2-10.

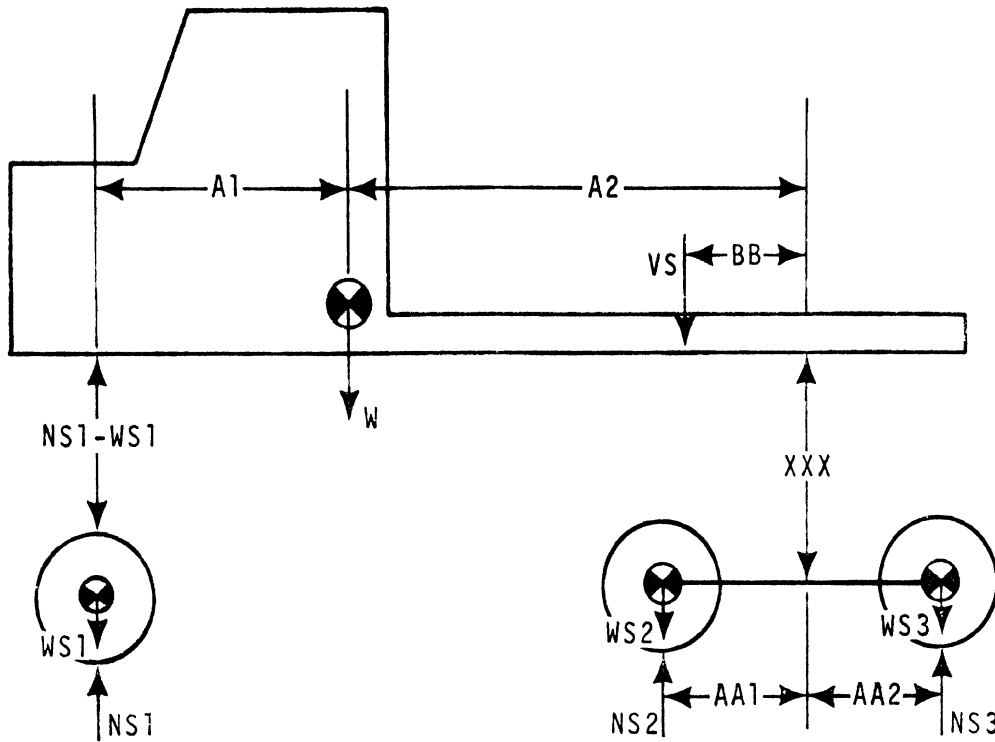


Figure 2-9. Static loading of a tractor with a walking beam suspension

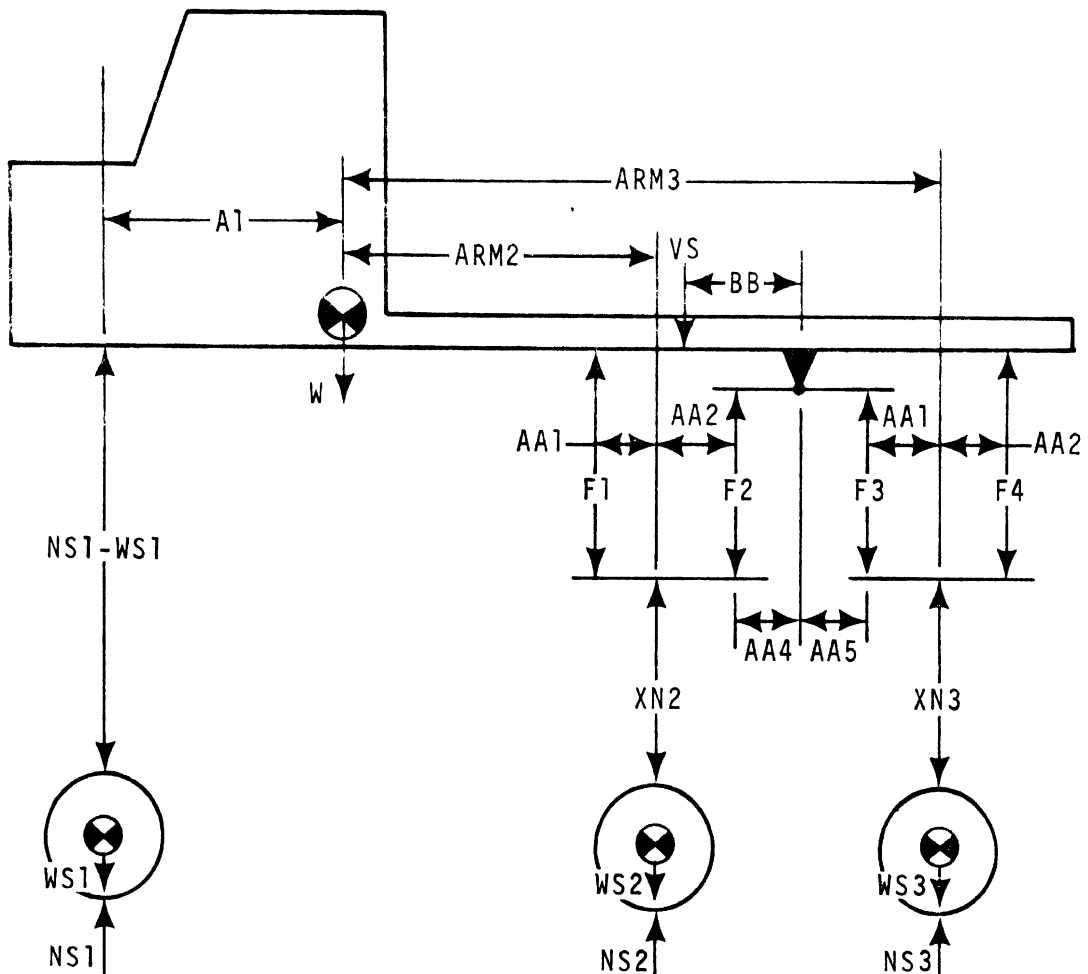


Figure 2-10. Static Loading of a tractor with a four spring suspension

Since the calculations for this case are directly analogous to those performed for the trailer, only the results are given:

$$XN3 = \frac{W(A1) + VS(A1+A2-BB)}{A1 + ARM3 + \left(\frac{AA5}{AA4}\right) \left(\frac{1 + AA2/AA1}{1 + AA1/AA2}\right) (A1 + ARM2)} \quad (2-16a)$$

$$XN2 = \frac{XN3(1 + AA2/AA1)}{\frac{AA4}{AA5}(1 + AA1/AA2)} \quad (2-16b)$$

$$NS3 = XN3 + WS3 \quad (2-16c)$$

$$NS2 = XN2 + WS2 \quad (2-16d)$$

$$NS1 = VS + W + WS1 - XN2 - XN3 \quad (2-16e)$$

2.3. SUSPENSION SYSTEMS

This section includes a detailed discussion of the suspension models along with the assumptions made in developing the models and some inherent limitations of the models.

2.3.1. ASSUMPTIONS. In deriving the equations for the suspension models, the following assumptions were made: (1) The force in the suspension is the sum of the forces due to coulomb friction, viscous friction, and the spring force. (2) The suspension forces are always in the "z" direction. The differences between results derived using this assumption and results derived assuming that the forces are perpendicular to the frame of the vehicle are negligible for small pitch angles.

2.3.2. THE COULOMB FRICTION. The classic expression usually denoted by the term "coulomb friction" is

$$f \leq \mu N \quad (2-17)$$

where f is the force of friction,

μ is an experimentally derived parameter,

N is the contact "normal force" between two sliding surfaces.

Equation 2-17 is empirical in nature, and describes approximately an observed phenomenon. To illustrate this point, consider the simple system shown in Figure 2-11.

The equation of motion of the mass M shown is

$$\overline{CF} = Mg + F(t) - Kz \quad (2-18a)$$

for

$$\dot{z}=0, \quad |\overline{CF}| < CF$$

otherwise,

$$M\ddot{z} + Kz + C\dot{z} + CF\frac{|\dot{z}|}{\dot{z}} = Mg + F(t) \quad (2-18b)$$

where \overline{CF} is the maximum allowable magnitude of the coulomb friction force CF , $F(t)$ is the driving force on the system, K is the spring rate, C is the viscous damping coefficient, z is the displacement of the mass M ($z=0$ at the free length of the spring), and g is the gravity constant.

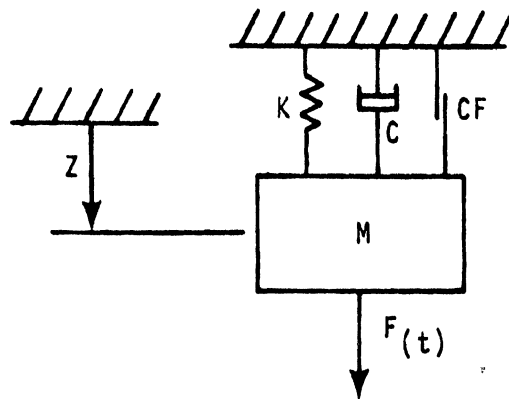


Figure 2-11. Mass spring system with viscous damping and coulomb friction

From equation 2-18a, it can be seen that no motion is possible for the system initially at rest until the magnitude of the quantity $Mg + F(t) - Kz$ becomes greater than $|CF|$. At this point, motion ensues, which is described by equation 2-18b. The motion of the mass will continue to be described by equation 2-18b, until the system again meets the conditions of equation 2-18a.

In developing a digital simulation of a system with coulomb friction, equations 2-18a and 2-18b present special problems. Since the velocity \dot{z} is known only at discrete points, the time when \dot{z} equals zero cannot easily be found. Thus, the actual time to switch from solution of equation 2-18b to solution of equation 2-18c is not known. There are a variety of ways to circumvent this problem, some of which are considered below:

- (a) Continuously solve equation 2-18b. This method is unsatisfactory (especially for large amounts of coulomb friction) since the system will "chatter" around the static equilibrium position. A slightly negative \dot{z} produces large coulomb friction, which causes large positive \ddot{z} . When the large positive \ddot{z} is integrated over a short time, positive \dot{z} results. The cycle then repeats with opposite signs. The period of this "chatter" is twice the integration time step.
- (b) Use an "equivalent viscous damping". By this method an increased value of C is chosen to compensate for the elimination of coulomb friction. This method can be useful when the coulomb friction forces are small compared to the velocity sensitive forces, but, in general, it cannot yield

satisfactory results in truck dynamics since the forces of coulomb friction are normally much larger than those of viscous friction.

- (c) Introduce a "dead zone" around static equilibrium. This method is shown schematically in Figure 2-12. This method has proven quite satisfactory for suspensions in which both viscous and coulomb friction are present. In the event that the viscous coefficient C is zero, however, the simulation allows velocity up to $|\dot{z}|=\delta$ with no energy loss. In digital computation this can cause the same type of chatter described in (b) above.
- (d) Use a limiting (saturation) function. A schematic diagram showing the function used in the simulation is given in Figure 2-13. This function effectively eliminates the problems with the methods described in (a), (b), and (c).

There is no free zone around static equilibrium. Thus, given large enough δ , all chatter is eliminated. The value of δ should be small enough, however, to preserve the character of coulomb friction. A method for the computation of δ is given below:

δ should be large enough so that if the coulomb friction were the only force applied to the unsprung mass and the sprung mass, the velocity in the suspension could not change from δ to a negative value in one integration time step. This precludes the onset of chatter.

The free body diagram of a system of sprung and unsprung masses, which can represent a truck or a tractor, is shown in Figure 2-14. The relative velocity between the sprung mass and the unsprung mass may be written:

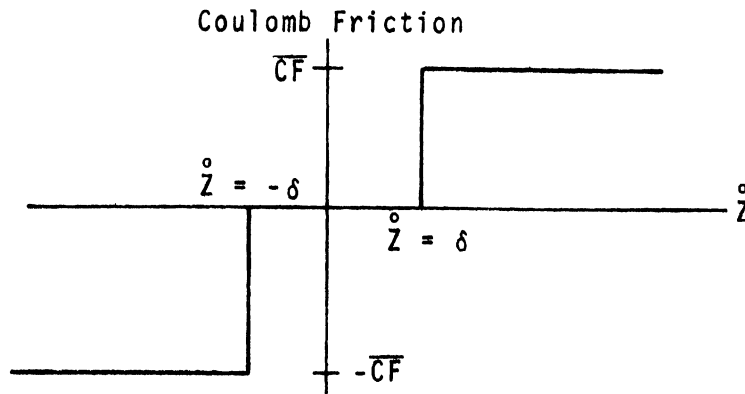


Figure 2-12. Coulomb friction with dead zone

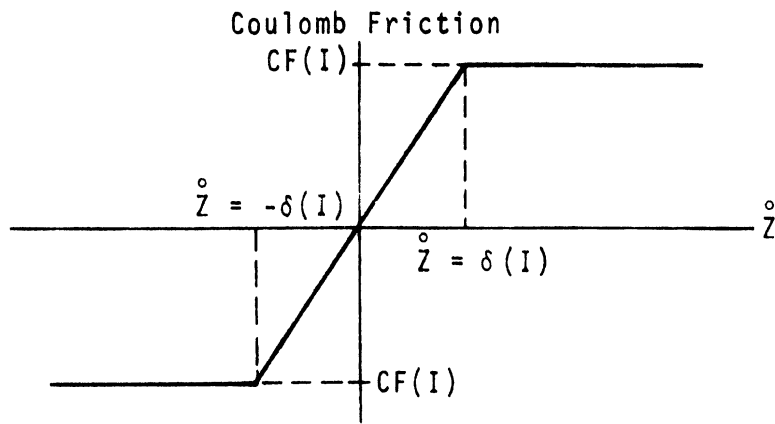


Figure 2-13. Coulomb friction represented by limiting (saturation) functions

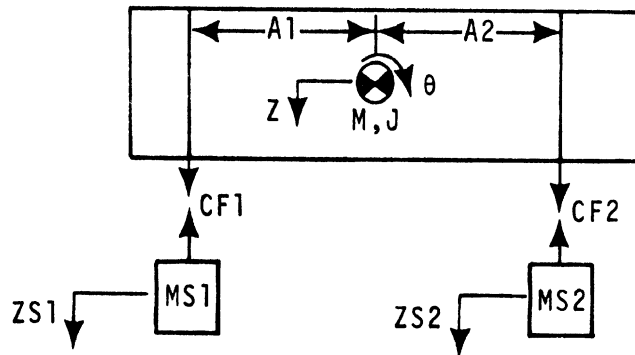


Figure 2-14. System used in sample calculations of δ

$$SD1 = Z\dot{S}1 + A1\dot{\theta} - \dot{z} \quad (2-19)$$

$$SD2 = Z\dot{S}2 - A2\dot{\theta} - \dot{z} \quad (2-20)$$

Thus:

$$|\ddot{z}| \leq \frac{1}{M}(CF1+CF2) \quad (2-21)$$

$$|\ddot{\theta}| \leq \frac{1}{J}(CF1(A1)+CF2(A2)) \quad (2-22)$$

$$|\ddot{zS1}| \leq \frac{CF1}{MS1} \quad (2-23)$$

$$|\ddot{zS2}| \leq \frac{CF2}{MS2} \quad (2-24)$$

During a time interval Δt , the changes in suspension velocities are

$$|\Delta S1D| \leq \Delta t [CF1(\frac{1}{MS1} + \frac{1}{M} + \frac{A1^2}{J}) + CF1(\frac{1}{M} + \frac{(A2)A1}{J})] \quad (2-25)$$

$$|\Delta S2D| \leq \Delta t [CF2(\frac{1}{MS2} + \frac{1}{M} + \frac{A2^2}{J}) + CF2(\frac{1}{M} + \frac{(A1)A2}{J})] \quad (2-26)$$

The coulomb friction break points, $\pm\delta(I)$ in figure 2-13, for suspensions 1 and 2 are set at

$$DEL1 = |\Delta S1D| \quad (2-27)$$

$$DEL2 = |\Delta S2D| \quad (2-28)$$

In a similar manner, it can be shown that, for a trailer suspension

$$DEL3 \leq \Delta t [CF3(\frac{1}{M1} + \frac{A4^2}{J})] \quad (2-29)$$

Since, in the program, the integration time step Δt is always .0025 seconds, calculations lead to typical values for the break points in the neighborhood of 3 inches/second. Thus, the simulated "frozen" suspension will allow small relative velocities (less than, say, 3 inches/second) rather than holding relative velocity to zero, and the possibility of numerical instability due to the coulomb friction is thereby eliminated.

2.3.3. VISCOUS FRICTION. The viscous friction coefficient is the slope of the force-velocity curve for the shock absorber. The user may select the slope in rebound and compression as is shown in Figure 2-15*.

Viscous friction is available at all axle locations; this will, in many cases, require the user to set the C values to zero in all but the front suspension. If the viscous friction is considered to

*To conform with popular shock absorber test practice, compression is shown positive.

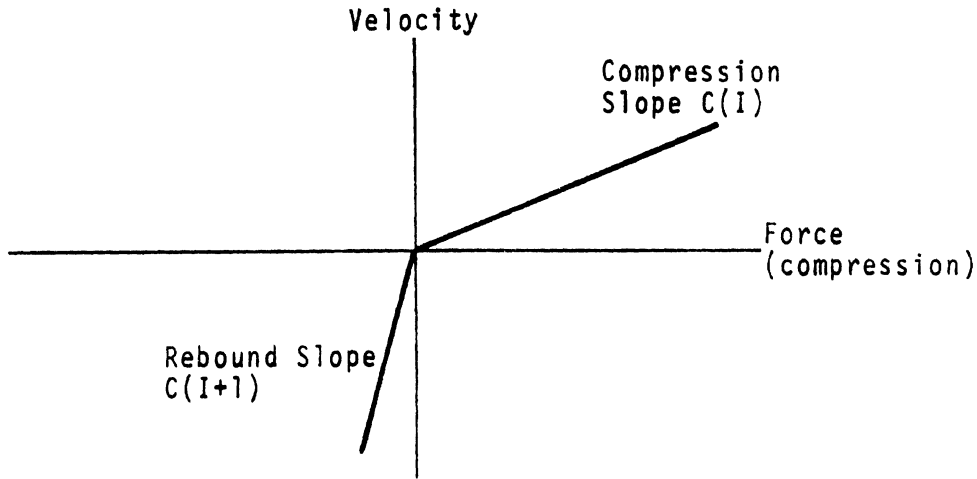


Figure 2-15. Force-velocity characteristic of shock absorbers

have an important effect (this will be unlikely in the presence of large amounts of coulomb friction), the user should carefully assess the effect of the shock absorber orientation. To determine the effective value of C for solid axles, the coefficients $C(I)$ are multiplied by the square of the cosine of the angle between the centerline of the shock absorber and the vertical. Other suspension geometries will require individual analysis by the user.

2.3.4. SPRING FORCES. The spring force at axle I may be denoted by a linear relationship

$$F(I) = K(I) * S(I) \quad (2-30)$$

where $K(I)$ is the slope of the force deflection curve in pounds/inch,

$S(I)$ is the suspension deflection from its static length in inches.

Alternatively, a nonlinear force deflection relationship may be used*. An example is shown in Figure 2-16, in which four points are used. The force in the spring will then be found through linear interpolation. (Note the table lookup "squares off" the spring force at the first and last points.)

2.3.5. SINGLE AXLE SUSPENSION MODEL. A schematic diagram of a single axle is given in Figure 2-17. The equations of motion are written in terms of the variables given in Table 2-1.

*To specify a nonlinear spring rate, the user enters any negative number for spring constant $K(I)$. This sets a flag which causes the program to read as input a set of tabulated force-deflection points.

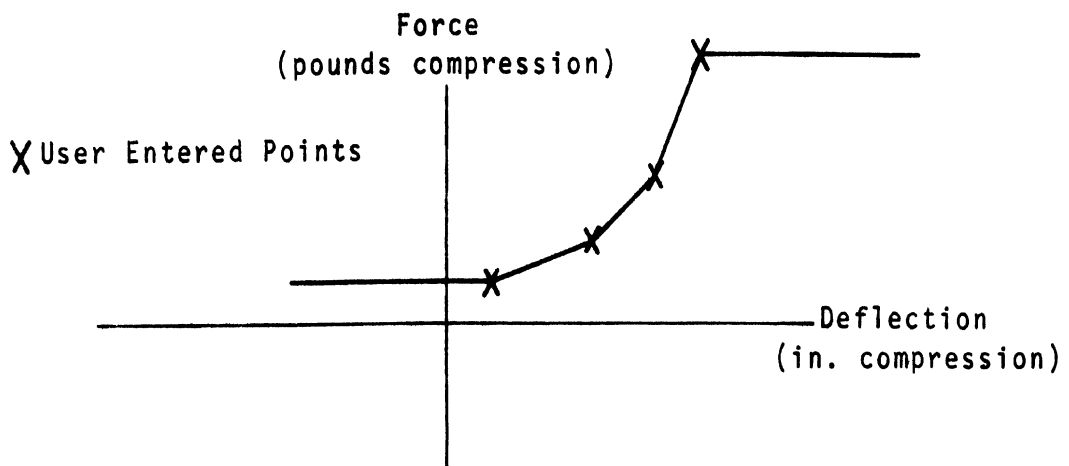


Figure 2-16. Nonlinear spring force-deflection characteristics

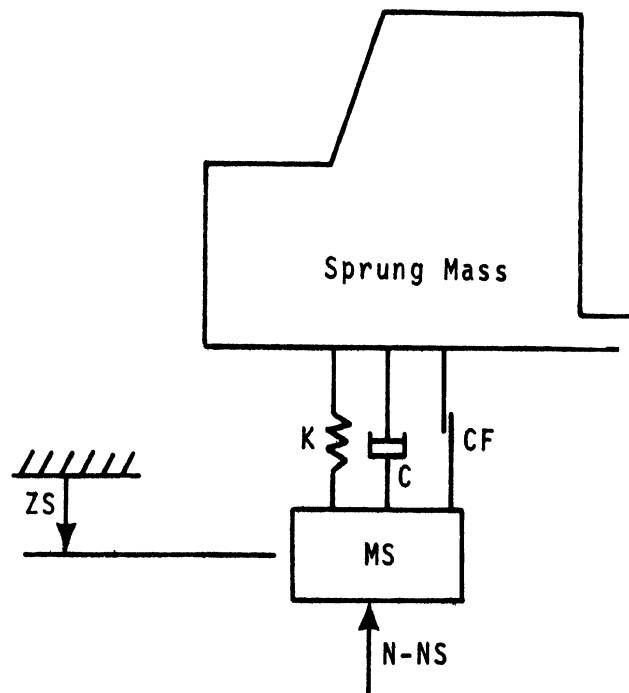


Figure 2-17. Single axle suspension model

TABLE 2-1
Variables in the Equations for the Single Axle Suspension

C	Viscous damping coefficient
CF	Coulomb friction
K	Spring rate
N	Normal force on the tire
NS	Static normal load on the tire
MS	Unsprung mass
S	Distance suspension has extended
SD	Velocity of suspension extension
ZS	Position of unsprung mass, ZS=0 for static equilibrium

The parameters C and K may be a function of \dot{ZS} and ZS respectively, and the dependence of CF on \dot{ZS} is taken from a functional relationship analogous to that shown in Figure 2-13.

The equation of motion is determined by summing the vertical forces acting on the unsprung mass*:

$$MS(\ddot{ZS}) + C(\dot{ZS}) + K(ZS) + CF = NS - N \quad (2-31)$$

2.3.6. WALKING BEAM SUSPENSION MODEL. A diagram of the walking beam is shown in Figure 2-18. Nomenclature is listed in Table 2-2. It should be noted that the torque rods are assumed to remain horizontal and the center of mass of the tandem assembly is assumed to be on the line of wheel centers. The analysis given here is for the suspension mounted on a tractor; application to a trailer is analogous. Applying Newton's second law in the "ZT" direction yields:

$$NS2 + NS3 - N2 - N3 - SF2 = [MS(2) + MS(3)](\ddot{ZT}) \quad (2-32)$$

The moment of momentum about the point P is defined as

$$\bar{H} = \sum_{\substack{\text{all} \\ \text{particles}}} \bar{r}_i \times dm_i \bar{V}_i \quad (2-33)$$

where

\bar{r}_i is the vector from point P to the ith particle,

dm_i is the mass of the ith particle,

\bar{V}_i is the velocity vector of the ith particle.

The point P is chosen as the mass center of the walking beam suspension. From Figure 2-18, note that the velocity of the ith particle on the front axle assembly is

*Note that (MS)g has been eliminated from the equation by setting ZS=0 at static equilibrium.

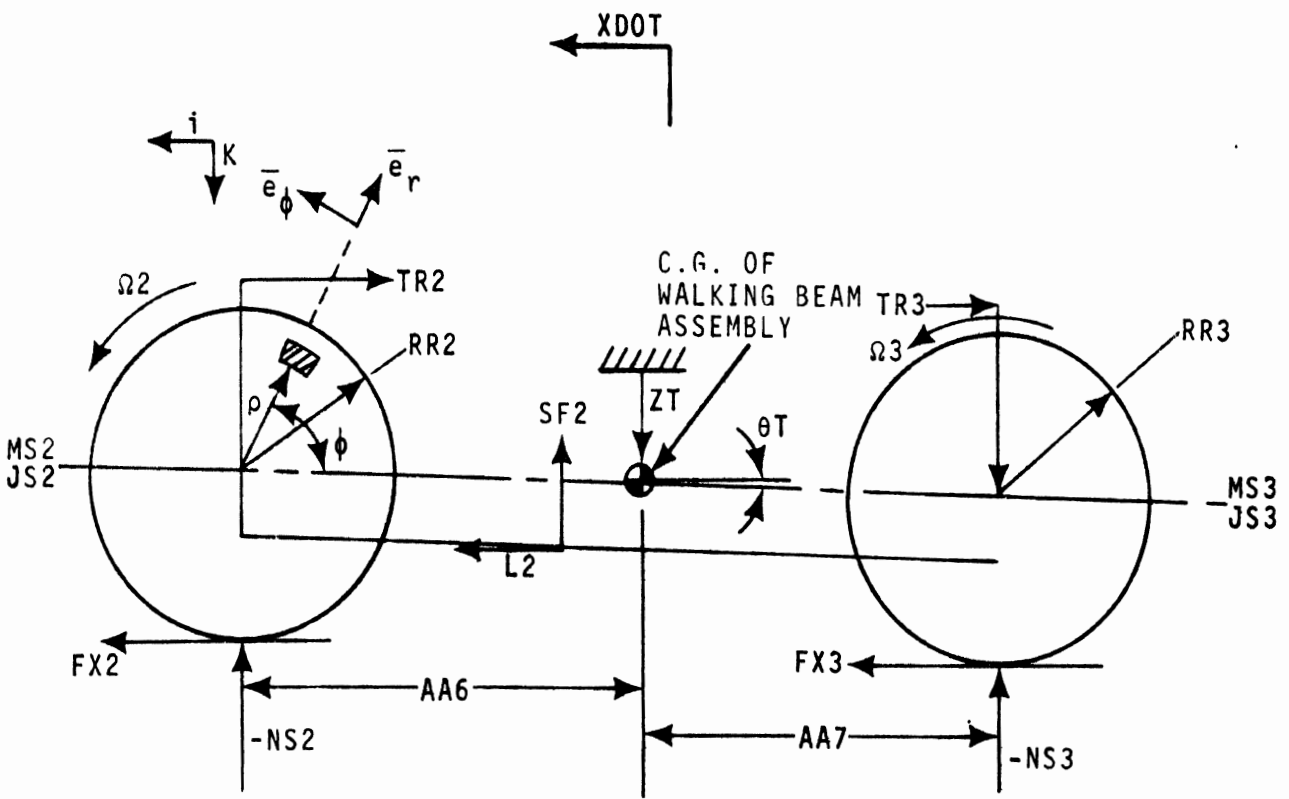
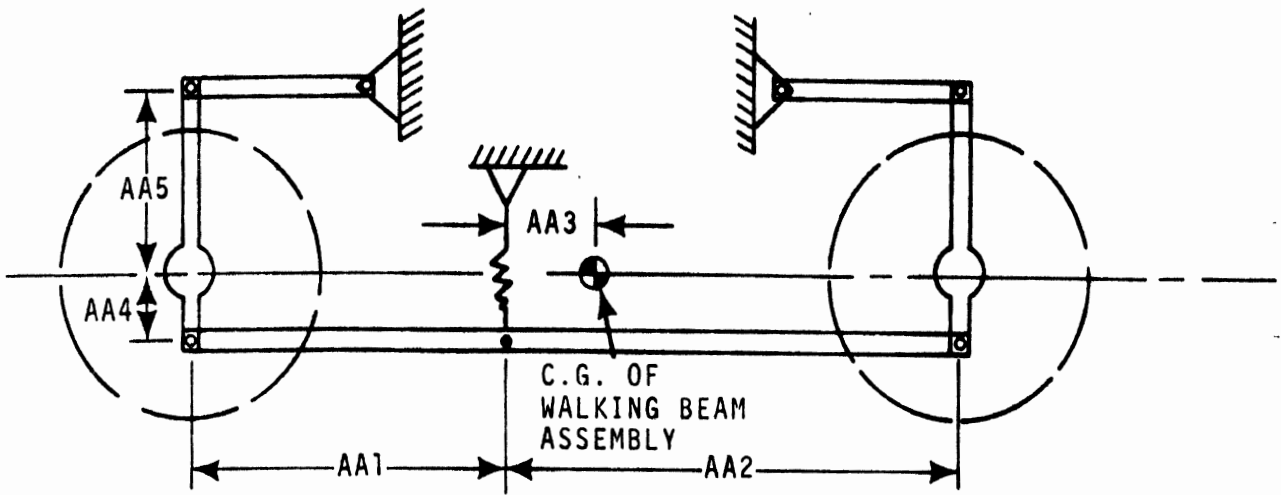


Figure 2-18. Walking beam suspension model

TABLE 2-2
Nomenclature for Walking Beam Suspension

AA1	Horizontal distance from walking beam pin to front axle
AA2	Horizontal distance from walking beam pin to rear axle
AA3	Horizontal distance from walking beam pin to suspension CM (computed)
AA4	Vertical distance from axle to walking beam
AA5	Vertical distance from axle to torque rod
AA6	Horizontal distance from front tandem axle to CM (computed)
AA7	Horizontal distance from rear tandem axle to CM (computed)
PERCNT	Number between 0 and 100 describing the effectiveness of the torque rods. User choice of 0 signifies no torque rods; choice of 100 signifies 100 percent effective torque rods and hence no inter-axle load transfer due to brake torque.

$$\bar{V}_i = [Z\dot{T}2 - AA6(\dot{\theta}T)]k + |\rho|(\Omega 2)\bar{e}\bar{\phi} \quad (2-34)$$

where the second term applies only to those particles following $\Omega 2$. Using equations 2-33 and 2-34, the moment of momentum for the front axle assembly is:

$$\bar{H}_{FA} = \sum_i dm_i (AA6i + |\rho|\bar{e}\bar{r}) \times [(Z\dot{T}2 - AA6\dot{\theta}T)k + \rho\Omega 2\bar{e}\bar{\phi}] \quad (2-35)$$

Completing the cross product and noting that

$$\sum_i dm_i = MS2, \quad (2-36a)$$

$$\bar{e}\bar{r} = -\cos\phi i - \sin\phi k, \quad (2-36b)$$

$$\bar{e}\bar{\phi} = -\cos\phi k + \sin\phi i, \quad (2-36c)$$

the angular momentum for the front axle about the mass center is:

$$\bar{H}_{FA} = [MS2(AA1)^2\dot{\theta}T - \dot{\phi} \int |\rho|^2 dm]j \quad (2-37)$$

But $\int |\rho|^2 dm$ is the polar moment of inertia of wheel 2;

$$\int |\rho|^2 dm = JS2 \quad (2-38)$$

Using equations 2-37 and 2-38, and performing similar operations to include the rear axle, leads to

$$\bar{H} = \{ [MS2(AA6)^2 + MS3(AA7)^2] \dot{\theta}T - JS2(\dot{\Omega}2) - JS3(\dot{\Omega}3) \} j \quad (2-39)$$

Summing moments around the mass center:

$$\begin{aligned} & (W2-WS2)(AA6) - (N3-NS1)(AA7) + SF2(AA3) + L2(AA4) \\ & + (TR2+TR3)(AA5) + FX2(R2) + FX3(R3) = [MS2(AA6)^2 \\ & + MS3(AA7)^2] \ddot{\theta}T - JS2(\ddot{\Omega}2) - JS3(\ddot{\Omega}3) \end{aligned} \quad (2-40)$$

Figure 2-19 is a free body diagram of the various parts of the assembly. Applying Newton's second law in the "X" direction, the following equations are obtained:

$$FX2 - FAX2 = (MW2)\ddot{X} \quad (2-41)$$

$$H2 - TR2 + FAX2 = (MAX2)\ddot{X} \quad (2-42)$$

Summing equations 2-41 and 2-42:

$$FX2 + H2 - TR2 = (MS2)\ddot{X} \quad (2-43)$$

In the same manner, it can be shown that

$$FX3 + H3 - TR3 = (MS3)\ddot{X} \quad (2-44)$$

Summing moments about the center of axles shown in figure 2-19 yields:

$$(H2 + V2\alpha2)AA4 + TR2(AA5) = T2 \quad (2-45)$$

$$(H3 + V3\alpha3)AA4 + TR3(AA5) = T3 \quad (2-46)$$

But from figure 2-19:

$$H3 + H2 = L2 \quad (2-47)$$

Using equations 2-45 and 2-46 in equation 2-47 yields:

$$L2(AA4) = T2 + T3 - (TR2+TR3)AA5 = (V2\alpha2+V3\alpha3)AA4 \quad (2-48)$$

Using equation 2-48 in equation 2-40 yields:

$$\begin{aligned} & (N2-NS2)(AA6) - (N3-NS3)(AA7) + SF2(AA3) - V2\alpha2+V3\alpha3)AA4 \\ & + [T2 + (FX2)RR2 - (JS2)\dot{\Omega}2] + [T3 + (FX3)RR3 + (JS3)\dot{\Omega}3] \\ & = [MS3(AA6)^2 + MS3(AA7)^2] \ddot{\theta}T \end{aligned} \quad (2-49)$$

An examination of the rotational equations for the wheels shows that the terms in brackets on the left-hand side of equation 2-49 are identically zero. Thus, $V2\alpha2$ and $V3\alpha3$ need to be determined to complete the equations.

Those unknown terms are a function of the many compliances in the suspension. Since V may be very large and α quite small, this term is difficult to model analytically. Rather, it is assumed that

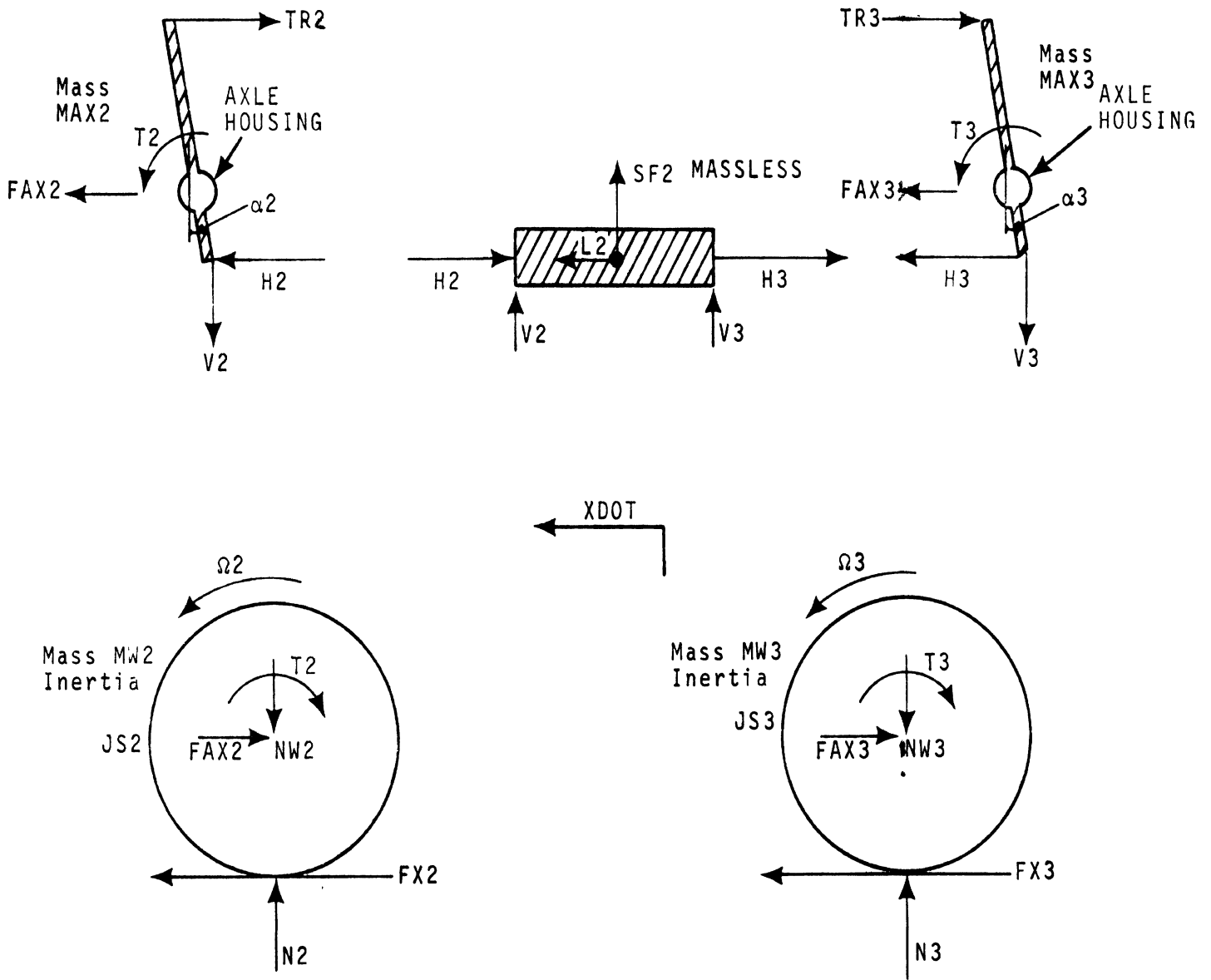


Figure 2-19. Free body diagrams: walking beam suspension

$$V2\alpha2(AA4) = P(TR2)(AA5) \quad (2-50)$$

$$V3\alpha3(AA4) = P(TR3)(AA5) \quad (2-51)$$

i.e., the moment of the vertical force around the axle center will be proportional to the moment of the torque rod about the axle center. Therefore, equations 2-45 and 2-46 may be written:

$$H2(AA4) + (1+P)(TR2)(AA5) = T2 \quad (2-52)$$

$$H3(AA4) + (1+P)(TR3)(AA5) = T3 \quad (2-53)$$

TR2 and TR3 can now be determined from equations 2-43, 2-44, 2-52, and 2-53:

$$TR2 = \frac{T2 - AA4(MS2\ddot{X} - FX2)}{AA4 + (1+P)AA5} \quad (2-54)$$

$$TR3 = \frac{T3 - AA4(MS3\ddot{X} - FX3)}{AA4 + (1+P)AA5} \quad (2-55)$$

Now equations 2-50 and 2-51 may be used to find $V2\alpha2(AA4)$ and $V3\alpha3(AA4)$.

Lastly, the pitch moment applied to the frame must be determined. A free body diagram of the rear portion of the frame is given in figure 2-20. (Note $\delta 2$ is the vertical distance from cm (center of mass) to the static position of the axle centers. The small changes in the vertical position of the height of the axle centers are neglected.)

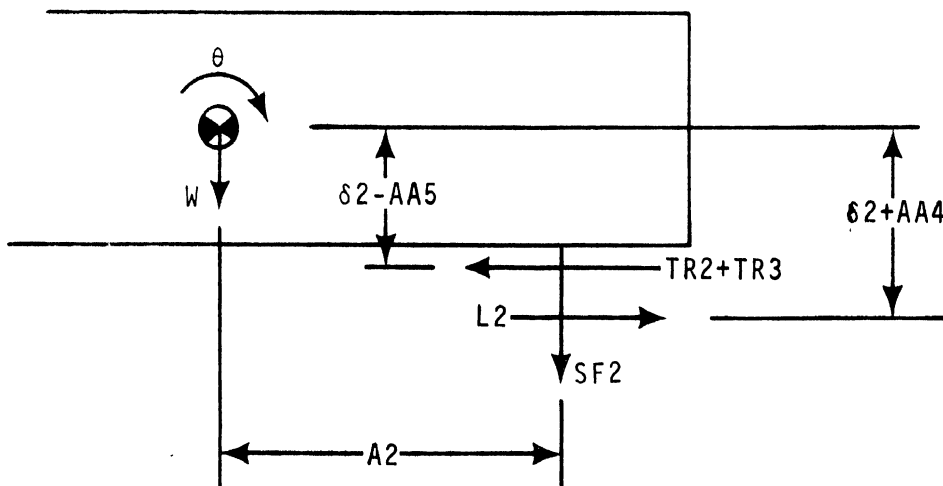


Figure 2-20. Free body diagram: frame with walking beam suspension

Thus, the moment applied by the tandem assembly is

$$\Sigma M_{cm} = SF2(A2) + (TR2+TR3)(\delta 2-AA5) - L2(\delta 2+AA4) \quad (2-56)$$

This may be written

$$\Sigma M_{cm} = SF2(A2) + (TR2+TR3-L2)\delta 2 - L2(AA4) - (TR2+TR3)AA5 \quad (2-57)$$

From equations 2-43, 2-44, and 2-47:

$$(TR2+TR3-L2) = FX2 + FX3 - (MS2+MS3)\ddot{X} \quad (2-58)$$

and from equation 2-48

$$-L2(AA4) - (TR2+TR3)AA5 = -T2 - T3 + (V2\alpha 2+V3\alpha 3)AA4 \quad (2-59)$$

Therefore, equation 2-57 may be written:

$$\Sigma M_{cm} = SF2(A2) + \delta 2 [FX2+FX3 - (MS2+MS3)\ddot{X}] - T2 - T3 + (V2\alpha 2+V3\alpha 3)AA4 \quad (2-60)$$

It is shown above that P is the ratio of the moment of vertical force around the axle center to the moment of the torque rod around the axle center.

The variable which is input to the program to define the ratio P is PERCNT, where

$$P = \frac{100 - \text{PERCNT}}{\text{PERCNT}} \quad (2-61)$$

Thus, if PERCNT = 100, P=0 and the torque rods will be "perfect", i.e., there will be no inter-axle load transfer due to brake forces. On the other hand, smaller PERCNT will result in increasing load transfer in braking. Equations 2-54 and 2-55 show that as P becomes larger, TR2 and TR3 become smaller, and equations 2-45 and 2-46 show that V2 α 2 and V3 α 3 become larger. Choice of PERCNT=0 will produce the load transfer of a system with no torque rods.

At this point, some remarks on inter-axle load transfer during braking are in order. Equation 2-49 may be re-written in the following form:

$$\ddot{\theta T} = \frac{N2(AA6) - N3(AA7) + SF2(AA3) - (V2\alpha 2+V3\alpha 3)(AA4)}{MS2(AA6)^2 + MS3(AA7)^2} \quad (2-62)$$

Consider the case in which the walking beam pin is at the mass center of the axle assembly, AA3=0. Also, at static equilibrium, N2(AA6)=N3(AA7). Since the normal forces are a function of position only, θT remains zero unless the V α terms are non-zero. Thus, there can be no inter-axle load transfer due to braking if the experimentally determined variable P is zero.*

From equation 2-62 it is apparent that the pitching motion of the walking beam assembly is undamped. This will lead to unrealistic bouncing in the presence of excitation from the last two terms on the right-hand side of the equation. However, there is in fact

*In the general case, there is a small effect due to non-zero AA3. The direction of the transfer depends on the sign of AA3 and is not related to what is commonly called axle hop.

energy dissipation in the tires. This energy dissipation or damping is modelled by putting a dashpot between the tire and the road. The damping coefficient CT has been chosen as 2% critical:

$$CT = .04 [(KT) (MS)]^{1/2} \quad (2-63)$$

While this parameter is not an exact representation of the dynamic characteristics of the tire, it is reasonable (see reference 8), and it has the desired effect of limiting continued pitching of the walking beam assembly. Two percent critical damping is quite small dissipation, however, and thus has negligible effects on the overall vehicle motion.

2.3.7 THE FOUR SPRING SUSPENSION. A schematic and a free body diagram of the suspension is shown in Figure 2-21. Note that the geometry of front and rear axles are identical. Nomenclature relevant to the four spring suspension is given in Table 2-3. The analysis given here is for the tandem suspension mounted on the tractor. Analysis of this suspension mounted on a trailer is analogous.

This analysis is based upon four important assumptions:

- (1) For the purposes of calculation of inter-axle load transfer, the leaves are considered rigid links. They will, however be considered as springs in the sprung mass pitch and bounce calculations.
- (2) The slight shift of spring and axle positions due to the rotation of the load leveler and horizontal movement of the spring frame contact points is neglected.
- (3) Only vertical forces exist at the contact points characterized by TN1, TN2, TN3, and TN4.
- (4) The connection between the load leveler and the frame is considered to be a frictionless pin.

TABLE 2-3
Nomenclature for Four Spring Suspension

AA1	Horizontal distance from front leaf - frame contact to axle center
AA2	Horizontal distance from rear leaf - frame contact to axle center
AA4	Horizontal distance from front leaf contact to load leveler "pin"
AA5	Horizontal distance from rear leaf contact to load leveler "pin"
AA6	Vertical distance from axle down to torque rod
AA7	Angle between torque rod and horizontal
AA8	Horizontal distance from axle center forward to torque rod
ARM1	Perpendicular distance from torque rod to axle center (computed)
ARM2	Horizontal distance from TN1 to sprung mass cm (computed)
ARM3	Horizontal distance from TN4 to sprung mass cm (computed)

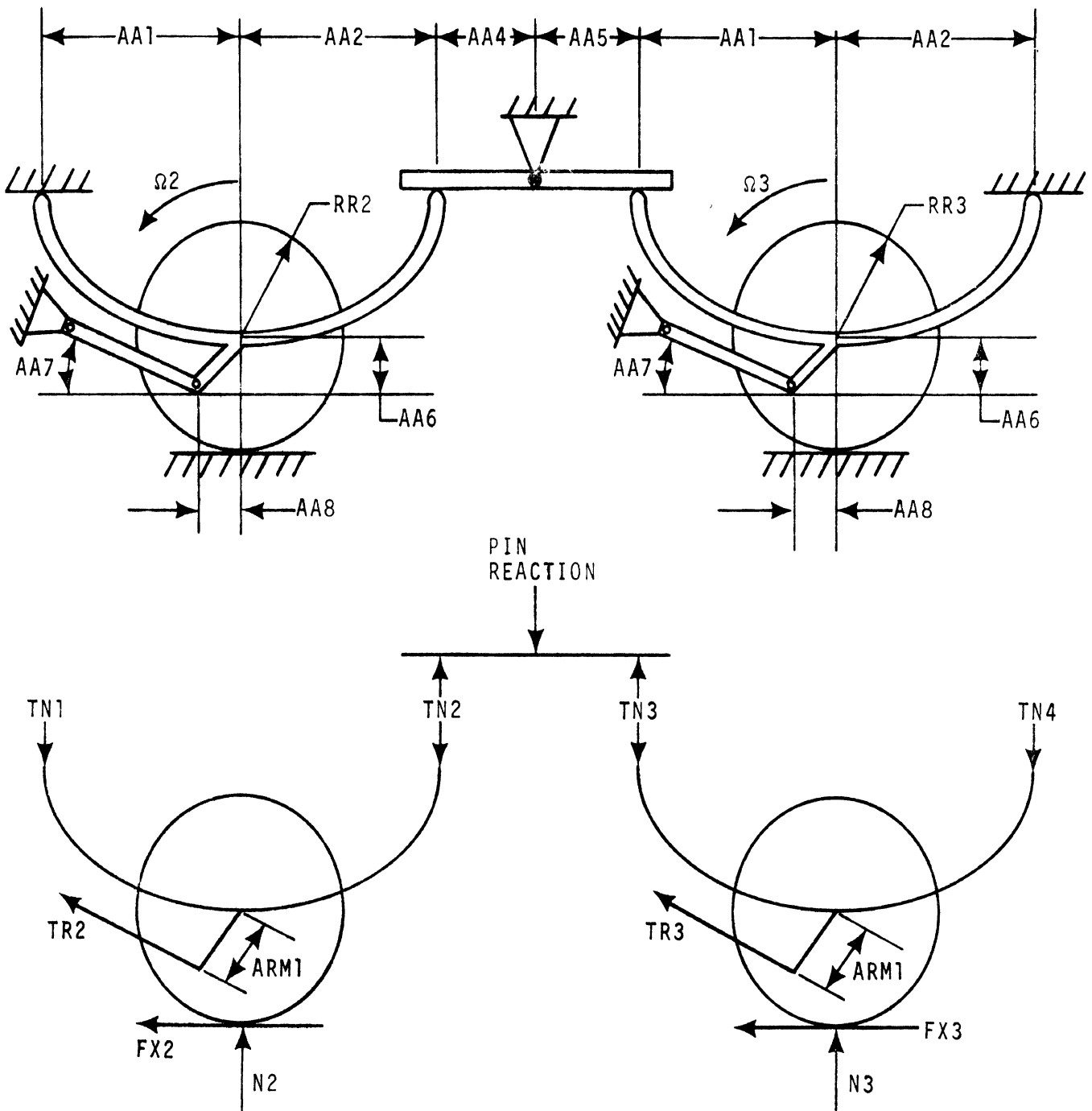


Figure 2-21. Free body diagram: four spring suspension

These simplifying assumptions are necessary to allow generation of a tractable set of equations which describe fairly accurately the dynamics of the suspension. The assumptions apparently result in the prediction of somewhat more inter-axle load transfer than one might find experimentally.

Applying Newton's second law in the "X" direction to each of the axles in Figure 2-21, yields:

$$TR2 \cos AA7 = MS2(\ddot{X}) - FX2 \quad (2-64)$$

$$TR3 \cos AA7 = MS3(\ddot{X}) - FX3 \quad (2-65)$$

Summing moments about the axle centers yields:

$$TN1(AA1) - TN2(AA2) = JS2(\dot{\Omega}2) + TR2(ARM1) + FX2(RR2) \quad (2-66)$$

$$TN3(AA1) - TN4(AA2) = JS3(\dot{\Omega}3) + TR3(ARM1) + FX3(RR3) \quad (2-67)$$

And from the load leveler we get:

$$TN2(AA4) - TN3(AA5) = 0 \quad (2-68)$$

The torque rod forces can be found from equations 2-64 and 2-65. Equations 2-66, 2-67, and 2-68 supply information about the four contact forces, TN. The fourth equation relates the suspension to the frame. With KK designated as the sum of the spring rates of all four leaf springs and CC the sum of all coulomb friction in the leaves, the following expression is assumed:

$$TN1 + TN2 + TN3 + TN4 = -KK(\delta) - CC + \text{Static Load} \quad (2-69)$$

where δ is the vertical displacement of the midpoint between the axle centers. The use of an average spring deflection to calculate forces transmitted to the frame is somewhat arbitrary.* This technique is useful, however, for calculating the effect of the load transfer from the tandem axles onto the truck front axle during braking. Note that, in contrast to what may be observed in practice, the mathematical model will allow an asymmetric vibration mode (such as brake hop) independent of the coulomb friction. As a remedy to this problem, CT has been chosen to be 10% critical damping.

$$CT = .2 [KS \cdot MS]^{1/2} \quad (2-70)$$

An appropriate sketch is shown in Figure 2-22.

A free body diagram of the wheels is shown in Figure 2-23. The equations of vertical wheel motion are:

$$-TR2 \sin(AA7) + TN1 + TN2 - N2 = MS2(\dot{Z}\dot{S}2) \quad (2-71)$$

$$-TR3 \sin(AA7) + TN3 + TN4 - N3 = MS3(\dot{Z}\dot{S}3) \quad (2-72)$$

Lastly, the sprung mass pitch dynamics are considered, using the free body diagram of the sprung mass given in Figure 2-24. The pitch moment equation is

$$J\ddot{\theta} = F1 \cdot A1 - TN1(ARM2-AA1) - TN2(ARM2+AA2) - TN3(ARM3-AA1) - TN4(ARM3+AA2) - TT1 - L1 \cdot S1 - TR2 \cdot DT2 - TR3 \cdot DT3 \quad (2-73)$$

*Note that use of the non-linear deflection-force characteristic for the four spring suspension model is not justified due to this assumption.

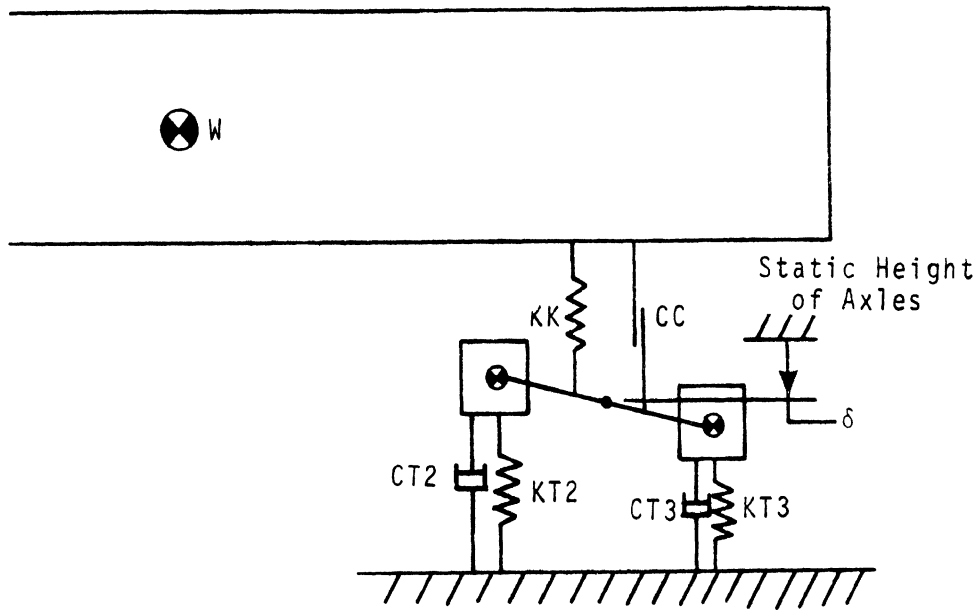


Figure 2-22. Four spring suspension model

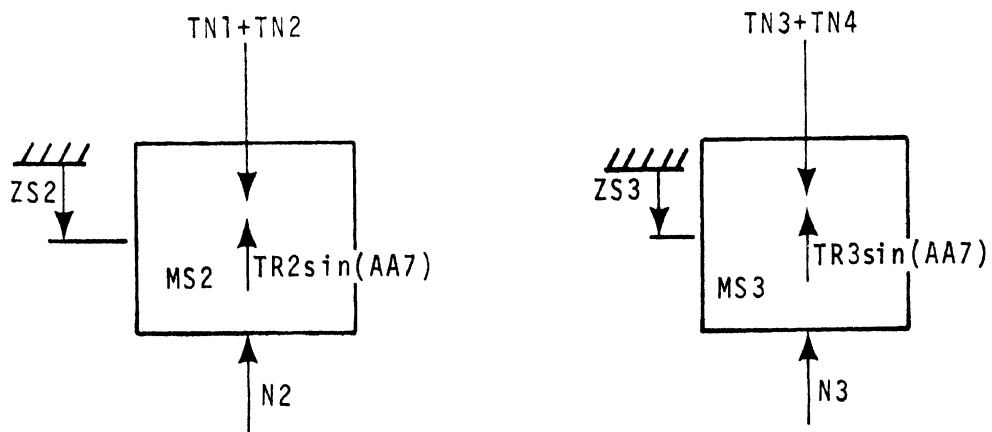


Figure 2-23. Free body diagram: unsprung masses of the four spring suspension model

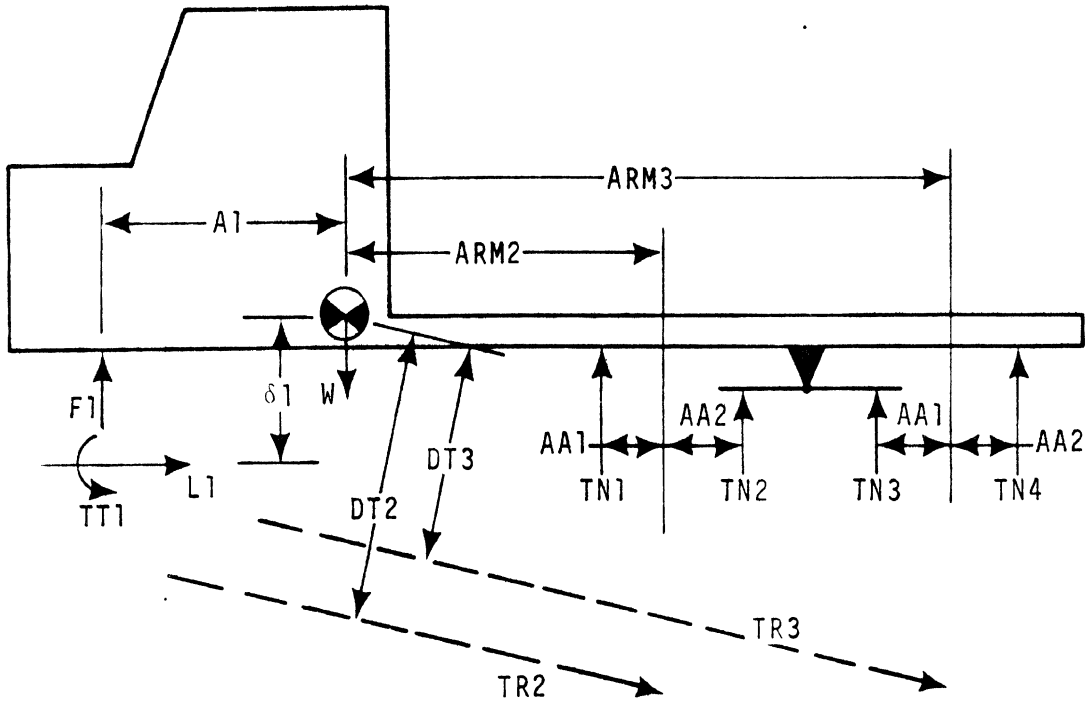


Figure 2-24. Free body diagram: frame with four spring suspension

The moments from the torque rods may be written:

$$TR2(DT2) = -TR2[\sin(AA7) \cdot ARM2 - \cos(AA7) \cdot \delta 2 - ARM1] \quad (2-74a)$$

$$TR3(DT3) = -TR3[\sin(AA7) \cdot ARM2 - \cos(AA7) \cdot \delta 2 - ARM1] \quad (2-74b)$$

Therefore, equation 2-73 may be written:

$$\begin{aligned} J\ddot{\theta} = & F1 \cdot A1 - TN1(ARM2-AA1) - TN2(ARM2+AA2) - TN3(ARM3-AA1) \\ & - TN4(ARM3+AA2) - TT1 - L1 \cdot \delta 1 - (\cos AA7) \cdot \delta 2 + ARM1 (TR2+TR3) \\ & + \sin(AA7) \cdot (ARM2 \cdot TR2 + ARM3 \cdot TR3) \end{aligned} \quad (2-75)$$

2.4 THE TIRE MODEL

The tire model used in this program is adapted from a more general model developed for use in a previous study. In this model, the tire-road shear force is generated on the basis of equations which approximately describe the deformation field over the tire-road contact patch. The location of the point on the tire carcass associated with the point in the contact patch where sliding starts in a braking maneuver is evaluated as a function of longitudinal slip between the tire and the road, vertical load, and sliding velocity. A thorough

discussion of these equations, including comparisons of predicted tire force data to experimental data have been reported in reference 9. The tire parameters needed for the model (which in this program considers longitudinal and rotational motion of the tire only) are CS, the rate of change of brake force with slip at zero slip, μ , the low speed locked wheel friction coefficient, and FA, the friction reduction parameter.

Since the tire model uses wheel rotational velocity to calculate tire longitudinal slip, wheel rotational dynamics are discussed before defining the equations for the tire model.

2.4.1. WHEEL ROTATIONAL DYNAMICS. Figure 2-25 is a free body diagram of a typical wheel.

The wheel rotational equation of motion is

$$J_S(\dot{\Omega}) = -TT - FX(RR) \quad (2-76)$$

where

- FX is the longitudinal force at the tire-road interface
- JS is the polar moment of inertia
- N is the normal force at the tire-road interface
- RR is the effective tire radius
- TT is the applied brake torque
- XDOT is the vehicle velocity
- XDD is the vehicle acceleration
- $\dot{\Omega}$ is the wheel angular acceleration

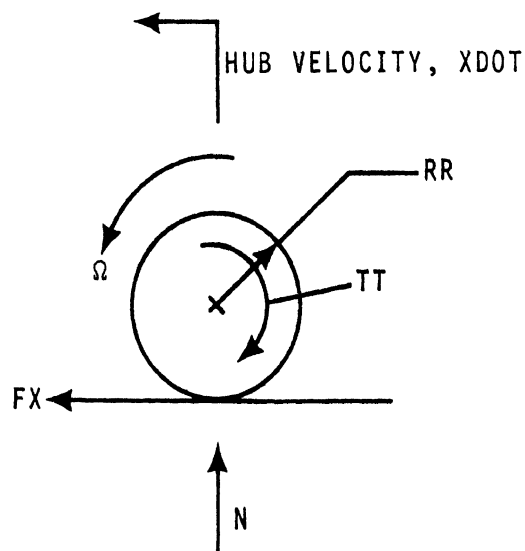


Figure 2-25. Free body diagram: wheel with braking

Wheel slip SLIP is defined as

$$SLIP = 1 - \frac{(RR)\Omega}{XDOT} \quad (2-77)$$

which when combined with Equation 2-76 yields:

$$\frac{d}{dt} (SLIP) = \frac{-RR}{XDOT \cdot JS} [-TT - FX(RR)] + XDD \frac{(1-SLIP)}{XDOT} \quad (2-78)$$

Let SZERO be the value of SLIP at $t=t_0$ for a μ -slip curve in the form shown in Figure 2-26, $FX = -\mu N$. At $SLIP = SZERO$,

$$FX = MULOCAL(N) \quad (2-79)$$

Expanding the μ -slip relationship in a Taylor series about $SLIP = SZERO$,

$$\mu = MULOCAL + \frac{\partial \mu}{\partial (SLIP)} (SLIP - SZERO) + \text{higher order terms} \quad (2-80)$$

Neglecting the higher order terms, FX may be written

$$FX = \bar{\eta} + \bar{\beta} (SLIP) \quad (2-81)$$

where

$$\bar{\eta} = -N[MULOCAL - \frac{\partial \mu}{\partial S} (SZERO)] \quad (2-82)$$

$$\bar{\beta} = \frac{\partial \mu}{\partial (SLIP)} (N) \quad (2-83)$$

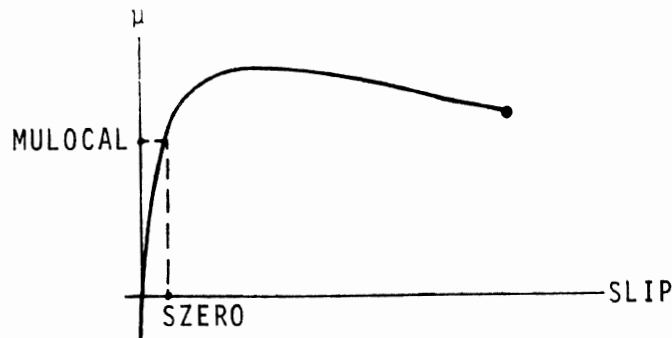


Figure 2-26. A typical μ -slip curve for tire/road interface.

Combining equations 2-82, 2-83, and 2-78 yields

$$\frac{d}{dt}(\text{SLIP}) + Q(\text{SLIP}) = F \quad (2-84)$$

where

$$\eta = -\text{TT}/\text{JS} \quad (2-85)$$

$$\beta = -\text{RR}/\text{JS} \quad (2-86)$$

$$F = \frac{-\text{RR}}{\text{XDOT}} (\eta + \beta\bar{\eta}) + \frac{\text{XDD}}{\text{XDOT}} \quad (2-87)$$

$$Q = \frac{\text{RR}}{\text{XDOT}} \beta\bar{\beta} + \frac{\text{XDD}}{\text{XDOT}} \quad (2-88)$$

The solution to equation 2-84 is

$$\text{SLIP} = (\text{SZERO} - \frac{F}{Q})e^{-Q(t-t_0)} + F/Q \quad (2-89)$$

In the program, slip is constrained to be in the range

$$0 \leq \text{SLIP} \leq 1 \quad (2-90)$$

where $\text{SLIP} = 1$ indicates a locked wheel. In the locked wheel case, the actual torque is the product of the brake force F_x and the rolling radius RR . In calculating the torque, the attempted torque input is designated by T , the actual torque applied by TT .

Thus, for $\text{SLIP} < 1$

$$\text{TT} = T \quad (2-91)$$

and for $\text{SLIP} = 1$

$$\text{TT} = -F_x(\text{RR}) \text{ for } T > -F_x(\text{RR}) \quad (2-92)$$

or

$$\text{TT} = T \text{ for } T \leq -F_x\text{RR} \quad (2-93)$$

2.4.2. SHEAR FORCES AT THE TIRE/ROAD INTERFACE. The brake force versus slip equations given in detail in reference 9 are summarized as follows:

$$\text{SLIP} = \frac{1 - \text{RR}(\Omega)}{\text{XDOT}} \quad (2-77)$$

$$F_x = \frac{-\text{CS}(\text{SLIP})}{1 - \text{SLIP}} f(\lambda) \quad (2-94)$$

$$\begin{aligned} f(\lambda) &= (2-\lambda)\lambda \quad \lambda < 1 \text{ (high SLIP)} \\ &= 1 \quad \lambda > 1 \text{ (low SLIP)} \end{aligned} \quad (2-95)$$

$$\lambda = \frac{-\text{MUZERO} (N) (1 - \text{FA} \cdot \text{XDOT} \cdot \text{SLIP}) (1 - \text{SLIP})}{2\text{CS}(\text{SLIP})} \quad (2-96)$$

where

CS is longitudinal stiffness, in pounds

FA is the friction reduction parameter, in sec/ft

MUZERO is the low speed friction coefficient.

These parameters are calculated using results from tire tests. CS for a wide variety of truck tires and load conditions is given in Table 4-4. Since very little experimental data exists from which FA and MUZERO can be determined, it is suggested that these parameters be determined heuristically. Two methods are suggested in Appendix E. Some μ -slip curves generated by using the tire model are shown in Figure 2-27.

2.4.3 NORMAL FORCES AT THE TIRE/ROAD INTERFACE. The vertical force on the tire from the road through the contact patch is a function of the static load, the tire spring rate, and viscous damping in the tire. Values for the rolling spring rates of various truck tires, as determined from experiment, are given in Table 4-3. Although no similar data is available on values for truck tire viscous damping coefficients, it is reasonable to assume (for example, see references 8 and 10) that the tire damping coefficient is of the order of 2% critical.

2.4.4 ROUGH ROAD SIMULATION. Road profile data in functional or coordinate form may be introduced into the programs. It was noted above that a linear vertical spring rate at the tire-road interface is assumed. Since there is no provision in this program to model the enveloping characteristics of the tire, use of short wave length "bumps" should be avoided.

2.5 BRAKES AND BRAKE SYSTEMS

In the preceding section, we have considered the effect of the application of brake torque to the wheels. This section is concerned with the calculation of that torque.

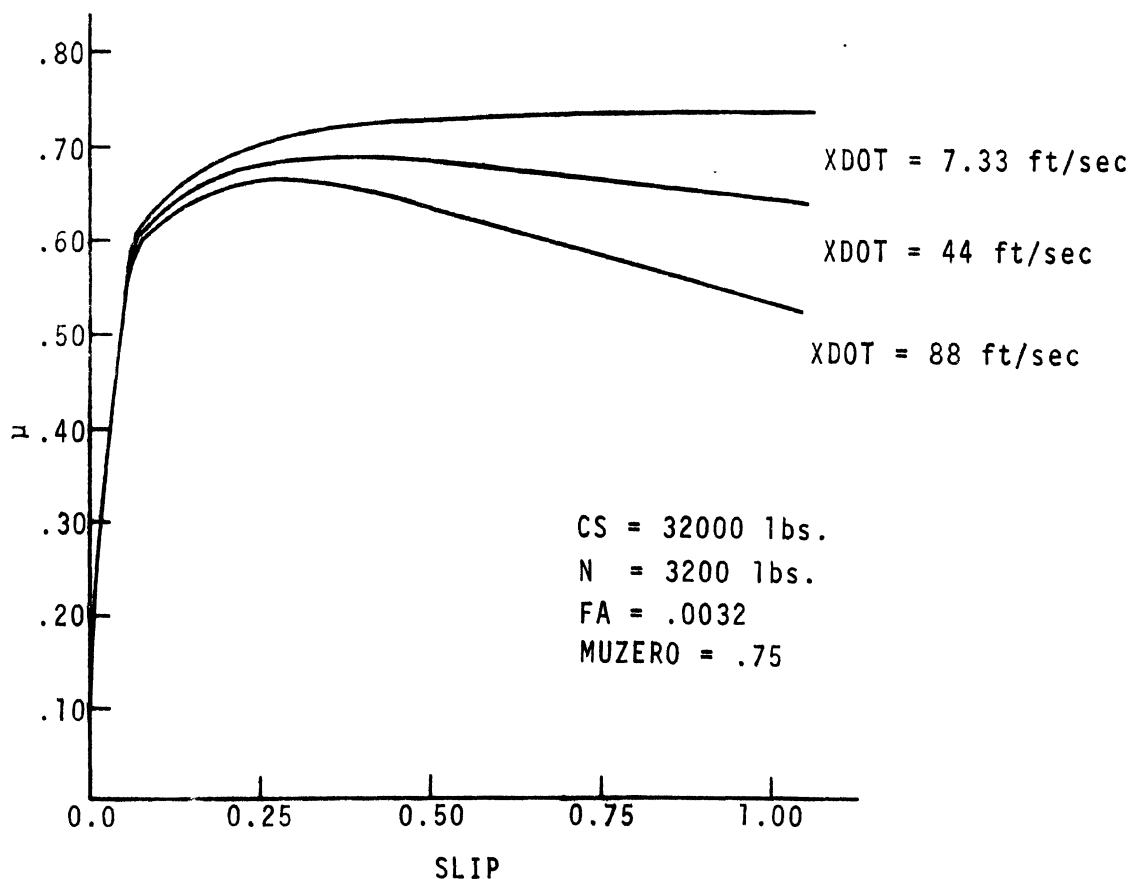


Figure 2-27. μ -slip curves generated using the tire model

2.5.1 DELAYS AND LAGS IN BRAKE SYSTEM RESPONSE. In this program, the response of the brake system to control inputs applied at the treadle valve is characterized by two parameters (per axle): the time delay, and the rise time. The time delay is defined as the time elapsed from the instant that the pressure starts to rise at the output of the treadle valve to the instant that pressure starts to rise in a given brake actuator. For the purposes of this program, rise time of the brake is defined as the time elapsed from the instant that pressure starts to increase in the brake chamber to the instant that the pressure reaches 63% of the commanded value, as a result of a step application of pressure at the treadle valve. The simulated pressure response at any given axle is given by the equation

$$\frac{dP(I)}{d\bar{t}} + \frac{(P-P(I))}{TQ(I,2)} = 0 \quad (2-97)$$

where

P is the treadle valve pressure at time t

P(I) is the pressure at the Ith axle

$$\bar{t} = t - TQ(I,1) \quad (2-98)$$

TQ(I,1) is the time delay

TQ(I,2) is the rise time.

Equation 2-97 can be solved for a step application of treadle pressure P_0 at time t_0 . The pressure response at the Ith axle is

$$P(I) = 0, \bar{t} \leq 0 \quad (2-99)$$

$$P(I) = P_0 (1 - \exp(-\frac{t-\bar{t}}{TQ(I,2)})), \bar{t} > 0 \quad (2-100)$$

where

$$\bar{t} = t - t_0 - TQ(I,1) \quad (2-101)$$

The response at the Ith axle to a step pressure at the treadle valve is delayed by time delay TQ(I,1). The pressure will then rise toward P_0 , reaching $.63P_0$ approximately TQ(I,1) + TQ(I,2) seconds after the step application at the treadle valve. Thus, the time delay is TQ(I,1), and the rise time is characterized by TQ(I,2).

In general, the pressure at the treadle valve varies with time. Thus, provision is made in the program for the user to specify a table of values for pressure versus time. An explanation of the use of the table and the appropriate differential equation is given below:

- (a) For the time step beginning at t_0 , the line pressure at the Ith wheel is P(I).
- (b) Perform the integration for the time step from t_0 to $t_0 + \Delta t$.
- (c) Set $POLD(I) = P(I)$.

(d) Look up treadle valve pressure P in Table 1 at time $t_0 + \Delta t - TQ(I,1)$.*

$$(e) P(I) = [POLD(I) - P] \exp\left(\frac{-\Delta t}{TQ(I,2)}\right) + P$$

An example is given for illustration. Typical brake pressure response curves are given in Figure 2-28. The curves calculated using steps (b) through (e) above are given in Figure 2-29. The time pressure points used to produce the treadle valve curve in Figure 2-29 were:

<u>Time, sec</u>	<u>Pressure, psi</u>
0.0	0
0.1	100

The brake time response parameters used were:

$$TQ(1,1) = TQ(2,1) = 0$$

$$TQ(3,1) = 0.15$$

$$TQ(1,2) = TQ(2,2) = TQ(3,2) = 0.23$$

2.5.2 CALCULATION OF BRAKE TORQUE. Brake torque may be generated by means of torque-line pressure curves, such as would be obtained from a brake dynamometer, or by means of brake modules in which detailed design parameters for the brakes on each axle must be specified.

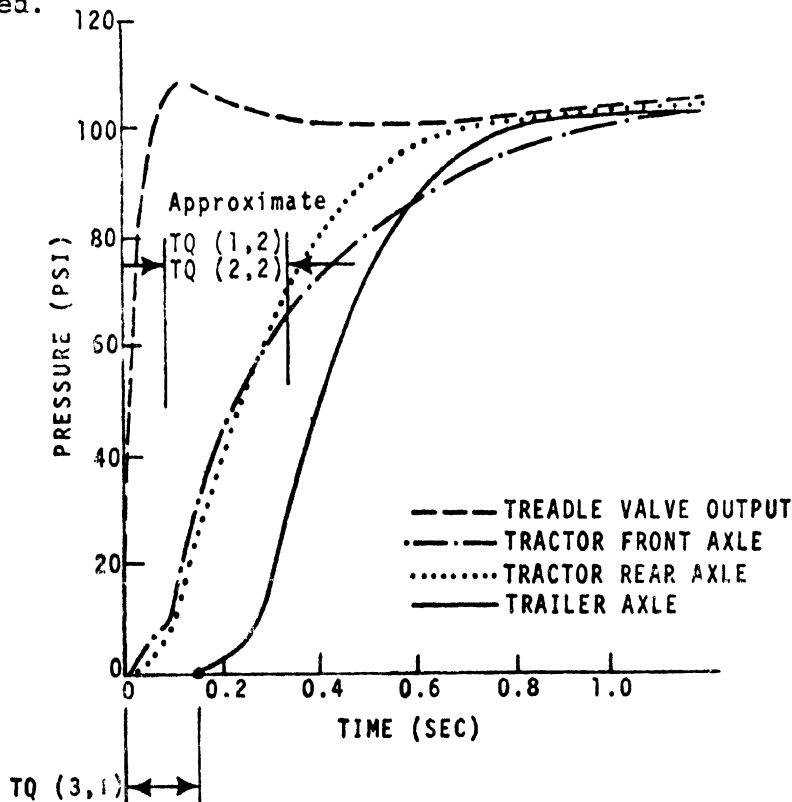


Figure 2-28. Typical empirical brake pressure application response curves

* $P(I)$ is found by linear interpolation of the user input pressure-time points.

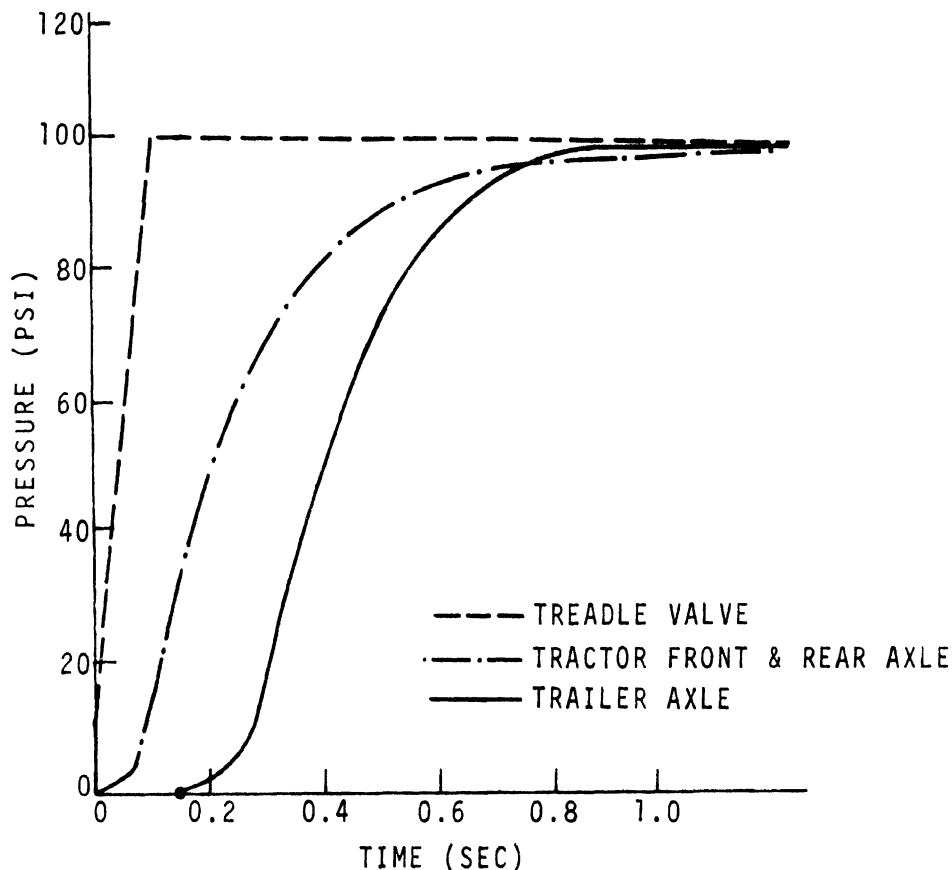


Figure 2-29. Simulated brake pressure application response curves

If dynamometer curves are used, one table of values of line pressure versus torque must be supplied for each axle. Then, in the course of the integration process during the simulation, a linear interpolation is made to produce the value of brake torque for the given instantaneous value of brake line pressure at each axle.

If, on the other hand, brake modules are specified, the brake torque is calculated using the brake system parameters specified by the user. Brakes must be specified on an axle by axle basis. Options include: no brakes, S-cam, dual or single wedge, duo-servo self-actuating, duplex, and disc. The brake torque produced at each axle is calculated by means of the following equation [11]:*

$$T(I) = PB(I) \cdot Q(I) \cdot BF(I) \quad (2-102)$$

where

- T(I) is the attempted brake torque on the Ith axle
- PB(I) is the effective line pressure at the brake minus the pushout pressure
- Q(I) is the brake system constant
- BF(I) is the brake factor, defined as the ratio of drum drag to the actuating force of the brake shoes [5].

*Numbers in brackets designate references.

For hydraulic brake systems,

$$Q(I) \triangleq 2A_{wc} \cdot \eta_c \cdot r \quad (2-103)$$

where

A_{wc} = area of wheel cylinder
 η_c = mechanical efficiency of the brake
 r = drum radius

For air brakes,

$$Q(I) \triangleq 2A_c \cdot \eta_m \cdot BF \cdot r \cdot \rho \quad (2-104)$$

where

A_c = brake chamber area
 η_m = mechanical efficiency between brake chamber and shoe actuation
 ρ = lever ratio between brake chamber and brake shoe.

For S-cam brakes, the lever ratio is given by

$$\rho = \frac{l_s}{2l_c} \quad (2-105)$$

where

l_s = effective slack adjuster length
 l_c = effective cam radius.

For wedge brakes, the lever ratio is related to the wedge angle, α :

$$\rho = \frac{1}{2\tan(\alpha/2)} \quad (2-106)$$

If the brakes are in good mechanical condition, the mechanical efficiencies exhibited by S-cam and wedge brakes range from 0.70 to 0.75 and 0.80 to 0.88, respectively [13].

The value of the brake factor for the various types of drum and disc brakes required in equation 2-102 is calculated by means of analytical expressions in which brake factor is given as a function of brake type, brake geometry, and the coefficient of friction between the lining and the drum or disc. Brake factor - lining friction coefficient relationships for three commonly used brake types are given in Figure 2-30 [11].

2.5.3. BRAKE FACTOR CALCULATIONS. This section contains a description of the brake factor calculations for the several types of brakes used in the program [12,14]. Except for disc brakes and dual servo self actuating brakes, the calculations are made for each shoe, and the total brake factor is the sum of the brake factors calculated for each shoe. The three types of brake shoes available in the program are: a pinned leading shoe, a pinned trailing shoe, or a leading

shoe supported by an abutment. The following three equations are used for calculation of brake factors for these individual shoes:

Pinned Leading Shoe (see Figure 2-31)

$$BF = \frac{\mu \cdot D}{E - \mu \cdot G} \tag{2-107}$$

where

$$D = HB/RD$$

$$ALPH3 = ALPH0 + 2.0 \cdot ALPH1$$

$$E = \frac{APRIM}{RD} \left[\frac{ALPH0 - \sin(ALPH0) \cdot \cos(ALPH3)}{4.0 \cdot \sin(ALPH0/2) \cdot \sin(ALPH3/2)} \right]$$

$$G = 1 + \frac{APRIM}{RD} \cdot \cos(ALPH0/2) \cdot \cos(ALPH3/2)$$

μ = coefficient of friction of the linings

and all other angles and dimensions are as shown in Figure 2-31.

Pinned Trailing Shoe (see Figure 2-32) The expression for the brake factor for the pinned trailing shoe is the same as Equation 2-107 except for a sign change in the denominator:

$$BF = \frac{\mu \cdot D}{E + \mu \cdot G} \tag{2-108}$$

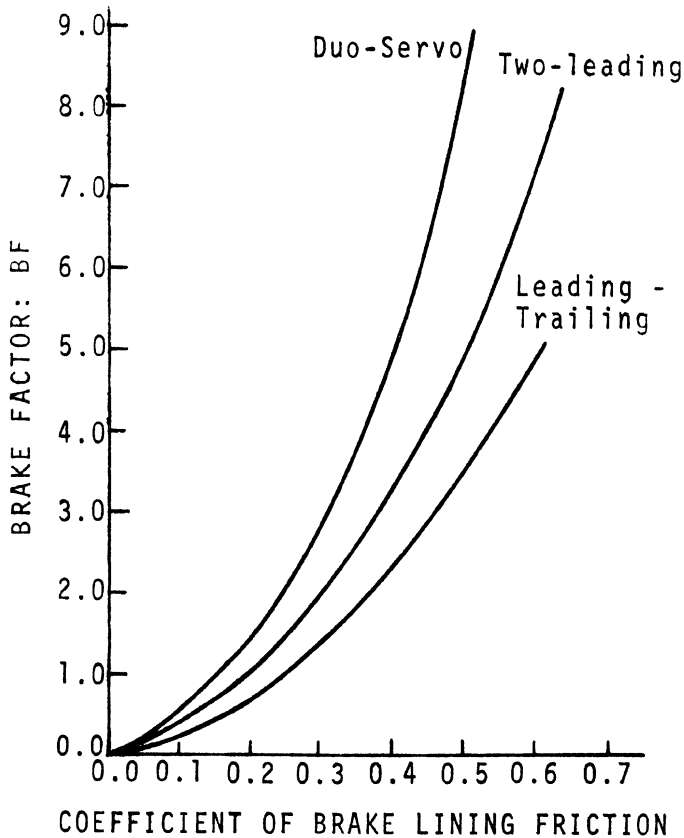


Figure 2-30. Typical brake factor-lining friction curves for typical drum brakes

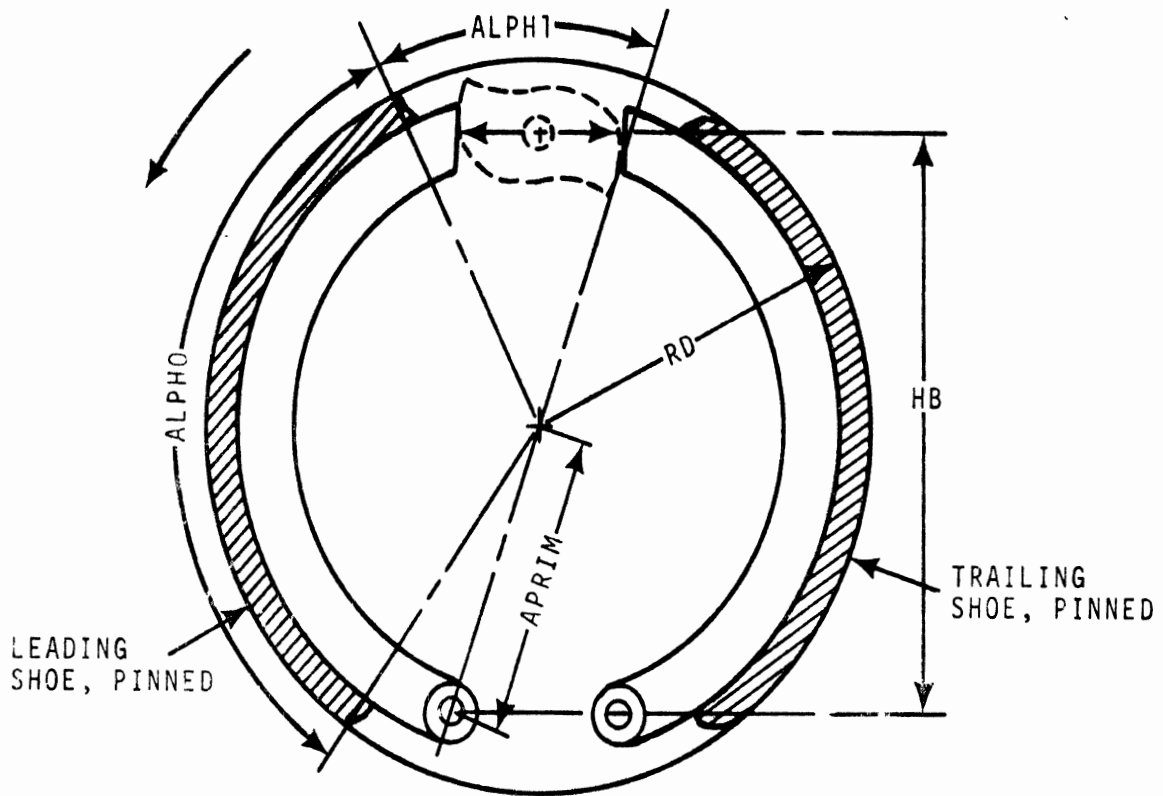


Figure 2-31. Leading shoe-trailing shoe brake

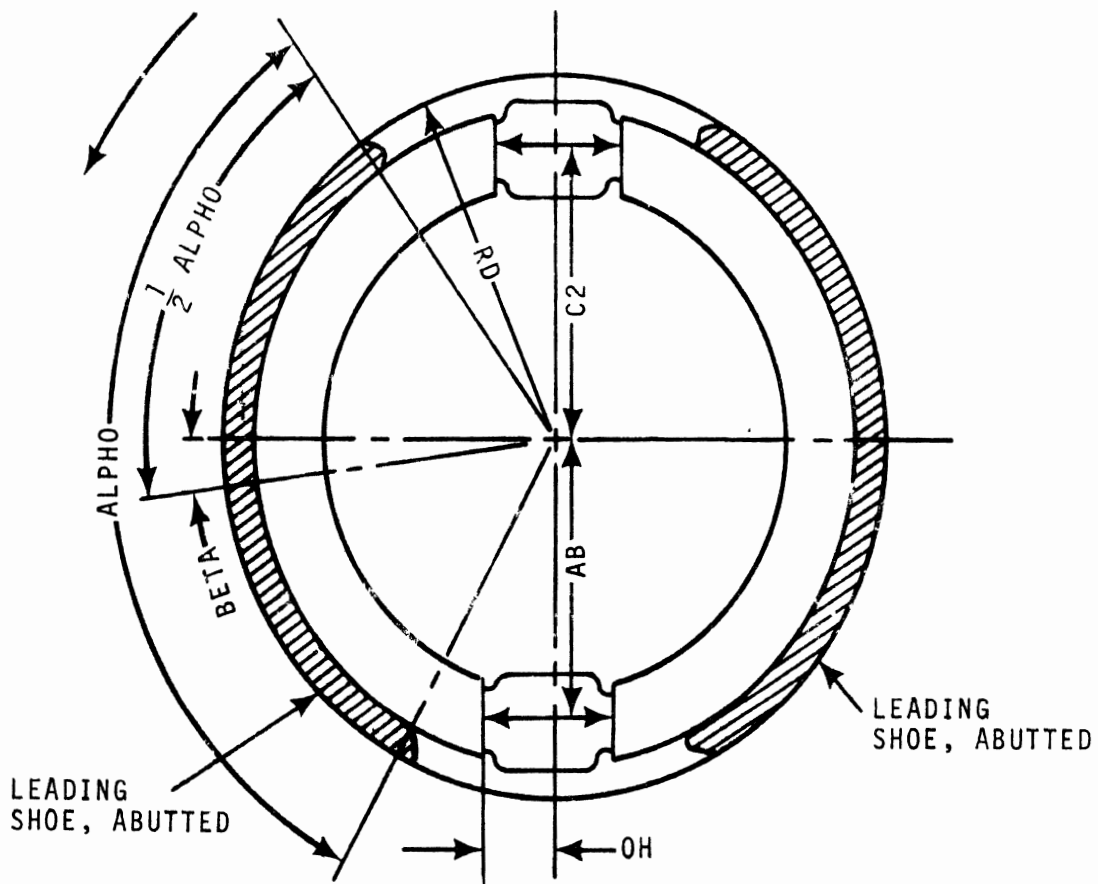


Figure 2-32. Two leading shoe brake

Leading Shoe Supported by an Abutment

$$BF = \frac{\mu \cdot D + \mu^2 \cdot E}{F2 - \mu G + \mu^2 H2} \quad (2-109)$$

where in this case:

$$D = \left[\frac{C2}{RD} + \frac{AB}{RD} + 0.25 \frac{OH}{RD} \right] \cdot \cos(\text{BETA}) + 0.25 \cdot \frac{C2}{RD} \cdot \sin(\text{BETA})$$

$$E = 0.25 \cdot \frac{C2}{RD} \cdot \cos(\text{BETA}) - \left[\frac{C2}{RD} + \frac{AB}{RD} + 0.25 \cdot \frac{OH}{RD} \right] \cdot \sin(\text{BETA})$$

$$MM = \frac{\text{ALPHO} + \sin(\text{ALPHO})}{4.0 \cdot \sin(\text{ALPHO}/2)}$$

$$F2 = MM \left[\frac{AB}{RD} + 0.25 \frac{OH}{RD} \right]$$

$$G = \cos(\text{BETA}) + 0.25 \cdot \sin(\text{BETA})$$

$$H2 = MM \left[\frac{AB}{RD} + 0.25 \frac{OH}{RD} \right] - (0.25 \cos(\text{BETA}) - \sin(\text{BETA}))$$

Angles and dimensions are as shown in Figure 2-32.

The equations used in the program to calculate the brake factors are (with the exception of disc brakes) combinations of the above three equations.

For S-cam brakes, the program sums the brake factors calculated for the leading and trailing shoes using:

$$BF = \frac{\mu \cdot D}{E - \mu \cdot G} + \frac{\mu \cdot D}{E + \mu \cdot G} \quad (2-110)$$

where the first term is from equation 2-107 (a pinned, leading shoe) and the second term is from equation 2-108 (a pinned, trailing shoe).

For each of the shoes of a 2-Wedge brake, the program calculates the brake factor using equation 2-109. The brake is assumed to consist of two identical leading shoes whose ends are supported by abutments. Thus the total brake factor is:

$$BF = 2 \left[\frac{\mu \cdot D + \mu^2 \cdot E}{F2 - \mu \cdot G + \mu^2 \cdot H2} \right] \quad (2-111)$$

For a single wedge brake the brake factor is calculated as if the leading and trailing shoes are pinned as in equation 2-110.

For the duo-servo self-actuating brake the program calculates the brake factor for each shoe separately and then combines them to solve for the total brake factor. The primary shoe is considered equivalent to the leading shoe supported by an abutment, whose brake factor can be calculated using equation 2-109.

$$BF1 = \frac{\mu \cdot D + \mu^2 \cdot E}{F2 - \mu \cdot G + \mu^2 \cdot H2} \quad (2-112)$$

The brake factor for the secondary shoe is calculated in two steps. First, the secondary shoe is assumed to be a pinned leading shoe and BF2 is calculated using equation 2-107:

$$BF2 = \frac{\mu \cdot D2}{E2 - \mu \cdot G2} \quad (2-113)$$

Since the brake factor is the drum drag divided by the actuating force on the shoe from the wheel cylinder, the brake factor, BF2 (for the secondary shoe), must be corrected due to the fact that, not only is there the actuating force from the wheel cylinder, but there is also the (tangential) force generated by the friction between the primary shoe and the drum, which adds to the force actuating the secondary shoe. In order to give the brake factor in terms of the actuating force from the wheel cylinder, BF2 must be multiplied by

$$\frac{\text{Actual actuating force on secondary shoe}}{\text{Force from wheel cylinder}} = \left[\frac{C2}{AB} + \frac{BF1 \cdot RD}{AB} \right] \quad (2-114)$$

The brake factor for the whole brake is given as:

$$BF = BF1 + BF2 \left[\frac{C2}{AB} + \frac{BF1 \cdot RD}{AB} \right] \quad (2-115)$$

For a 2-leading shoe brake, the shoes are assumed to be supported by abutments rather than pins and the brake factor is calculated the same as for a 2-Wedge brake using equation 2-111.

The brake factor for a disc brake is:

$$BF = 2 \left[\frac{F_{\text{tangential}}}{F_{\text{wheel cylinder}}} \right] \quad (2-116a)$$

or

$$BF = 2 \left[\frac{\mu \cdot F_{\text{wheel cylinder}}}{F_{\text{wheel cylinder}}} \right] \quad (2-116b)$$

which reduces to

$$BF = 2 \cdot \mu \quad (2-116c)$$

2.5.4 BRAKE FADE. If the value of the lining friction coefficient is held constant in the calculation of brake torque as a function of brake line pressure, the brake factor remains constant, and the line pressure-torque characteristic is a straight line. However, test results indicate that the line pressure-torque relationship may be nonlinear, especially when loaded vehicles are decelerated from higher speeds. This nonlinearity results from variations in brake factor due to changes in the brake lining friction coefficient.

Therefore, the technique described in the following paragraphs was devised to take fade effects into account by proper adjustment of the lining friction coefficient. In addition to the tests conducted for this program, results from an earlier vehicle test program were used to verify the technique [11].

A nonfaded operating design point is established on a brake factor vs. lining coefficient curve by the value for μ (designated as μ_{Lh}) provided by the vehicle or brake manufacturer as shown in Figure 2-33. (Typical values of μ_{Lh} for S-cam or wedge brakes are 0.35 to 0.38 and 0.45 to 0.48, respectively.)

The lining friction coefficient, μ_L , is a function of temperature, sliding velocity, and pressure at the lining-drum interface, i.e., $\mu_L = F(T, V, pd)$. For a series of vehicle tests in which

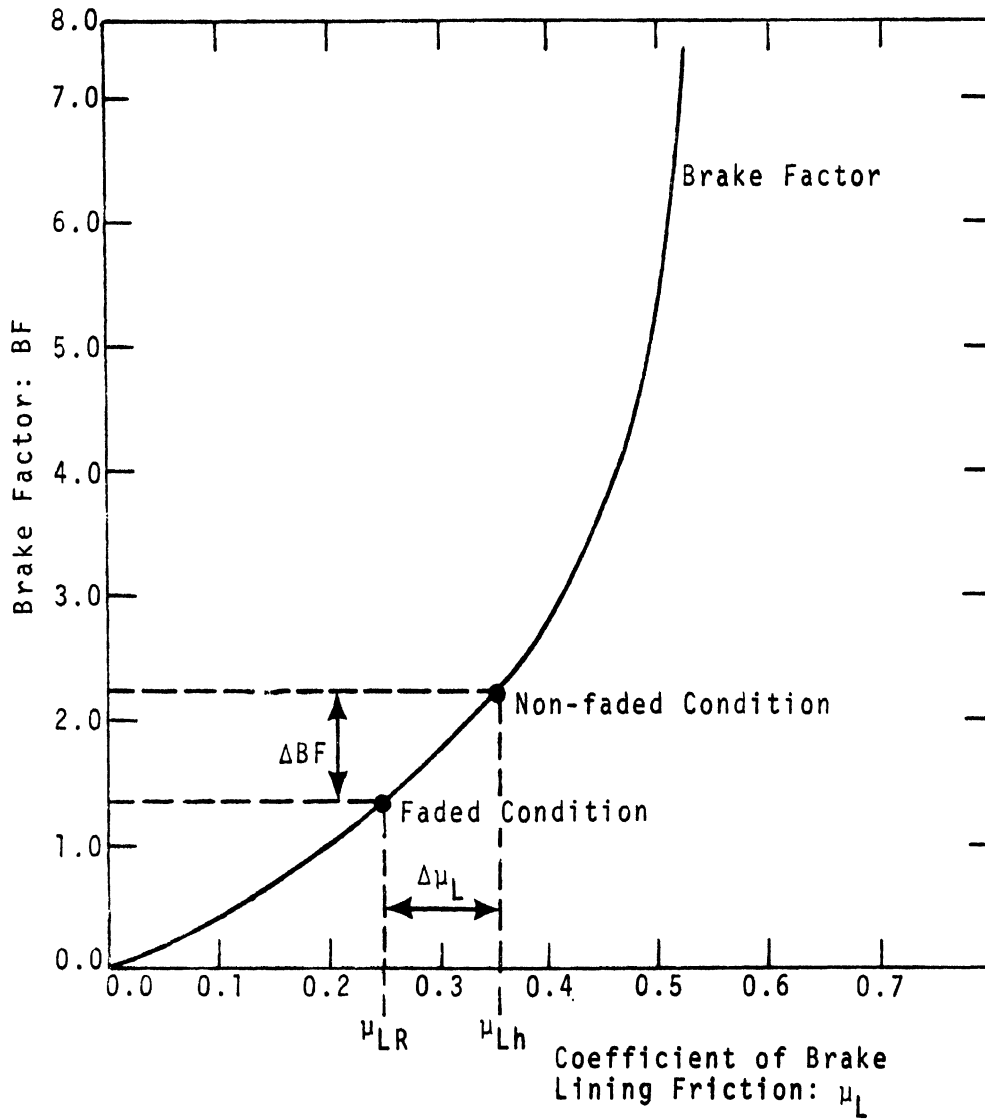


Figure 2-33. Effect of brake fade on brake factor

velocity, ambient temperature, and brake temperatures do not vary considerably from vehicle to vehicle, the lining-drum coefficient of friction may be assumed to be a function of pressure only. This is an extremely significant assumption which bears heavily on the usefulness of the model, but is certainly justified within the limitations specified for its use. A mathematical model was devised in which an exponentially decreasing dependence of the lining friction coefficient upon pressure was assumed, as given by the following expression [11]:

$$\mu_L = \mu_{Ll} + (\mu_{Lh} - \mu_{Ll})e^{-\bar{f}p_m} \quad (2-117)$$

where

μ_{Ll} = lower value of lining friction coefficient

μ_{Lh} = upper value of lining friction coefficient

\bar{f} = a brake fade coefficient

p_m = mean pressure between shoe and drum

Since there is a direct relationship between lining-drum interface pressure and brake chamber pressure, the mean pressure between shoe and drum can be replaced by the line pressure at the individual wheel cylinders or brake chambers with the proper adjustment in the fade coefficient, f . Thus, if line pressure is designated by p , and

$$p_m \cong Kp \quad (2-118a)$$

and

$$f = K\bar{f} \quad (2-118b)$$

equation 2-117 may be written

$$\mu_L = \mu_{Ll} + (\mu_{Lh} - \mu_{Ll})e^{-fp} \quad (2-119)$$

The coefficient f , as well as the lower limit for the lining friction coefficient, μ_{Ll} , are determined from test data and curve fitting procedures. Vehicles with air brake systems yielded fade coefficients f in the range .012 to .0045. Analysis of the experimental data indicates that the maximum reduction in lining friction coefficient could be approximated reasonably well by assuming that

$$\mu_{Ll} = 0.70\mu_{Lh}.$$

Typical parameters required for brake factors and brake effectiveness calculations are shown in Table 2-4.

TABLE 2-4
 Typical Parameters for Brake Factor
 and Brake Effectiveness Calculations

Input Parameter Table for Brake Force Calculation Subroutine

Symbol	Description	Initial Value
FRAY	Brake Fade Coefficient	0.0160
Axle 1		
IBRT(1)	Brake Type	2-Wedge
AC(1)	Brake Chamber Area (Sq In)	12.000
EM(1)	Mechanical Efficiency	0.800
PO(1)	Pushout Pressure (PSI)	7.500
RD(1)	Drum Radius (In)	7.500
ULH(1)	MU Lining, High	0.500
ULL(1)	MU Lining, Low	0.350
AB(1)	Distance from Horizontal Centerline of Drum to Parallel Line Through Shoe Contact Point (In)	5.400
ALPH0(1)	Lining Contact Angle (Deg)	125.000
ALPHW(1)	Wedge Angle (Deg)	12.000
BETA(1)	Lining Offset Angle (Deg)	0.0
C2(1)	Distance from Horizontal Centerline of Drum Parallel Line Through Point of Actuating Force (In)	5.400
OH(1)	Distance from Vertical Centerline of Drum to Parallel Line Through Shoe Contact Point (In)	3.000
Axle 4		
IBRT(4)	Brake Type	S-Cam
AC(4)	Brake Chamber Area (Sq In)	30.000
EM(4)	Mechanical Efficiency	0.700
PO(4)	Pushout Pressure (PSI)	2.500
RD(4)	Drum Radius (In)	8.250
ULH(4)	MU Lining, High	0.350
ULL(4)	MU Lining, Low	0.150
ALPH0(4)	Lining Contact Angle (Deg)	111.000
ALPH3(4)	ALPH0(4) + 2*ALPH1(4) (Deg)	207.000
APRIM(4)	Radial Distance from Center of Drum to Shoe Pin (In)	6.900
HB(4)	Distance from Horizontal Centerline Through Shoe Pin to Parallel Line Through Connector Contact Point (In)	12.600
RC(4)	Cam Radius (In)	0.500
SAL(4)	Slack Adjuster Length (In)	6.000

2.5.5 MECHANICAL ACTUATION OF PARKING BRAKES. In light trucks the parking brakes may be applied to the rear wheels by a mechanical linkage. Therefore it is assumed that the parking brakes described here will be applied to the rear axle. Since the linkage is purely mechanical, no provision is made for simulating time lags. To utilize the parking brake, brake torque versus time points are placed in the appropriate table as explained in Appendix D.

2.5.6 BRAKE TORQUE APPLIED TO THE DRIVE SHAFT. There are a variety of ways in which brake torque may be applied to the drive shaft. The simulation includes:

- a) engine braking
- b) exhaust braking
- c) prop shaft braking
- d) auxiliary retarders.

It is assumed that in all these cases the applied torque depends on engine RPM and on the drive axle design. Thus it is necessary to know what gear the vehicle is in during the course of the braking.

It is assumed that the gear utilized is a function of vehicle speed, and hence the appropriate information must be supplied to the program as explained in Appendix D. Note that the simulated shift in gears is instantaneous--no effort has been made to model a time lag to change gears.

It is assumed that drive shaft rotation rate is equal to the product of the wheel rotation rate and a gear ratio. Thus the user must input a table of gear ratios for each gear selected as explained in Appendix D. Engine RPM is then calculated from the wheel rotation rate and the gear ratio.

Lastly, a table of engine RPM versus applied brake torque must be input. This torque will be applied to axle 2, in the case of a single rear axle, or divided between axles 2 and 3, in case of tractor tandem axles, with a given percentage of the torque (denoted by EBPER) being applied to the front tandem axle.

A short diagram of the procedure is given in Figure 2-34.

2.5.7 USE OF PROPORTIONING VALVES. The assumed input-output relationship for a brake proportioning valve is given in Figure 2-35.

The slope of the line used to characterize the proportioning at axle I is calculated on the basis of two parameters supplied by the user.

- (1) EMPTY (I), the slope of the proportioning valve input-output characteristic specified for the empty vehicle.
- (2) MAXAX (I), the maximum expected axle load on axle I.

The load on a given axle of an empty vehicle can be calculated from the input parameters WS, W, and W1*. For the loaded vehicle, the load on the axle can be calculated from WP and the empty weights WS, W, and W1. For purposes of illustrating the calculation procedure, the loads on the axle for the empty and laden case are designated LOAD1 and LOAD2, respectively. The slope of the input-output characteristic of the proportioning valve used at axle I in the simulation is

$$\text{SLOPE (I)} = \frac{\text{LOAD2 (I)} - \text{LOAD1 (I)}}{\text{MAXAX (I)} - \text{LOAD1 (I)}} (1.0 - \text{EMPTY (I)}) + \text{EMPTY (I)}; \text{LOAD2 (I)} \leq \text{MAXAX (I)} \quad (2-120)$$

$$\text{SLOPE (I)} = 1.0, \text{LOAD2 (I)} > \text{MAXAX (I)} \quad (2-121)$$

*We are assuming an articulated vehicle here. The same logic applies to the straight truck where W1=0.

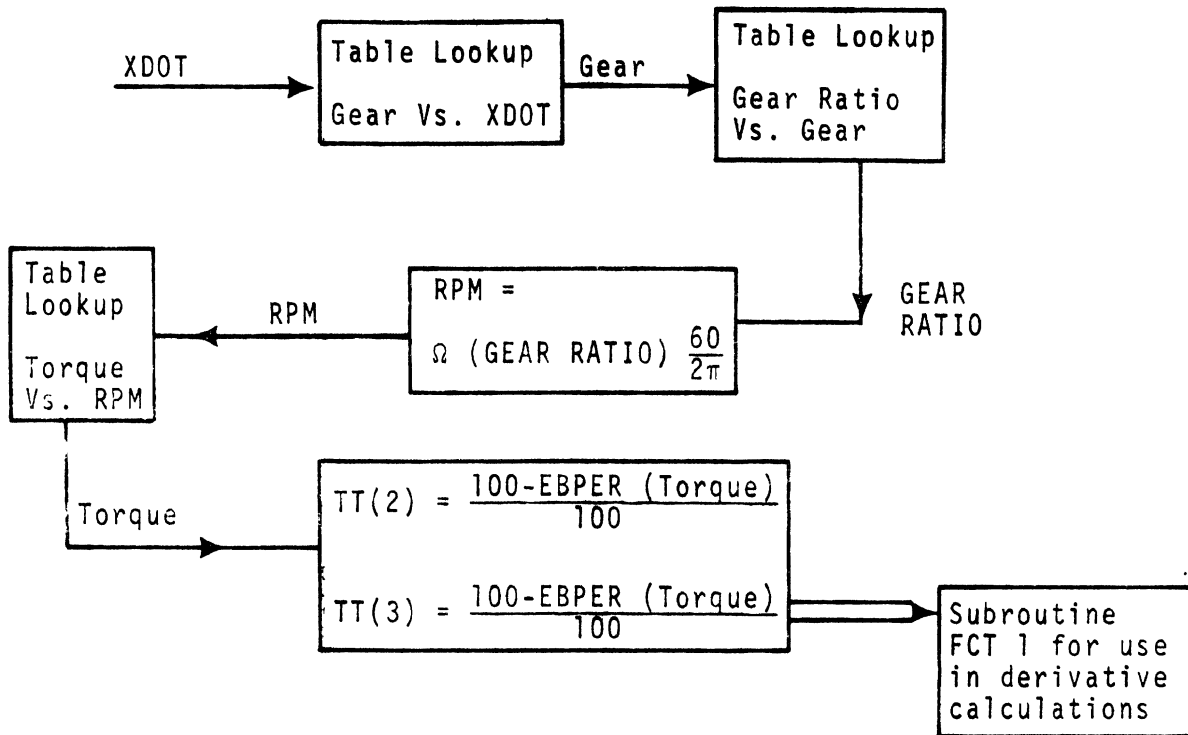


Figure 2-34. Procedure for determination of engine rate sensitive brake torque

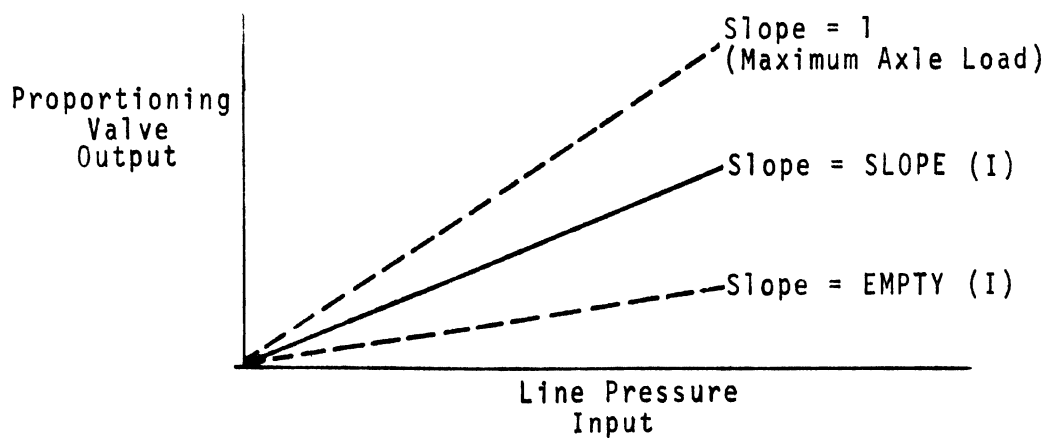


Figure 2-35. Proportioning valve input/output pressure characteristic

Note that SLOPE (I) is linearly interpolated between EMPTY (I) and 1.0 based on the axle load. If the axle load is above the rated load MAXAX (I), SLOPE (I) takes on its maximum allowable value, namely, 1.0. If the line pressure called for at axle I without proportioning, is P(I), with proportioning it is P(I)·SLOPE(I). This pressure is then used with pressure-torque curves determined from either the dynamometer table lookup or the brake modules to specify brake torque.

2.5.8 SPRING ACTUATION OF FOUNDATION BRAKES. On many large trucks, parking and emergency braking are accomplished by the actuation of the foundation brakes on one or more axles through the action of a preloaded, mechanical spring. In the simulation, this process is modeled through the use of the following parameters:

ONTIME	The time at which brake application is initiated.
TMAX(I)	The maximum torque to be applied at axle I (I=2, KAXLE)*.
RISET	The number of seconds after ONTIME until the applied torque at axle I reaches 0.63 TMAX(I).

Thus,

$$T(I) = 0, \quad t \leq \text{ONTIME} \quad (2-122a)$$

$$T(I) = TMAX(I) (1 - \exp(-t/\text{RISET})) \quad (2-122b)$$

2.5.9 ANTILOCK SYSTEM SIMULATION - A SUGGESTED APPROACH. In this section a brief outline of the steps necessary to add a wheel antilock system to the simulation is given.

It is assumed that the antilock system reduces the line pressure based on its measurement of certain variables, which typically might be circumferential slip, vehicle speed, wheel rotation rate, derivative of the wheel rotation rate, and vehicle linear acceleration. Analytical expressions describing the antilock system using these variables should be inserted just below the TORQUE entry of subroutine OUTPUT.

The following variables are in the OUTPUT common block, and may be utilized in this subroutine:

SLIP (I)	- longitudinal slip of the wheels on the Ith axle
OMEGAD (I)	- wheel acceleration
XDOT	- vehicle velocity
XDD	- vehicle acceleration.

Individual wheel rotation rate can be calculated using the following expression:

$$\text{OMEGA} = \text{XDOT} * \text{SLIP}(I) \quad (2-123)$$

An illustration is given to explain the programming technique. Consider a system in which line pressure at wheel I will be set to zero for .01 seconds if the circumferential slip at axle I exceeds .5. In

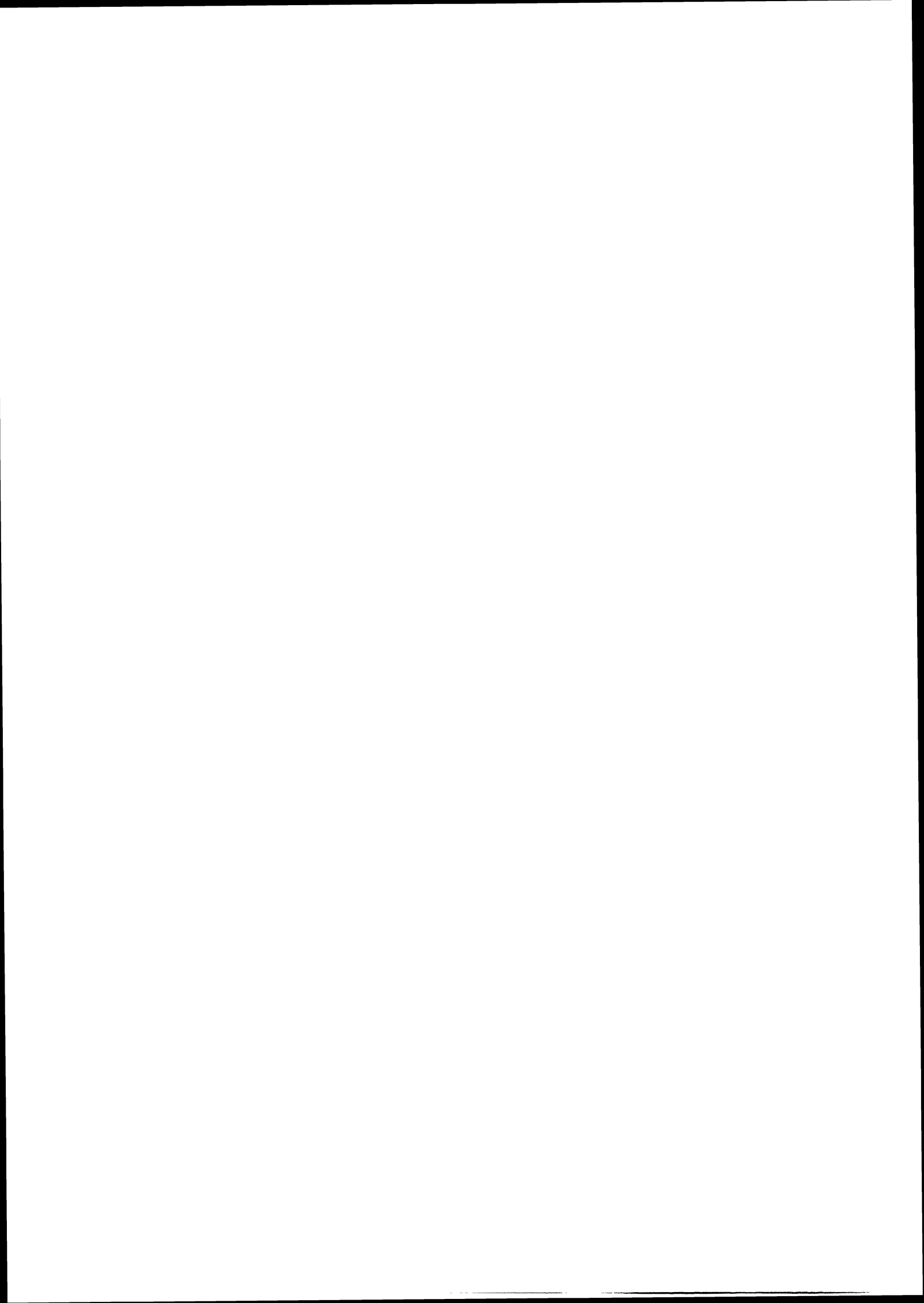
*Spring actuation of foundation brakes is not commonly used on the front axle.

subroutine OUTPUT below entry TORQUE, the following statements are inserted (Note X is time in subroutine OUTPUT):

```
C
C ENTER TORQUE
C
    ENTRY TORQUE(X)
    NO=1
    NUMB=NUM(1)
    TIME=X-XPRINT
    DO 1250 I=1,KAXLE
C
C ANTI-LOCK SYSTEM ...CHECK TO SEE IF SLIP(I) IS GREATER THAN 0.5
    IF ((TLOCK(I)-X).GT.0.0) GO TO 3
    IF(SLIP(I).LT.0.5) GO TO 2
    TLOCK(I) = X + 0.01
    GO TO 3
    2 CONTINUE
C
C TABLE LOOK-UP FOR PRESSURE
    Z = XPRINT-TQ(I,1)
    CALL TABLE(1,NUMB,XX,YY,Z,Q)
C
C OPTION 2
C STATIC LOAD SENSING BRAKE PROPORTIONING
    Q=Q*PROP(I)
C
C PRESSURE EQUATION
    P(I)=(POLD(I)-Q)*EXP(-TIME/TQ(I,2))+Q
    GO TO 4
C
C SLIP(I) IS GREATER THAN 0.5 ...SET P(I) = 0.0 FOR 0.01 SECONDS
    3 P(I)=0.0
C
    4 CONTINUE
```

The variables TLOCK (I) must be dimensioned to 5 in subroutine OUTPUT and initialized to zero. The program as modified will then be ready to run.

In general, an antilock control system may be expected to be more complex than the one modeled here. This will necessitate dimensioning of new variables and perhaps additions to the tables and changes in the common blocks. The location of the algorithm, however, should be the same as the example given in this section.



3.0 THE SIMULATION PROGRAMS

3.1 PROGRAM SPECIFICATIONS

The entire program has been written in Fortran IV. The core storage requirements for the articulated vehicle and the straight truck programs, and the integration routine, HPCG, on MTS* are as follows:

Articulated Vehicle	69648	BYTES
Straight Truck	43962	BYTES
HPCG	1882	BYTES

3.2 PROGRAM STRUCTURE

An overview of the program is given in Figure 3-1. With the exception of HPCG, which is an IBM system subroutine, the flow diagrams for each separate subroutine are given in Appendix C. For an explanation of HPCG, the user should consult the HPCG list and reference [15].

Most algebra is in its most expanded form, and comment cards are used frequently to explain tedious computations. Thus, even a casual Fortran user should be able to follow the logic of all the separate small algorithms that make up the whole. Therefore, changes may easily be made; more variables may be output and certain algorithms may be modified.

Certain aspects of the program, however, should be handled with extreme care, as inadvised changes may result in errors which may prove difficult to detect and debug. These are listed below:

- a) The integration time step, PRMT(3). This has been carefully chosen based on the physics of the system. While the increase in PRMT(3) from its set value of .0025 may save computer time, it would entail danger of numerical instability and thus incorrect results.
- b) The slip loop (do loop 5 in subroutine FCT1). The wheel rotational equations of motion are integrated to produce wheel velocities and accelerations and brake forces. Any changes should be made only after careful reference to section 2.4.1.
- c) The initializations in the beginning of subroutine OUTPUT. A false step in this section may result in seemingly correct results which, in fact, are seriously in error.

3.3 SIMULATION COSTS

The cost of the computations will, of course, depend on the options utilized in a particular run. If the most time consuming options on the articulated vehicle are utilized, the run costs are less than three dollars per simulated second on MTS. The straight truck runs for about one dollar per simulated second.

*MTS stands for Michigan Terminal System which is implemented on the IBM 360/67 at the University of Michigan.

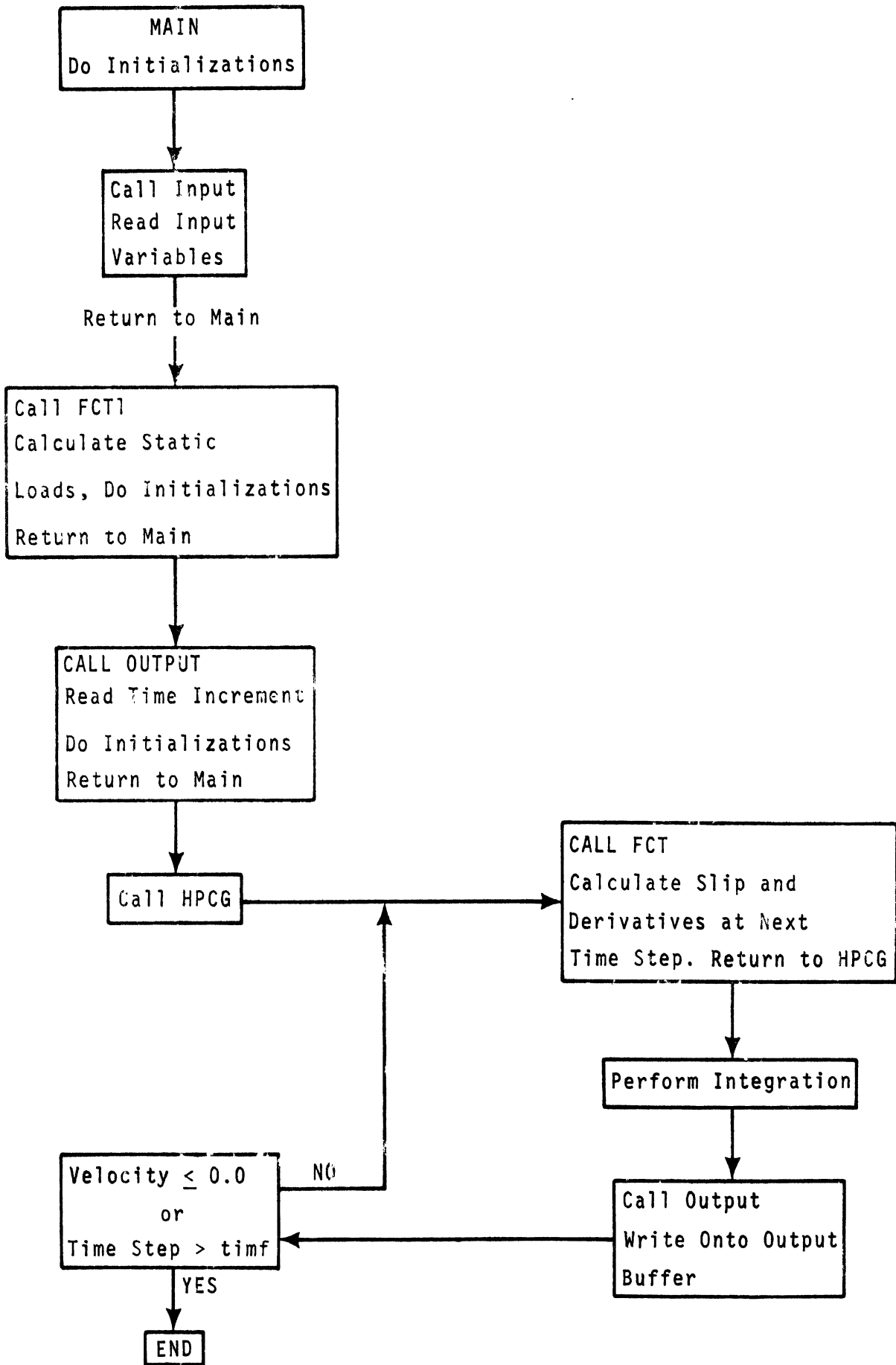


Figure 3-1. Simplified flow diagram, braking performance program

4. MEASUREMENT OF VEHICLE PARAMETERS

The parameters necessary for describing the vehicles whose braking performance is to be simulated can be separated into six different categories:

1. vehicle geometry
2. suspension characteristics
3. inertial properties of vehicle and payload
4. tire properties
5. tire-road interface characteristics
6. brake and brake system characteristics

Extensive parameter measurements were made for the two vehicles tested in this program.* Where it was feasible to make measurements, parameters were calculated or estimated from design drawings and specifications. Test procedures used to determine suspension characteristics, inertial properties, and tire properties for the two vehicles are given in the following paragraphs.

4.1 SUSPENSIONS

4.1.1 REAR SUSPENSION PARAMETERS. Parameter measurements on the rear suspensions of the two vehicles were made by applying a vertical force to the frame rails and measuring appropriate fore-aft (x) and vertical (z) displacements of the suspensions. The tractor was equipped with a four spring suspension; the truck with a walking beam suspension.

In order to apply a vertical force to the rear suspension of the two vehicles, the 40-foot van-type trailer, parked and resting on its landing gear, was loaded with some 60,000 pounds of concrete blocks. Each vehicle, in turn, was backed under the trailer. Two hydraulic axle jacks, placed on the vehicle frame rails at the suspension centerline, were then used to raise the trailer, thus causing a transfer of load from the trailer landing gear to the vehicle rear suspension. (see Figure 4.1.) This technique allowed for the smooth application of a rear suspension gross load of 53,000 pounds on the tractor and 55,000 pounds on the straight truck, as measured by load scales placed under each wheel.

The load on the vehicle being tested was increased in increments of 4000 to 6000 pounds, keeping the distribution between wheels as even as possible. After achieving maximum load, the load was removed in similar increments.

After each increment of loading, x and z displacements relative to the vehicle frame were measured at the axle center of each wheel. In addition, on the straight truck with the walking beam suspension, z displacements at the center line between the rubber springs were measured on each side of the vehicle. (See Figure 4.2.)

Vertical deflection data gathered from these tests are presented graphically in Figures 4.3 through 4.11. Included are plots of vertical load vs. vertical deflection for

1. each axle center of both vehicles,
2. averaged data for axle centers on each side of the vehicles,
3. averaged data for all four axle centers of each vehicle.

In addition, for the walking beam suspension, plots are presented for

1. rubber springs, each side,
2. averaged data for rubber springs,
3. averaged data for bushing and structural member deflections.

*The two vehicles tested were: a 50,000 lb. gwv Diamond Reo straight truck and a tractor-trailer consisting of a 6x4 COE White tractor and a 40 ft. Fruehauf van trailer. Vehicle specifications are given in Section 5.

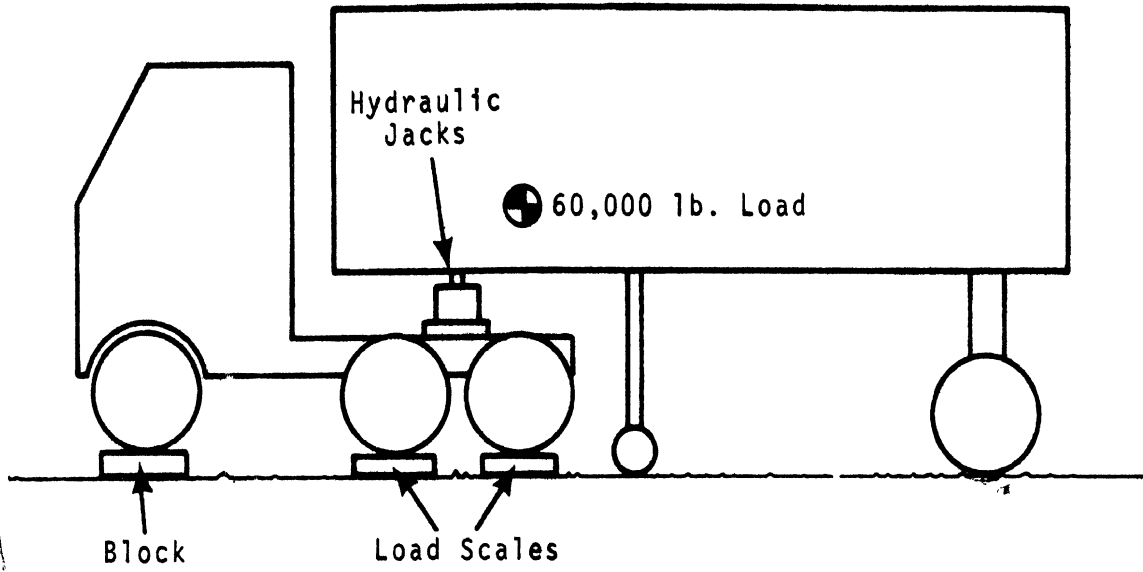


Figure 4-1. Loading scheme for rear axle suspension measurements.

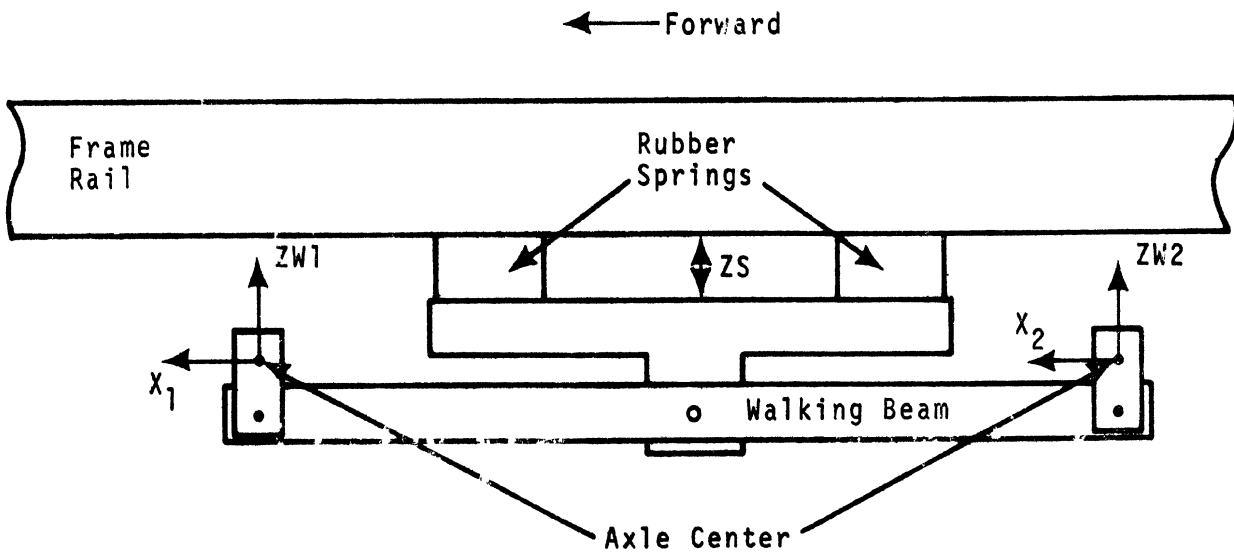


Figure 4-2. Measurement scheme for walking beam suspension.

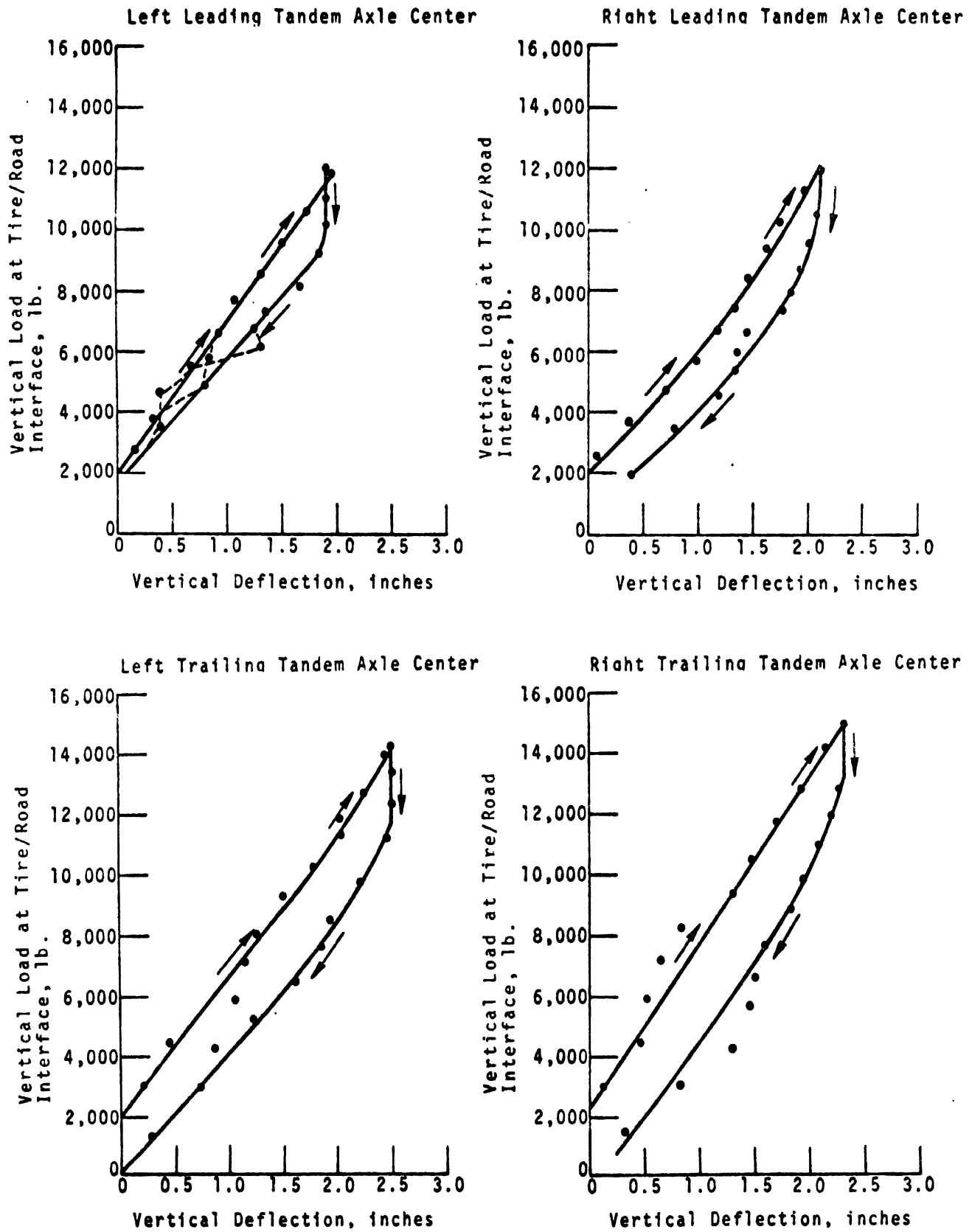


Figure 4-3. Vertical force-deflection characteristics measured at each wheel center, four spring suspension.

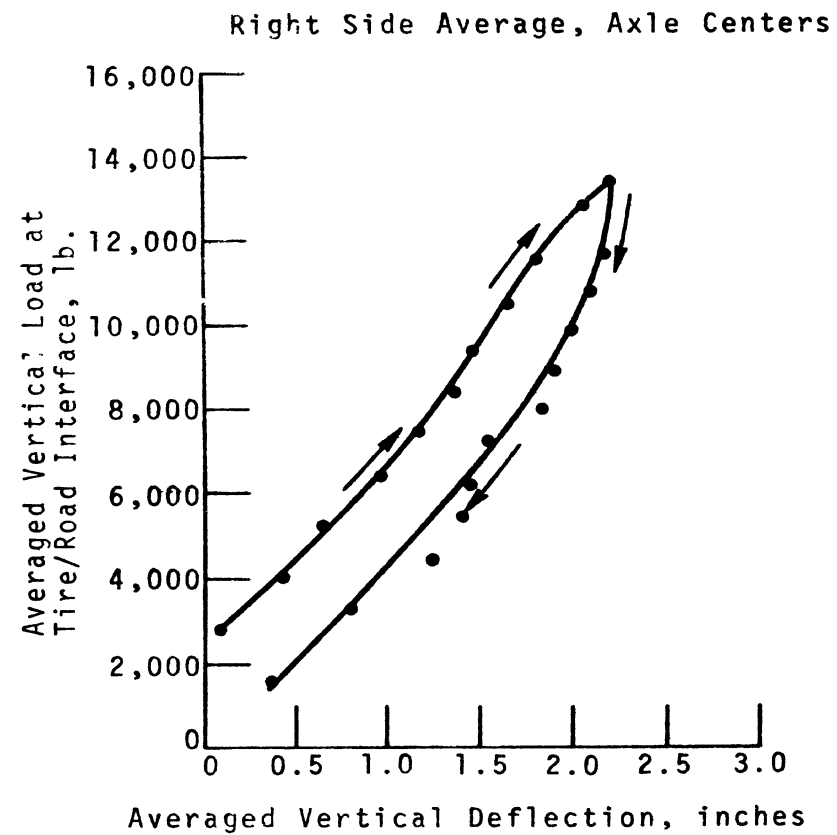
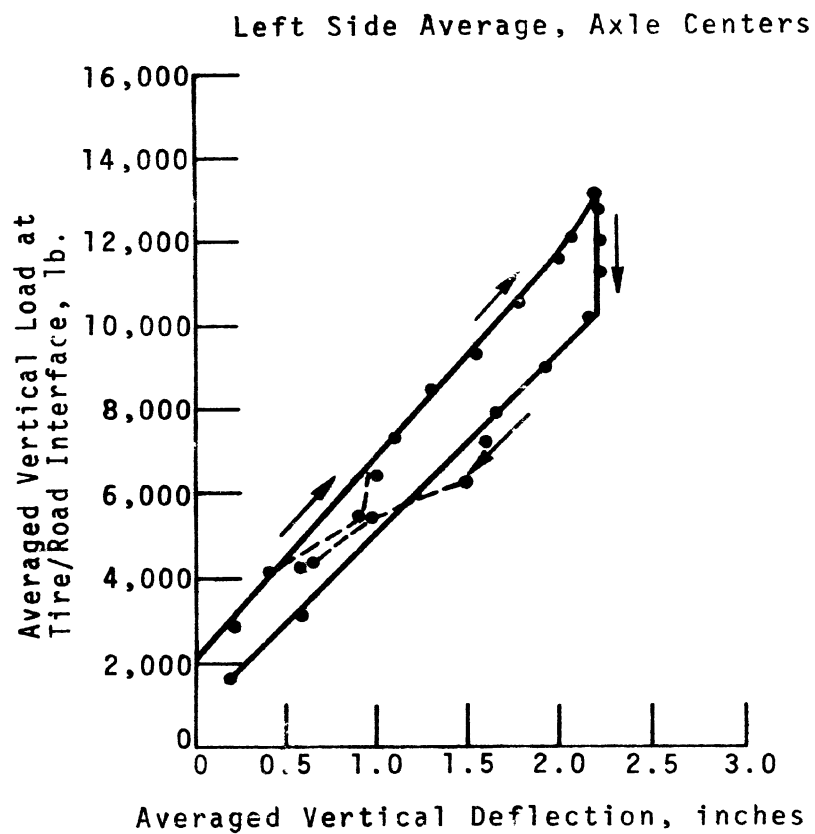


Figure 4-4. Vertical force-deflection characteristics, averaged for each side, four spring suspension.

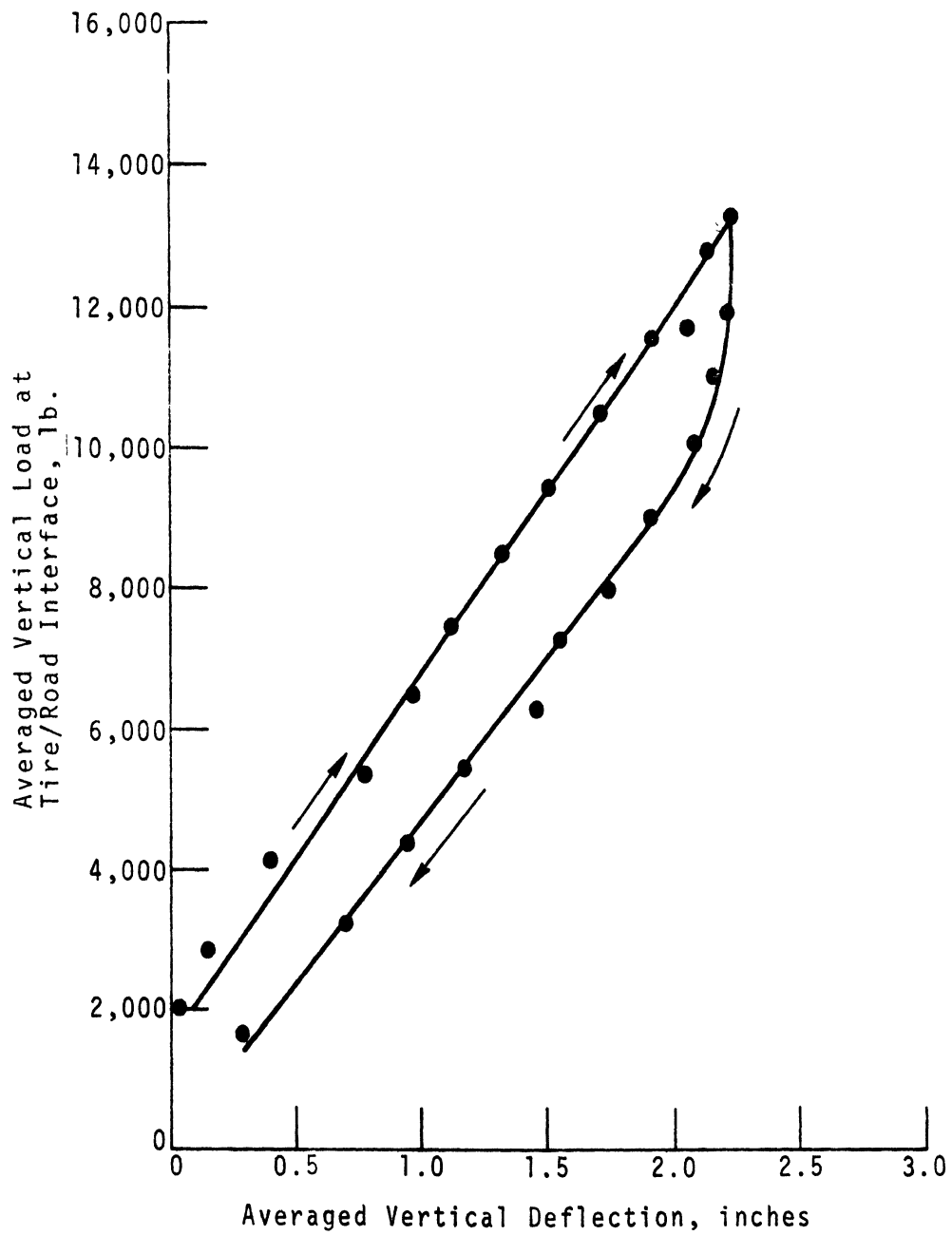


Figure 4-5. Vertical force-deflection characteristics, averaged for all four wheels, four spring suspension.

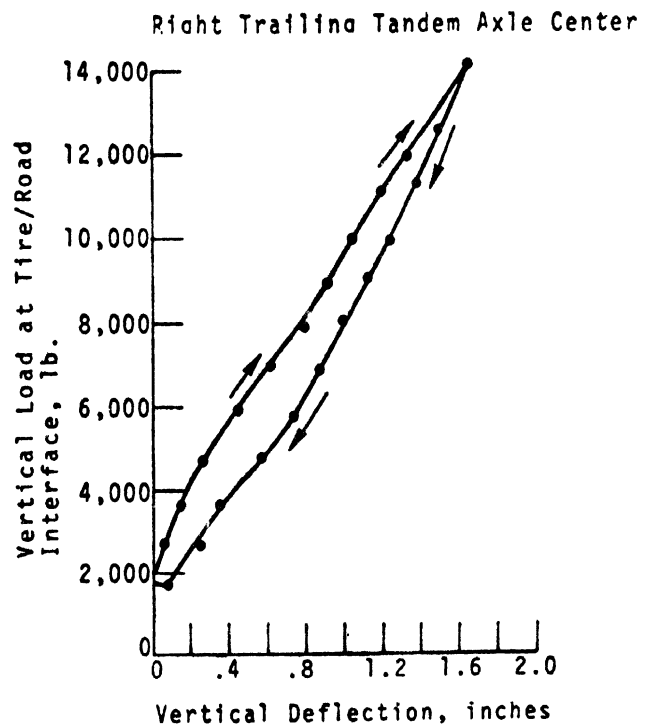
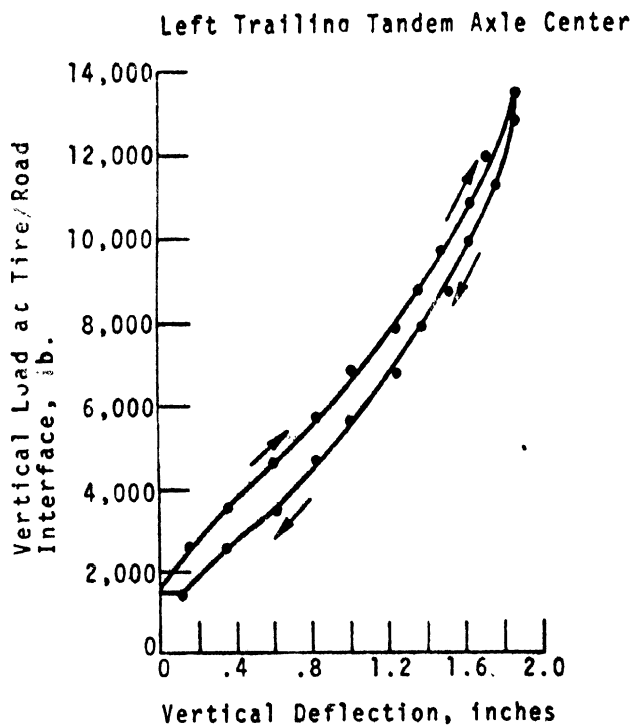
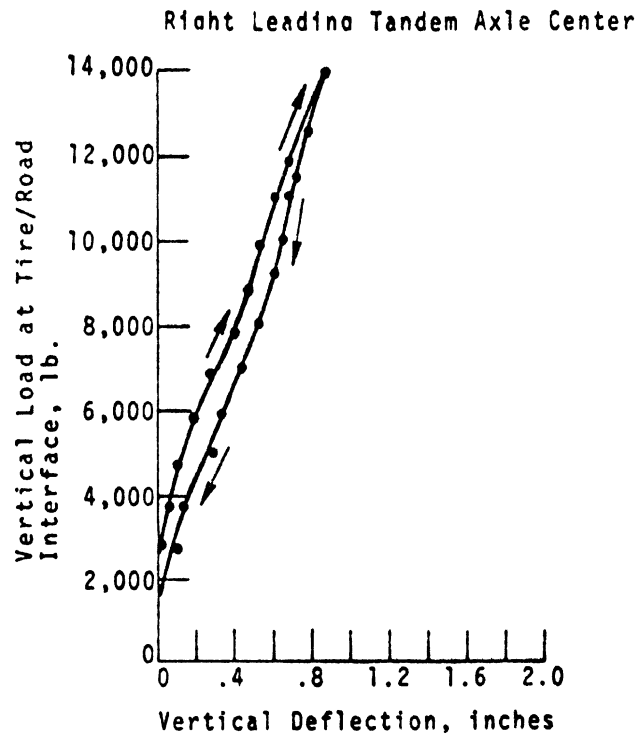
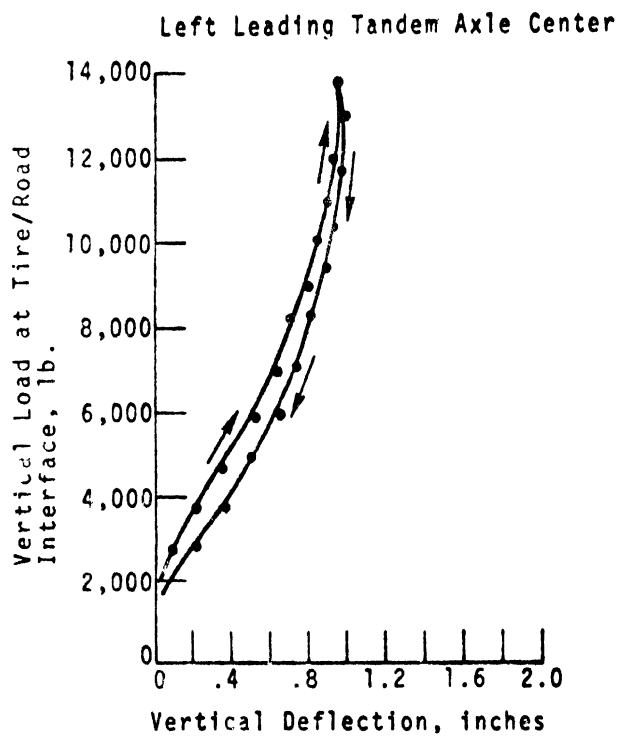
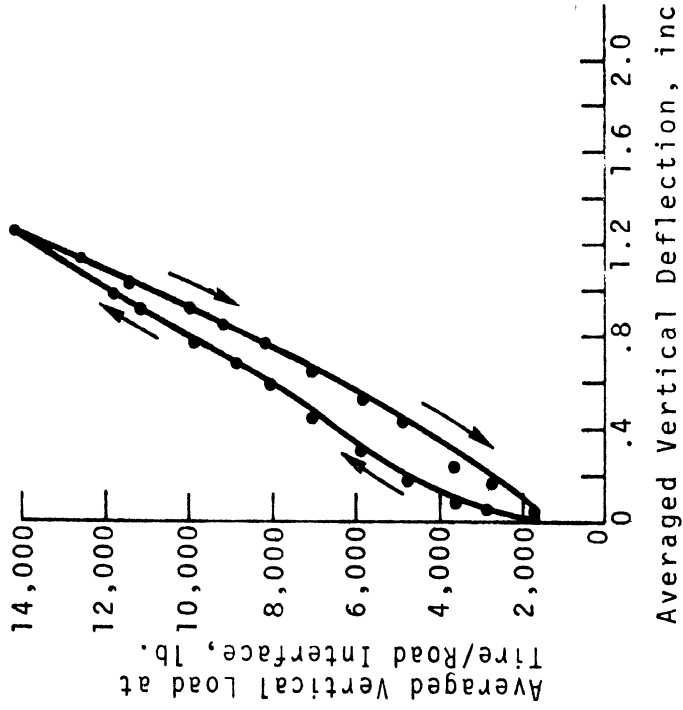


Figure 4-6. Vertical force-deflection characteristics measured at each wheel center, walking beam suspension.

Right Side Average, Axle Centers



Left Side Average, Axle Centers

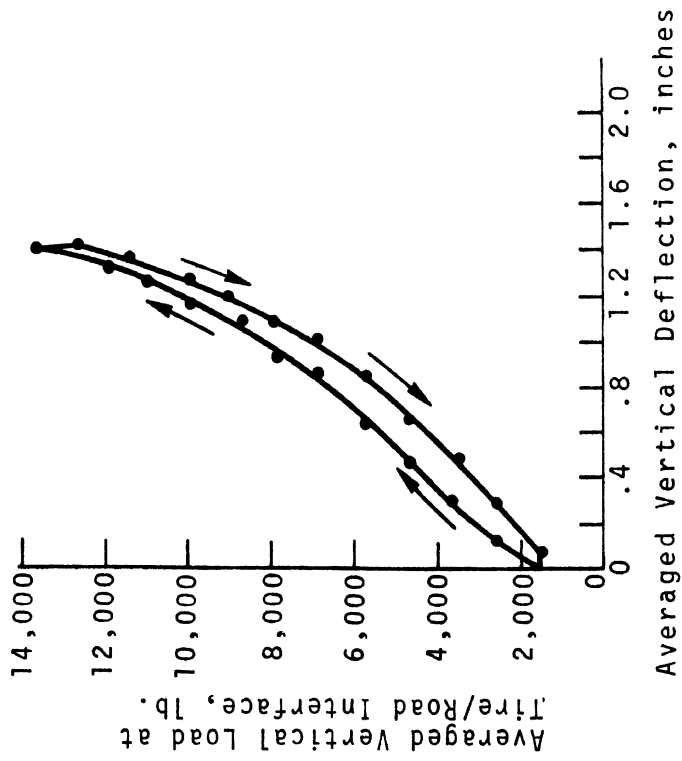


Figure 4-7. Vertical force-deflection characteristics, averaged for each side, walking beam suspension.

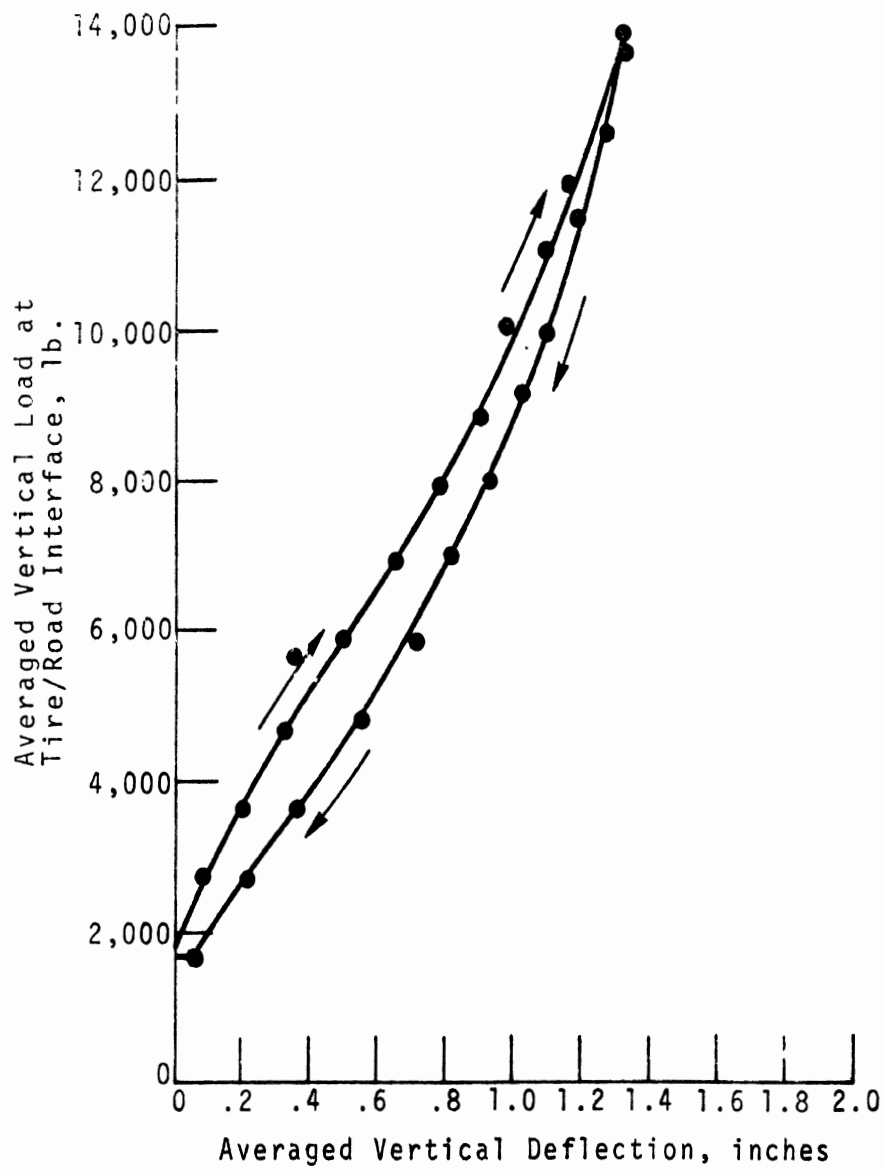
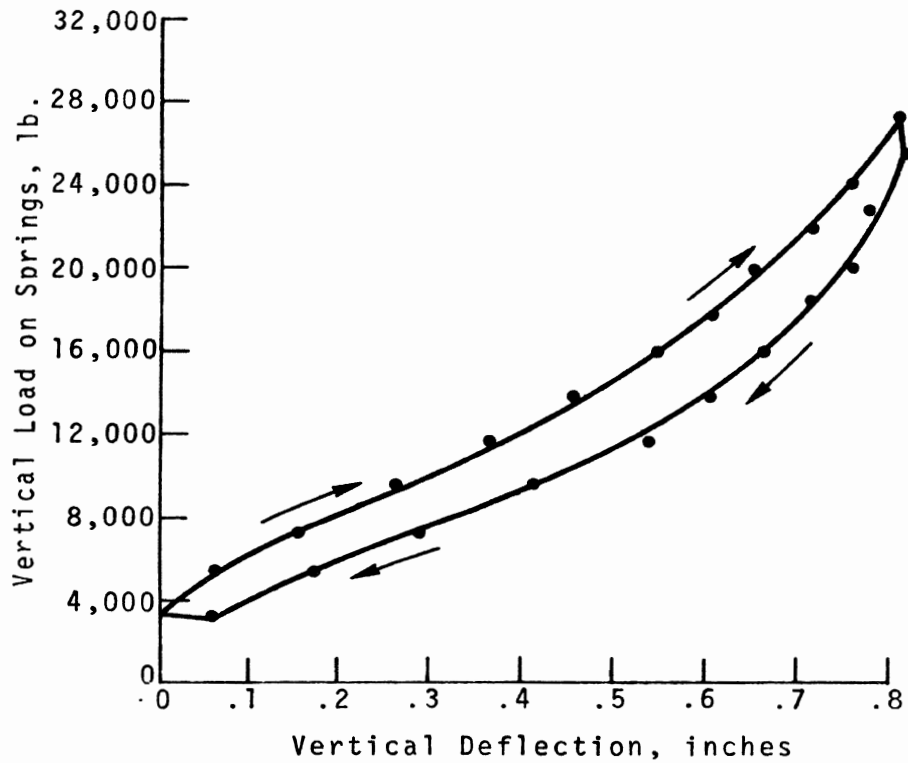


Figure 4-8. Vertical force-deflection characteristics, averaged for all four wheels, walking beam suspension.

Rubber Springs, Left Side



Rubber Springs, Right Side

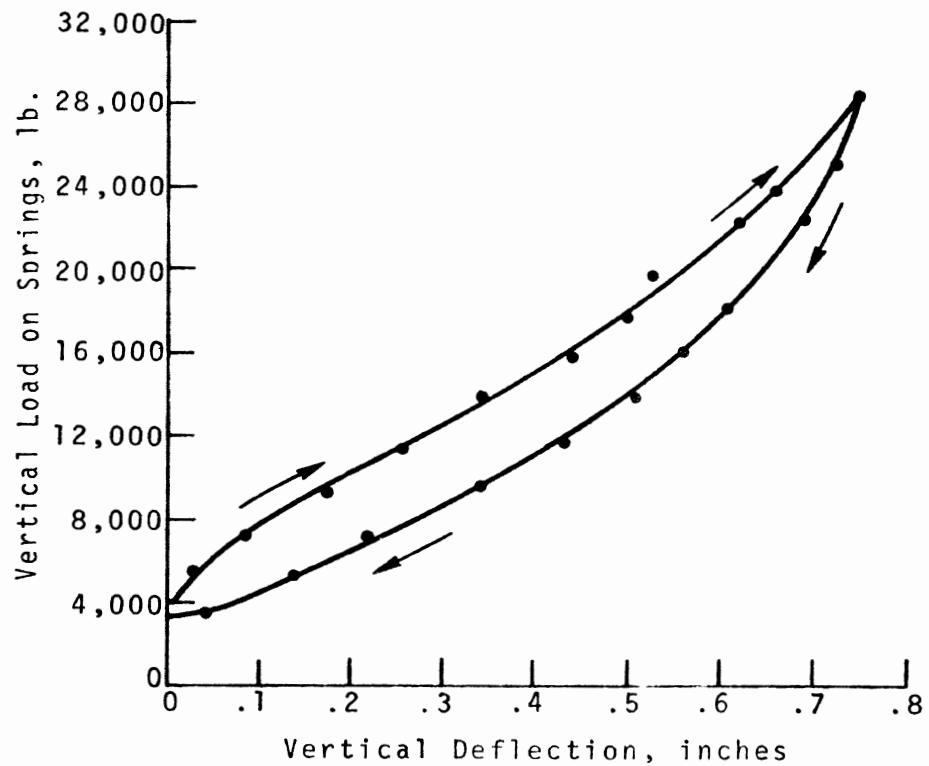


Figure 4-9. Vertical force-deflection characteristics for rubber springs on walking beam suspension, averaged for each side.

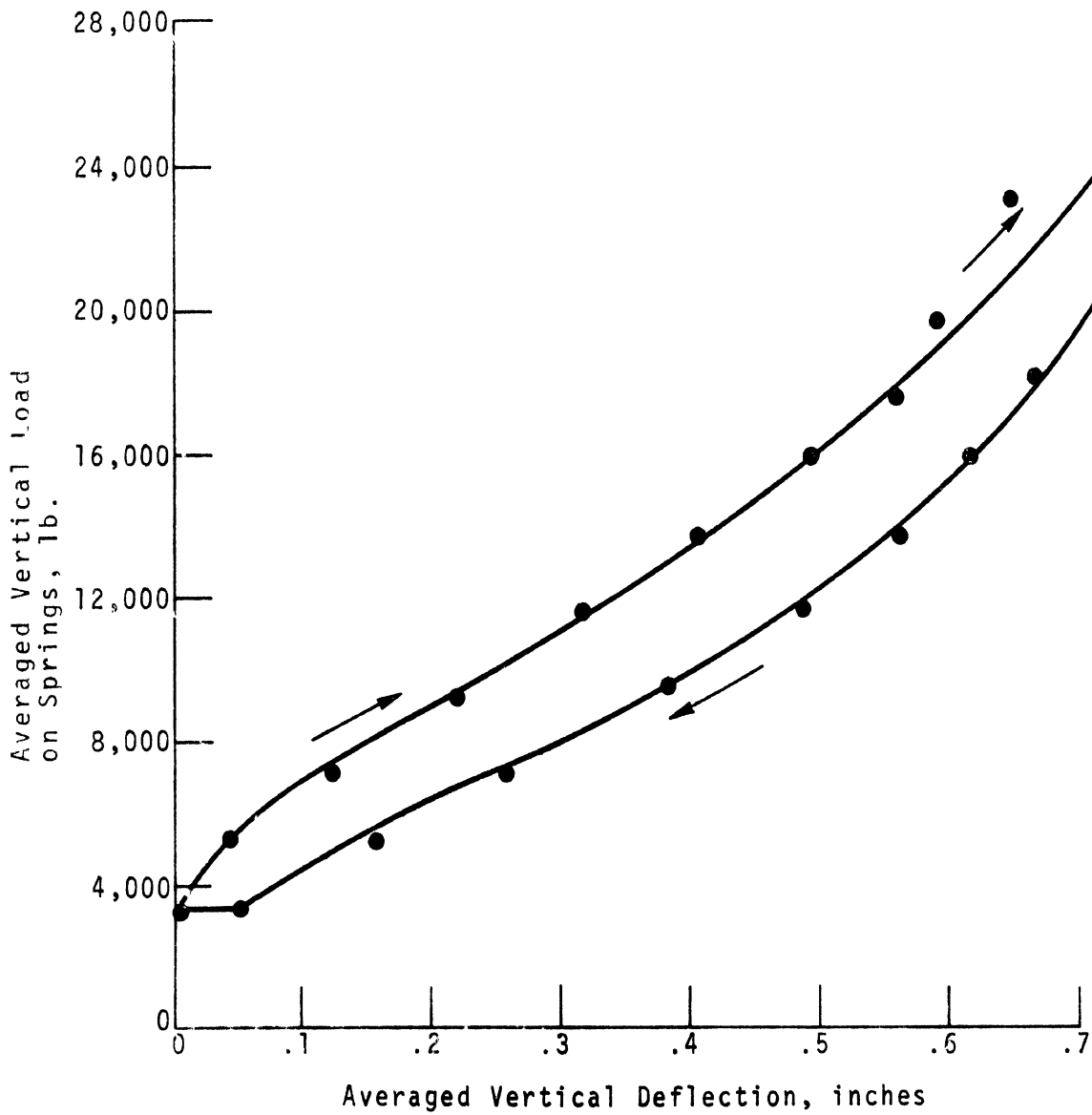


Figure 4-10. Averaged vertical force-deflection characteristics for rubber springs, walking beam suspension.

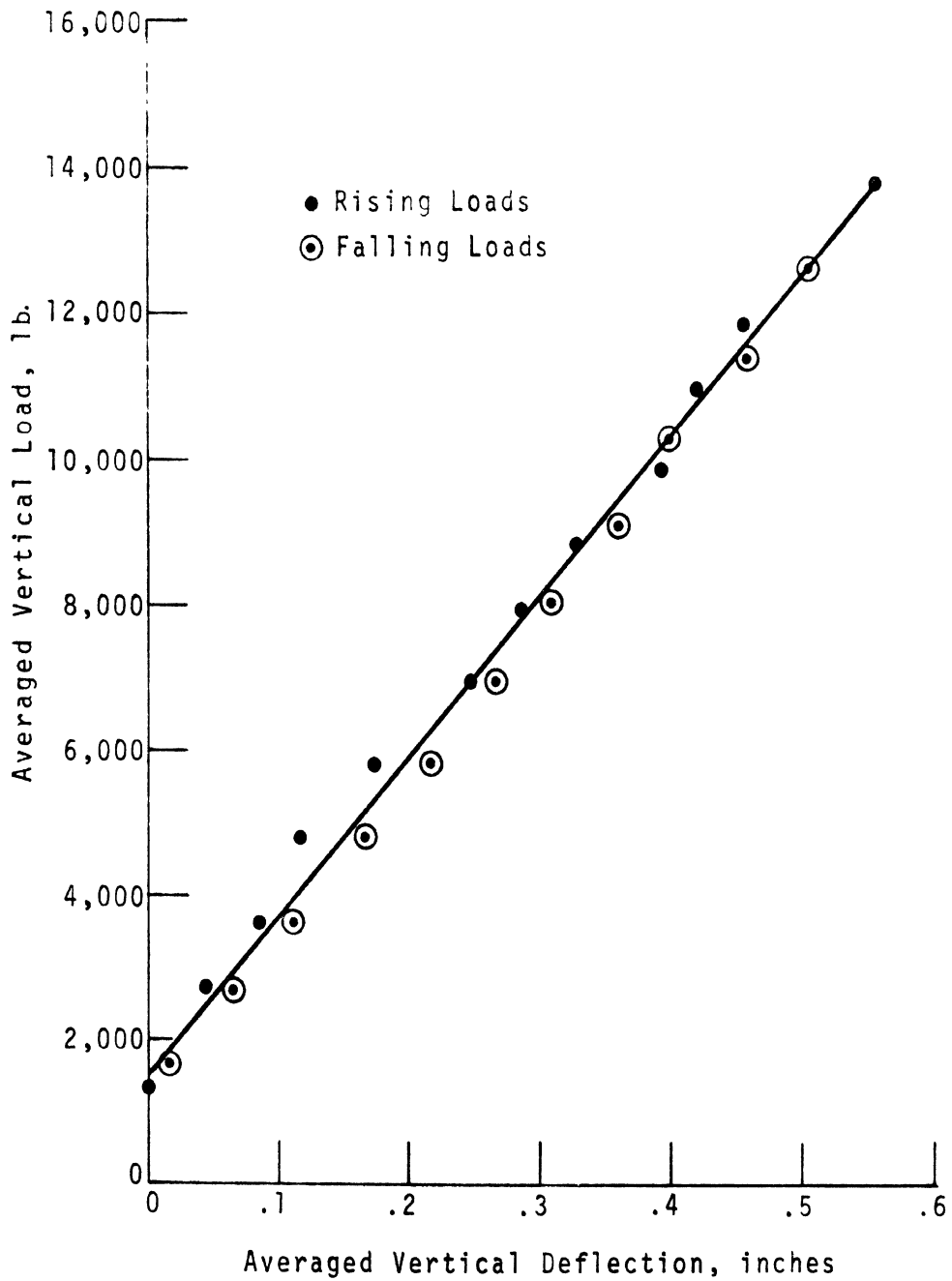


Figure 4-11. Averaged vertical force-deflection characteristics for bushings and structural members only, walking beam suspension.

Inasmuch as equal side-to-side load distribution was maintained during the tests, the axles remained approximately parallel to the plane of the frame rails as they displaced. Thus, the effective spring rates and horizontal displacements measured at the wheels were approximately equal to the actual spring rates and displacements at the spring-axle connection points.

Empirical analysis of the four spring suspension of the tractor is based on the model illustrated in Figure 4-12. Note that the total vertical spring deflection ZS is the sum of the spring compression, $f(FS)$, due to the vertical load on the spring, FS , and the spring deflection due to load leveler movement, Z_ℓ .

Thus:

$$ZS = f(FS) + Z_\ell \quad (4-1)$$

However, since the axles experienced approximately equal loading during the tests, load leveler motion was small, and only FS and ZS were measured during the testing. Furthermore, since Z_ℓ will be very nearly equal and opposite for wheels on one side of the vehicle, the effect of Z_ℓ on ZS may be removed by averaging the FS vs. ZS characteristics of the wheels on one side of the vehicle. (Of course, this is also true if the properties at all four wheels are averaged.) With Z_ℓ so removed, there is a one-to-one relationship between ZS , the parameter measured, and the desired spring deflection characteristic, $f(FS)$.

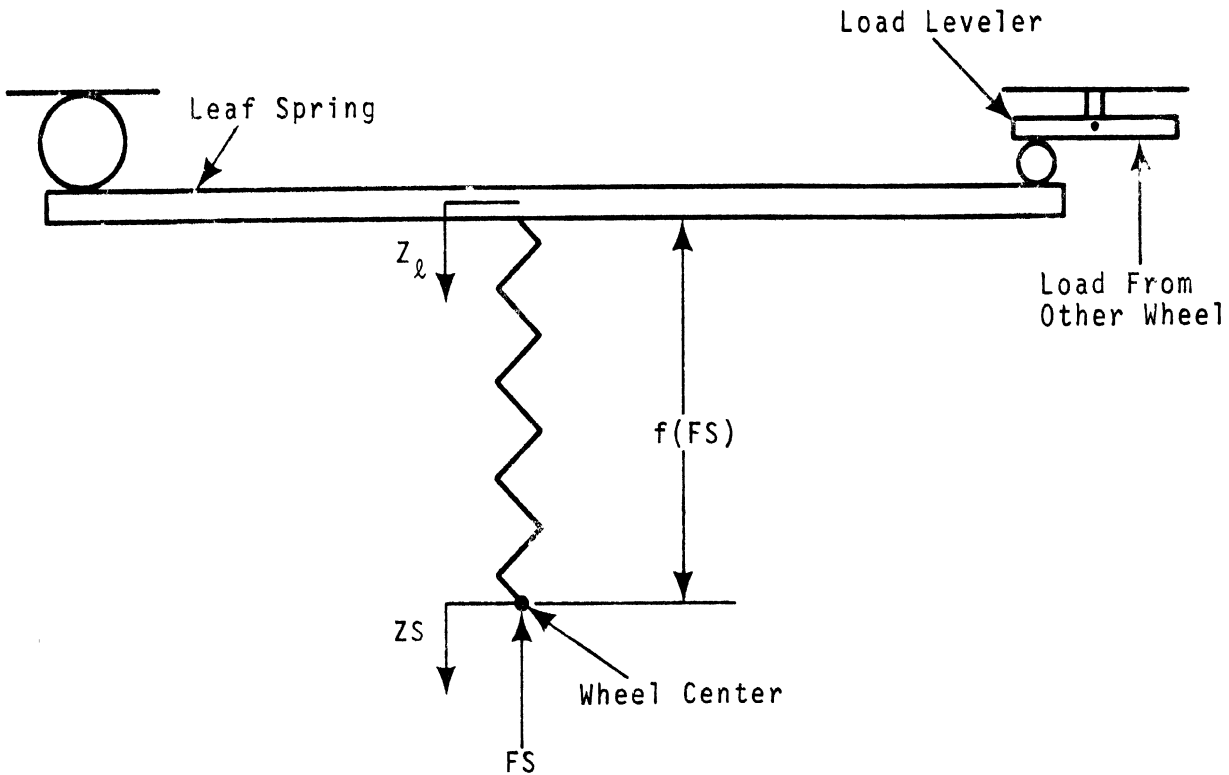


Figure 4-12. Measurement scheme, four spring suspension.

Thus, the functional relationship f , relating average vertical spring load to average vertical spring deflection, is provided directly by the experimental results and is obtained from Figure 4-5. The measurements indicate an average spring rate of 5200 lbs/inch at each wheel. Average coulomb friction properties are also contained in this graph, and are represented by half the vertical distance between points on the rising and falling portions of the graph. Coulomb friction varies from 900 lbs/wheel at light loads to 1300 lbs/wheel at heavy loads. The values of spring rate and coulomb frictions chosen for use in the simulation are total suspension values, and thus will be four times the "per wheel" values.

Empirical analysis of the walking beam suspension of the straight truck is based on a model illustrated by Figure 4-13. The additional subscripts, 1 and 2, used in Figure 4-13 refer to the forward and rear axle of the tandem, respectively. As illustrated in this figure, the total vertical compliance of the walking beam suspension is derived from the individual compliances of the rubber springs, axle bushings, walking beam pivot bushings, and structural members. Experimentation indicates that the rubber springs of this particular suspension, represented by spring parameter KR , typically account for about 60% of the total suspension compliance under evenly distributed loading conditions. The remaining compliances of various rubber bushings and structural members is assumed to be concentrated in the K' springs shown in Figure 4-13. Thus,

$$ZW1 = f(FS1+FS2) - (AA1)\theta_T + f'(FS1) \quad (4-2)$$

$$ZW2 = f(FS1+FS2) + (AA2)\theta_T + f'(FS2) \quad (4-3)$$

where θ_T is the walking beam rotation angle.

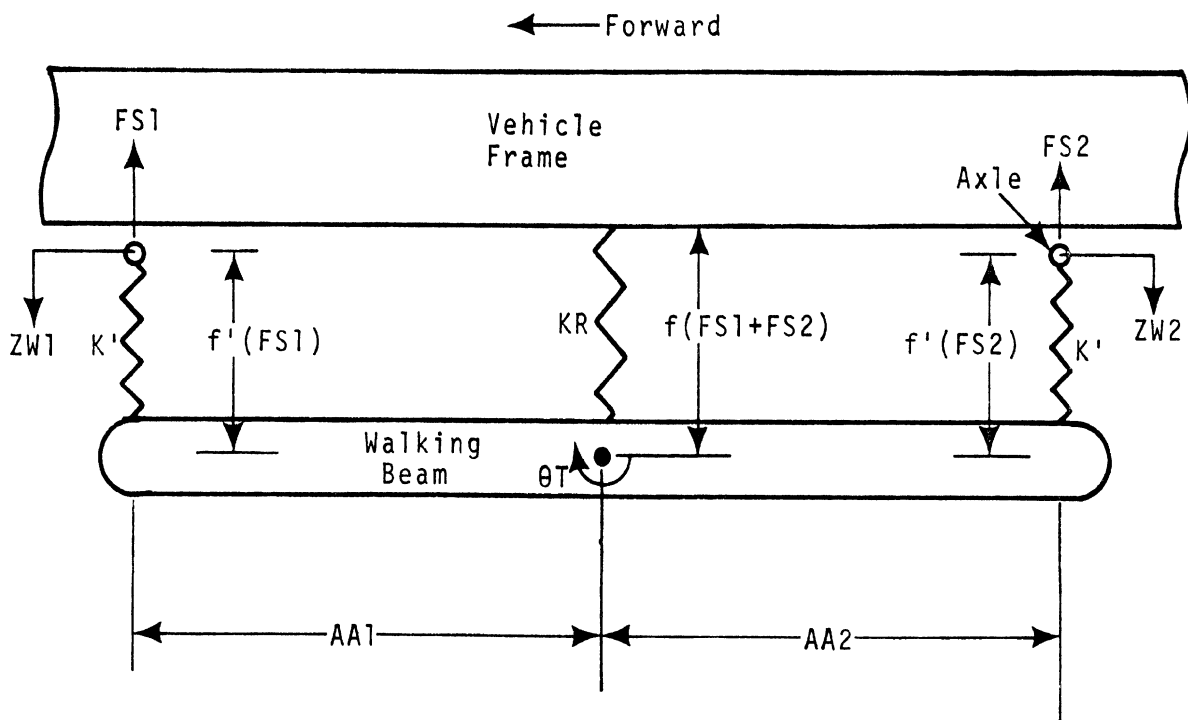


Figure 4-13. Detailed measurement scheme for walking beam suspension.

During the testing, $ZW1$, $ZW2$, $f(FS1+FS2)$, $FS1$ and $FS2$ were the measured parameters. Since $AA1$ and $AA2$ are nearly equal, θT remained small; thus the effect of the terms $AA1(\theta T)$ and $AA2(\theta T)$ can be neglected by averaging the results from the wheels on one side of the vehicle. The terms $f'(FS1)$ and $f'(FS2)$ can then be determined from the measured quantities by subtracting $f(FS1+FS2)$ from the average of $ZW1$ and $ZW2$.

The average functional relationships f and f' , as determined by experiment are illustrated in Figures 4-10 and 4-11, respectively. Figure 4-10 shows the average deflection of the rubber springs under vertical loading while Figure 4-11 shows the average bushing and structural deflection determined by subtracting rubber spring deflection from the average total axle deflection.

Although there is a slight hysteresis effect shown in Figure 4-11 the data indicates that it is reasonable to assume that for this suspension all coulomb friction can be attributed to the rubber spring assembly, which varies from 1200 lbs/side at light loads to as high as 1300 lbs/side at heavier loads.

The total effective spring constant for the rubber suspension is quite nonlinear, as can be seen from Figure 4-8, and varies from 7000 lbs/inch to 12,000 lbs/inch. The spring rate used in the simulation are total suspension values, and thus will be four times the "per wheel" values.

4.1.2 FRONT SUSPENSION PARAMETERS. The front suspensions of both the straight truck and tractor are similar in concept, being a beam axle assembly, suspended and located by two longitudinal multi-leaf springs. Therefore, the same test procedure and analysis were used for each front suspension.

The equipment for applying loads to the front suspensions of the test vehicle is illustrated in Figure 4-14.

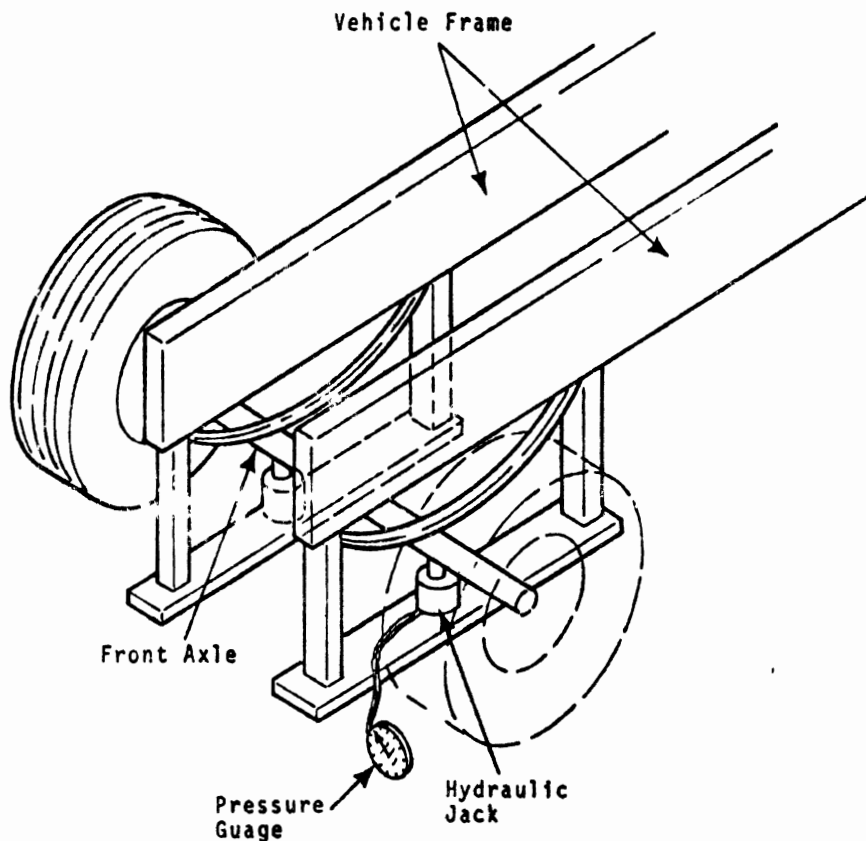


Figure 4-14. Scheme for loading front suspension.

The spring mounting brackets of the vehicles were fitted with new spring pins which are somewhat longer than the original pins. Two free swinging cradle assemblies were suspended from these pins such that each cradle hangs directly below the leaf spring assembly. Each cradle supported a hydraulic axle jack, located beneath the axle centerline. Each jack was fitted with a load calibrated pressure gauge. The jacks rested on five, one-inch diameter rollers placed so that the jack could freely translate longitudinally. A half-inch diameter rod was placed laterally between the jack and axle so that the jack could apply an upward force to the axle without applying any moment to the axle.

Using this equipment, the suspension was loaded equally, side-to-side, in increments of about 500 pounds per side until the axle hit the bump stops. The front axle of the straight truck was loaded to 31,000 pounds, while the front axle of the tractor was loaded to 22,700 pounds. Loads in both cases were removed in increments of 1000 pounds per side. At each increment of loading, vertical and fore-aft deflections of the spindle centers relative to the vehicle frame were measured at each wheel. To facilitate the study of steer effects for Phase II, two separate force-deflection tests were run on each front suspension. Figures 4-15 and 4-17 give results for the individual test on the straight truck and the tractor, respectively. (Each graph shows vertical load vs. vertical deflection for both the right and left spindle centers.) Figures 4-16 and 4-18 show the averaged vertical deflections for the straight truck and tractor respectively. These latter two graphs consolidate the data obtained from the two separate tests conducted on each vehicle, thus displaying the excellent repeatability of the data.

Since equal side-to-side loading was maintained, the axle remained in a horizontal plane; therefore, vertical deflection of the spindles was equal to vertical spring deflection. Thus, the desired spring deflection and coulomb friction characteristics can be obtained directly from Figures 4-16 and 4-18. The average spring rate per wheel for the truck is approximately 2200 lbs/inch, while the coulomb friction varies from 500 lbs at light loads to as high as 3000 lbs. at heavy loads. On the tractor, the spring rate is fairly constant at 1200 lbs/inch with coulomb friction varying from negligible at light loads to 1500 lbs. at heavy loads. Since these average values are for one side only, they should be doubled for use in the simulation.

4.1.3 TRAILER SUSPENSION PROPERTIES. Since the trailer was equipped with a four spring suspension, the procedure for measuring the load-deflection characteristics was similar to that used for the tractor tandem. The spring rates were determined experimentally by loading the rear wheels to 62,500 lbs. in approximately 4000 lbs. increments, while measuring vertical load at each wheel, and vertical displacement of the axles relative to the trailer body.

The spring force-deflection curve obtained by averaging the results from the four wheels, is shown in Figure 4-19. The average spring constant is 7000 lbs/inch. The average coulomb friction is 900 lbs. Note again that these are "per wheel" values, and thus should be multiplied by four for use in the simulation.

4.2 INERTIAL PROPERTIES

The inertial properties of each vehicle are described by the following parameters: weights of the sprung and unsprung masses and the payload; the vertical and fore-aft position of the center of gravity of each mass; the pitch moment of inertia for the sprung mass, and the payload; and the polar moment of inertia of the wheels.

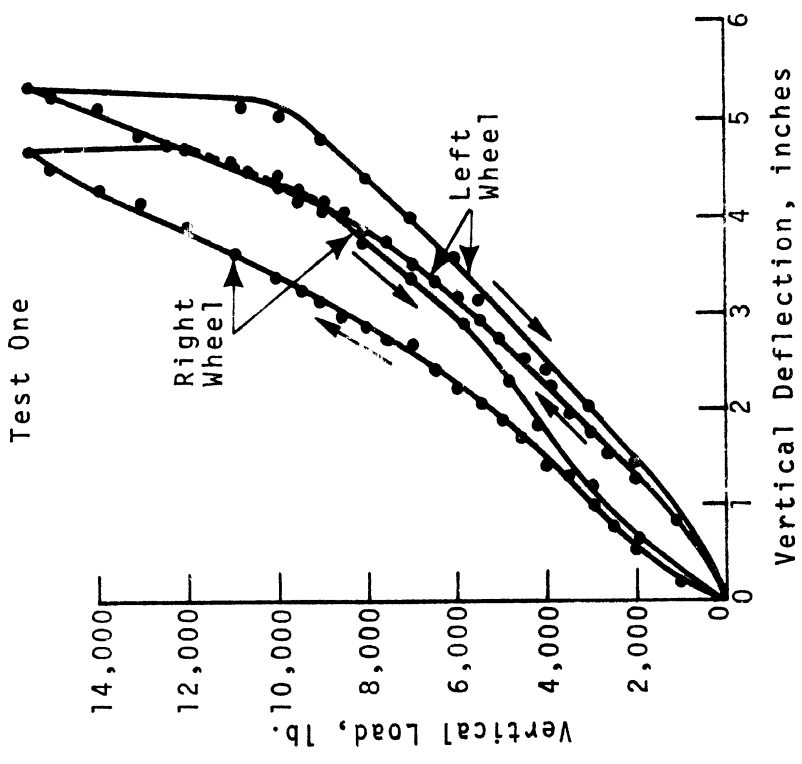
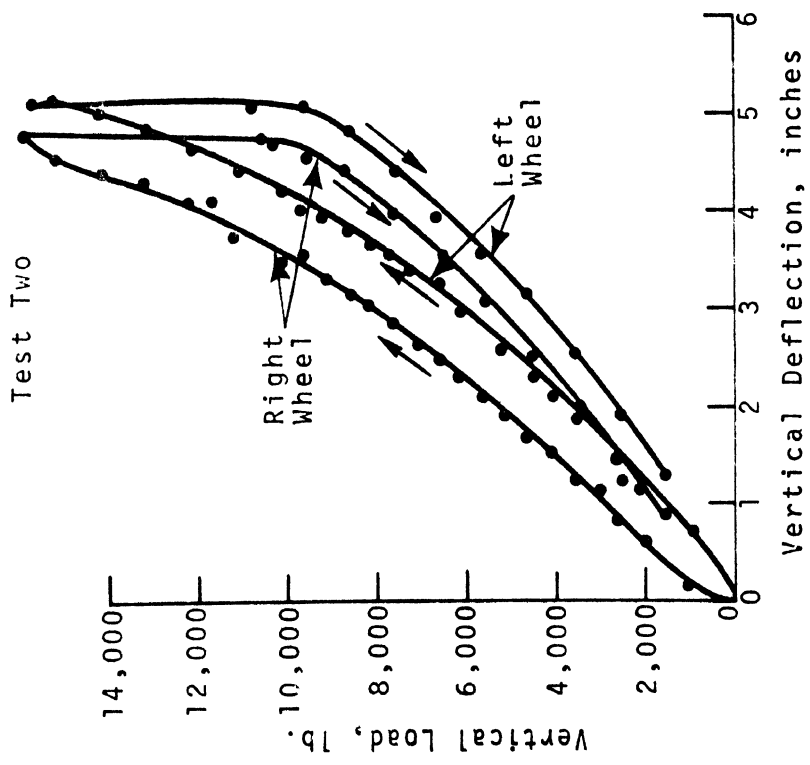


Figure 4-15. Axle spindle center deflections from tests of straight truck front suspension.

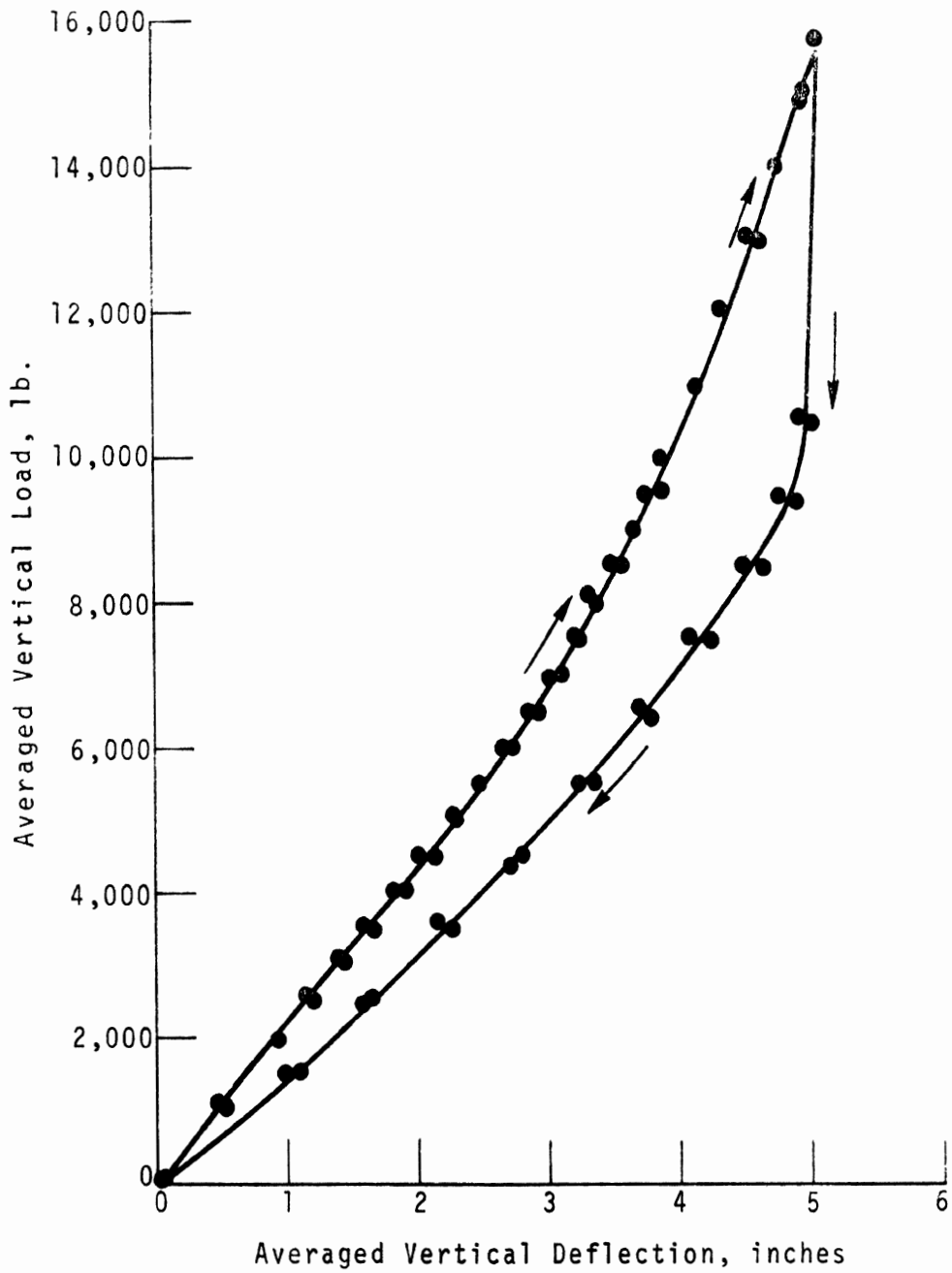


Figure 4-16. Averaged axle spindle center deflections from tests of straight truck front suspension.

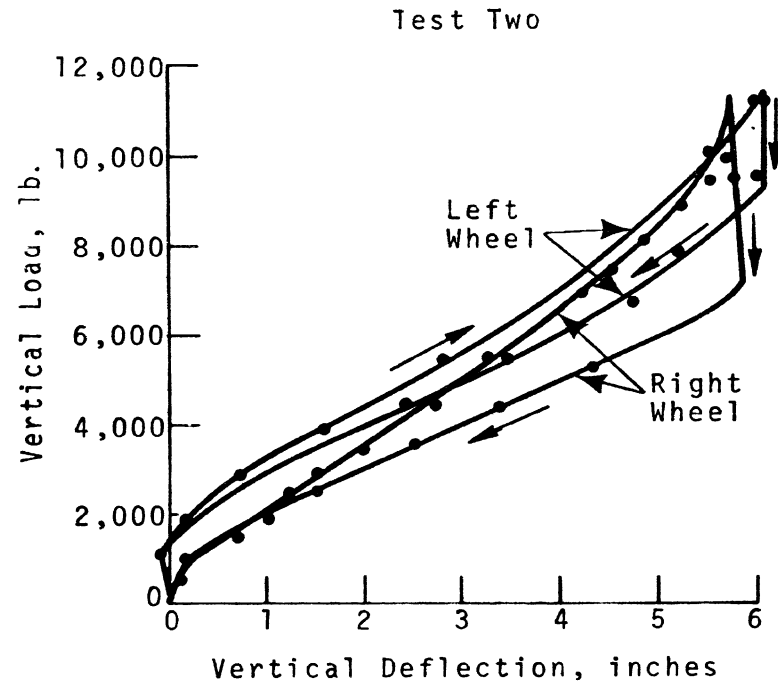
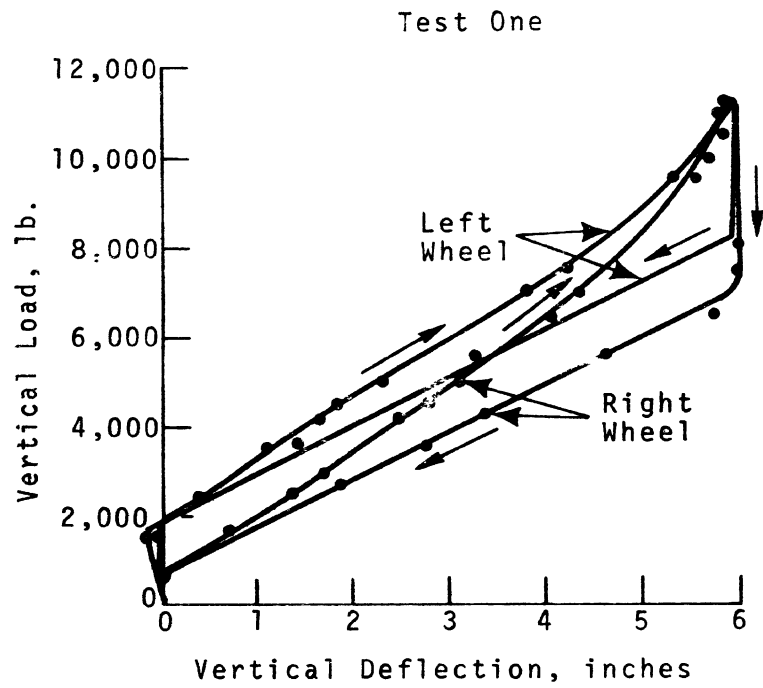


Figure 4-17. Axle spindle center deflection from tests of tractor front suspension.

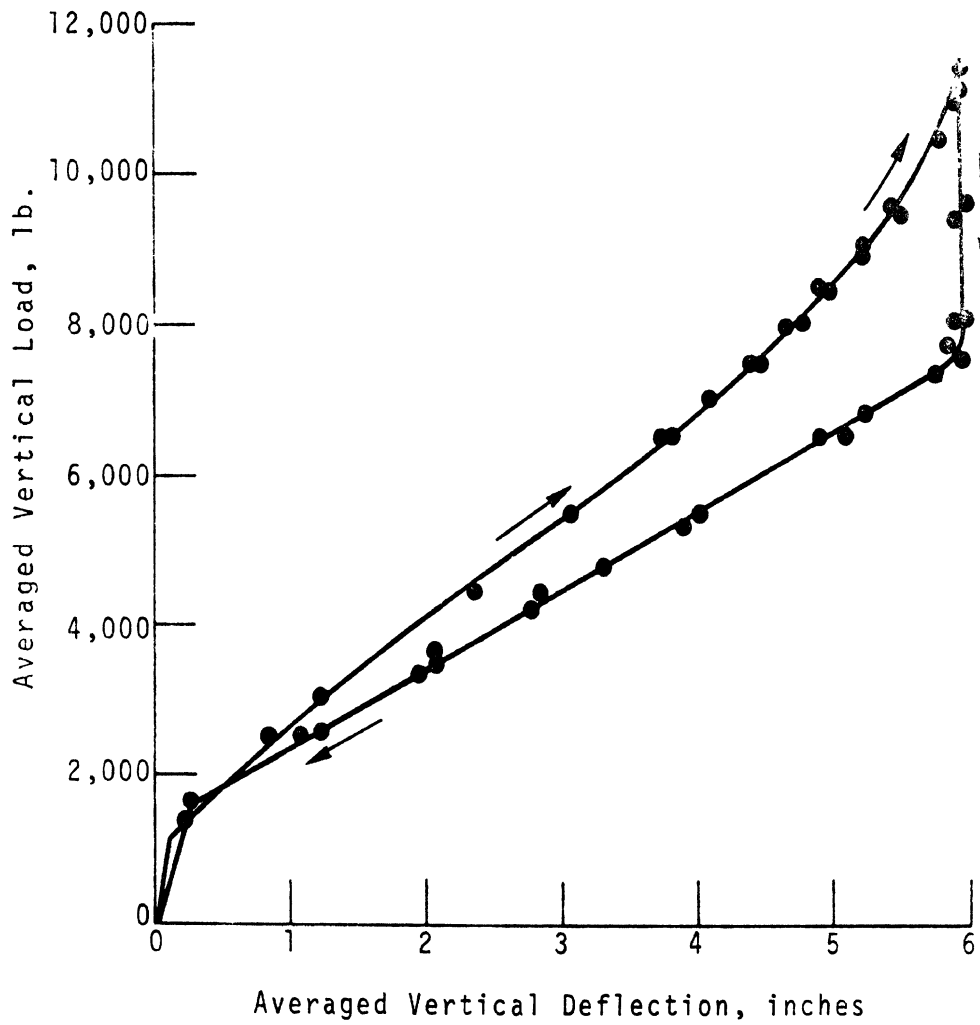


Figure 4-18. Averaged axle spindle center deflection from tests of tractor front suspension.

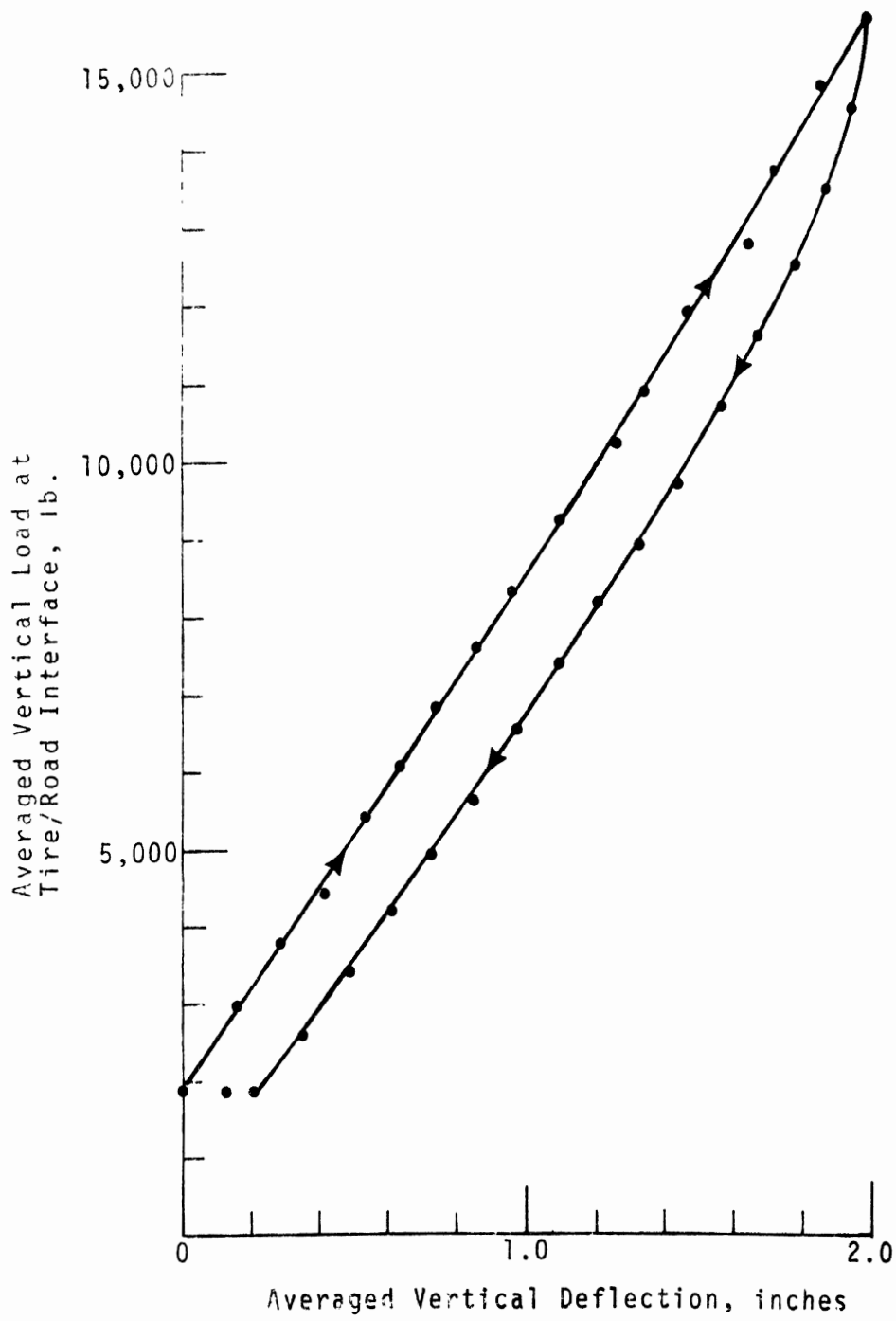


Figure 4-19. Averaged force-deflection characteristics for the four spring suspension of the trailer.

These parameters were measured for the truck and the tractor. For the trailer, the weights of the sprung and unsprung masses were measured, but the moments of inertia and the center of gravity locations were calculated.

In the following paragraphs, the measurement techniques for determining these parameters are described, and the actual parameter values for the test vehicles are given.

4.2.1 WEIGHTS. The truck and the tractor were weighed several times during the course of the program on truck scales at various locations and under a variety of loading conditions. The front and rear axles of the truck and tractor and the bogey on the trailer were removed and weighed individually using a hoist equipped with a carefully calibrated load cell. The total weight of each vehicle was established from the results obtained from the truck scales.* The weight of the sprung mass of each vehicle was determined by subtracting the weights of the unsprung masses from the total vehicle weight.

4.2.2 CENTER OF GRAVITY POSITION. To determine the fore-aft position of the c.g. for the truck and tractor, the vehicle is balanced on knife edges placed laterally under the frame rails in a trial and error manner.** Successful balancing indicates the c.g. position.

When the fore-aft c.g. position has been determined, the vertical position may be found. Hangers are constructed by which the vehicle may be supported on knife edges placed laterally and directly above the c.g. as shown in Figure 4-20. With the vehicle so supported, an inclinometer is used to determine the angle of inclination of the frame rails of the vehicle, θ_1 . A known weight, W_ℓ is then attached at a known horizontal distance, ℓ_h , and vertical distance, ℓ_v , from the knife edge supports, which causes the vehicle to rotate to a new equilibrium position. Again using the inclinometer, the new angle of inclination, θ_2 , is measured. Assuming the weight of the hangers is negligible, ℓ_o , the distance between the vertical c.g. position and the knife edge supports can be found from the following equation.

$$\ell_o = \frac{1}{W} [W_\ell (\ell_h \text{ctn}(\theta_2 - \theta_1) - \ell_v)] \quad (4-4)$$

where W is the gross vehicle weight. The c.g. location of the sprung mass is then determined by subtracting the effect of the unsprung weights.

The above method of determining c.g. position was applied to tractor and to the bare frame straight truck. The results are indicated in Figure 4-21.

However, during the brake performance testing program, the straight truck was fitted with a box as a means to carry load. Subsequently, the truck was tested in three load configurations: with the box empty, with the box loaded with gravel, and with the box

*The load on the front and rear axles was measured separately, as well as the total vehicle weight.

**It should be noted that in the tests for determining c.g. location and moment of inertia, the axles were chained to the frame of the vehicle to prevent suspension deflection when the wheel were lifted off the floor.

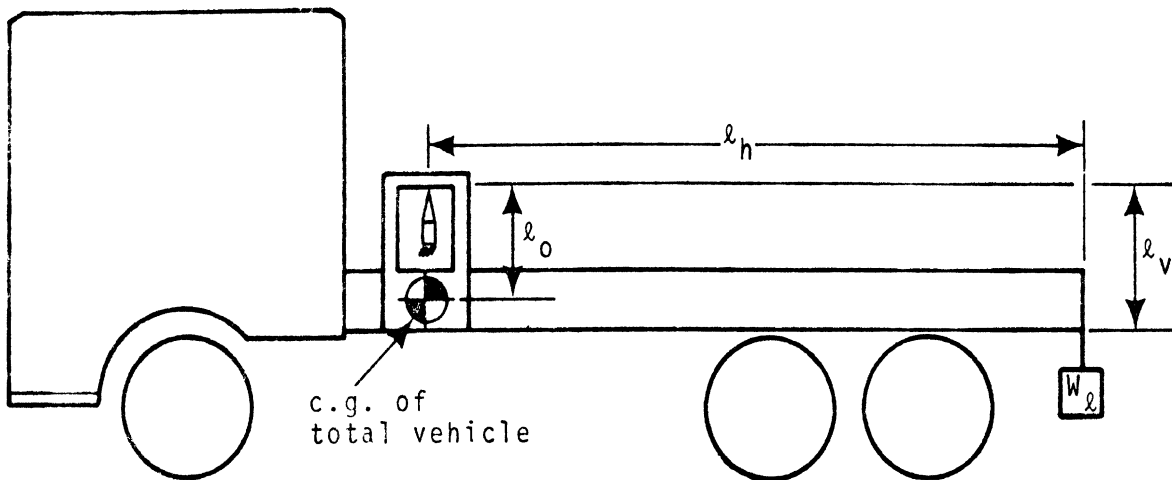


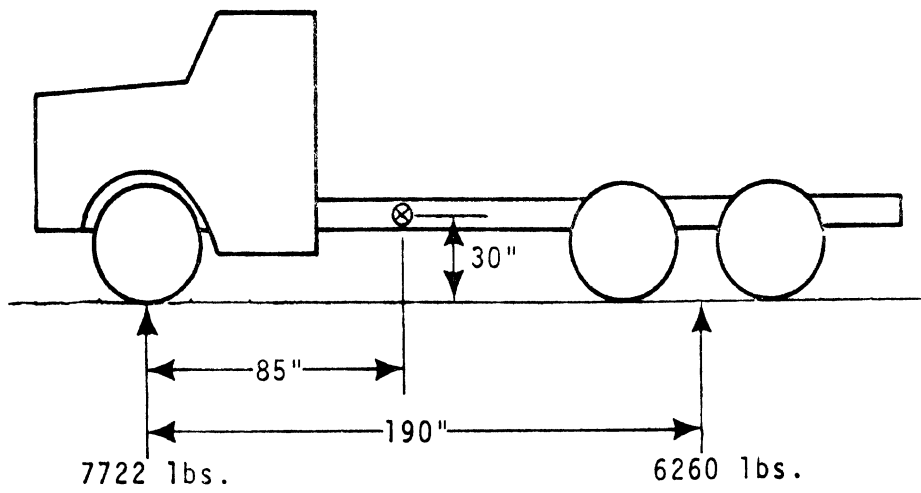
Figure 4-20. Scheme for determining center of gravity height.

loaded with steel blocks located to give the truck a c.g. height comparable to that of a concrete mixer truck. The weight and c.g. position of the box and the loads were calculated; this information, together with the empirical data for the sprung mass, allow calculation of the c.g. height for the total sprung mass of the vehicle in each of three load configurations. Vehicle weights and c.g. positions for the three load configurations are shown in Figure 4-22.

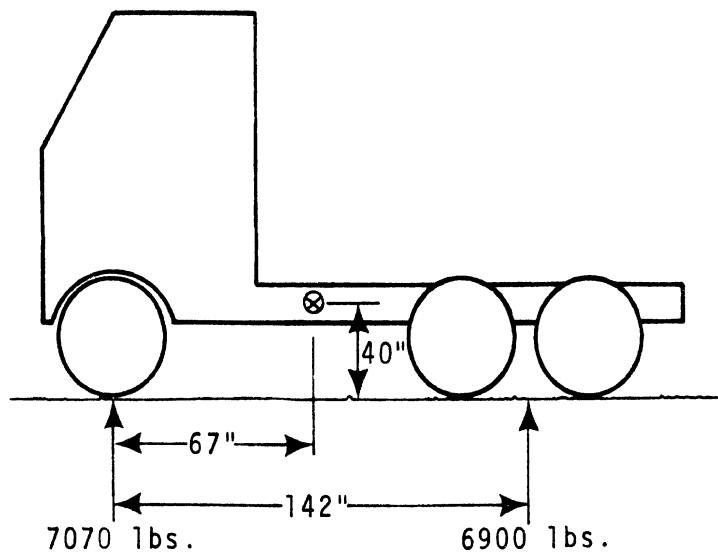
To determine the position of the trailer sprung mass center, the weights of its component parts were calculated. The following results were obtained:

Both Sidewalls.....	1408 lbs.
Front Wall.....	116 lbs.
Floor.....	3050 lbs.
Lower Side Rails.....	129 lbs.
Upper Side Rails.....	165 lbs.
Roof.....	234 lbs.
Pickup Plate.....	435 lbs.
Longitudinal I-Beams.....	415 lbs.
Front Bulkhead & Floorplate.....	319 lbs.
Support.....	290 lbs.
Rear Bumper, Header & Doors.....	669 lbs.
TOTAL.....	7230 lbs.

As a check, the calculated longitudinal position of the c.g. was compared to an empirical result. In order to experimentally determine the c.g. location of the trailer, weight measurements were taken at the trailer support (dolly) and at the rear wheels with the tandem axles set at the aftmost position. Figure 4-23 shows the values obtained. The bogey was then removed and weighed. The sprung weight



Straight Truck



Tractor

Figure 4-21. Weights and total vehicle c.g. locations of truck and tractor.

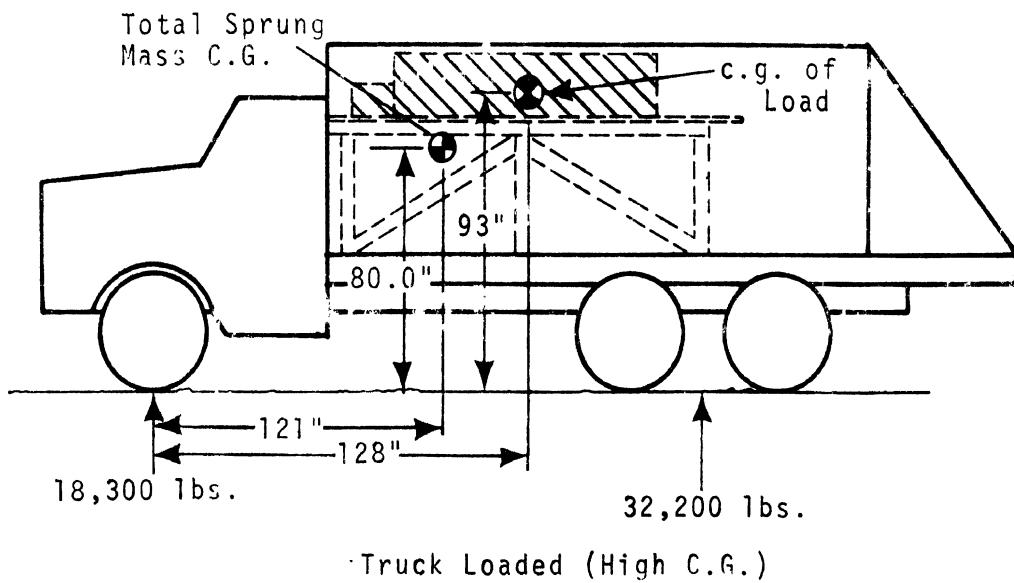
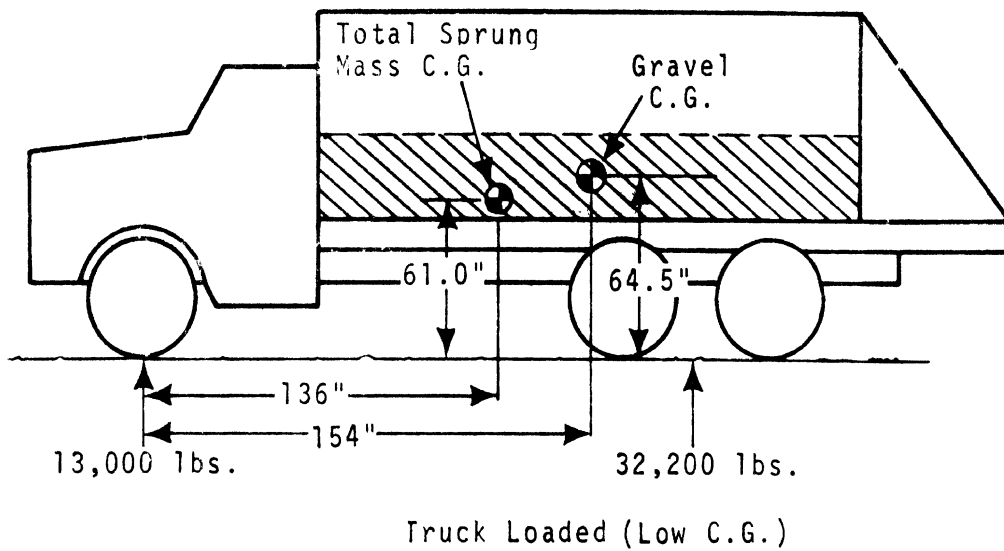
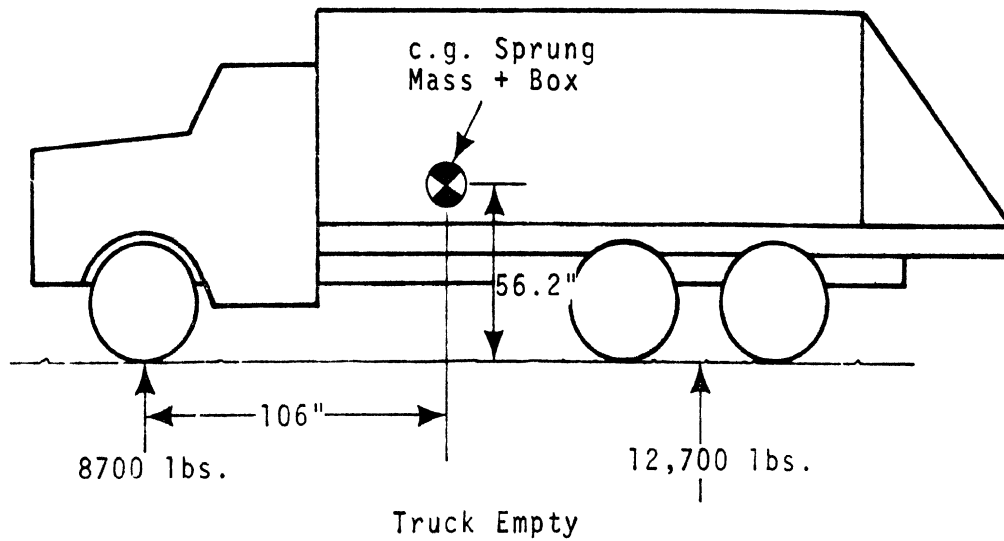


Figure 4-22. Weights and c.g. locations for truck in three load conditions.

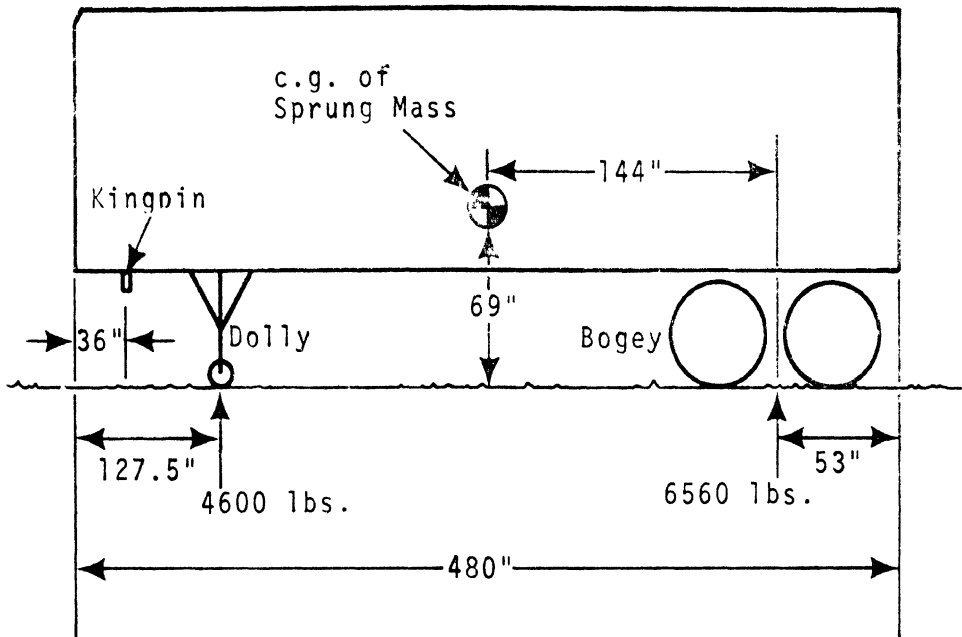


Figure 4-23. Weights and c.g. locations for the empty trailer.

(the part rigidly connected to the trailer) and the unsprung weight (tires, brakes, axles, springs) were obtained by suspending them from a hoist equipped with a load cell. Weights determined are as follows:

Sprung weight = 890 lbs.
 Unsprung weight = 3040 lbs.

Using these weights, the fore-aft location of the sprung mass center was computed. The value thus obtained agreed closely with the calculated value.

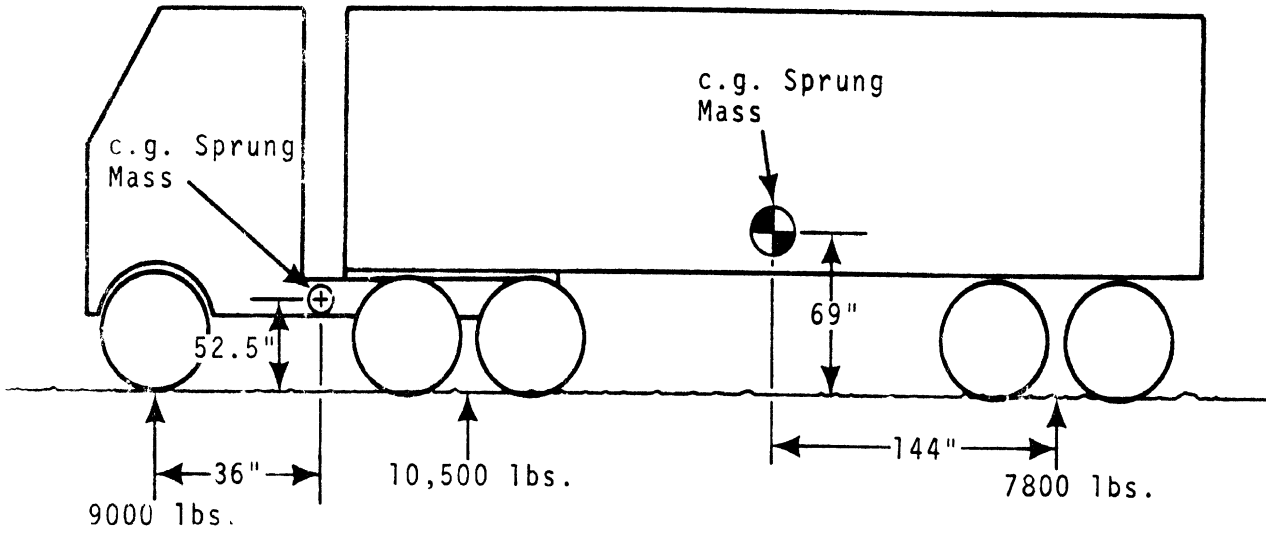
The tractor-trailer combination was tested in the empty and loaded condition, with weights and c.g. positions as indicated in Figure 4-24.

4.2.3 PITCH MOMENT OF INERTIA. The pitch moment of inertia of the bare frame truck and tractor were found by making further use of the hangers described above. (See Figure 4-25.) With the vehicle supported by knife edges placed laterally and directly above the c.g., a low amplitude swinging motion of the vehicle was initiated. Using a stopclock, the time period, T_n , for the vehicle to swing through n full cycles was obtained. The moment of inertia of the vehicle, in pitch, about its c.g. is given by:

$$I_p = Wl_o \left[\frac{(T_n/n)^2}{4\pi^2} - \frac{l_o}{g} \right] \quad (4-5)$$

The moment of inertia so determined includes the effects of both sprung and unsprung mass. Hence, it is necessary to subtract out

Empty Tractor-Trailer



Loaded Tractor-Trailer

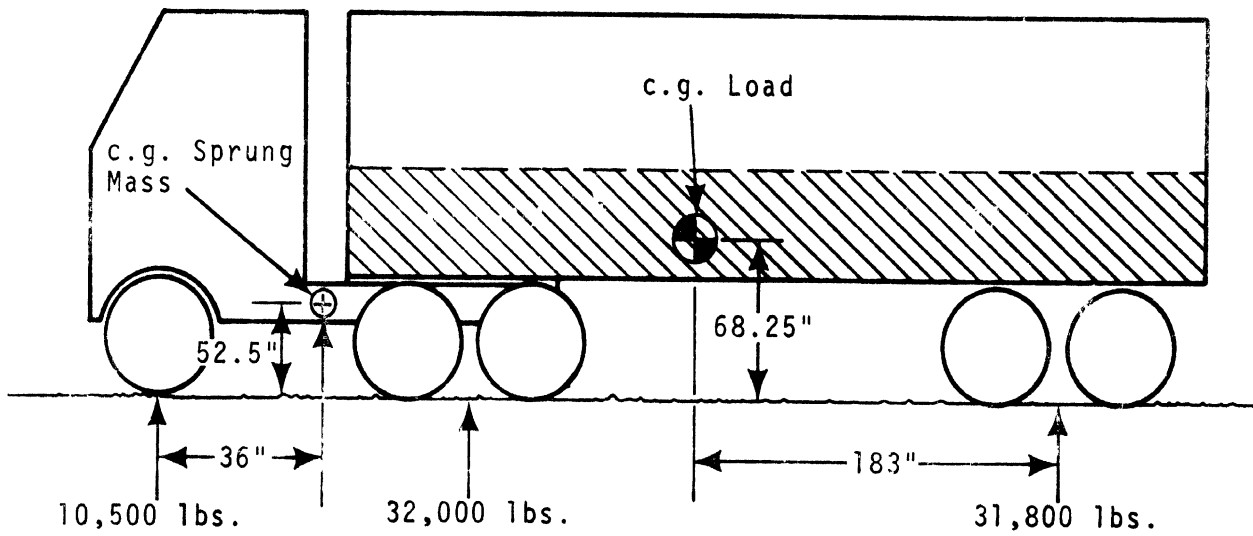


Figure 4-24. Weights and c.g. locations for tractor-trailer, in the empty and the loaded condition.

This page is reproduced at the back of the report by a different reproduction method to provide better detail.

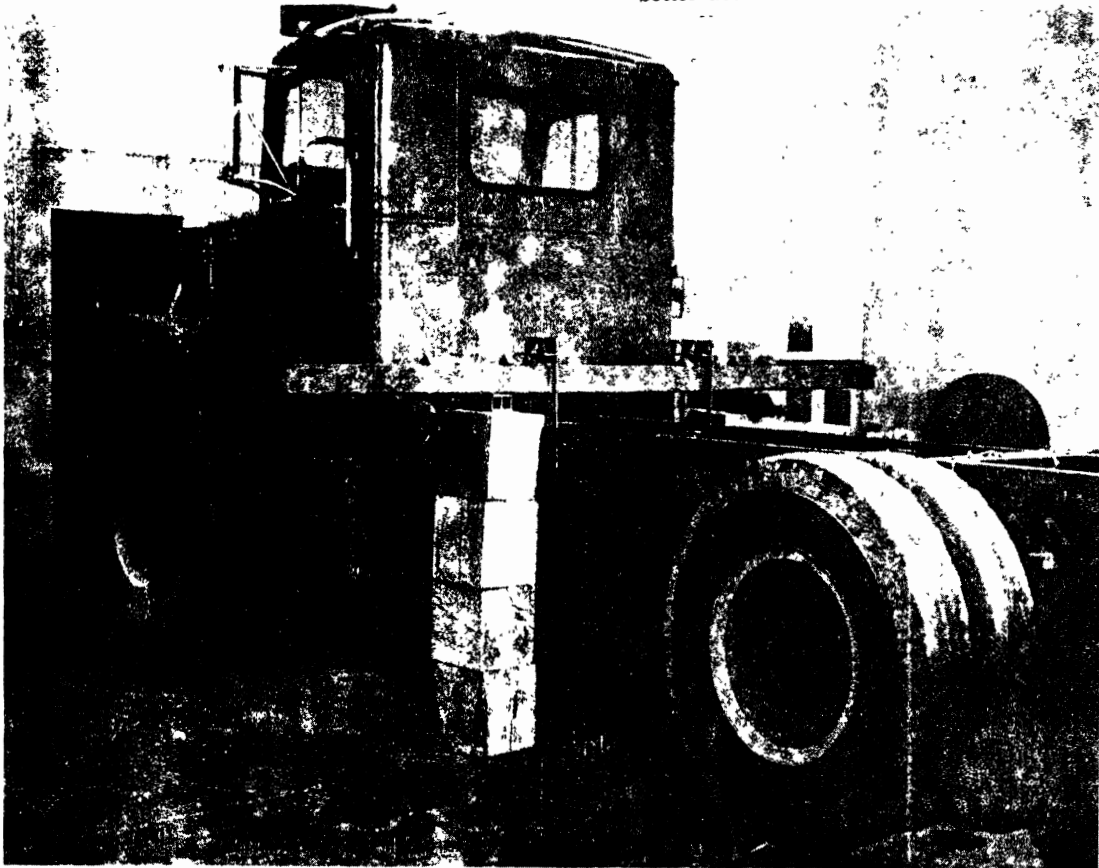


Figure 4-25. Pitch moment of inertia measurement.

the effects of unsprung masses, and add in the effects of additional masses (i.e., driver and passenger, instrumentation, and loads).

Equations for calculating the c.g. location and the moment of inertia of the sprung weight, making adjustments for the weights added and deleted, are given below:

Fore-aft c.g. position:

$$\ell = \frac{\sum_{i=1}^n {}_1W_i {}_1\ell_i - \sum_{j=1}^m {}_2W_j {}_2\ell_j}{W_0 + \sum_{i=1}^n {}_1W_i - \sum_{j=1}^m {}_2W_j} \quad (4-6)$$

Vertical c.g. position:

$$h = \frac{\sum_{i=1}^n {}_1W_i {}_1h_i - \sum_{j=1}^m {}_2W_j {}_2h_j}{W_0 + \sum_{i=1}^n {}_1W_i - \sum_{j=1}^m {}_2W_j} \quad (4-7)$$

Moment of inertia:

$$I = I_0 + \sum_{i=1}^n \left[{}_1I_i + \frac{{}_1W_i}{g} {}_1d_i^2 \right] - \sum_{j=1}^m \left[{}_2I_j + \frac{{}_2W_j}{g} {}_2d_j^2 \right] + \frac{W_0}{g} d^2 \quad (4-8)$$

where:

W_0 total weight of vehicle as originally tested for c.g. position (lb.)

${}_1W_i$ weights to be added to vehicle (lb.)

${}_2W_j$ weights to be subtracted from vehicle (lb.)

${}_1\ell_i$ horizontal distance in the pitch plane from c.g. of W_0 to c.g. of ${}_1W_i$. ${}_1\ell_i$ is positive if ${}_1W_i$ is forward of W_0 , negative if ${}_1W_i$ is aft of W_0 . (in.)

${}_2\ell_j$ horizontal distance in the pitch plane from c.g. of W_0 to c.g. of ${}_2W_j$. ${}_2\ell_j$ is positive if ${}_2W_j$ is forward of W_0 , negative if aft of W_0 . (in.)

ℓ horizontal distance in the pitch plane from c.g. of W_0 to adjusted c.g. position. ℓ is positive if new c.g. is forward of W_0 , negative if new c.g. is aft of W_0 . (in.)

${}_1h_i$ vertical distance in the pitch plane from c.g. of ${}_1W_i$ to c.g. of W_0 . ${}_1h_i$ is positive if ${}_1W_i$ is above W_0 , negative if below W_0 . (in.)

- ${}_2h_j$ vertical distance in the pitch plane from c.g. of ${}_2W_j$ to c.g. of W_0 . ${}_2h_j$ is positive if ${}_2W_j$ is above W_0 , negative if below W_0 . (in.)
- h vertical distance in the pitch plane from c.g. of W_0 to adjusted c.g. position. h is positive if new c.g. is above W_0 , negative if below W_0 . (in.)
- I_0 moment of inertia about the c.g. of the vehicle as originally tested. (in lb sec²)
- ${}_1I_i$ moments of inertia about their own c.g. of the masses to be added to the vehicle (in lb sec²)
- ${}_2I_j$ moments of inertia about their own c.g. of the masses to be subtracted from the vehicle (in lb sec²)
- I adjusted moment of inertia of the vehicle about the adjusted c.g. position (in lb sec²)
- ${}_1d_i$ total distance in the pitch plane from the c.g. of ${}_1W_i$ to the adjusted c.g. position (in.)
- ${}_2d_j$ total distance in the pitch plane from the c.g. of ${}_2W_j$ to the adjusted c.g. position (in.)
- d total distance in the pitch plane from the c.g. of W_0 to the adjusted c.g. position. (in.) $d = (\ell^2 + h^2)^{1/2}$
- n number of masses to be added.
- m number of masses to be subtracted
- g 386 in/sec²

Note that the moment of inertia cannot be calculated using equation 4-8 until the c.g. position as calculated using equation 4-6 and 4-7 has been determined. Further, note that weights affecting the calculations in equation 4-8 may be considered in two categories:

1. Those weights whose linear dimensions in the pitch plane are small relative to the vehicle and may be considered as point weights. Thus, ${}_1I_i$ or ${}_2I_j$ of these bodies can be assumed to be zero. Such masses include unsprung masses, driver and passenger, and instrumentation.
2. Masses whose linear dimensions in the pitch plane are large. These would include vehicle bodies and payloads. The moment of inertia of these masses about their own c.g. must be considered. Such moments of inertia can be determined by calculation or independent measurement.

If there is only one weight and/or inertia requiring addition (or subtraction) from the model, the computations above may be performed by the program through the use of PW and PJ as explained in Section 2.2.

The moment of inertia of the trailer was obtained by computing the moment of inertia of each part about its c.g., then using the parallel axis theorem to find the inertias about an axis through the vehicle c.g., and finally adding these. All moments of inertia are about an axis system having its origin at the c.g. of the sprung mass.

4.2.4 ROLLING INERTIA OF WHEELS. Rolling inertia of the tire-wheel-drum assemblies of the two vehicles were measured using the classical torsional pendulum technique [16]. The apparatus used is pictured in Figure 4-26. The half-shafts were included with the dual wheel assemblies for the inertia measurements.

The equation for calculating the moment of inertia about the c.g. of the assemblies is

$$I = \frac{W_r \tau^2}{4\pi^2 \ell} + \frac{W_b r^2}{4\pi^2 \ell} (\tau^2 - \tau_o^2) \quad (4-9)$$

where W = test weight of the assembly

W_b = weight of the supporting platform

ℓ = length of the supporting cables

r = horizontal distance from center of platform to supporting cables

τ = period of oscillation of platform plus assembly

τ_o = period of oscillation of platform only.

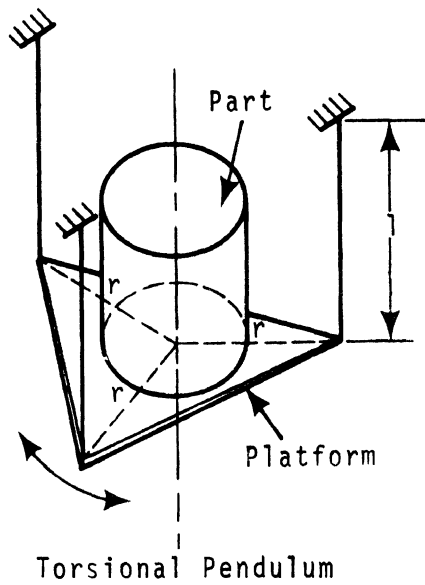
4.2.5 SUMMARY OF INERTIAL PARAMETER MEASUREMENTS. Tables 4-1 and 4-2 give a summary of the inertial parameters measured and/or calculated for the test vehicles.

4.3 TIRE PARAMETERS

The parameters required as inputs to the tire model, for the case when motion is restricted to the plane of the tire, were identified in section 2.2 as CS, the longitudinal stiffness, KT , the vertical rolling spring rate, and the tire-road interface parameters μ_o and FA.

KT and CS can both be measured by means of the HSRI Flat Bed Tire Test Machine. [17]. To measure KT , camber and sideslip angles are set to zero, the tire inflation pressure and load set at the specified values, and the bed is moved past the tire; the rolling height of the tire is measured while the tire rolls freely on the bed. The value of KT is determined from the slope of the vertical load versus rolling height characteristic plotted for a given tire inflation pressure. Values of vertical rolling spring rate, determined for various sizes and types of truck tires are given in Table 4-3.

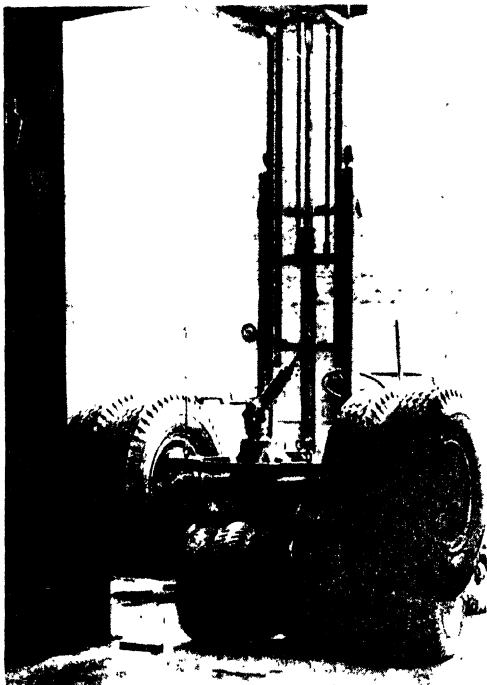
To determine the longitudinal stiffness, CS, of the tire, the same procedure as described for determining rolling height is used, except that a resisting or driving torque is applied to the tire. Longitudinal force is measured and plotted against the longitudinal slip of the tire on the bed. The slip values are calculated using rolling height, tire rotational velocity, and bed velocity. The force-slip characteristic is determined for each tire by making measurements at specified values of normal load and inflation pressure for several values of applied torque. Table 4-4 contains values of longitudinal stiffness for a wide variety of truck tires.



This page is reproduced at the back of the report by a different reproduction method to provide better detail.



Torsional Pendulum Platform With Tire, Wheel, & Brake Drum Assembly



Pendulum Suspended by Means of Lift Truck

Figure 4-26. Apparatus for measuring polar moment of inertia of wheels and rotating assemblies.

TABLE 4-1
INERTIAL PROPERTIES OF TEST VEHICLES

Vehicle	Total Weight lbs.	Unsprung Front lbs.	Unsprung Rear lbs.	Sprung Weight lbs.	Center of Gravity Total Vehicle a	Location* Sprung Weight h	Pitch Moment of Inertia About Sprung Weight c.g., in-lb-s
Truck							
bare frame	14,000	1750	4050	8200	85	395	103,491
empty box	21,400	1750	4050	15,600	116	106	378,434
loaded low c.g.	45,200	1750	4050	39,400	137	136	611,875
loaded high c.g.	50,500	1750	4050	44,700	106	121	601,000
Tractor							
bobtail	15,000	1300	4400	9300	67	36	53,374
Trailer							
empty	12,200	--	3000	9200	126	144	607,200
loaded	59,300	--	3000	56,300	173	177	2,055,000

* a = distance behind front axle, inches (or from centerline of rear suspension on the trailer)
h = distance above ground, inches

TABLE 4-2
POLAR MOMENTS OF INERTIA FOR ROTATING ASSEMBLIES*

	Truck	Tractor	Trailer
Front Wheel-Tire-Drum Assembly	163	103	---
Rear Dual Wheel-Tire-Drum Assembly	205	231	231

*Values given in inch-lb-sec².

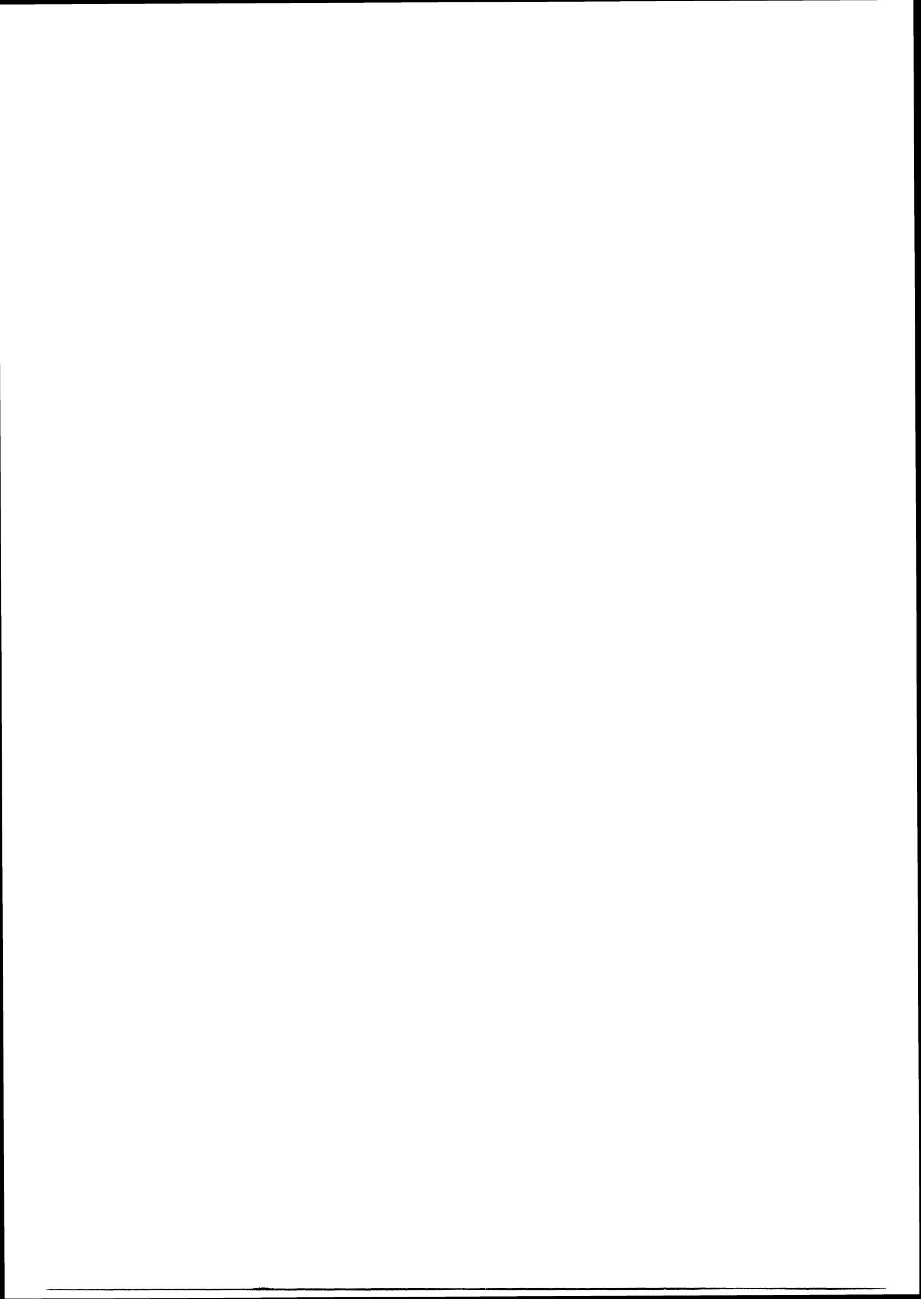
TABLE 4-3
VERTICAL SPRING RATE OF TRUCK TIRES

Tire	Inflation Pressure (psi)	Vertical Spring Rate (lb/in)
Highway Tread 10 X 20/F	50	2943
	85	4700
	100	4309
Highway Tread 10 X 20/G	50	2857
	85	4363
	100	5532
Lub Type Tread 10 X 20/F	50	3600
	85	4500
	100	5000
Competitive Highway Tread 10 X 20/F	50	2680
	85	5032
	100	5416
Half-Worn Highway Tread 10 X 20/F	85	3939
Full-Worn Highway Tread 10 X 20/F	85	4600
Highway Tread 15 X 22.5/H	90	5420
Highway Tread 11 X 22/F	85	5578
Highway Tread 11 X 22/G	90	5852
Highway Tread 12.50 X 22.5/G	90	4785
Highway Tread 12 X 22.5/F	85	4534
Highway Tread 12 X 20/G	80	4800
Highway Tread 11 X 22.5/F	85	5700
Highway Tread 1 X 20/E	80	3823
Highway Tread 9 X 20/F	85	4122
Highway Tread 8.25 X 20/E	85	3900

TABLE 4-4
LONGITUDINAL STIFFNESS OF TRUCK TIRES

Tire	Inflation Pressure (psi)	Vertical Load (lb)	C _s -Longitudinal Stiffness (lb/unit slip)
Highway Tread	50	5430	36,000
10 X 20/F	85	2800	28,000
	85	5430	42,000
	85	8100	42,000
	100	5430	40,000
Highway Tread	85	5430	50,000
10 X 20/G			
Lug Type Tread	85	5430	28,000
10 X 20/F			
Competitive	50	5430	70,000
Highway Tread	85	2800	33,000
10 X 20/F	85	5430	46,000
	85	8100	53,000
	100	5430	46,000
Half-Worn			
Highway Tread	85	5430	52,000
10 X 20/F			
Full-Worn			
Highway Tread	85	5430	60,000
10 X 20/F			
Highway Tread	90	2900	47,000
15 X 22.5/H		8640	85,000
		10,000	76,000
Highway Tread	85	2100	21,000
11 X 22/F		6290	47,000
		9800	48,000
Highway Tread	90	2100	23,000
11 X 22/G		6140	51,000
		10,000	60,000
Highway Tread	90	1960	21,000
12.50 X 22.5/G		5890	62,000
		9800	50,000
Highway Tread	85	2000	20,000
12 X 22.5/F		5920	58,000
		10,000	57,000
Highway Tread	80	2100	23,000
12 X 20/G		6140	60,000
		9900	74,000
Highway Tread	85	1800	18,000
11 X 22.5/F		5430	56,000
		8700	46,000
Highway Tread	80	1200	14,000
9 X 20/E		4160	41,000
		6500	52,000
Highway Tread	85	1400	16,000
9 X 20/F		4250	41,000
		6800	50,000
Highway Tread	85	1300	14,000
8.25 X 20/E		4050	22,000
		6500	36,000

Values of μ_0 and FA must be obtained from road tests, or estimated. Selection of appropriate values for μ_0 and FA is discussed in section 6.



5.0 VEHICLE BRAKING TESTS

5.1 INTRODUCTION

In order to provide experimental data suitable for verification of the Braking Performance Simulation Program, a straight truck and a tractor-trailer combination were subjected to a series of braking performance tests. These included brake effectiveness tests on high and low coefficient of friction surfaces, parking brake tests, static brake response time tests, and for the tractor-trailer, a brake balance test.

The straight truck, a 4X6, 50,000 lb. G.V.W. vehicle with a 190" wheel base, is pictured in Figure 5-1. It was fitted with a dump-type body for the test program. The tractor-trailer, a 4X6, 46,000 lb. G.V.W., 142" wheel base, cab-over-tractor in combination with a 40-foot, van-type, 2-axle trailer is pictured in Figure 5-2. Vehicle specifications are given in Tables 5-1 and 5-2. The straight truck was equipped with a walking beam type rear suspension, while the tractor and the trailer were each equipped with a four spring suspension. Thus, data was made available for verification of the walking beam and four spring suspension modules employed in the simulation.

During testing, the vehicles were loaded such that the center of gravity location generally corresponded to that of the normal service condition intended to be simulated. The straight truck was tested in the empty condition (i.e., with empty dump body), in a fully loaded condition (i.e., dump body loaded with gravel), and in a high c.g. load configuration. For the latter configuration, the center of gravity height of the vehicle-load combination approximated that of a typical concrete mixer truck. To achieve the high center of gravity, the vehicle was loaded with steel blocks on a platform placed on the floor of the dump body, as shown in Figure 5-3.

The tractor-trailer combination was tested with the trailer empty and with the trailer loaded to gross vehicle weight with con-trainerized gravel. Static axle loads and center of gravity position for the various loading conditions of the two vehicles are listed in Table 5-3.

Since the truck and tractor were both new vehicles, and the trailer had been reconditioned to the "as new" condition, a minimum amount of preparation was required to prepare the vehicles for brake performance testing. OEM tires on both vehicles were replaced with those tires specified for testing. A dump body was installed on the straight truck. The tractor-trailer combination was fitted with the articulation angle limiter pictured in Figure 5-4. (This device limits the vehicle articulation angle to a nominal value of $\pm 15^\circ$.) Both vehicles were fitted with a brake pedal stop, depicted in Figure 5-5, which could be adjusted for a given brake line pressure prior to testing and thus allowed an open loop quasi-step brake application.

The instrumentation installed in each vehicle was quite extensive. Table 5-4 and 5-5 list the equipment employed in the braking performance tests on the straight truck and tractor-trailer. Figure 5-6 shows the signal processing equipment which was installed in the cab of the truck above the stabilized platform unit. To eliminate any problem arising from motion of the tractor cab with respect to the vehicle frame, only the signal processing and recording equipment was mounted in the cab of the tractor (see Figure 5-7), and the inertial sensing unit was mounted outside the cab on the frame rails (see Figure 5-8).

All tests were conducted on the oval track or skid pad at the Bendix Automotive Development Center at New Carlisle, Indiana. Tests

Preceding page blank

This page is reproduced at the back of the report by a different reproduction method to provide better detail.

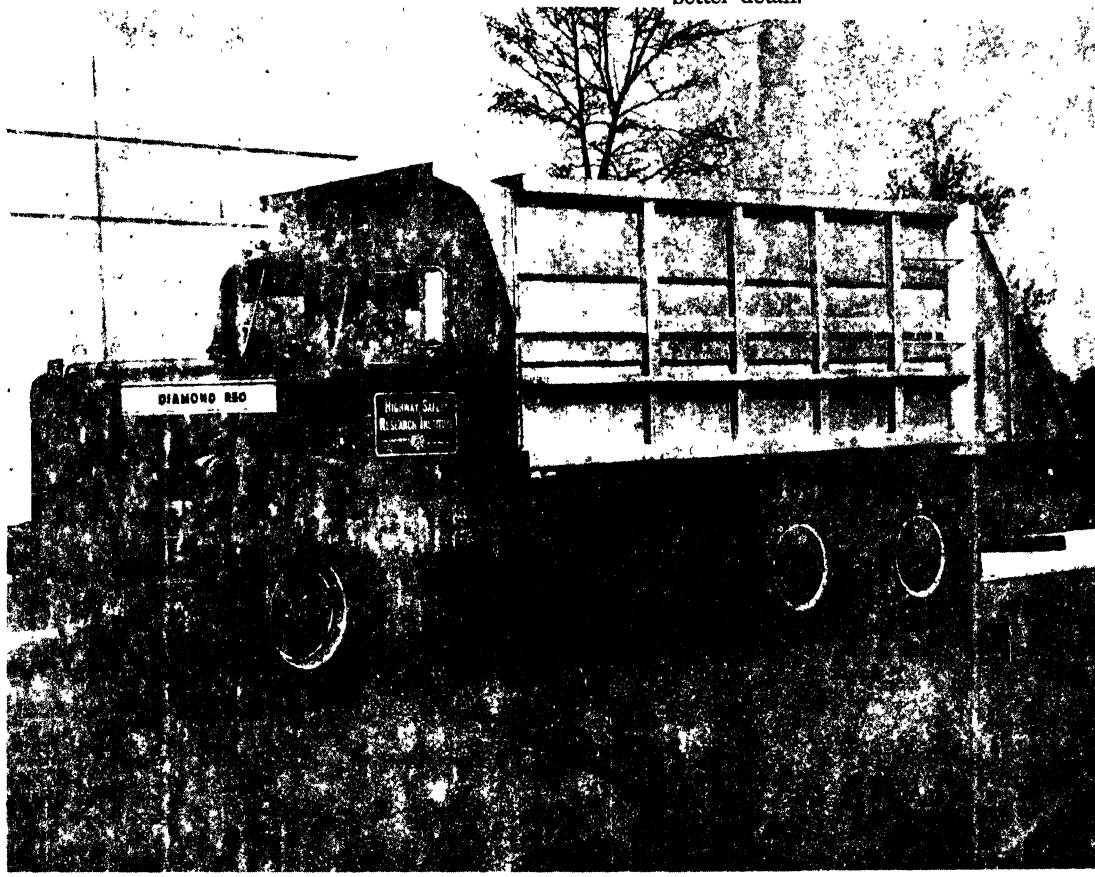


Figure 5-1. Test vehicle, straight truck

This page is reproduced at the back of the report by a different reproduction method to provide better detail.

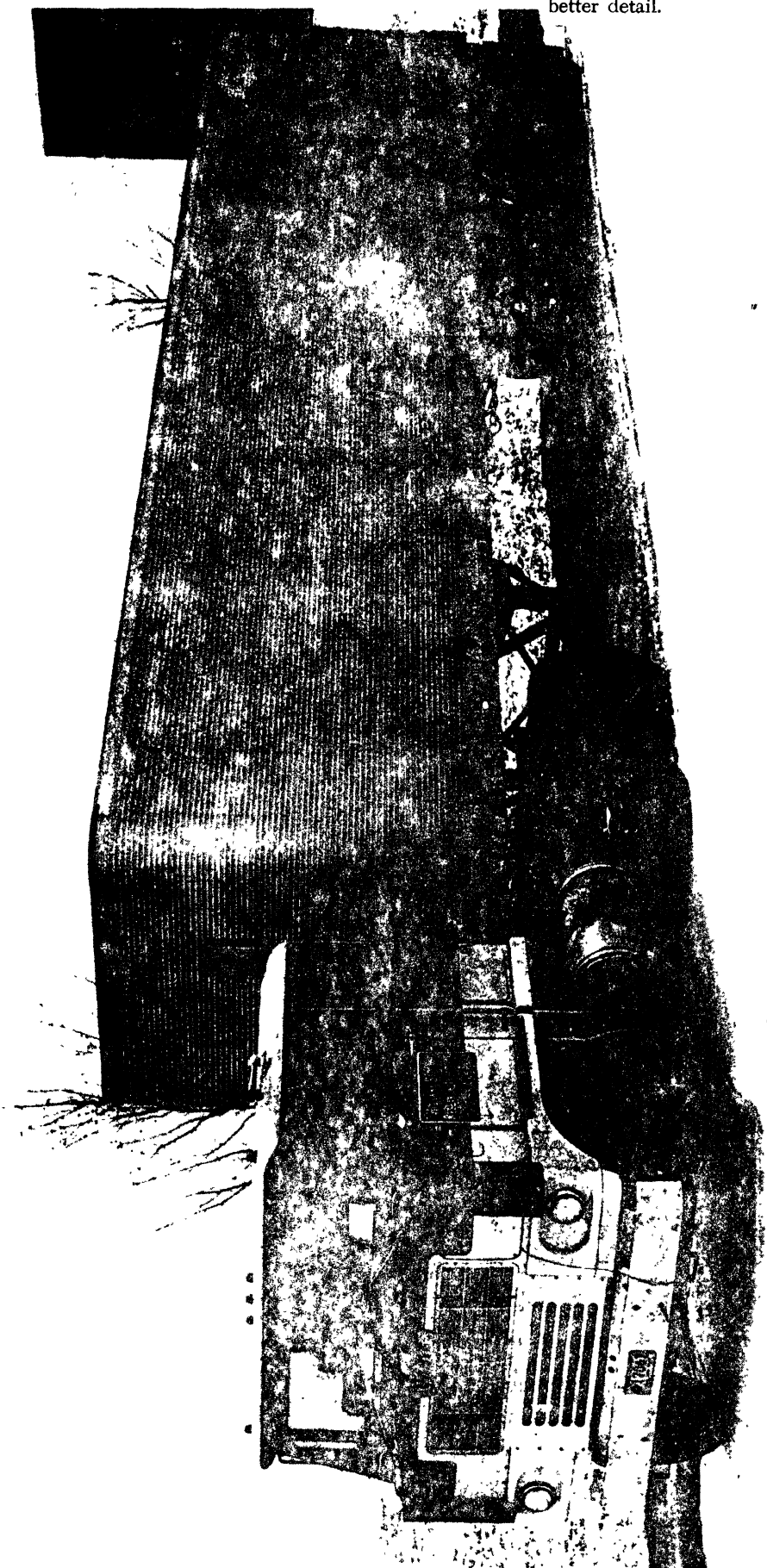


Figure 5-2. Test vehicle, tractor-trailer.

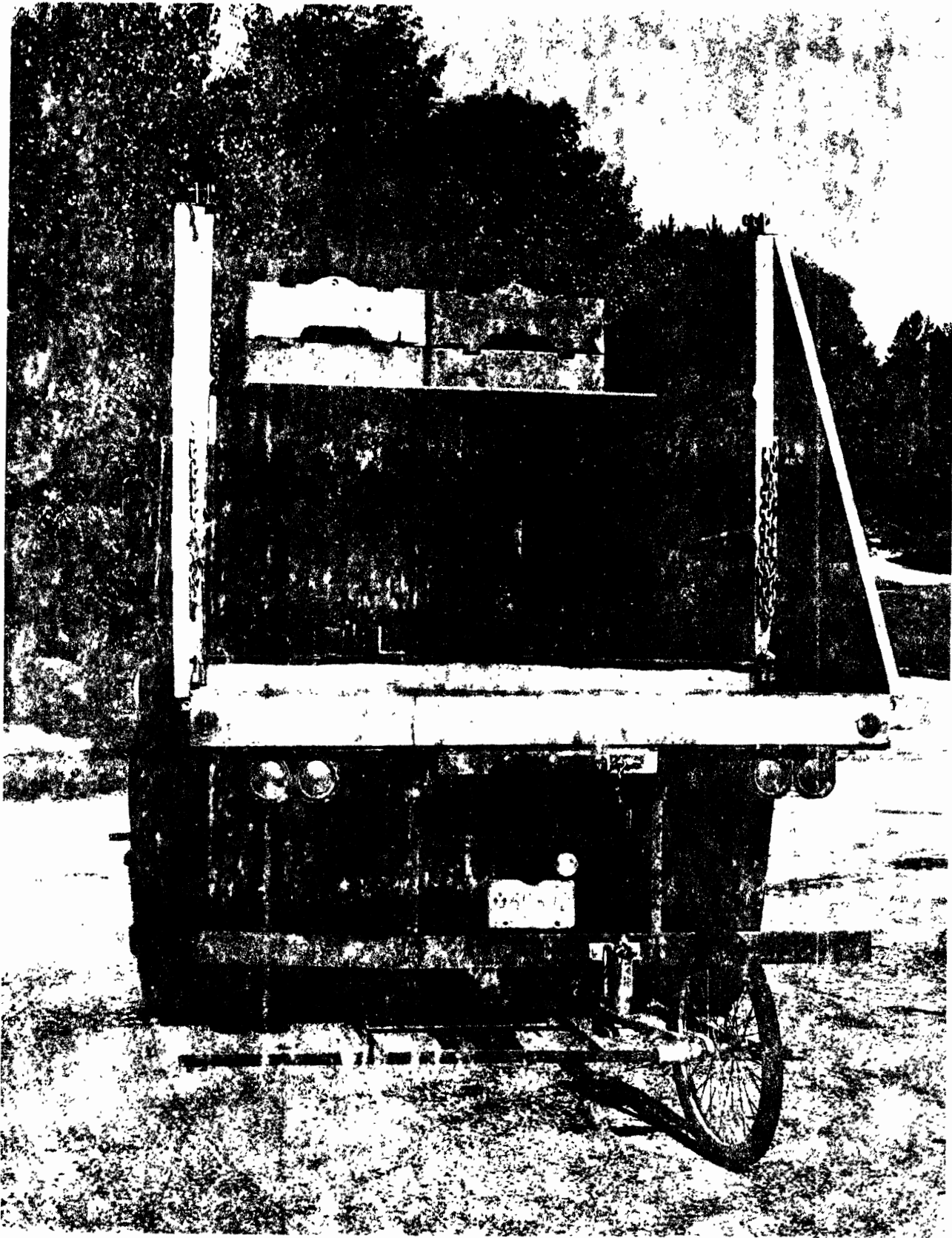


Figure 5-3. High c.g. load configuration

This page is reproduced at the back of the report by a different reproduction method to provide better detail.

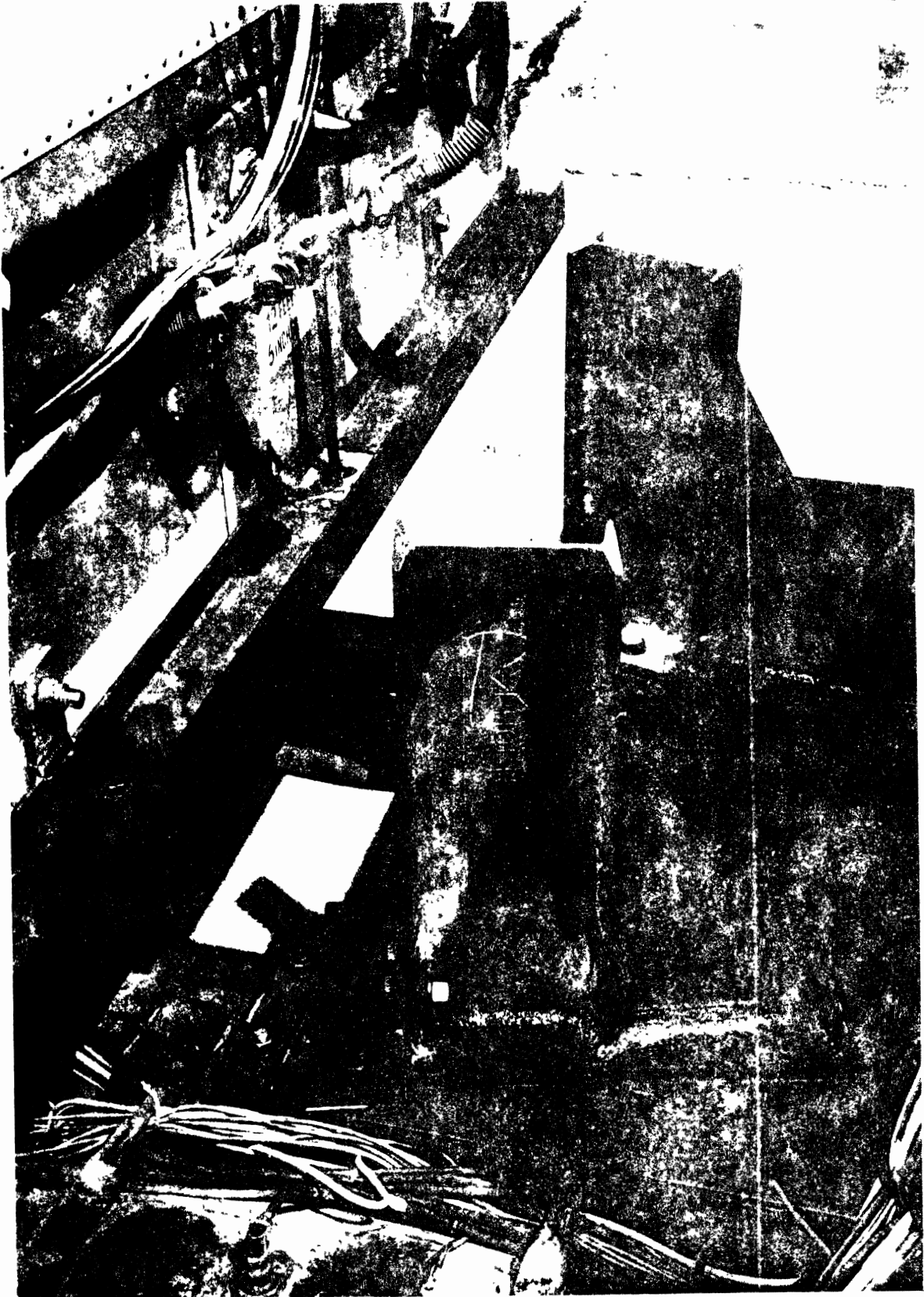


Figure 5-4. Articulation angle limiter

This page is reproduced at the back of the report by a different reproduction method to provide better detail.

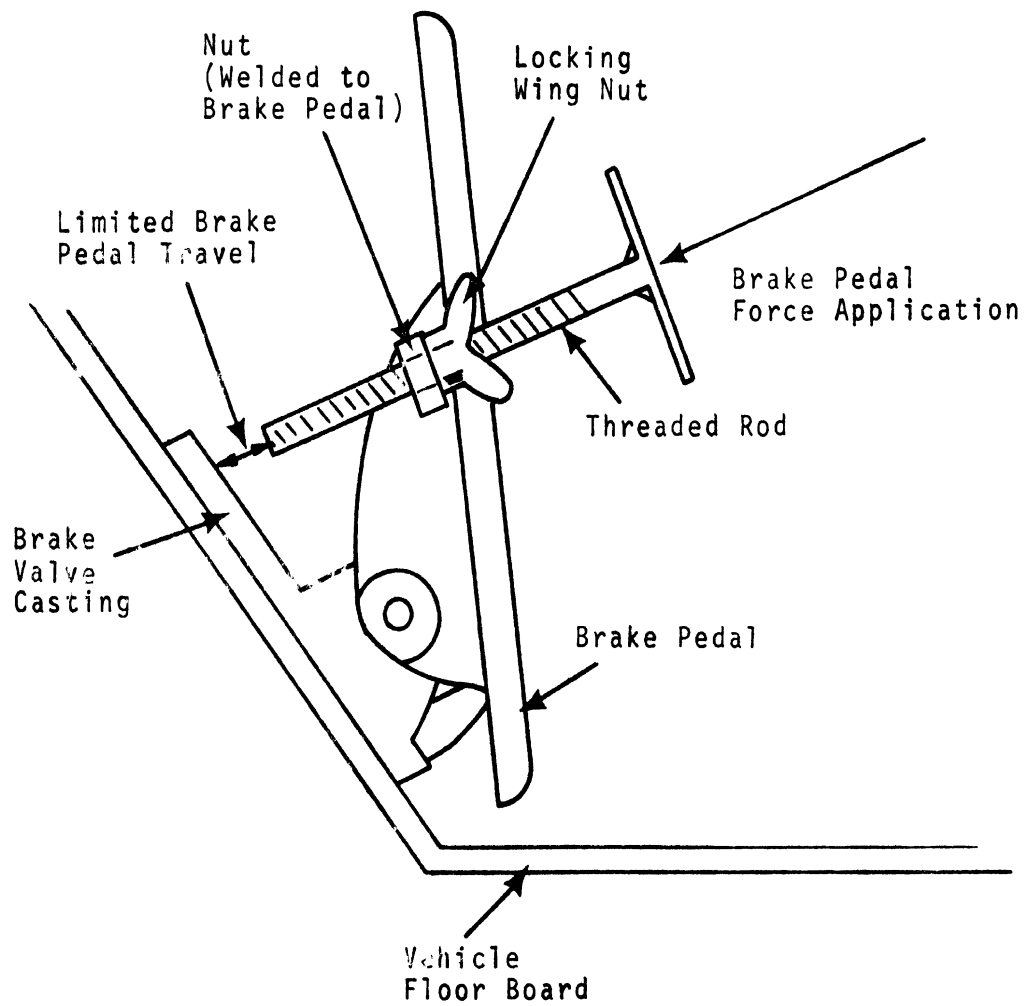


Figure 5-5. Brake pedal stop

This page is reproduced at the back of the report by a different reproduction method to provide better detail.

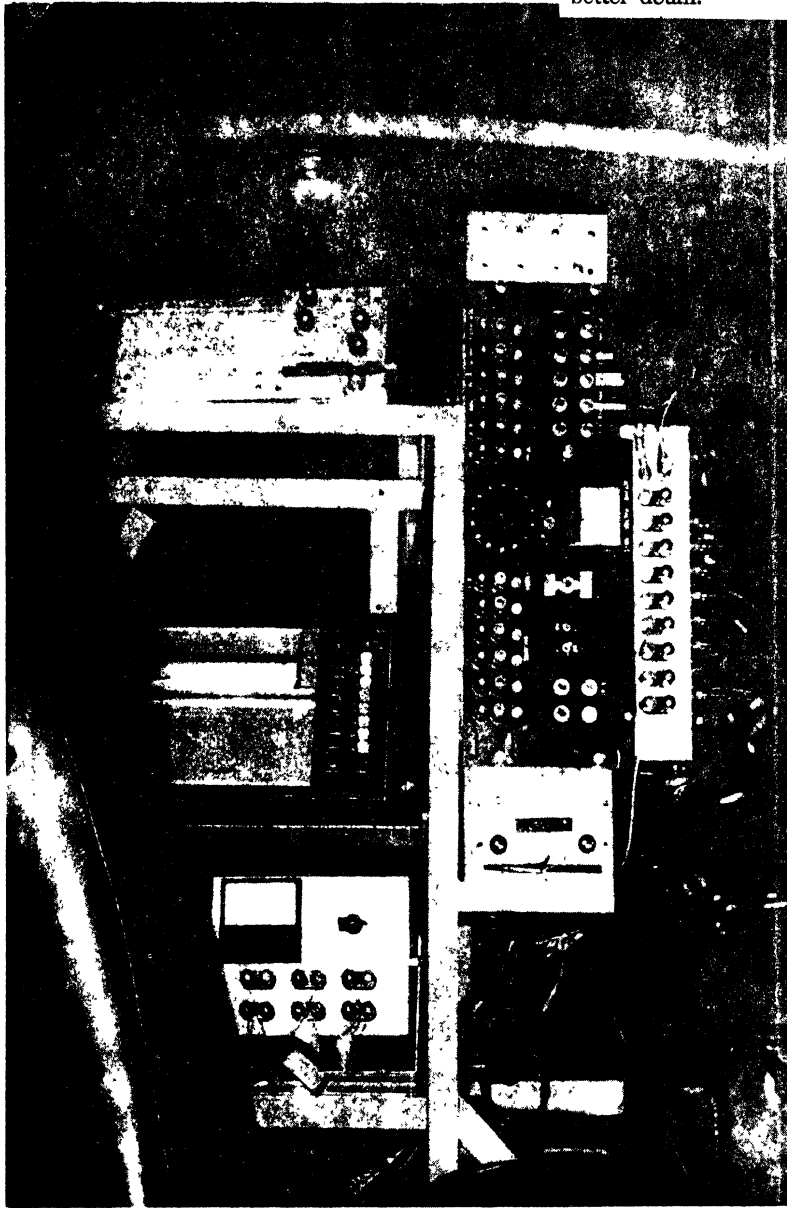


Figure 5-6. Signal processing equipment installed in truck

This page is reproduced at the back of the report by a different reproduction method to provide better detail.



Figure 5-7. Signal processing equipment installed in tractor cab

This page is reproduced at the back of the report by a different reproduction method to provide better detail.

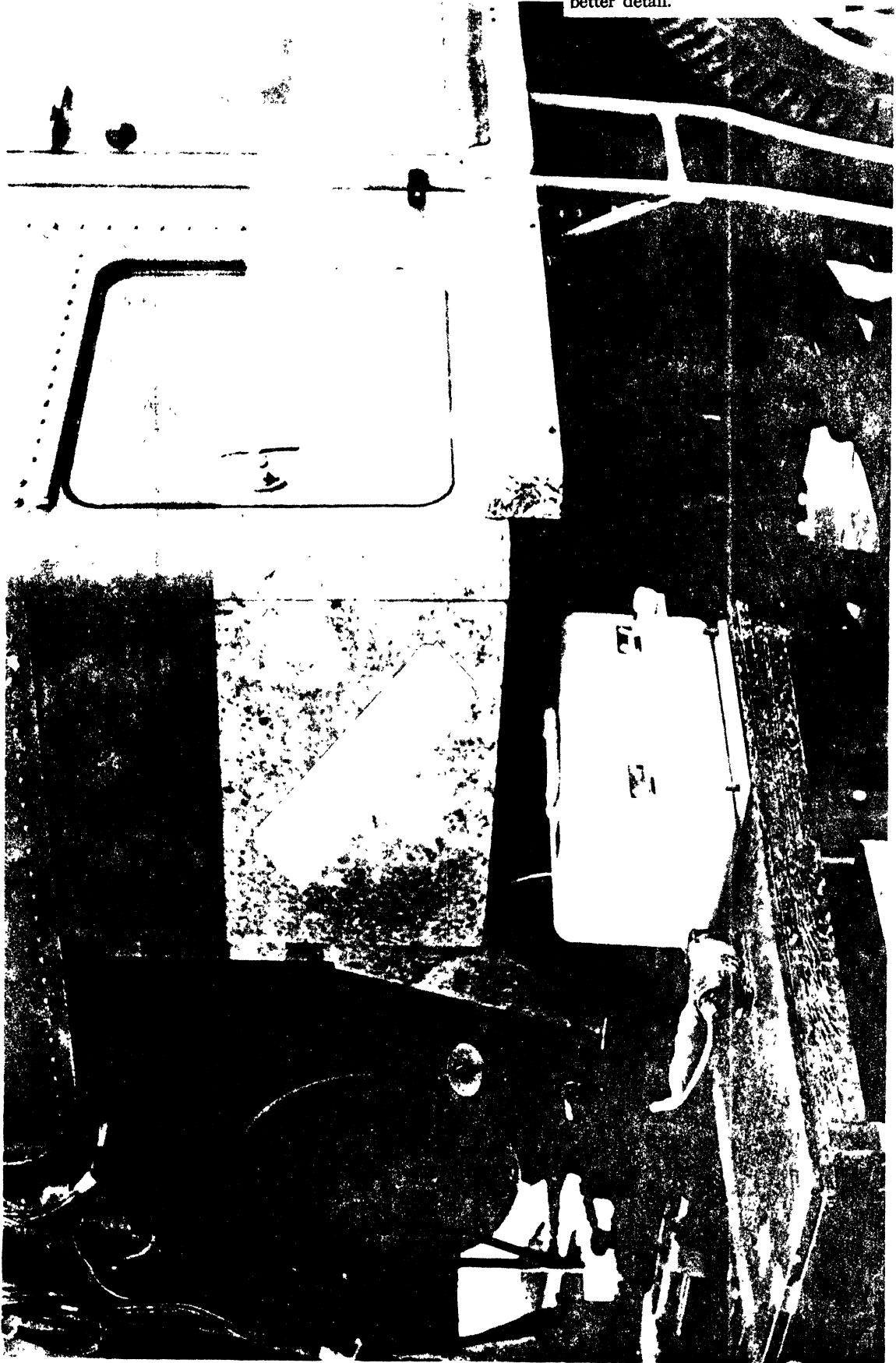


Figure 5-8. Stabilized platform unit mounted on tractor frame

TABLE 5-1
VEHICLE SPECIFICATIONS, STRAIGHT TRUCK

General	4X6, 50,000 lb. gw, straight truck, 190" wheel base	
Engine	V8-210	
Transmission	5 speed forward, 1 reverse with 4 speed auxiliary spicer	
Rear Axles	34,000 rated load with 7.8 ratio	
Steering Gear	19:24:19, hydraulic power	
Wheels	cast spoke	
Brakes	Front	Rear
	dual chamber wedge type	dual chamber wedge type
Air Chamber	type 9	type 12
Wedge Angle	12°	12°
Size	15 x 5	15 x 6
Linings	RM-MA-417A	ABB-693-551-D
Lining Area	314 sq. in.	752 sq. in.
Parking-Emerg.	-----	single wedge, spring actuated, 4 rear wheels
Axles	16,000 lb.	34,000 lb.
Suspension	leaf springs, 11 leaves, 7000 lb.	rubber springs, RSA-340, 34,000 lb., aluminum walking beam
Tires		
Size	highway tread, tubeless 15 - 22.5	highway tread, tube type 10.00 - 20
Load Range	H	F

TABLE 5-2
VEHICLE SPECIFICATIONS, TRACTOR-TRAILER

TRACTOR		
Model	4X6, 46,000 lb. gvwt, 142" wheel base, COE (sleeper type)	
Engine	V-8, 335	
Transmission	5 speed forward, 1 reverse, 2 speed auxiliary spicer	
Rear Axle	34,000 with 4.11 ratio	
Steering Gear	28:1 constant ratio, lock to lock	
Wheels	cast spoke	
Brakes	Front	Rear
Special Equip.	dual chamber wedge type limiting and quick release valve	dual chamber wedge type relay valve and quick release valve
Air Chamber	type 12	type 12
Wedge Angle	12°	12°
Size	15 X 4	15 X 7
Linings	RM-MR-417A	RM-MA-417A
Parking-Emerg.	-----	single wedge, spring actuated, 4 rear wheels
Axles	12,000 lb.	34,000 lb.
Suspension	leaf spring	4 spring
Tires	highway tread, tube type	deep lug, tube type
Size	10.00 - 20	10.00 - 20
Load Range	F	F
TRAILER		
Model	40 ft., van type, 2 axle, semitrailer	
Suspension	4 spring (3 leaf)	
Axles	34,000 lb.	
Brakes	S-cam, leading-trailing	
Air Chambers	type 30	
Slack Adjusters	6 inch length	
Size	16-1/2 X 7	
Linings	SAE friction code "EE"	
Tires	highway tread, tube type	
Size	10.00 X 20	
Load Range	F	

TABLE 5-3
LOADING CONDITIONS FOR TEST VEHICLES

Vehicle/ Condition	Weights (lb)				Total Vehicle C.G. Positions (in)			
	Front	Rear	Trailer	Total	Tractor-Truck		Trailer	
					Aft of Front Axle	Height	Aft of King Pin	Height
Straight Truck								
empty	8700	12,700	-----	21,400	116	46	-----	-----
loaded	13,000	32,200	-----	45,200	137	55	-----	-----
loaded high	18,300	32,200	-----	50,500	106	78	-----	-----
Tractor- Trailer								
bobtail	8100	6800	-----	14,900	67	40	-----	-----
Trailer empty	8900	10,500	7800	27,200	67	40	265	56
Trailer loaded	10,500	32,000	31,800	74,300	67	40	218	66

TABLE 5-4
INSTRUMENTATION, STRAIGHT TRUCK

Variable	Instrumentation
Brake line pressure at foot valve, P	CEC Type 40327 Strain Gauge Pressure Transducer
Brake line pressure at front axle, P ₁	Dynisco Model APT136 Strain Gauge Pressure Transducer
Brake line pressure at forward tandem axle, P ₂	Dynisco Model APT136 Strain Gauge Pressure Transducer*
Brake line pressure at rear tandem axle, P ₃	Dynisco Model APT136 Strain Gauge Pressure Transducer
Parking brake air pressure at forward tandem axle, P _p	Dynisco Model APT136 Strain Gauge Pressure Transducer*
Pitch Rate, $\dot{\theta}$, longitudinal acceleration, XDD	Humphrey Inc. Stabilized Platform Unit CF 18-0109-1
Wheel rotation lock-up for each of six wheels, LU ₁₋₆	Enwell Bicycle Generators for go/no-go indication
Vehicle velocity, XDOT	Tracktest Fifth Wheel
Stopping Distance, X	Bendix "Shotgun" Indicator
Brake lining temperature for each of six wheels, TEMP ₁₋₆	Serve-Rite, Iron-Constantan Thermocouple
Recorders:	(1) Honeywell Visicorder, Model 2206, 14 Channel, light beam oscillograph
	(2) Clevite-Brush, Model 2310, 16 Channel, light beam oscillograph

*This individual transducer is used in the two indicated applications.

TABLE 5-5
INSTRUMENTATION, TRACTOR-TRAILER

Variable	Instrumentation
Brake line pressure at foot valve, P	CEC Type 4-327 Strain Gauge Pressure Transducer
Brake line pressure at front axle, P ₁	Dynisco Model APT136 Strain Gauge Pressure Transducer
Brake line pressure at tractor rear axle, P ₂	Dynisco Model APT136 Strain Gauge Pressure Transducer*
Brake line pressure at trailer rear axle, P ₃	Dynisco Model APT136 Strain Gauge Pressure Transducer
Parking brake line pressure at forward tandem tractor axle, P _p	Dynisco Model APT136 Strain Gauge Pressure Transducer*
Tractor Pitch, θ ; and longitudinal acceleration, XDD	Humphrey Inc. Stabilized Platform Unit SA07-0114-1
Wheel rotation/lock-up for each of ten wheels, LU ₁₋₁₀	Enwell Bicycle Generators for go/no-go indication
Vehicle velocity, XDOT	Tracktest Fifth Wheel
Stopping Distance, X	Bendix "Shotgun" Indicator
Brake lining temperature for each of ten wheels, TEMP ₁₋₁₀	Serve-Rite, Iron-Constantan Thermocouple
Recorders: Two Honeywell Visicorders, Model 2206, 14 Channel, light beam oscillograph	

*This individual transducer is used in the two applications indicated.

were made on both high coefficient (dry asphalt) and low coefficient (wet jennite) surfaces. Skid trailer data for the surfaces, made available by Bendix, showed the dry asphalt surface has a nominal skid number of 93, and the wet jennite surface a nominal skid number of 24.

Prior to testing, brake burnishing was accomplished according to SAE J880. The new tires installed for testing were "worn in" during this process and on the trip from HSRI to the test site.

5.2 TEST PROCEDURES

The tests conducted for the purpose of providing data for validation of the braking performance computer simulation programs included: brake effectiveness tests, parking brake tests, brake balance tests, and brake response time tests. The effectiveness tests were run on both high and low coefficient surfaces, under a variety of load conditions, from various speeds. The parking brake test was conducted on the dry surface for both the empty and loaded condition. The brake balance test was run only on the loaded tractor-trailer. Static time tests were conducted on both vehicles. Table 5-6 indicates the various conditions for each test. A list of the signals recorded during each test is indicated in Table 5-7.

5.2.1 BRAKE EFFECTIVENESS TEST. With cold brakes (i.e., less than 200°F) and the vehicle traveling in a straight line at the test speed, the clutch was depressed and the brake pedal displaced in a quasi-step manner to a level determined by the position of the brake pedal stop. These conditions were maintained until the vehicle stopped. The steering wheel was held fixed at a nominal zero displacement during the stop.

The tests were conducted at a minimum of five line pressures corresponding to 25, 50, 75, 90 and 100% of the line pressure required to induce first wheel lockup. Within the limits of vehicle stability, line pressures were further increased in order to establish the order and level of occurrence of lockup of as many wheels as possible.

5.2.2 PARKING BRAKE TEST. With cold brakes, and the vehicle traveling in a straight line at 20 mph, the clutch was depressed and the parking brake applied. Input conditions were maintained until the vehicle stopped.

5.2.3 BRAKE BALANCE TEST. The tractor-trailer was subjected to a brake balance test as specified by SAE J-880, except that the vehicle was braked to a full stop from 20 mph, rather than snubbed from 20 mph to 10 mph. The brake pedal stop was used to obtain a nominal steady-state line pressure of 42 psi. Tests were conducted using (1) tractor front brakes only; (2) tractor rear brakes only; (3) trailer brakes only; (4) all brakes.

5.2.4 BRAKE RESPONSE TIME TESTS. The purpose of this test is to determine the response characteristics in application and release of each set of brakes on the vehicles. With the vehicle at rest on a flat level surface, the brake pedal is fully depressed as rapidly as possible, held for approximately 5 seconds, and then released as rapidly as possible.

5.3 TEST RESULTS

5.3.1 EFFECTIVENESS TESTS. Data from the effectiveness tests are presented graphically in Figures 5-9 through 5-15 for the straight truck, and Figures 5-16 through 5-21 for the tractor-trailer combination. Stopping distance and average deceleration as a function of line pressure for the straight truck are presented in Figures

TABLE 5-6
TEST CONDITION MATRIX

Test	Load Condition			
	empty	loaded	loaded high	loaded
Brake Effectiveness	dry asphalt 30&50 mph	dry asphalt 30&50 mph	dry asphalt 30 mph	dry asphalt 30&60 mph
	wet jennite 30 mph	wet jennite 30 mph	wet jennite 30 mph	wet jennite 30 mph
Parking Brake	dry asphalt 20 mph	dry asphalt 20 mph		dry asphalt 20 mph
Brake Balance				dry asphalt 20 mph
Brake Response Time	static			static
				empty
				Tractor-Trailer loaded

TABLE 5-7
TEST MEASUREMENTS

Variable*	Effectiveness Test	Parking Brake Test	Brake Balance Test	Brake Response Time
P	R		R	R
P1	R		R**	R
P2	R		R**	R
P3	R		R**	R
P _p		R		
θ	R	R		
XDD	R	R	R	
XDOT	R	R	R	
X	MEA	MEA	MEA	
LU _{1-6, 10} ⁺	R	R	R	
TEMP _{1-6, 10} ⁺	MON	MON	MON	

Key: R - Recorded continuously on light beam oscillograph.
 MON - Monitored before and after test.
 MEA - Shotgun indication measured before and after test.

* See Tables 5.4 and 5.5 for variable definitions.

** Recorded as appropriate for test conditions.

+ Straight Truck, 6 channels; tractor-trailer, 10 channels.

TABLE 5-8
 MAXIMUM PERFORMANCE, STRAIGHT TRUCK

Initial Velocity Nominal (mph)	Loading Condition	Test Surface	Maximum Deceleration (ft/sec ²)		Minimum Stopping Distance (ft) (corrected to nominal v ₀)	
			No Wheel Lock	All Runs	No Wheel Lock	All Runs
30	empty	dry asphalt	17.9	25.4	67	45
30	loaded	dry asphalt	18.5	19.8	69	52
50	empty	dry asphalt	14.4	21.3	187	220
50	loaded	dry asphalt	18.8	18.8	189	189
30	high c.g.	dry asphalt	16.9	19.3	68	62
50	high c.g.	dry asphalt	13.9	14.9	208	194
30	empty	wet jennite	11.4	13.4	99	88
30	loaded	wet jennite	7.4	11.4	140	103

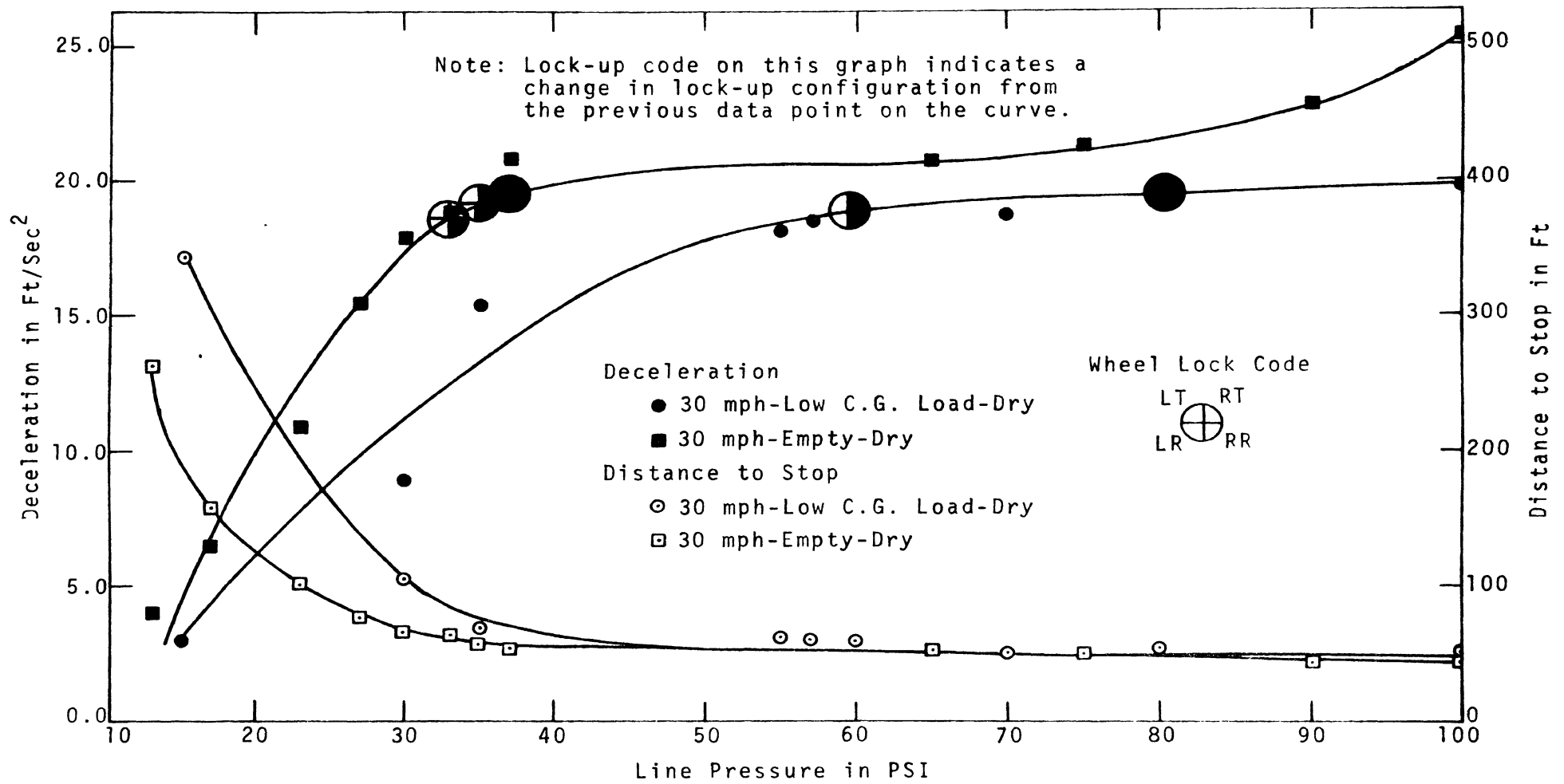


Figure 5-9. Results from effectiveness tests on straight truck from 30 mph, empty and loaded on dry surface

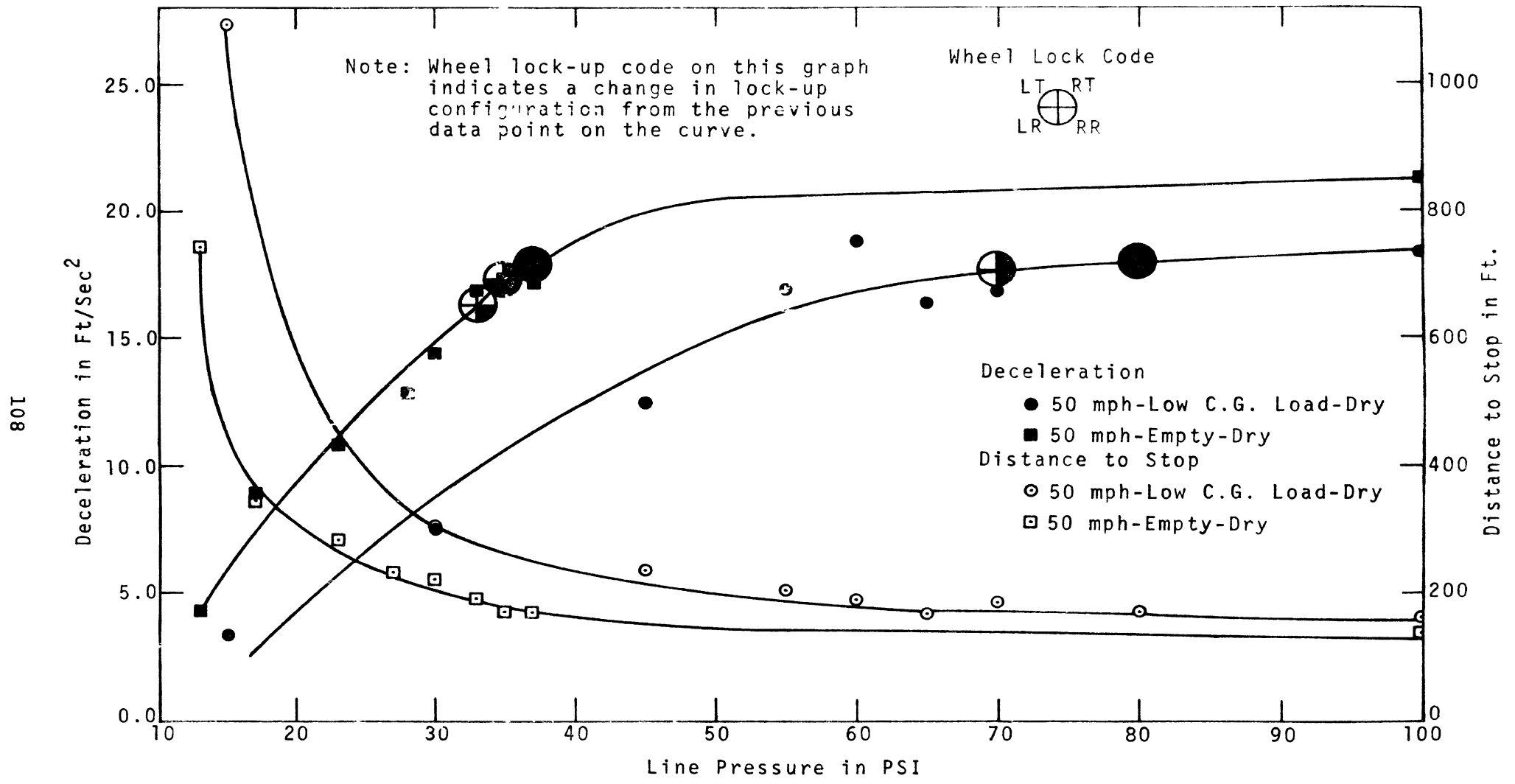


Figure 5-10. Results from effectiveness tests on straight truck from 50 mph, empty and loaded on dry surface

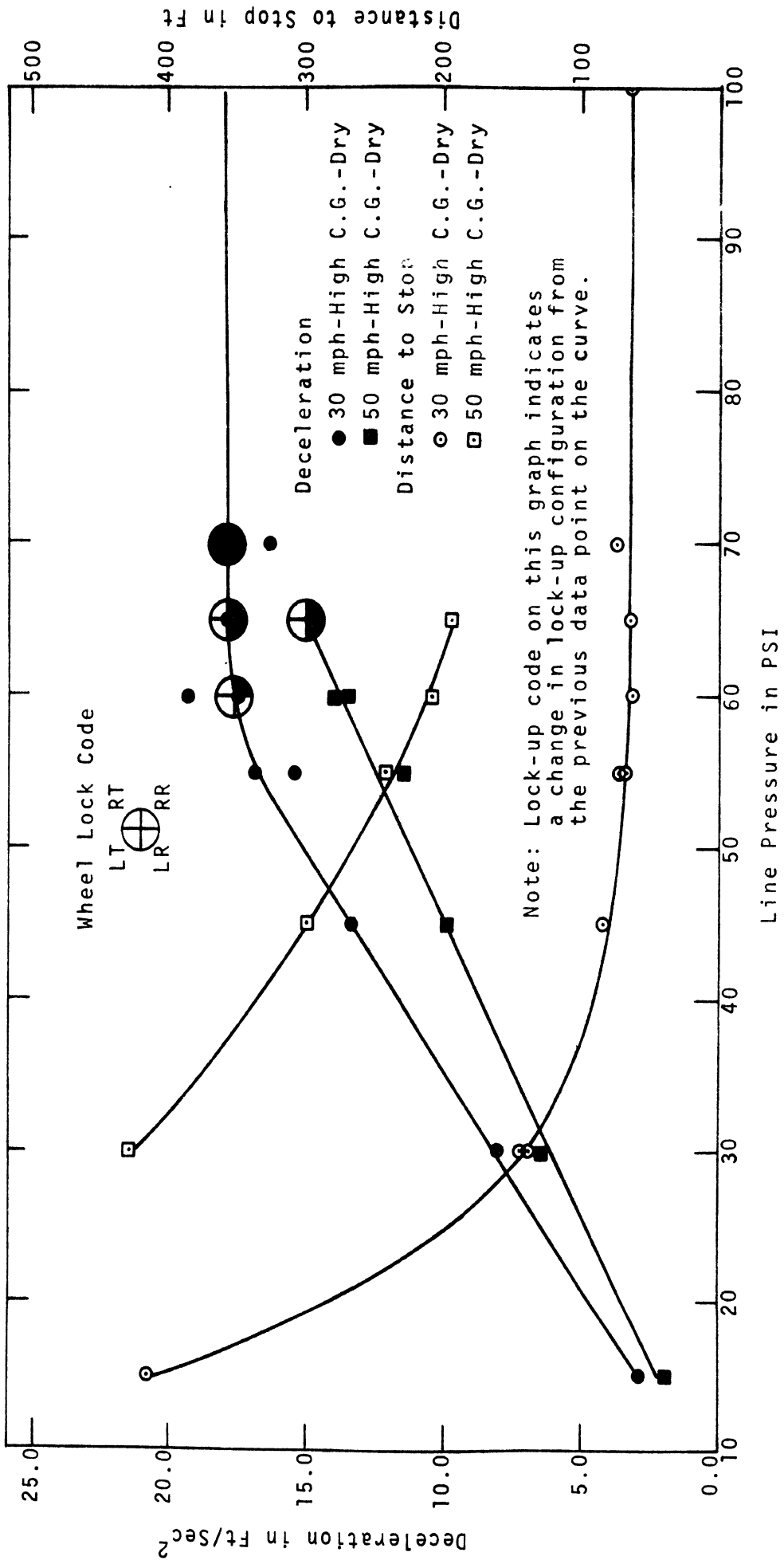


Figure 5-11. Results from effectiveness tests on straight truck from 30 mph, with high c.g. load

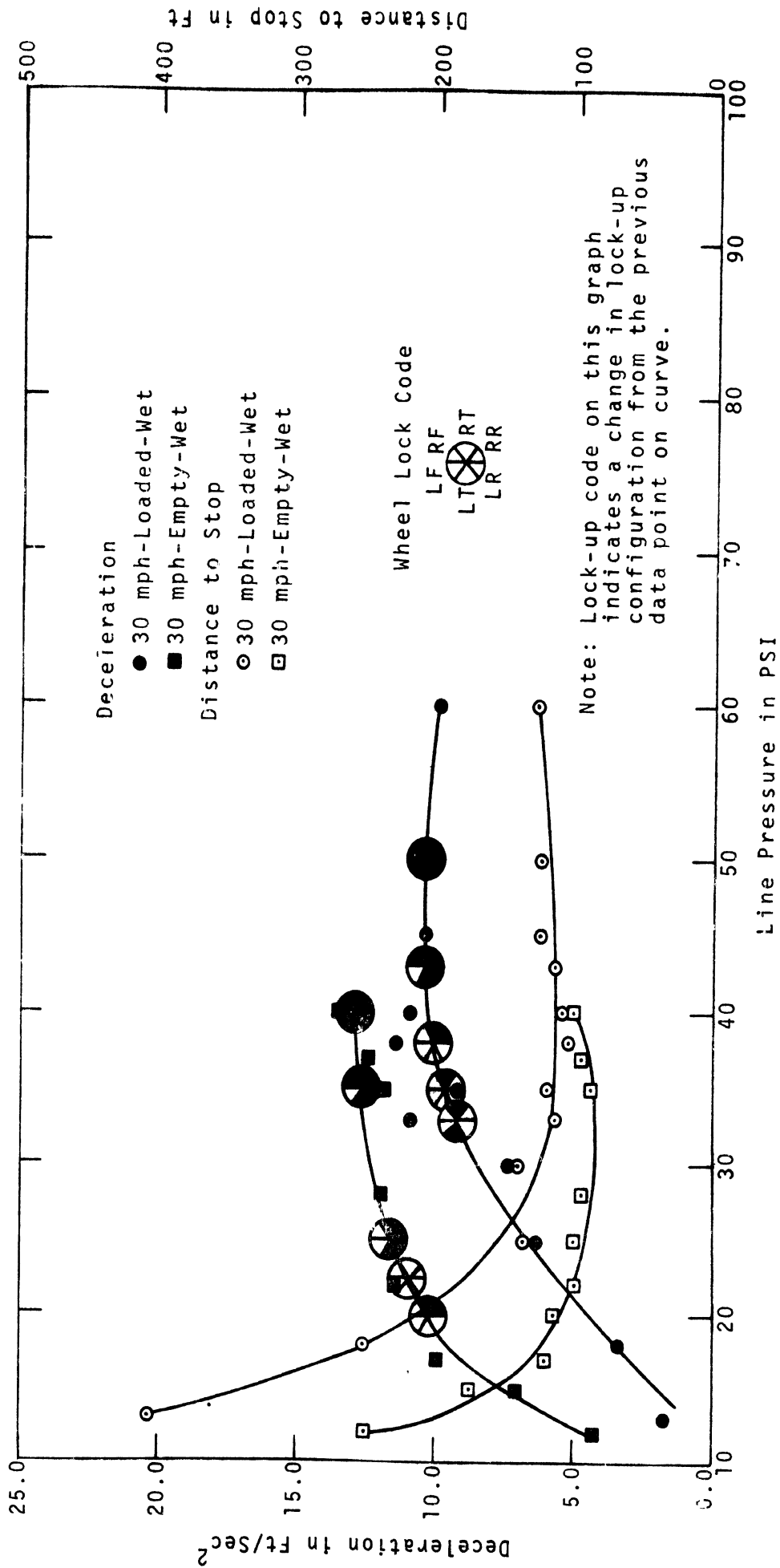


Figure 5-12. Results from effectiveness tests on straight truck from 30 mph, empty and loaded, on wet surface

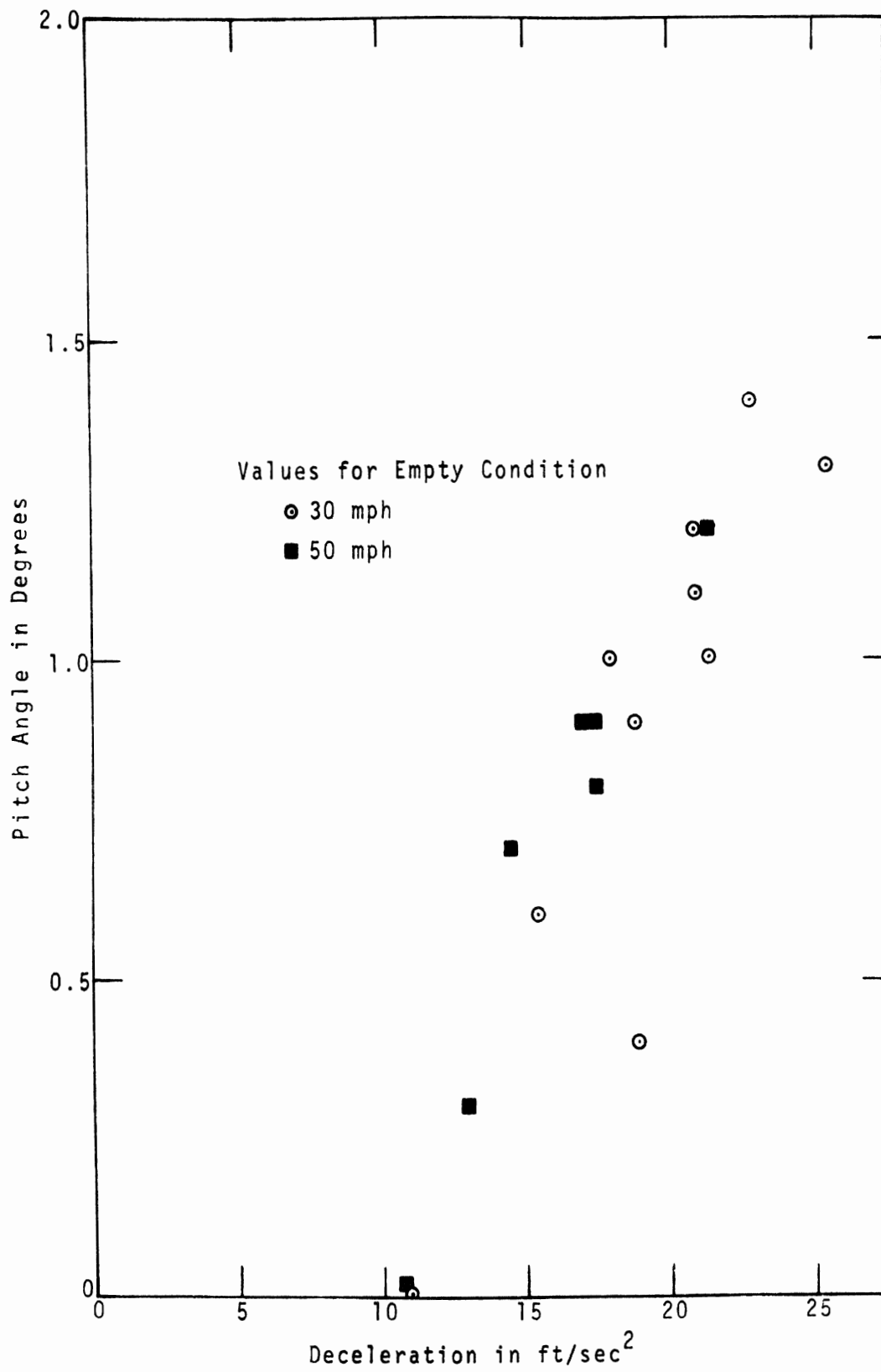


Figure 5-13. Pitch-deceleration data for the empty straight truck

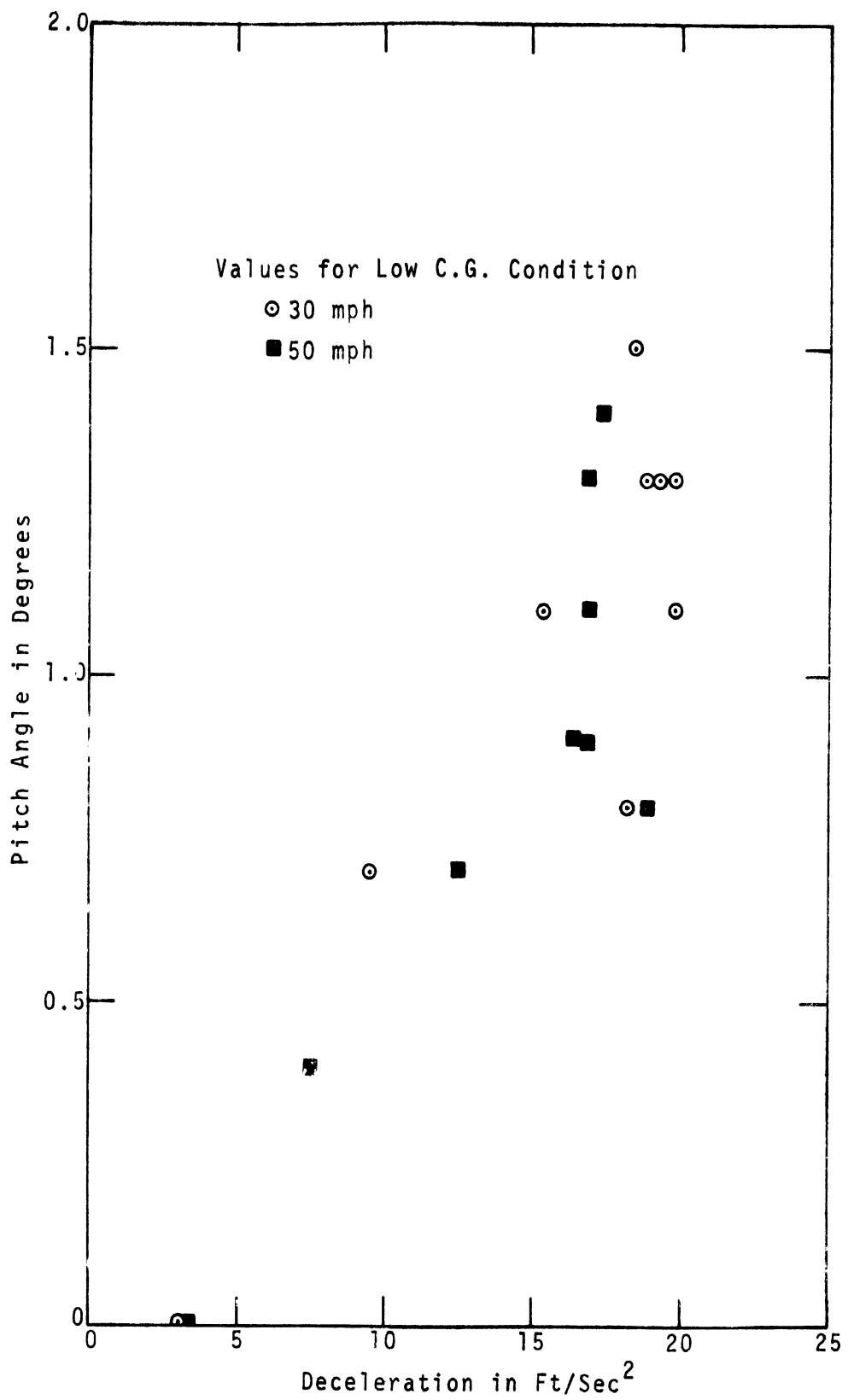


Figure 5-14. Pitch-deceleration data for the loaded (low c.g.) straight truck

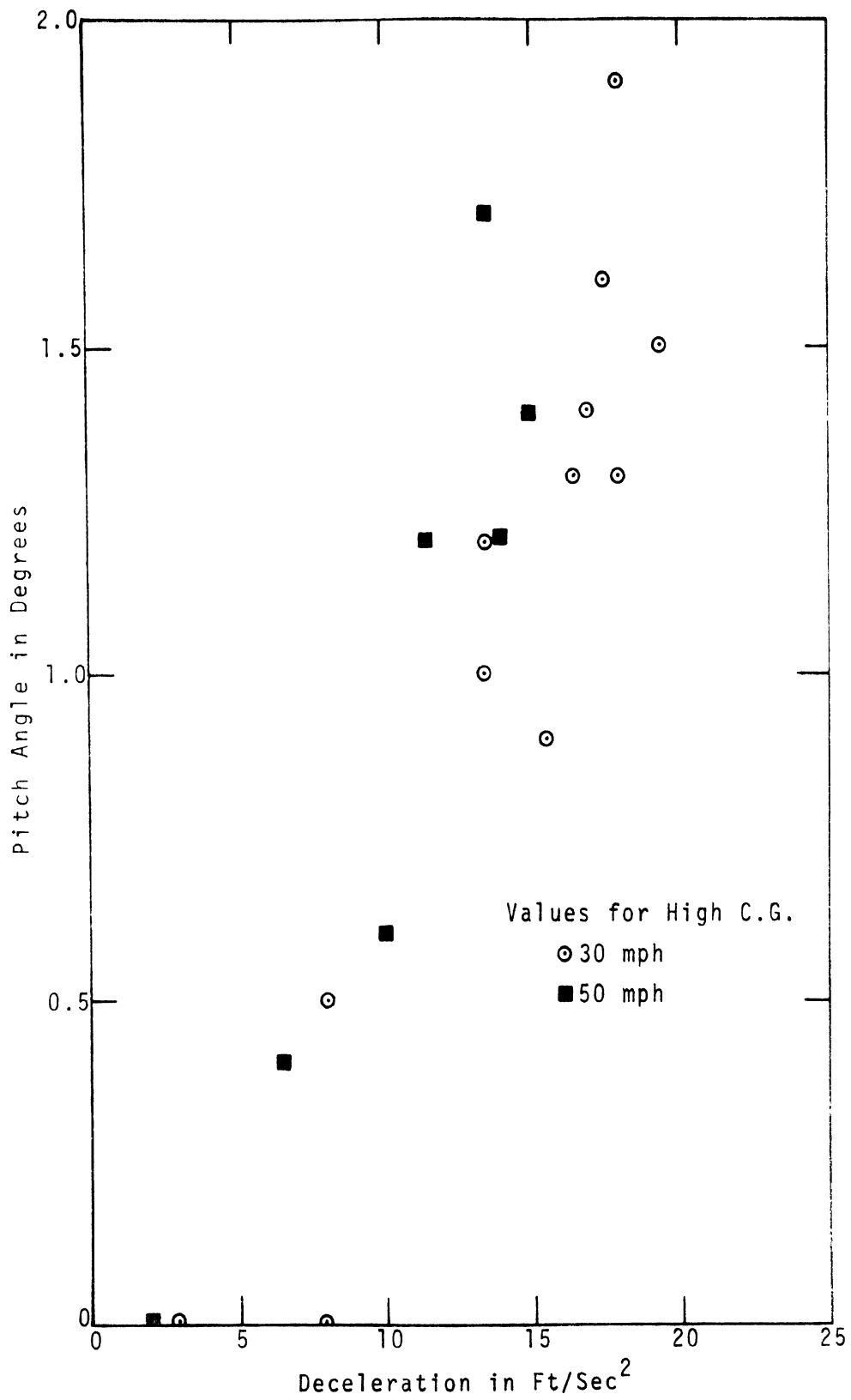


Figure 5-15. Pitch-deceleration data for the loaded (high c.g.) straight truck

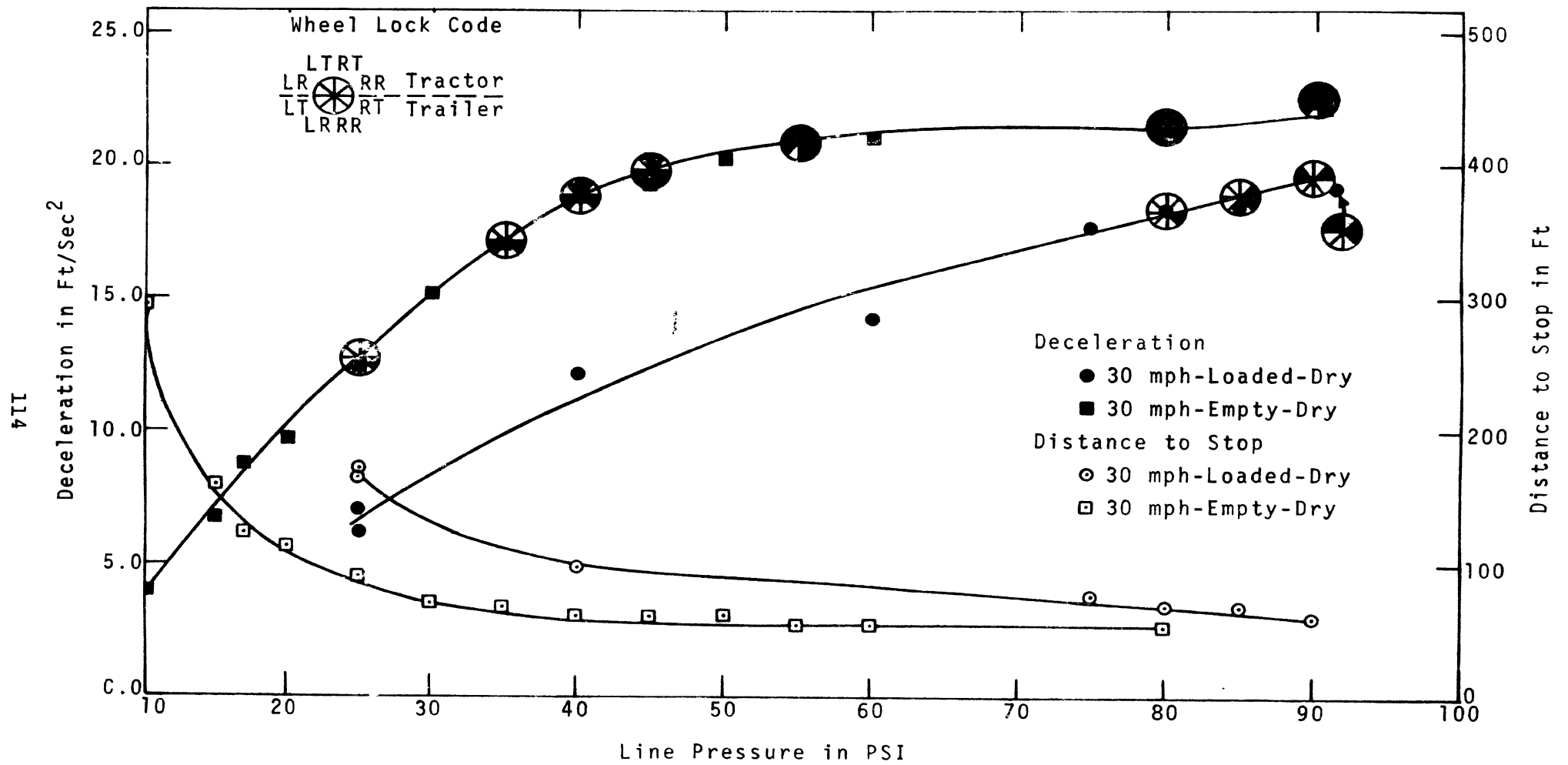


Figure 5-16. Results from effectiveness tests on tractor-trailer from 30 mph, empty and loaded, on dry surface

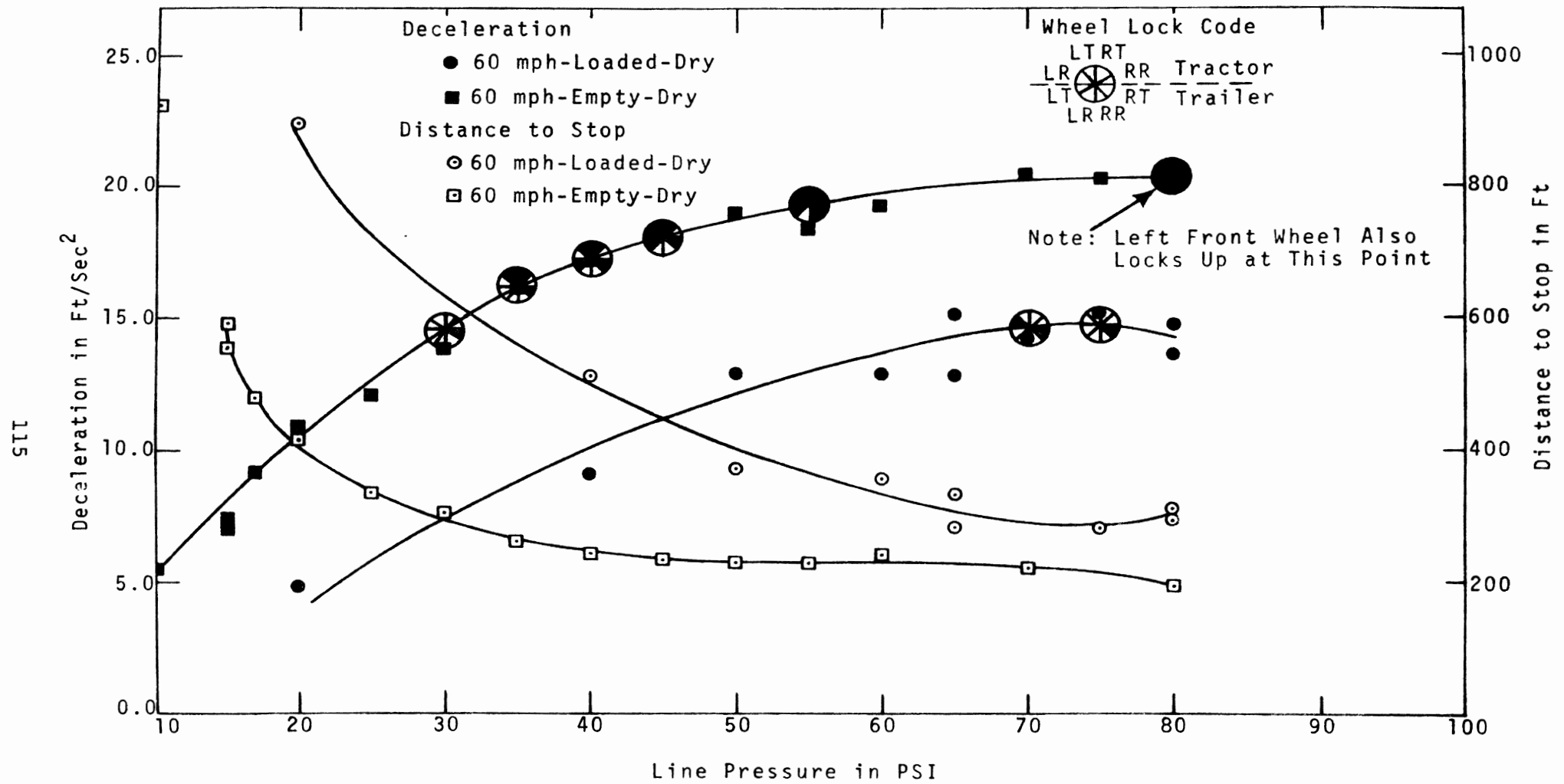


Figure 5-17. Results from effectiveness tests on tractor-trailer from 60 mph, empty and loaded, on dry surface

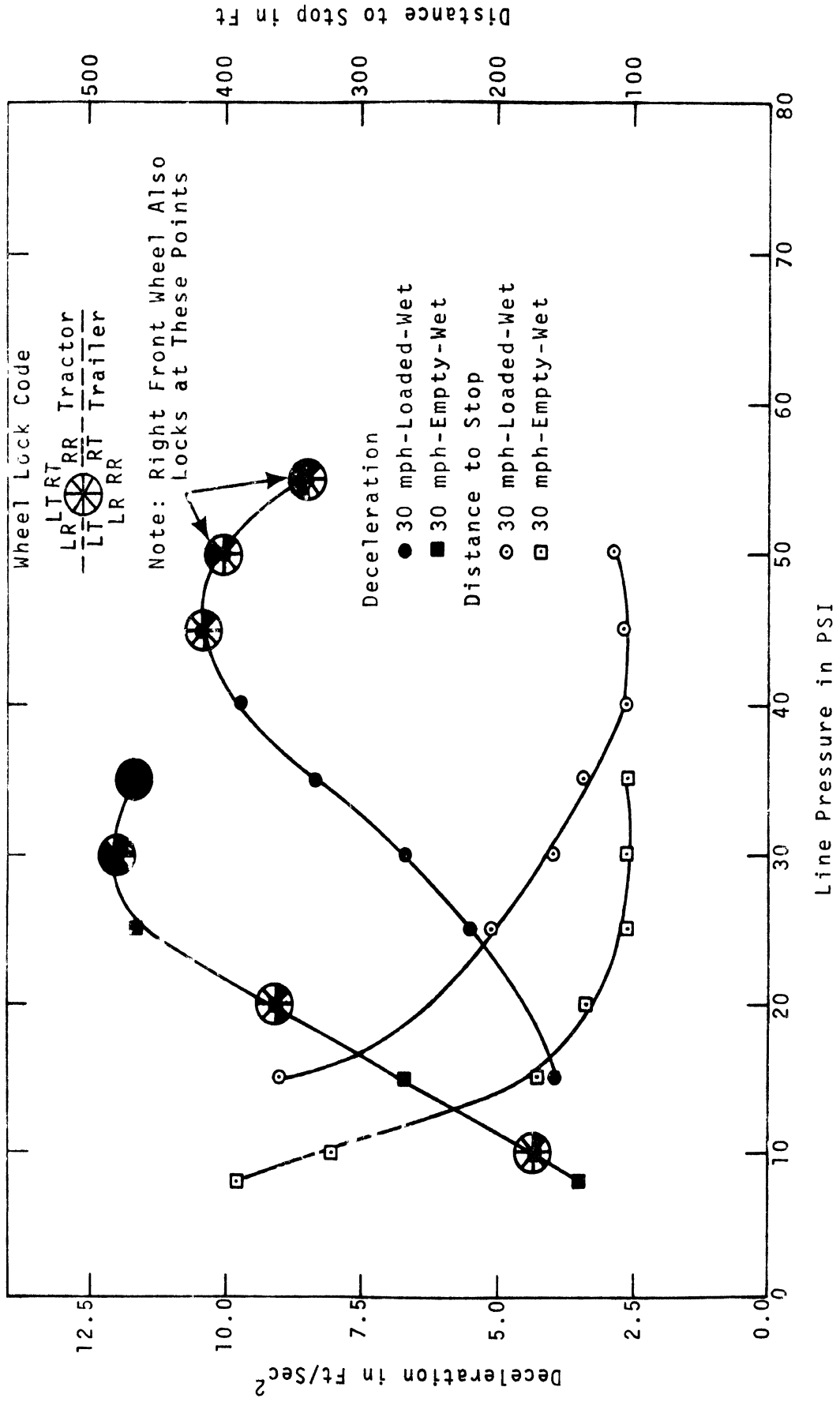
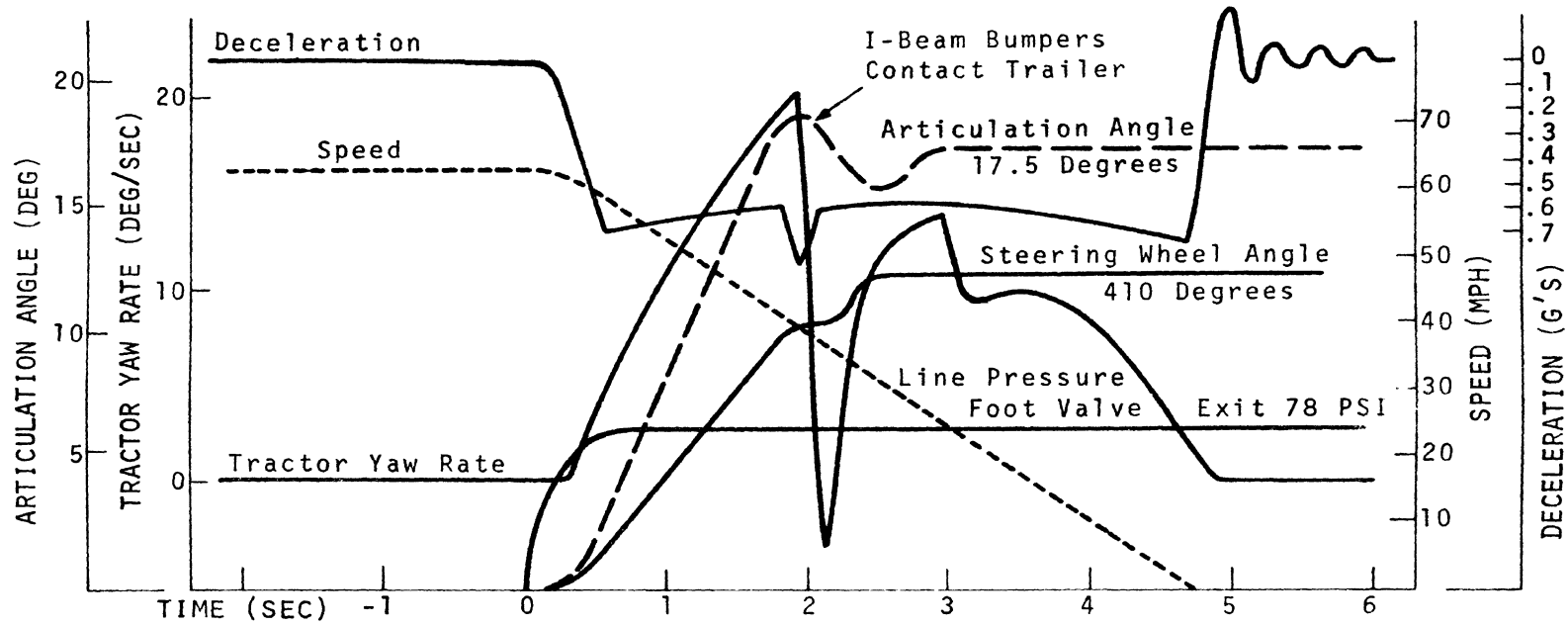


Figure 5-18. Results from effectiveness tests on tractor-trailer from 30 mph, empty and loaded, on wet surface

STRAIGHTLINE BRAKING TEST



117

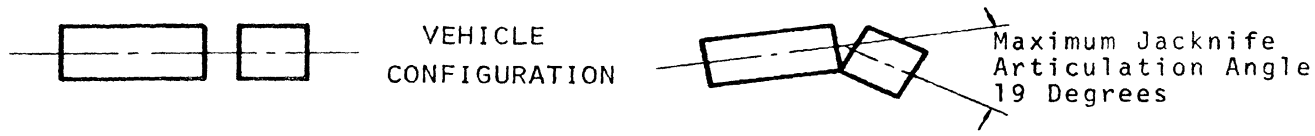


Figure 5-19. Jackknifing of tractor-trailer in brake effectiveness test

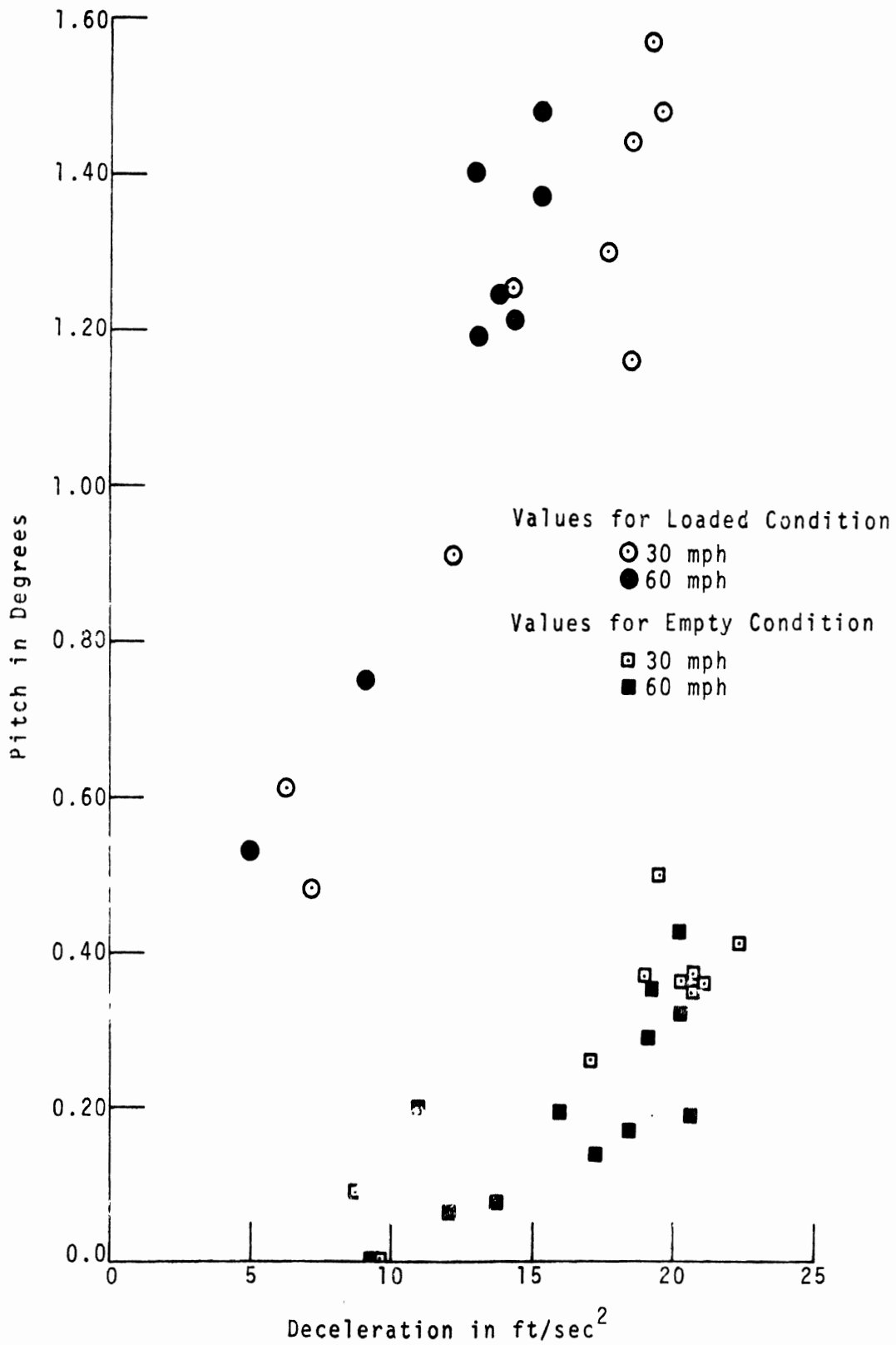


Figure 5-20. Tractor pitch-deceleration characteristic, in combination with trailer; empty and loaded

5-9 to 5-12. Stops were made at increasingly higher line pressures until first wheel lock was obtained. Line pressures were further increased to obtain stops with as many wheels locked as possible. Maximum performance data for the straight truck are presented in Table 5-8. The maximum average deceleration for this vehicle, 25.4 ft/sec², was obtained on dry asphalt with the vehicle empty and a nominal initial velocity of 30 mph. To achieve this deceleration, full brake line pressure was applied. It should be noted that on the high coefficient surface front wheel lockup was never attained regardless of loading condition, and that in all the effectiveness tests undertaken the vehicle remained stable even with all four wheels of the tandem suspension locked.

Initial wheel lock generally occurred on the right side of the vehicle. However, wheels on the leading and trailing axles of the walking beam suspension tended to lock at very nearly the same steady-state line pressure. Only in tests in which the vehicle was subjected to the high c.g. load was there a definite tendency for the wheels of the rear tandem axle to lock first.

Pitch angle versus deceleration data for the straight truck is presented in Figures 5-13 through 5-15. This data shows a good deal of scatter. However, comparison of the data for low and high c.g. loading configurations show the expected trend of larger pitch angles for the high c.g. loading condition.

Deceleration and stopping distance versus line pressure data for the tractor-trailer combination are presented in Figures 5-16, 5-17, and 5-18. Maximum performance data attained under the various test conditions are tabulated in Table 5-9. The maximum average deceleration for all tests was 22.4 ft/sec². This level of performance was attained with the vehicle empty, on dry asphalt, and a nominal initial velocity of 30 mph.

Unlike the straight truck with walking beam suspension, the four spring suspension of both the tractor and trailer showed a definite tendency for wheels on the leading axle to lock at lower line pressures than wheels on the trailing axle. Also, in contrast to the straight truck, it was possible to lock the front wheels on the tractor of the tractor-trailer combination in stops from 60 mph with the vehicle empty.

In the final two runs in the braking effectiveness test from 60 mph with the empty vehicle and with all the wheels on the tandem axles of the tractor locked, jackknifing did occur. The driver was able, by steering, to maintain the vehicle on the roadway during the stop, since the articulation angle of the vehicle was constrained to a limiting value by the bumper. Oscillograph traces showing the deceleration, yaw rate, speed, articulation angle, steering wheel angle, and brake line pressure for this stop are given in Figure 5-19.

Tractor pitch angle versus deceleration data (see Figure 5-20) again shows considerable scatter, but the expected higher levels of pitch for the loaded vehicle are readily apparent.

5.3.2 PARKING BRAKE TEST. Results of the parking brake tests for both vehicles are tabulated in Table 5-10. All parking brake tests were made on the high coefficient surface.

For the straight truck, the spring actuated parking brakes provided sufficient torque to lock all tandem wheels when the vehicle was empty, thus attaining a deceleration of 12.4 ft/sec². With the vehicle loaded, no locking of wheels occurred and deceleration was as high as 11.4 ft/sec².

TABLE 5-9
 MAXIMUM PERFORMANCE, TRACTOR-TRAILER

Initial Velocity Nominal (mph)	Loading Condition	Test Surface	Maximum Deceleration (ft/sec ²)		Minimum Stopping Distance (ft) (corrected to nominal v ₀)	
			No Wheel Lock	All Runs	No Wheel Lock	All Runs
30	empty	dry asphalt	9.7	22.4	113	53
30	loaded	dry asphalt	17.7	19.5	77	60
60	empty	dry asphalt	12.2	20.5	338	197
60	loaded	dry asphalt	15.2	15.2	282	282
30	empty	wet jennite	3.5	12.0	391	102
30	loaded	wet jennite	9.7	10.5	106	106

TABLE 5-10
PARKING BRAKE TESTS

Vehicle/ Condition	Initial Velocity, mph	Deceleration (ft/sec ²)	Wheels Locked	Stopping Distance, ft
Straight Truck				
empty	24.6	12.4	all tandems	54
loaded	21.3	11.4	none	--
	21.3	11.4	none	--
	21.3	11.0	none	61
Tractor- Trailer				
loaded	20.0	4.5	none	134

For the tractor-trailer, tests were made only with the vehicles loaded. No wheels were locked and deceleration was 4.5 ft/sec².

5.3.3 BRAKE BALANCE TEST. Results of the brake balance test of the tractor-trailer are tabulated in Table 5-11.

TABLE 5-11
BRAKE BALANCE TEST RESULTS
TRACTOR-TRAILER

Test No.	Brake Pressure, psi				Deceleration, ft/sec ²	
	P _F	P ₁	P ₂	P ₃	Measured	Corrected
1	42.1	41.2	39.0	40.1	9.72	9.72
2	40.1		36.7		3.41	3.61
3	39.5	37.8			1.58	1.72
4	40.1			39.0	4.25	4.38
Total of Test 2,3,4						9.71

Since brake line pressures were not precisely repeatable from test to test, a correction factor was applied to the deceleration data. The correction method as it would be applied to tests 2, 3, and 4 is given below:

$$A_{x\text{corr.}} = A_{x\text{meas.}} \times \frac{P_{i,1}}{P_{i,j}} \quad (5-1)$$

where

$A_{x\text{corr.}}$ = corrected deceleration

$A_{x\text{meas.}}$ = measured deceleration

$P_{i,l}$ = brake pressure at brake (i) as measured in test l

$P_{i,j}$ = brake pressure at brake (i) as measured in test j

The brake force distribution of the tractor-trailer was found to be

$$\phi_{1F} : \phi_{1R} : \phi_{2R} = 17.7 : 37.2 : 45.1,$$

where

ϕ_{1F} = % of total brake force on tractor front wheels

ϕ_{1R} = % of total brake force on tractor rear wheels

ϕ_{2R} = % of total brake force on trailer wheels

5.3.4 BRAKE RESPONSE TIME TESTS. Figures 5-21 and 5-22 show typical results from a brake response time test in the truck and tractor-trailer in which pressure-time relationships for each brake in application and release is given. It should be noted that no attempt was made on either of the vehicles to change the air brake control system configuration in any way or to alter the response times. Table 5-12 gives the time delay and rise time (as defined in Section 2.5) in addition to the total response time and release time for each vehicle.* Total response time is measured from first instant of pressure increase as measured at the output of the treadle valve in a full 100 psi brake application to the time at which the pressure measured at the axle reaches 60 psi. Thus the total response time for a given brake is the sum of the time delay and response lag for that brake. Release time is measured from the first drop in pressure at the output of the treadle valve in a full release to the time when the pressure measured at the brake reaches 5 psi.

*Note that the response times as given in the Table are the averaged results from 3 tests on each vehicle, while the curves in the figures are from one typical test.

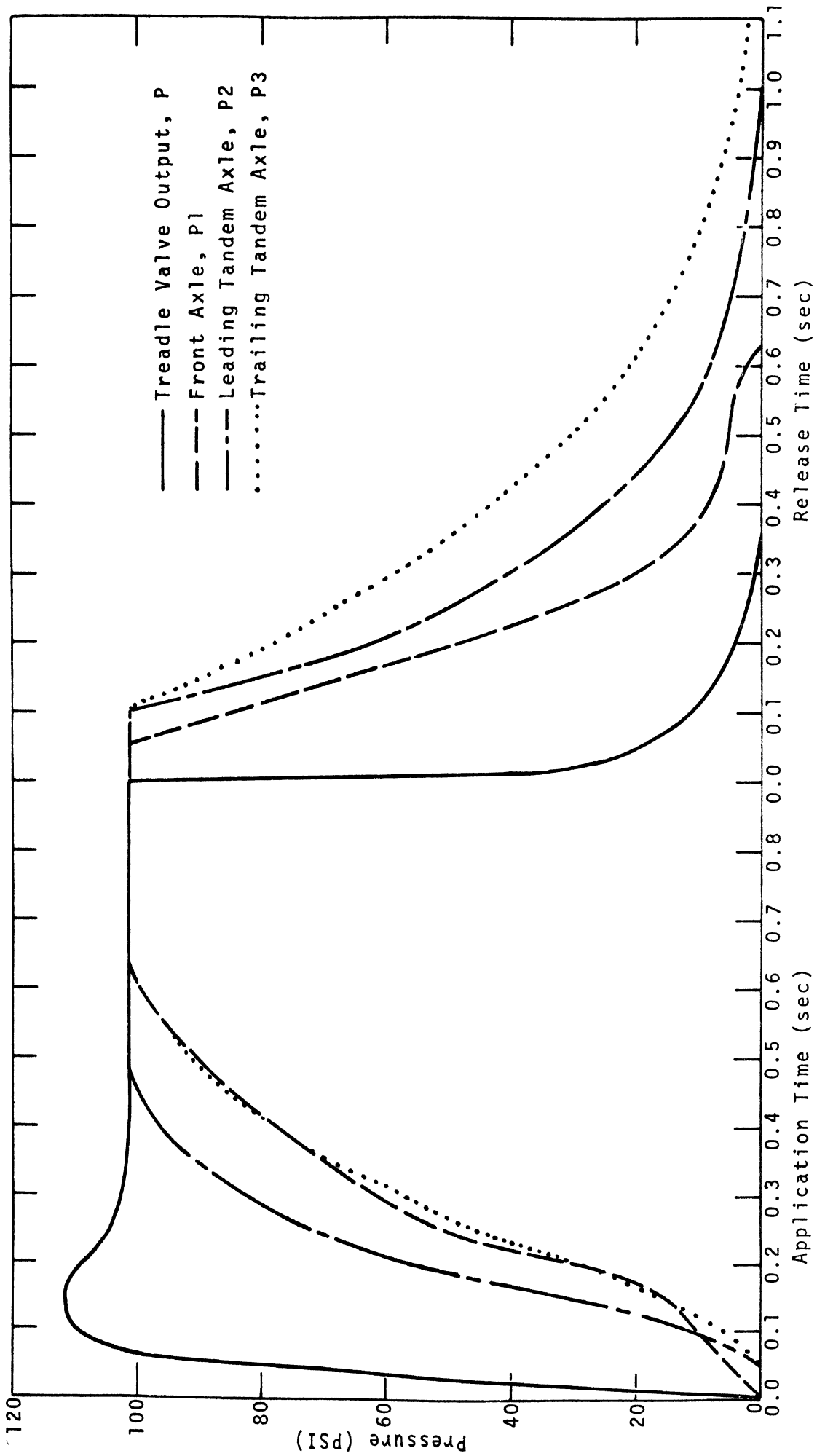


Figure 5-21. Results from brake response time tests on the straight truck

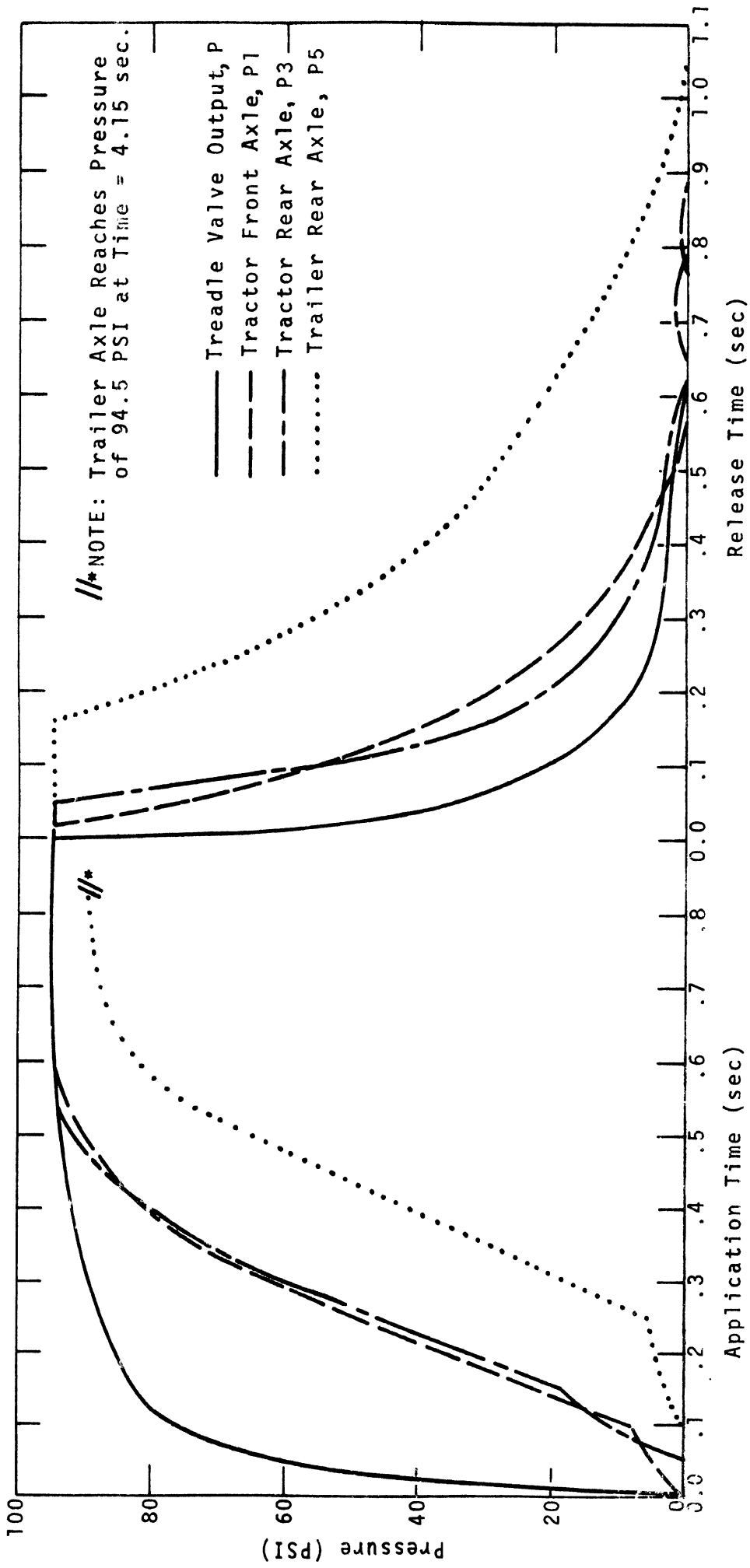


Figure 5-22. Results from brake response time tests on tractor-trailer

TABLE 5-12
BRAKE RESPONSE AND RELEASE TIMES

Vehicle	Axle	Time Delay Sec.	Rise Time Sec.	Response Time Sec.	Release Time Sec.
Truck	Front	.032	0.296	0.328	0.500
	Leading Tandem	0.070	0.181	0.251	0.700
	Trailing Tandem	0.073	0.276	0.349	0.950
Tractor	Front	0.050	0.270	0.320	0.400
	Trailing Tandem	0.075	0.245	0.320	0.450
Trailer	Trailing Tandem	0.175	0.305	0.475	0.880

6.0 RESULTS AND CONCLUSIONS

In this section the results from the vehicle braking performance tests are compared with results from the simulation programs. The choices required in brake system and tire-road interface parameters necessary to optimize correspondence between simulation and test results are discussed. The complete set of vehicle, brake system, and tire-road interface parameters used in the simulation programs are given in Appendix F.

6.1 CORRELATION OF RESULTS FROM TESTS AND SIMULATION: PROGRAM VALIDATION

6.1.1 VALIDATION PROCEDURE. The basis for the simulation program validation was a series of brake effectiveness tests run on the two test vehicles. These tests have been described in detail in Chapter 5. For the purpose of validation, a similar series of "effectiveness tests" were performed using the computer simulation.

A listing of the input data used in the simulation for the brake effectiveness test series is given in Appendix F. The majority of input data required to exercise the simulation was obtained from the results of the parameter measurement program (see Chapter 4) and from measurements taken from the vehicles or their component drawings as supplied by the manufacturer. The remaining parameters are the coefficients of friction and friction reduction parameters (MUZERO(I) and FA(I), I=1, KAXLE) required for the tire model, the brake timing constants (TQ(I, J), I=1, KAXLE; J=1,2), the two brake lining coefficients and the brake fade coefficient (ULH(I), and ULL(I), I=1, KAXLE and FRAY) required for the brake modules, and, for the walking beam suspension, the percent effectiveness of the torque rods (PERCENT).

Preliminary computer runs, simulating the sliding stop tests, were made to obtain the necessary tire parameters. In these computer runs, the values of the MUZERO(I) and the FA(I) were adjusted until the simulated deceleration-velocity relationships matched those obtained in testing as well as possible. These values were further adjusted to obtain good wheel lock correlation.

In the case of the straight truck, PERCENT=100 was chosen to characterize the walking beam suspension, since the leading and trailing axles tended to lock up at about the same time.* It was found necessary to use a significantly higher friction coefficient and lower friction reduction parameter for the trailing tandem in the straight truck wet surface tests to get proper lock correspondence. This, apparently, results from a wiping effect in which the leading tires partially clear the road surface of water for the trailing tires, thus allowing the leading tires to lock first.

The brake timing tests were employed to determine the response characteristics in the application of each set of brakes on the vehicle. (Release time was not considered here.) With the vehicle at rest on a flat level surface, the brake pedal is fully depressed as rapidly as possible, and held until a steady state line pressure is reached at each axle. The line pressure measured at the treadle valve is therefore approximately a step function; the pressure at each axle, after a finite delay, then tends to rise to the treadle valve pressure asymptotically, taking perhaps half a second to reach, for all practical purposes, the treadle valve pressure. Results from typical brake timing tests are given in Figures 5-21 and 5-22.

*Had the trailing axle locked up at significantly lower line pressure than the leading, correspondingly lower PERCENT would have been chosen.

Preceding page blank

The simulation of brake timing is explained in Section 2.5.1. It was assumed that the line pressure at axle I could be described by the time delay $TQ(I,1)$ and the rise time $TQ(I,2)$.

The choice of time delay $TQ(I,1)$ was straightforward; it was only necessary to measure the time from the initiation of the "step" application until the first rise in pressure could be detected at axle I. The choice of rise time $TQ(I,2)$ is complicated by the fact that the pressure measured at the treadle valve is not actually a step; thus the number of seconds to rise to 63% of the steady state treadle valve pressure is not readily apparent from the empirical data. This problem was solved in the following manner: it was assumed that the pressure measured at the treadle valve was a step, and $TQ(I,2)$ was taken directly from the experimental result. The simulation was then run with a very rapid rise time at the treadle valve, rather than using the actual measured treadle valve response. In figures 6-1 and 6-2 results from the simulation are superimposed on the test results given in 5-21 and 5-22. Note that the values for $TQ(I,J)$ used in the simulation, which are listed in Table 5-12, are chosen to match as closely as possible the average of the results from three tests on each vehicle. The empirical curves in Figures 6-1 and 6-2 are from one typical test on each vehicle. The results from the simulation fall within the scatter of the experimental data. The simulated pressure time relations are thus a reasonable approximation of the test data.

Simulations of the brake balance tests* were conducted in order to establish the relative magnitudes of ULL and ULH at each axle. Further refinements of the lining friction coefficients and establishment of the FRAY value was accomplished through curve fitting of simulation results with the effectiveness test data. In this manner, the lining friction coefficients were established for the brakes on each axle. These coefficients were then held constant throughout all subsequent simulation exercises. FRAY, however, was allowed to vary with the test conditions. Best correlation was obtained by making FRAY sensitive only to velocity; higher initial velocities necessitated the use of higher values of FRAY.

6.1.2 VALIDATION RESULTS--EFFECTIVENESS TEST. With the input data obtained as described above, the entire series of effectiveness tests conducted on the two test vehicles was simulated. The results of the simulation are superimposed on the experimental results in Figures 6-3 through 6-16. (Keys for these figures are given in Tables 6-1, 6-2, and 6-3.) Stopping distances are tabulated in Table 6-4.

At this point it should be noted that there is some difficulty in defining the values which should be plotted as deceleration in the effectiveness test plots. In the deceleration vs. time plots obtained from the vehicle tests, deceleration is not constant over the time of the stop. Particularly in more severe stops, deceleration rises rapidly in the first half second or so to a peak value followed by a decline to a steady state level. In high deceleration stops, this peak may be 30 or 40% greater than the steady state value. Then, late in the stops with locked wheels, deceleration increases gradually until the vehicle comes to rest. This behavior is due to the improvement of tire/road friction with decreasing velocity. Thus, in Figures 6-3 through 6-16, a time averaged deceleration, excluding the initial period of rapid deceleration rise, is plotted as the characteristic level of deceleration for an effectiveness test run.

*Since a full brake balance test on the straight truck was not accomplished at the Bendix Development Center, a series of front brake effectiveness checks were done on this vehicle at HSRI. In this manner, the brake force distribution for this vehicle was established.

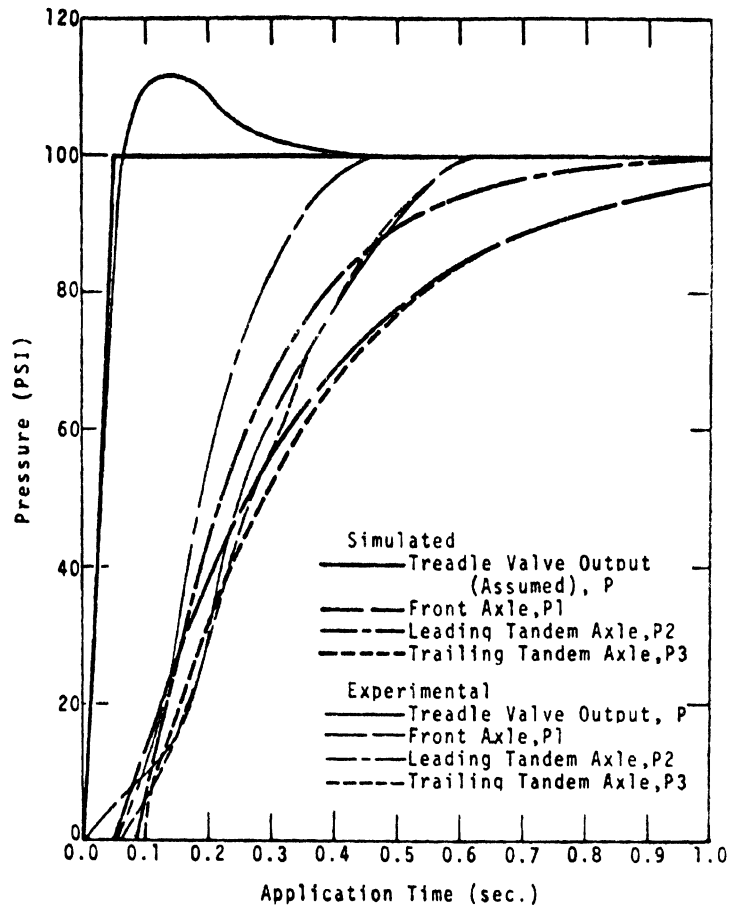


Figure 6-1. Straight truck brake timing

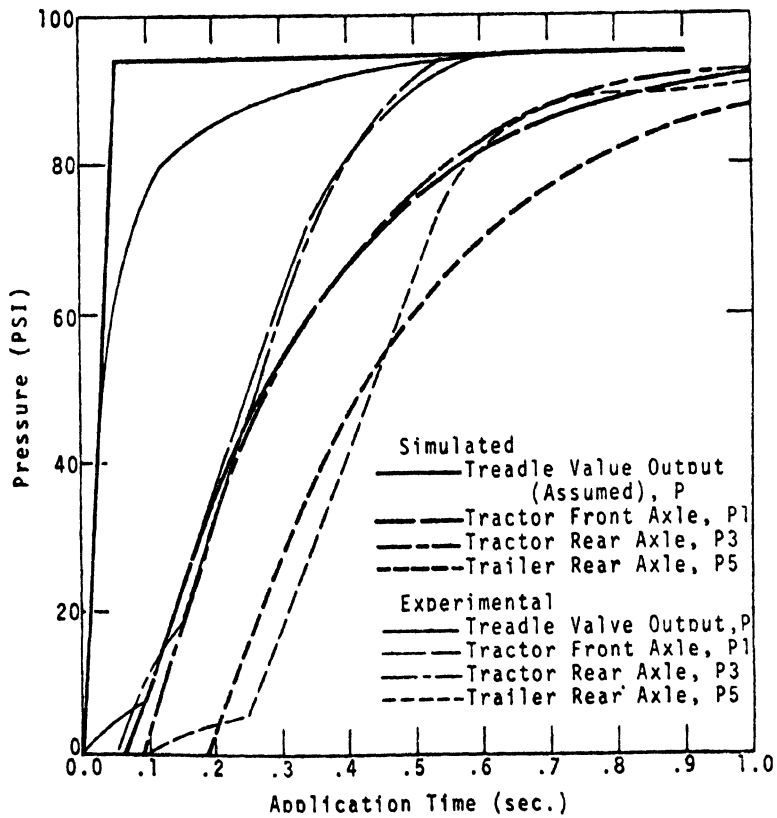


Figure 6-2. Tractor-Trailer Brake Timing

TABLE 6-1
KEY FOR FIGURES 6-3 THROUGH 6-8

DATA SOURCE	DECELERATION	STOPPING DISTANCE	WHEEL LOCK CODE
Simulation			LI→ Indicates minimum line pressure at which wheels of axle I lock.
Experimental			<div style="display: flex; justify-content: space-between;"> <div style="text-align: center;"> Left Leading Tandem </div> <div style="text-align: center;"> Right Leading Tandem </div> </div> <div style="display: flex; justify-content: space-between;"> <div style="text-align: center;"> Left Trailing Tandem </div> <div style="text-align: center;"> Right Trailing Tandem </div> </div> <p>Indicates a change in wheel lock configuration from the previous data point.</p>

[Note that experimental data is represented only by points and that the light lines are faired in only for the reader's convenience.]

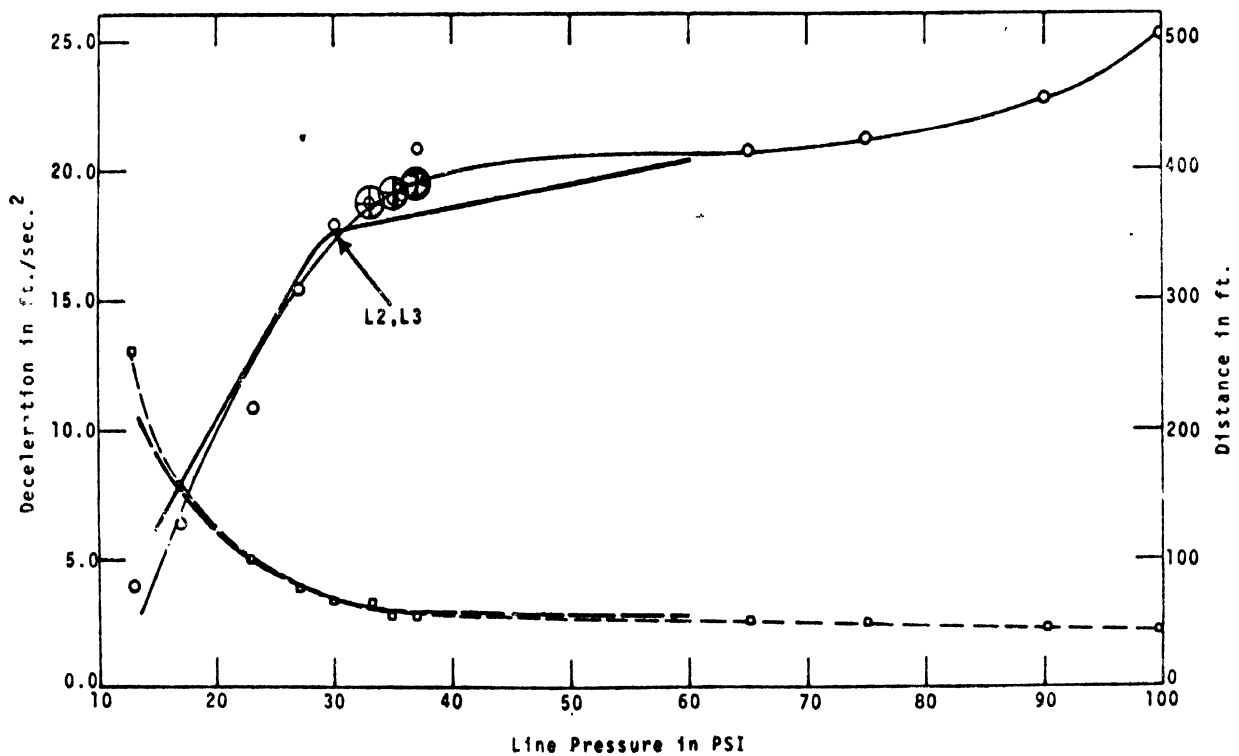


Figure 6-3. Effectiveness test validation: straight truck, empty, 30 mph, dry surface

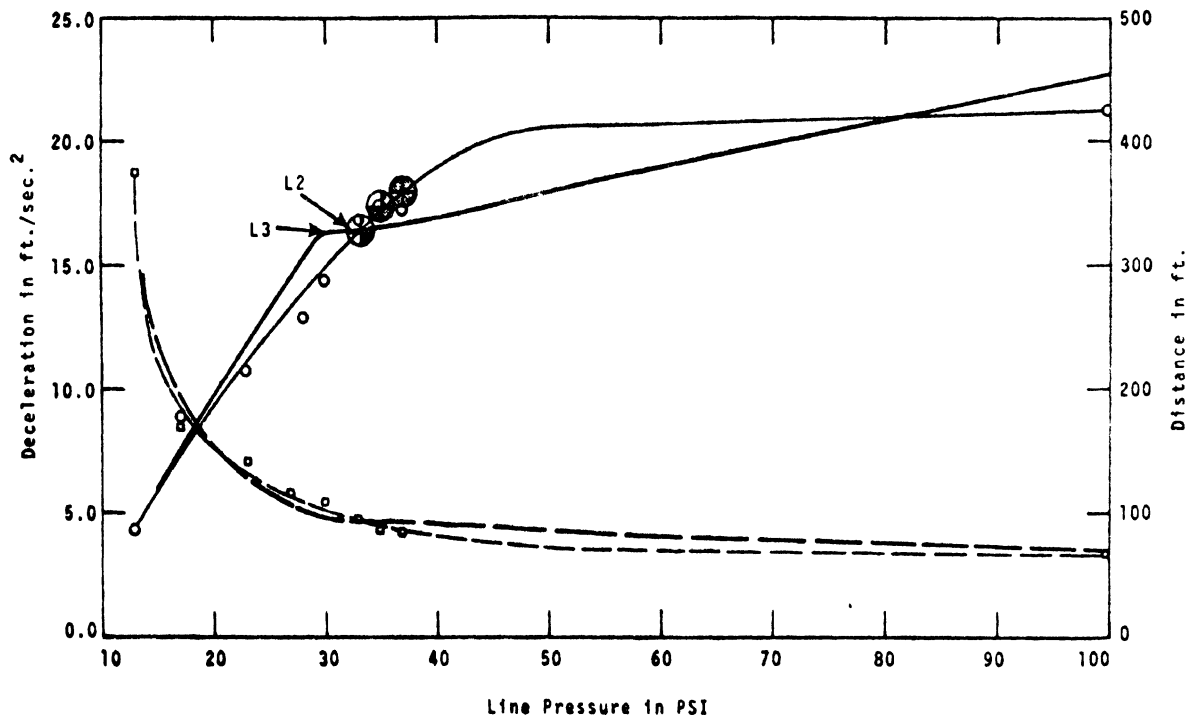


Figure 6-4. Effectiveness test validation: straight truck, empty, 50 mph, dry surface

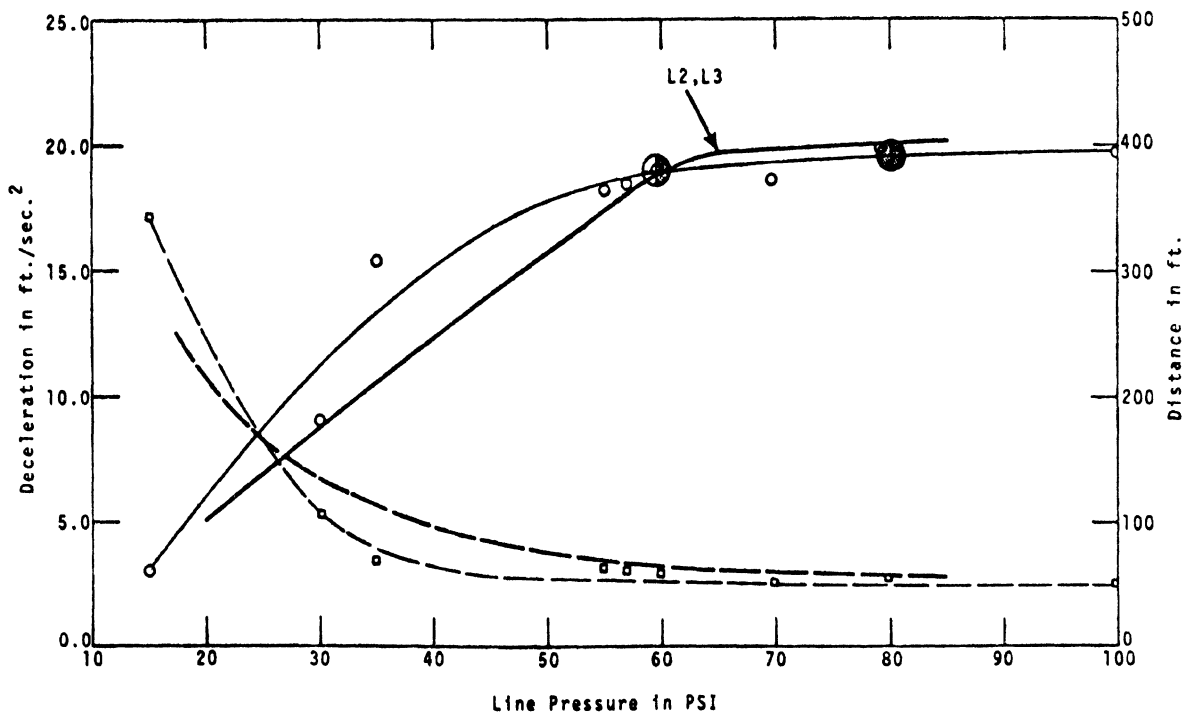


Figure 6-5. Effectiveness test validation: straight truck, low c.g. load, 30 mph, dry surface

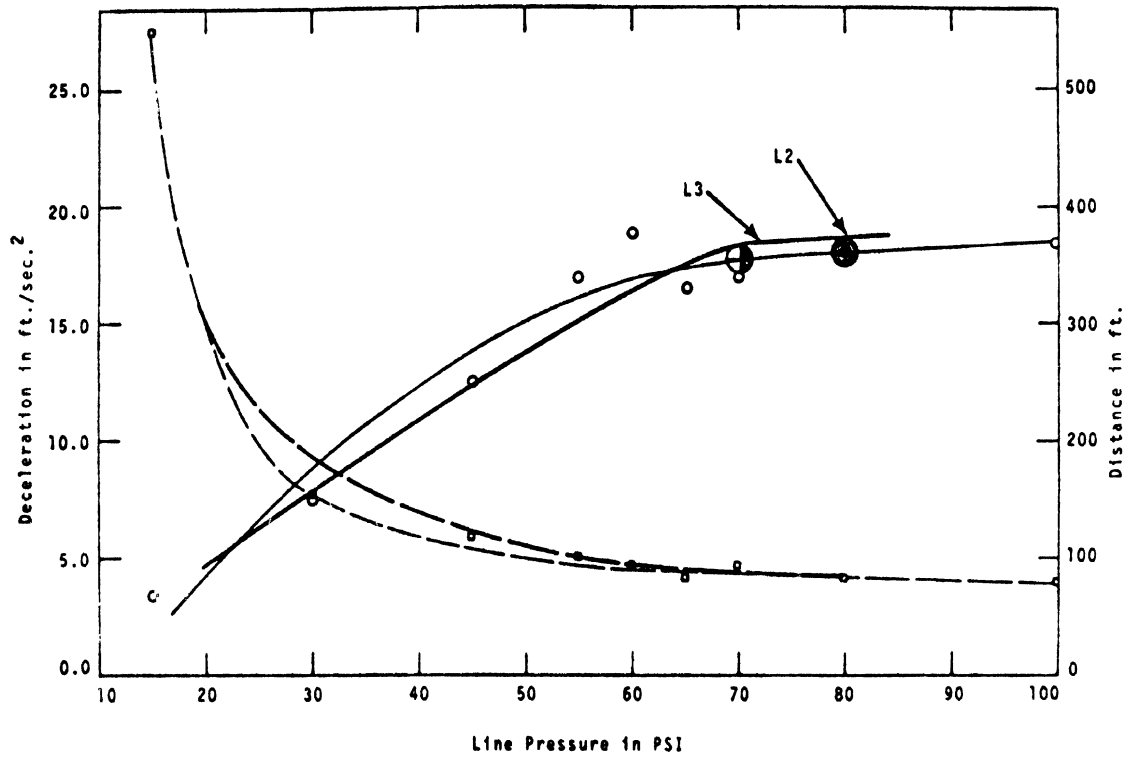


Figure 6-6. Effectiveness test validation: straight truck, low c.g. load, 50 mph, dry surface

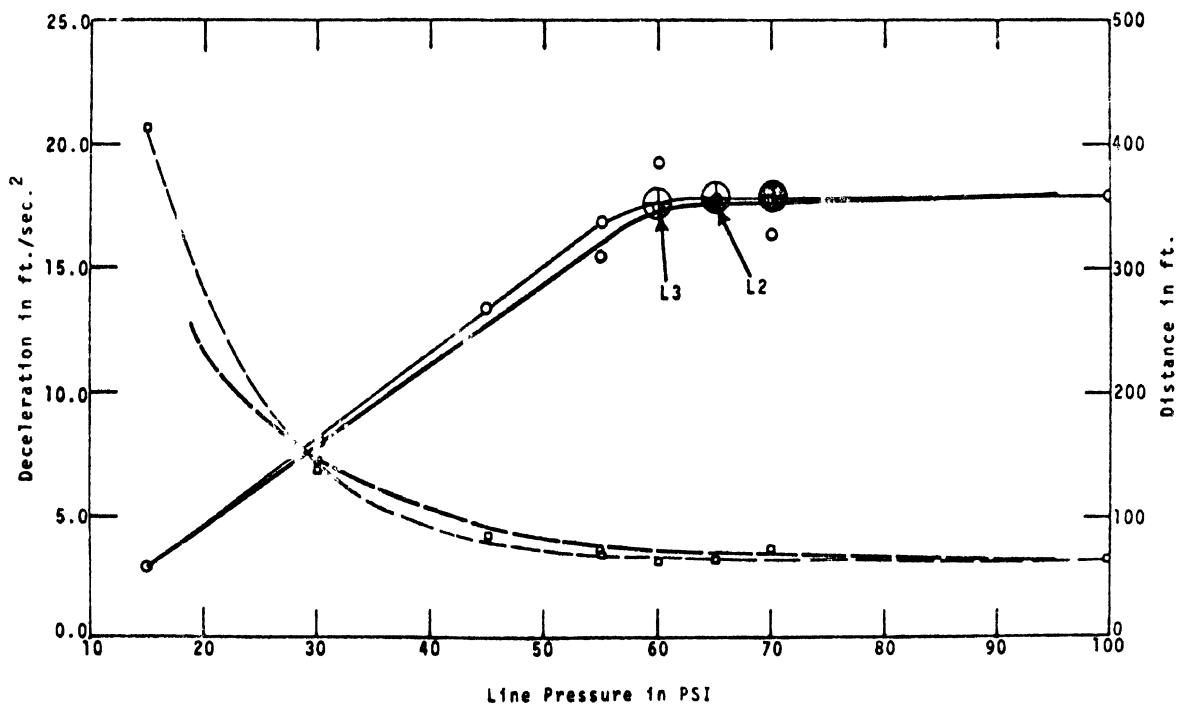


Figure 6-7. Effectiveness test validation: straight truck, high c.g. load, 30 mph, dry surface

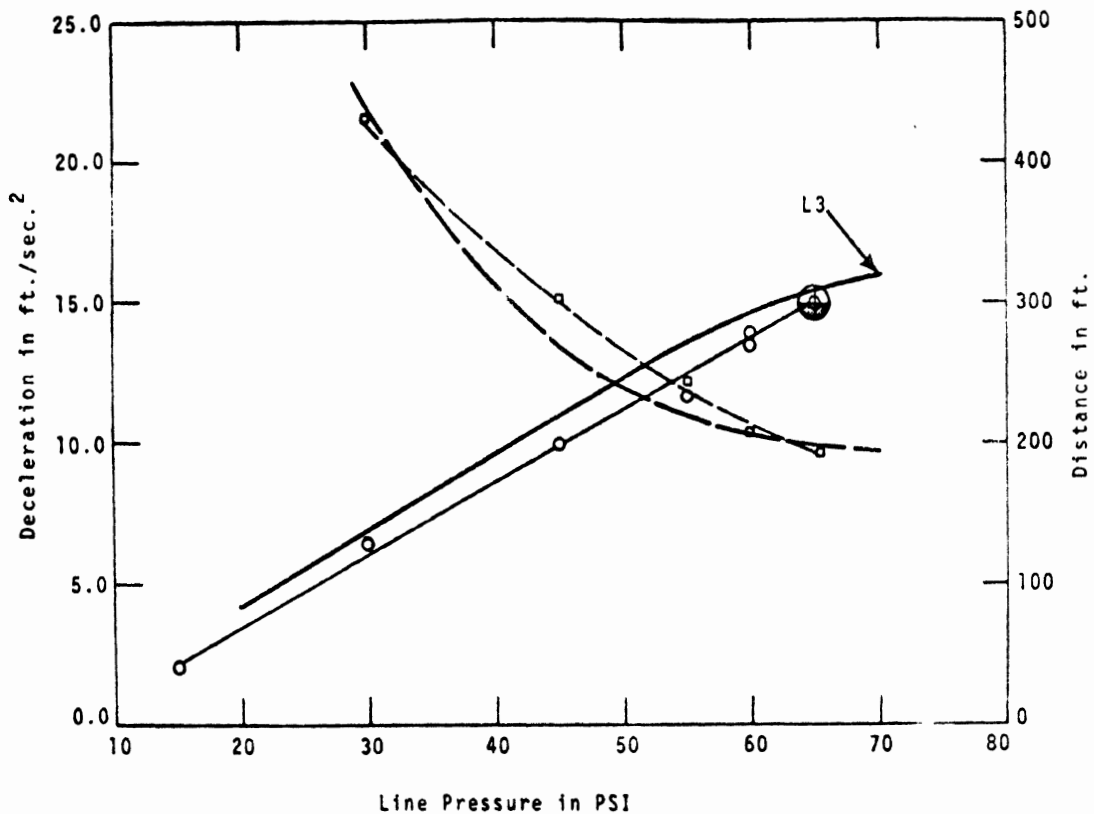


Figure 6-8. Effectiveness test validation: straight truck, high c.g. load, 50 mph, dry surface

TABLE 6-2
KEY FOR FIGURES 6-9 and 6-10

DATA SOURCE	DECELERATION	STOPPING DISTANCE	WHEEL LOCK CODE
Simulation			LI+ Indicates minimum line pressure at which wheels of axle I lock.
Experimental	 [Note that experimental data is represented only by points and that the light lines are faired in only for the reader's convenience.]		<div style="display: flex; justify-content: space-around;"> <div style="text-align: center;">Left Front</div> <div style="text-align: center;">Right Front</div> </div> <div style="display: flex; justify-content: space-around; margin-top: 5px;"> <div style="text-align: center;">Left Trailing Tandem</div> <div style="text-align: center;">Right Trailing Tandem</div> </div> <p>Indicates a change in wheel lock configuration from the previous data point.</p>

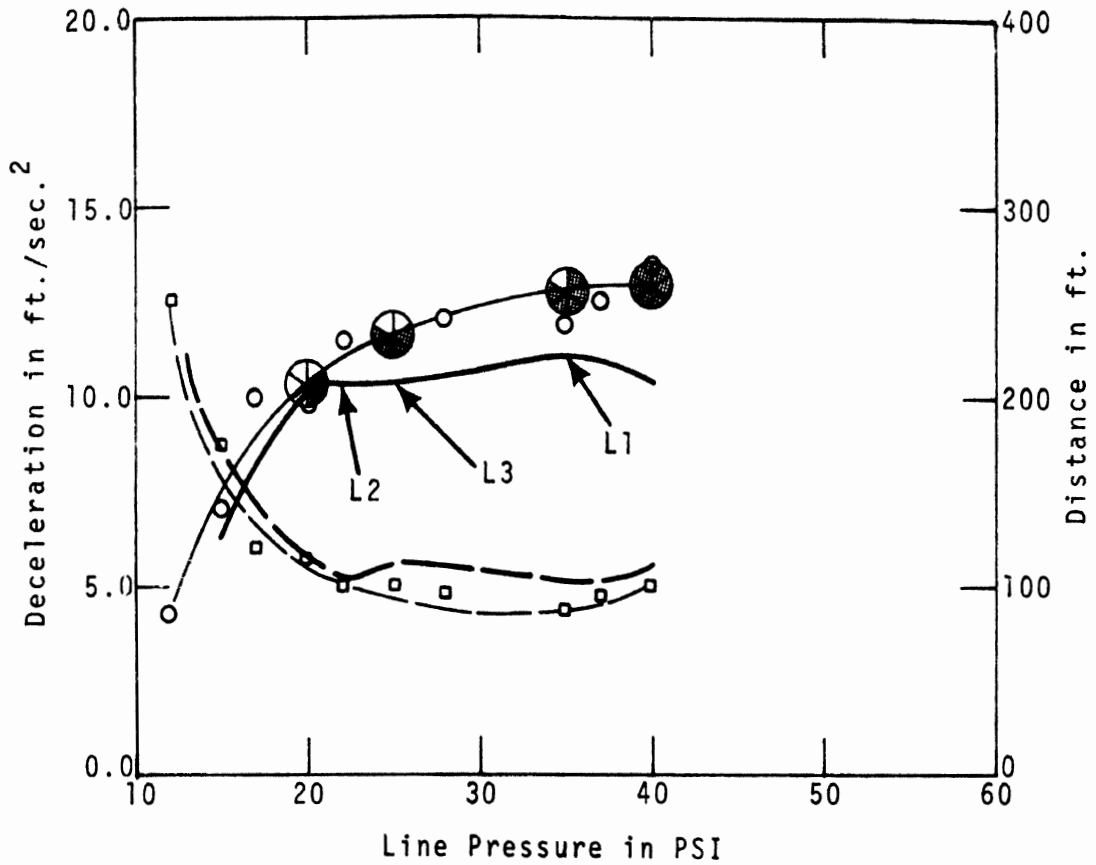


Figure 6-9. Effectiveness test validation: straight truck, empty, 30 mph, wet surface

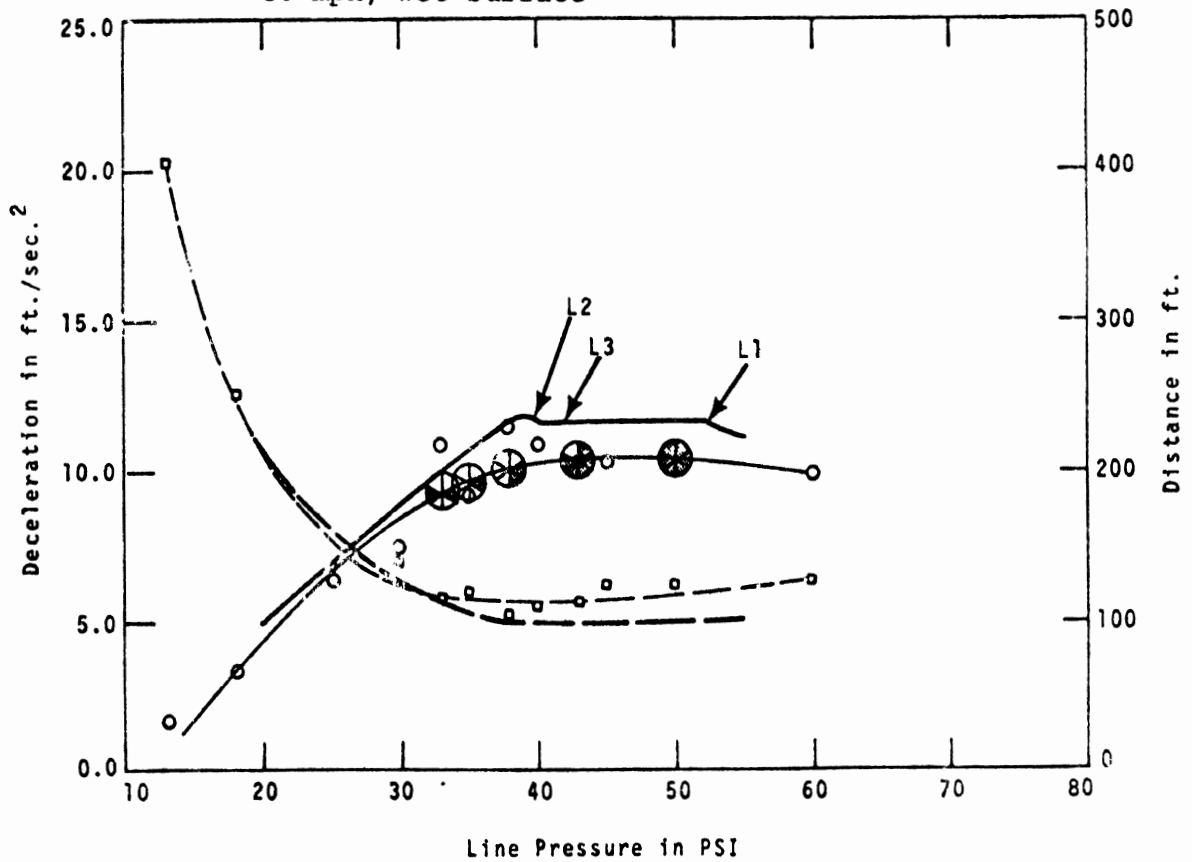


Figure 6-10. Effectiveness test validation: straight truck, low c.g. load, 30 mph, wet surface

TABLE 6-3
KEY FOR FIGURES 6-11 THROUGH 6-16

DATA SOURCE	DECELERATION	STOPPING DISTANCE	WHEEL LOCK CODE
Simulation			LI→ Indicates minimum line pressure at which wheels of axle I lock.
Experimental	 [Note that experimental data is represented only by points and that the light lines are faired in only for the reader's convenience.]		<div style="display: flex; justify-content: space-between;"> <div style="width: 30%;"> <p>Left Leading Tandem</p> <p>TRACTOR Left Trailing Tandem</p> <p>TRAILER Left Leading Tandem</p> <p>Left Trailing Tandem</p> </div> <div style="width: 30%; text-align: center;"> </div> <div style="width: 30%;"> <p>Right Leading Tandem</p> <p>TRACTOR Right Trailing Tandem</p> <p>TRAILER Right Leading Tandem</p> <p>Right Trailing Tandem</p> </div> </div>

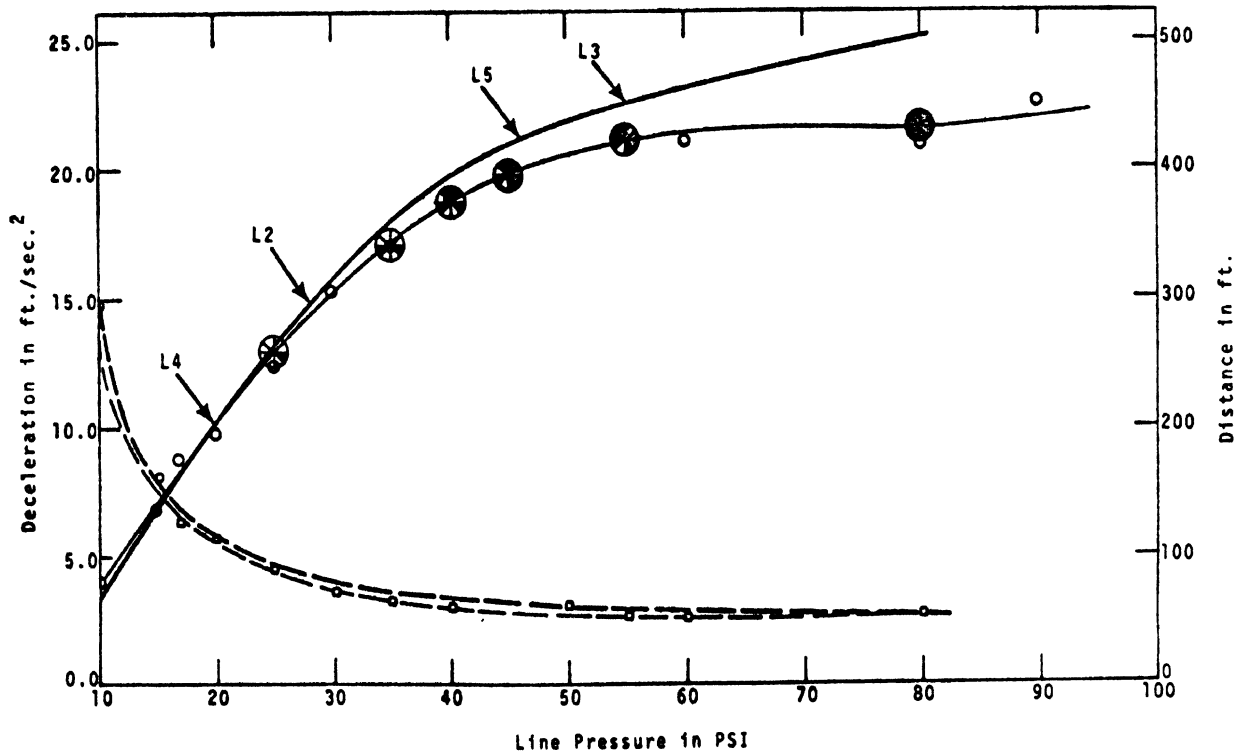


Figure 6-11. Effectiveness test validation: tractor-trailer, empty, 30 mph, dry surface

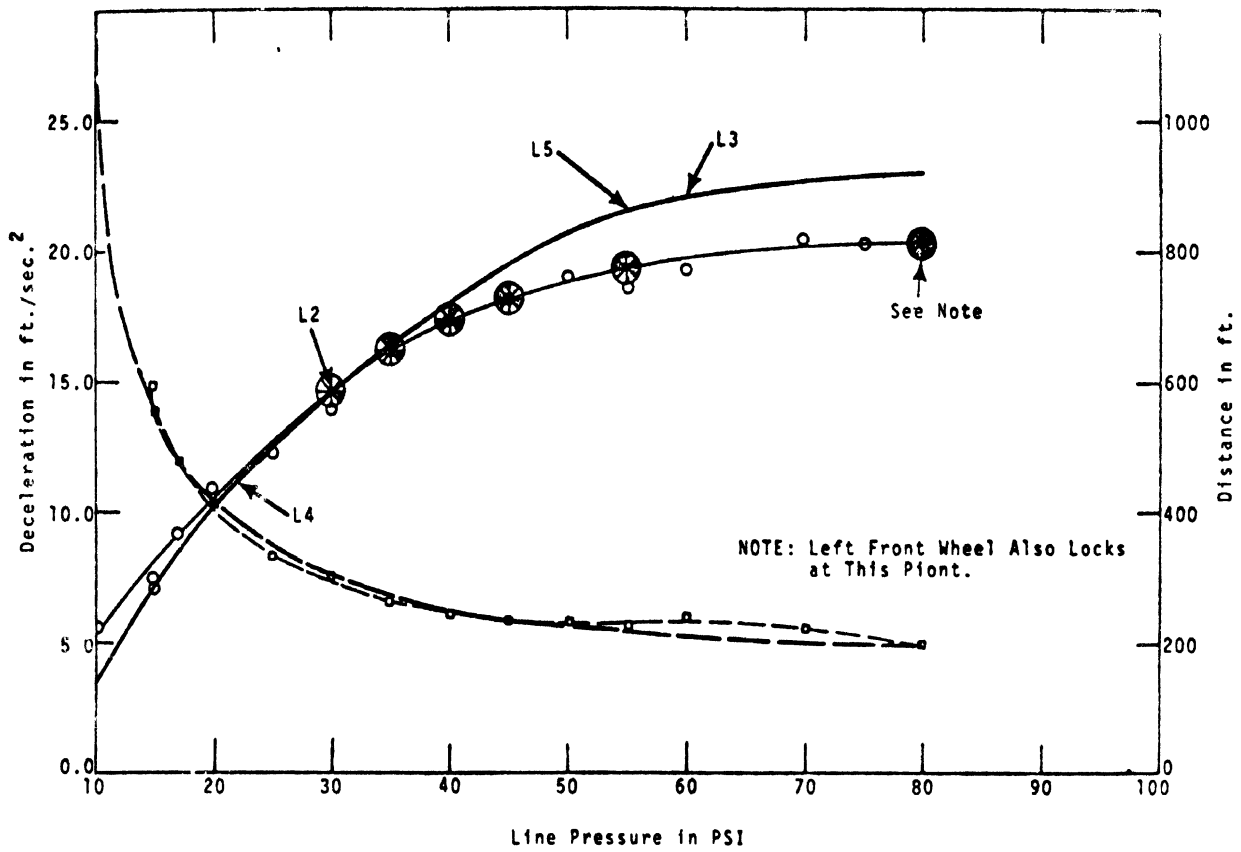


Figure 6-12. Effectiveness test validation: tractor-trailer, empty, 60 mph, dry surface

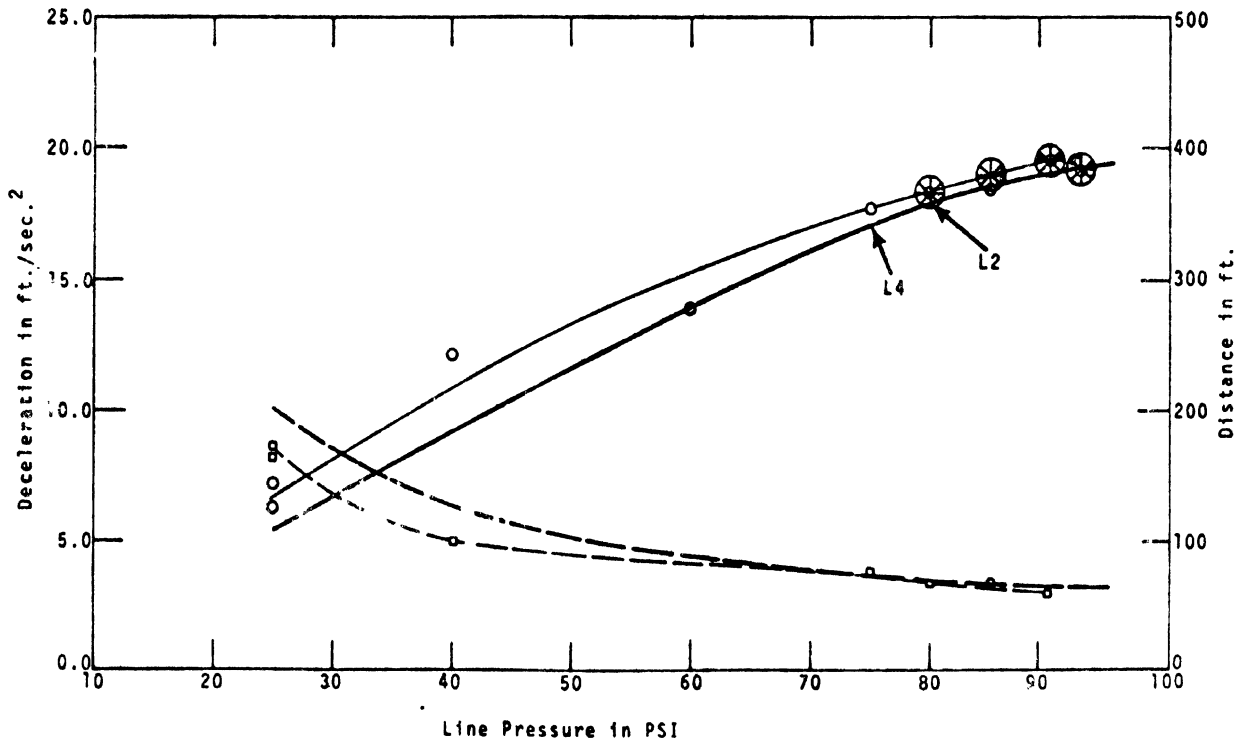


Figure 6-13. Effectiveness test validation: tractor-trailer, loaded, 30 mph, dry surface

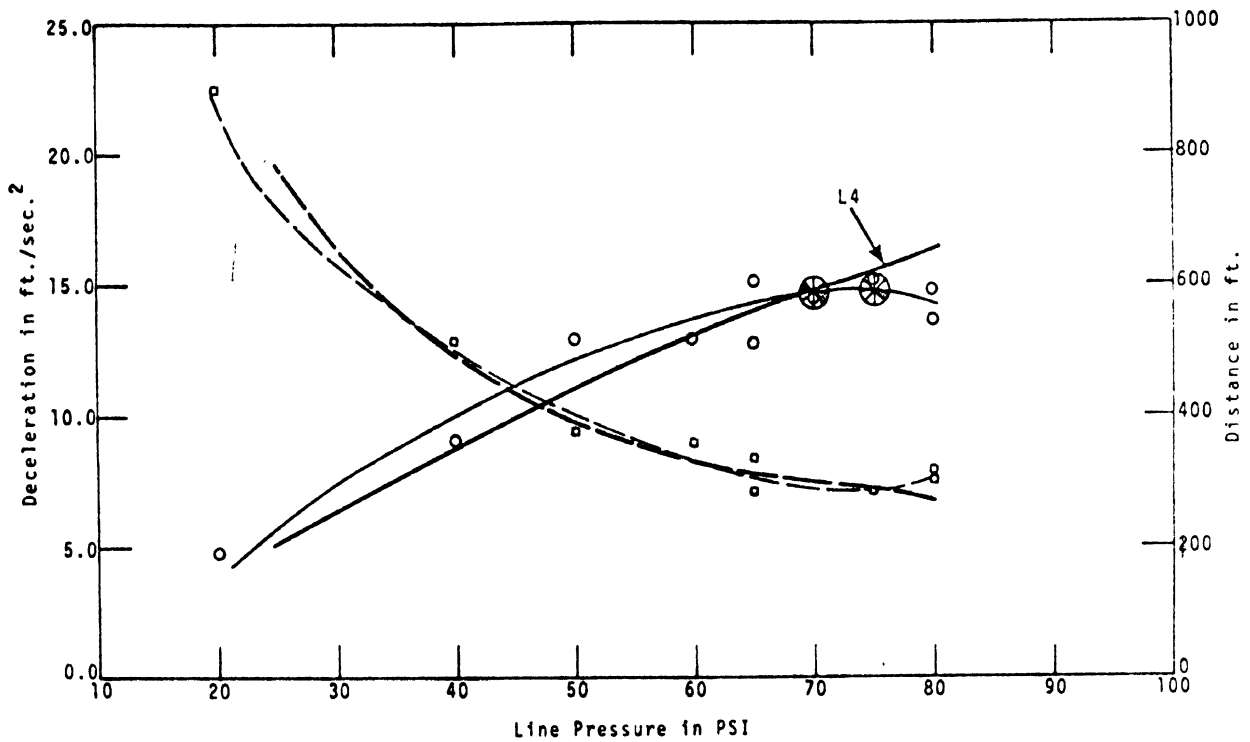


Figure 6-14. Effectiveness test validation: tractor-trailer, loaded, 60 mph, dry surface

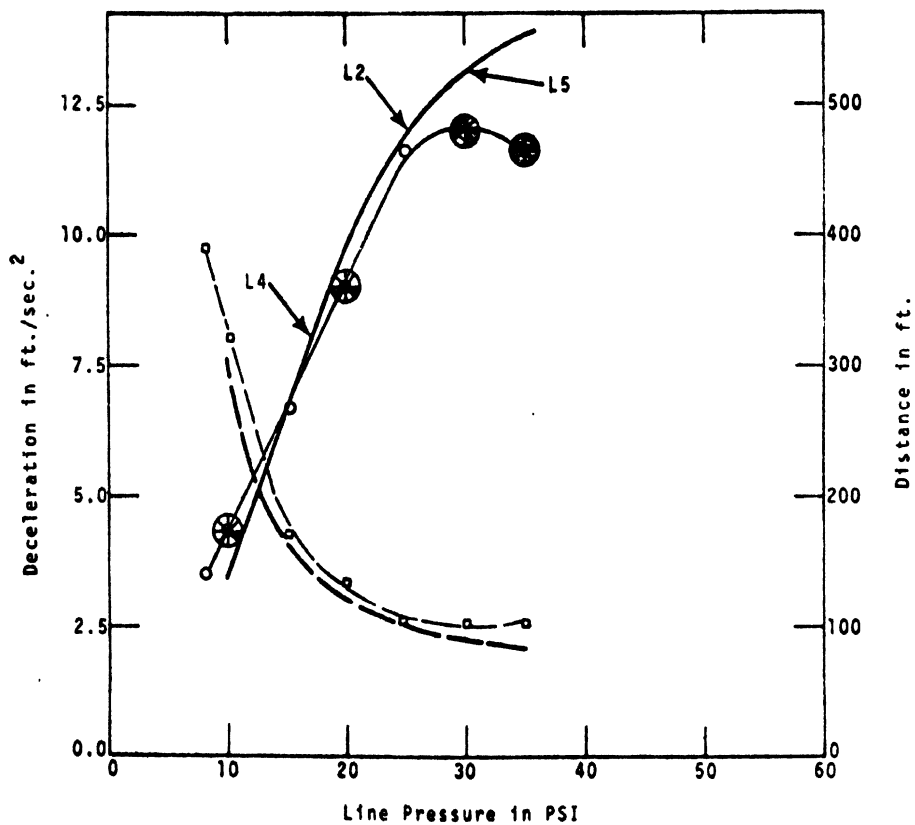


Figure 6-15. Effectiveness test validation: tractor-trailer, empty, 30 mph, wet surface

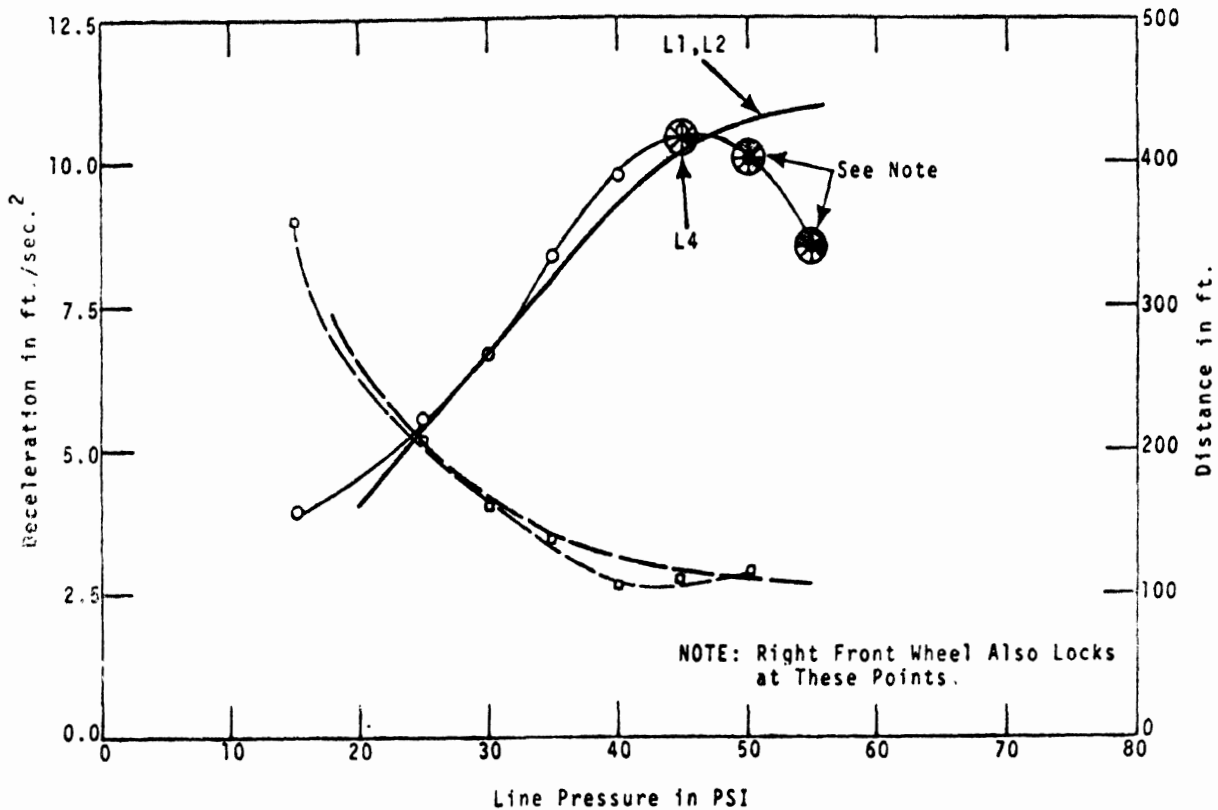


Figure 6-16. Effectiveness test validation: tractor-trailer, loaded, 30 mph, wet surface

In the simulation, due to the nature of the brake fade model (i.e., no time dependence) and the tire model, deceleration increases rapidly with time (mainly as a function of the TQ) and levels off with a much less dramatic peaking effect. Without wheel lock, a steady state deceleration is established and used in the effectiveness test plots. In stops in which wheels are locked, the tire model allows no steady state deceleration to be reached. After the initial transient, the deceleration increases gradually throughout the test. For these cases, a time average of deceleration during this portion of the test is plotted. Consequently, in Figures 6-3 through 6-16, it is somewhat difficult to correlate simulated and experimental deceleration particularly in locked wheel stops. Rather, it is stopping distance and wheel lock behavior which should be valued as a measure of simulated performance.

The results plotted in Figure 6-3 through 6-8 show good correlation between test and simulation for stops with the straight truck on the dry surface. The walking beam suspension model has accurately predicted the line pressure at which wheels of axles 2 and 3 lock. The results also show that stopping distance and sustained deceleration predicted by means of the simulation correlate well with the experimental data.

Results from the simulation of the straight truck effectiveness tests on the wet surface are given in Figures 6-9 and 6-10. The values for the friction reduction parameters used in the tire model are typically larger for a wet surface than for the dry. Thus on the wet surface, the sustained deceleration drops noticeably at points where wheels lock. Note in particular, the correspondence between the behavior of the individual experimental data points and the simulated individual experimental data points and the simulation results at the wheel lock points.

TABLE 6-4
TABULATED STOPPING DISTANCES
Straight Truck

Brake Line Pressure, psi	Stopping Distance, ft.		Brake Line Pressure, psi	Stopping Distance, ft.	
	Measured	Simulated		Measured	Simulated
Empty, 30 mph, Dry Surface			High c.g. Load, 30 mph, Dry Surface		
13	264	220	15	416	350
17	158	155	30	138/145	150
23	99	100	45	86/83	92
27	77	80	55	68/71	77
30	67	72	60	62	72
33	66	70	65	64	71
35	59	69	70	74	70
37	55	60	100	64	62
65	53	55			
75	50	53	High c.g. Load, 50 mph, Dry Surface		
90	46	50	30	430	435
100	45	48	45	300	270
			55	242	220
Empty, 50 mph, Dry Surface			60	208/208	205
13	744	665	65	194	198
17	352	390	Empty, 30 mph, Wet Surface		
23	283	258	12	250	278
27	234	217	15	175	178
30	220	192	17	120	145
33	187	190	20	115	114
35	169	189	22	99	105
37	172	187	25	100	112
100	140	138	28	96	110
Low c.g. Load, 30 mph, Dry Surface			35	88	103
15	344	320	37	95	100
30	106	133	40	101	112
35	70	111	Low c.g. Load, 30 mph, Wet Surface		
55	62	70	13	407	375
57	61	68	18	252	245
60	60	65	25	138	160
70	52	61	30	140	125
80	57	60	33	115	110
100	56	53	35	122/118	106
Low c.g. Load, 50 mph, Dry Surface			38	103	99
30	306	360	40	109	98
45	237	243	43	115	98
55	203	206	45	125	99
60	189	189	50	125	100
65	168	180	60	128	105
70	183	169			
80	172	166			
100	164	152			

TABLE 6-4 (continued)
TABULATED STOPPING DISTANCES

Tractor-Trailer

Brake Line Pressure, psi	Stopping Distance, ft.		Brake Line Pressure, psi	Stopping Distance, ft.	
	Measured	Simulated		Measured	Simulated
Empty, 30 mph, Dry Surface			Loaded, 60 mph, Dry Surface		
10	295	305	40	517	490
15	160	160	50	377	395
17	125	136	60	358	325
20	113	115	65	282/336	310
25	91	95	75	284	290
30	72	80	80	314	269
35	68	72	Empty, 30 mph, Wet Surface		
40	61	69	10	321	304
45	61	64	15	170	142
50	62	60	20	132	120
55	53	58	25	103	100
60	54	56	30	104	91
80	54	52	35	102	85
Empty, 60 mph, Dry Surface			Loaded, 30 mph, Wet Surface		
10	923	1178	15	360	370
15	566/558	550	25	206	205
17	469	490	30	160	168
20	414	425	35	137	142
25	338	350	40	106	124
30	308	302	45	107	113
35	262	275	50	116	108
40	244	250			
45	238	237			
50	230	228			
55	227	216			
60	243	212			
70	221	205			
80	197	198			
Loaded, 30 mph, Dry Surface					
25	164/171	200			
40	94	127			
75	77	74			
80	68	71			
85	69	69			
90	60	66			
91.5	61	66			

Results of the effectiveness test simulation effort for the tractor-trailer are presented in Figures 6-11 through 6-16. Stopping distances for this vehicle were predicted with good accuracy as were decelerations at the lower line pressures prior to wheel lock. However, significant errors in the predicted deceleration levels at which wheel lock occurred and errors in the sustained decelerations at higher line pressures are apparent.

From an examination of the results of the dry surface tests (Figures 6-16 through 6-18), it is apparent that the simulation always predicts wheel lock on the leading axle of each four spring suspension (axles 2 and 4) at a lower deceleration than is actually the case. Conversely, the wheels of the trailing axles (axles 3 and 5) do not lock in the simulation until higher decelerations than those reached in testing are attained. This behavior leads to the conclusion that the four spring suspension model is predicting greater load transfer to the trailing axle than is actually the case. A possible explanation for this discrepancy is that horizontal forces existing at the spring contact points, and which are not considered in the four leaf suspension model (see Chapter 2), contribute to the resistance of the brake force torque about the axle center and thus reduce the inter axle load transfer.

The behavior of the four spring suspension model made it difficult to refine the tire parameters for wet surface testing to include the wiping effect discussed in Section 6.1.1. This fact contributes to the inaccuracies of the simulation results displayed in Figures 6-15 and 6-16.

6.1.3 VALIDATION RESULTS - PITCH ANGLE. Simulated pitch angle results for the straight truck are superimposed in the experimental data in Figures 6-17, 6-18, and 6-19. The agreement between

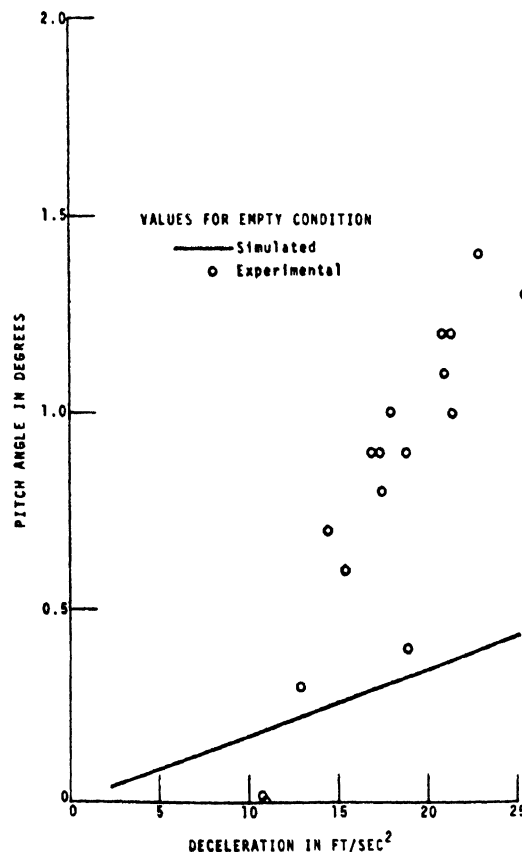


Figure 6-17. Pitch angle validation: straight truck, empty

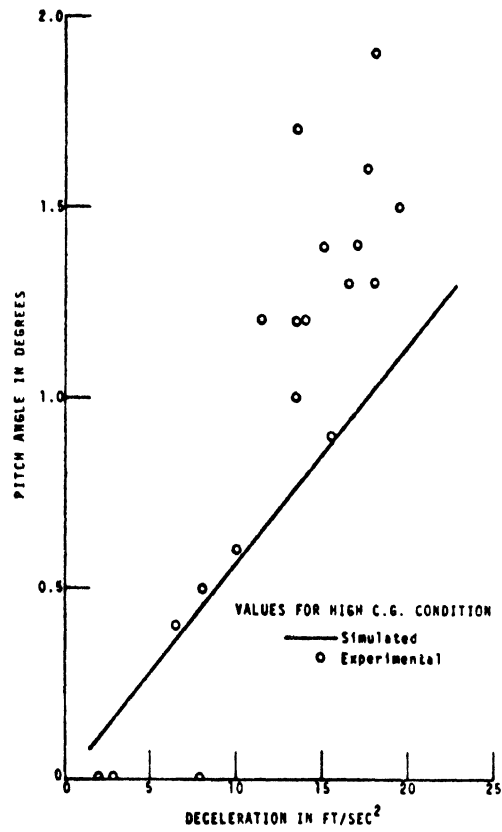


Figure 6-18. Pitch angle validation: straight truck, low c.g. load

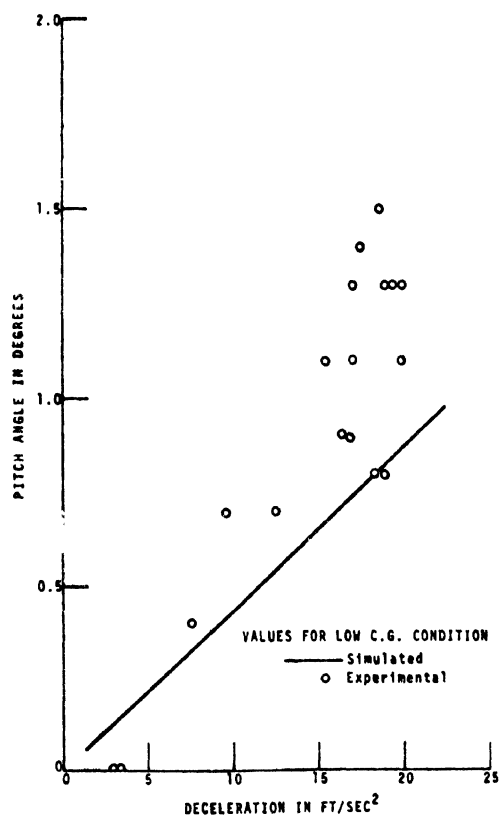


Figure 6-19. Pitch angle validation: straight truck, high c.g. load

simulation and experiment is quite good for the loaded vehicle. However, in the case of the empty vehicle, there is significant deviation between the simulated results and test data. This can be attributed at least in part to limitations of the coulomb friction model (see Section 2). Since the simulated coulomb friction cannot actually "freeze" the suspension, the simulation model must reach the same pitch angle as would be expected in the complete absence of coulomb friction. In actual tests, however, the effects of coulomb friction are apparent, especially in the empty condition.

Simulated pitch angle results for the tractor-trailer are superimposed on the experimental data in Figure 6-20. Again, the agreement is quite good for the loaded vehicle, but shows poor correlation for the empty vehicle.

6.1.4 VALIDATION RESULTS--PARKING BRAKE TEST. The computer program contains a separate module for the simulation of stops under the action of spring-actuated foundation brakes (i.e., parking/emergency brakes). Input data required for this module are ONTIME, the time at which brake torque is first applied, TMAX(I), I=2, KAXLE, the maximum brake torque attained at axle I, and RISE, the characteristic rise time (60%) of the brake torque.

Pressure vs. time traces obtained from the parking brake tests indicate that, after a short time lag which follows activation of the parking brake system by the driver, the air pressure in the brake chamber of the spring brake begins to fall linearly in time. This period is followed by a subsequent period of quasi-exponential decay of the chamber air pressure. This behavior is characterized in Figure 6-21.

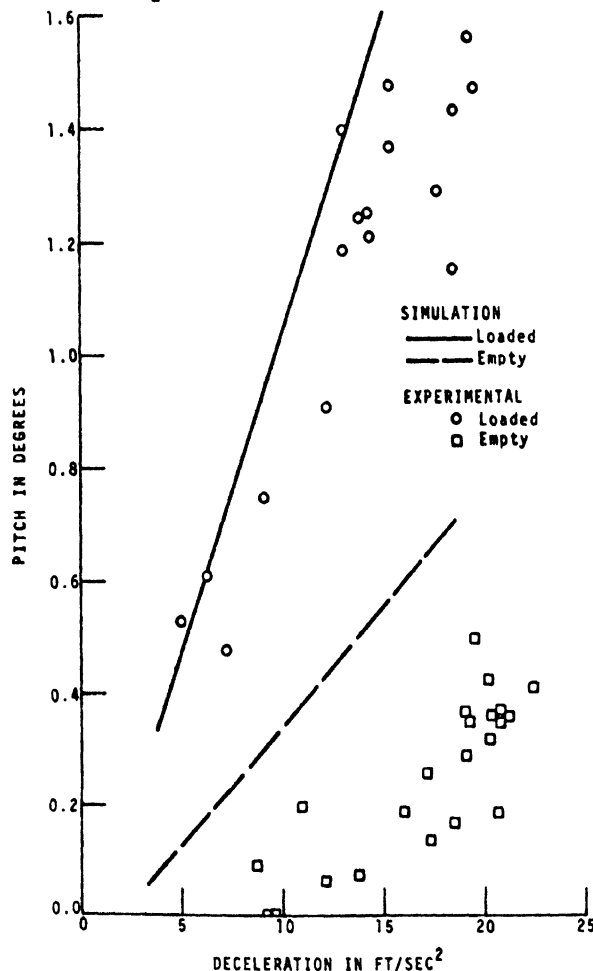


Figure 6-20. Pitch angle validation: tractor-trailer

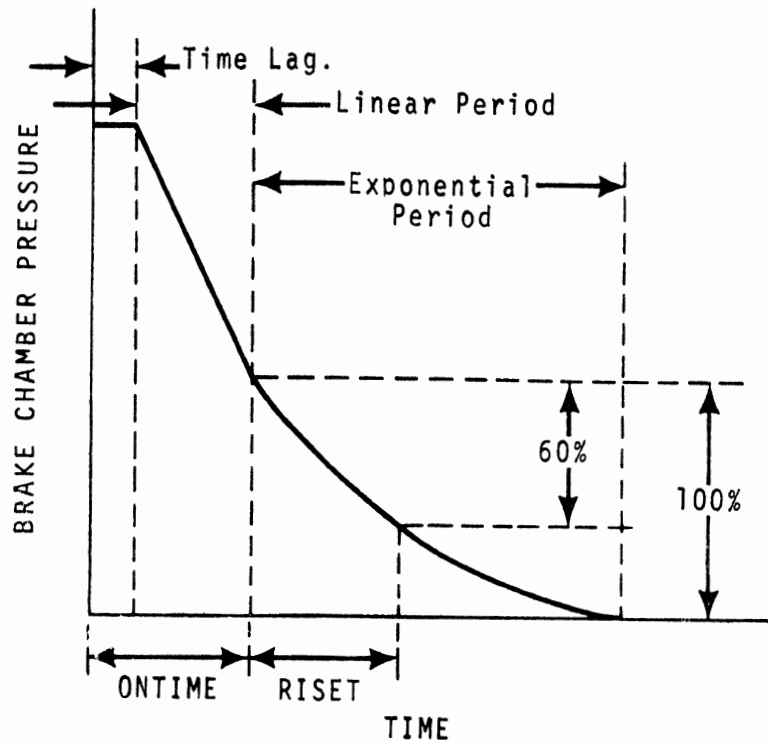


Figure 6-21. Parking brake air pressure behavior

It is assumed that during the time period of linear behavior, the chamber size is decreasing toward the point where shoe-drum contact first takes place. Therefore, brake torque is not initiated until the time period of exponential behavior begins. (Deceleration vs. time data obtained from the parking brake tests support this assumption.)

Therefore, values used for ONTIME in the simulation are the summation of the time lag plus the duration of the linear period of the pressure trace. RISET is then the 60% rise time of the exponential period only. (See Figure 6-21).

Values for TMAX(I) are calculated using the sustained vehicle deceleration from tests of the loaded vehicles (in which no wheels locked) with the assumption that brake torque is evenly distributed between the braking axles. The calculation is indicated in Equation 6-1.

$$TMAX(I) = \frac{GVW}{N} \cdot \frac{a}{32.2} \cdot ALPHA \quad (6-1)$$

where

- TMAX(I) = Maximum torque for each of the braking axles (in-lb)
- N = Number of braking axles
- GVW = Gross vehicle weight (lb.)
- a = Sustained test deceleration (ft/sec²)
- ALPHA = Rolling radius of the wheels of the braking axles (in)

The values used in the simulation are given in Table 6-4.

TABLE 6-5
PARKING BRAKE MODUAL DATA

VEHICLE	ONTIME (sec.)	TMAX(I) (in-lb)	RISSET (sec.)
Straight Truck	0.285	158000., I=2	0.358
		158000., I=3	
Tractor-Trailer	0.370	102000., I=2	0.385
		102000., I=3	
		0., I=4	
		0., I=5	

The results of the parking brake validation tests appear in Table 6-5.

The results of the straight truck loaded test are quite good. Discrepancies in the stopping distance of the tractor-trailer tests are probably due to the limitations of the assumptions made in determining ONTIME and RISSET. Stopping distance errors in the straight truck empty tests result from the limitations of the tire model and the input parameter values of FA(I) and MUZERO(I).

TABLE 6-6
PARKING BRAKE TESTS VALIDATION

VEHICLE CONDITION	STRAIGHT TRUCK EMPTY	STRAIGHT TRUCK LOADED, LOW C.G.	TRACTOR- TRAILER LOADED
Stopping Distance, ft.			
Simulation	63.0	63.7	116.6
Experimental	54.0	61.0	134.
Sustained Deceleration, ft/sec ² *			
Simulation	13.7	11.0	4.5
Experimental	12.4	11.0	4.5
Locked Wheels			
Simulation	ALL REARS	NONE	NONE
Experimental	ALL REARS	NONE	NONE

*Sustained deceleration data is subject to those difficulties discussed in Section 6.1.2.

6.2 CONCLUSIONS

The primary objective of the Phase I study was to develop a computer-based mathematical method for predicting the braking performance of trucks and tractor-trailers. This objective has been achieved. The dynamic simulation programs developed for the study have been validated. The validation process included making the necessary parameter measurements on a truck and tractor-trailer, using the parameter data as input to the simulation program, and comparing the results of the simulation program to the results from road tests on the truck and tractor-trailer. With certain minor qualifications, it can be stated that the results from the simulation programs agree well with the results from the tests. It can be further stated that the programs developed for predicting vehicle braking performance are relatively easy to use, allow a large number of options to the user, are efficient and cost effective.

The limitations of the mathematical models of certain of the modules utilized by the program have been alluded to in Section 6.1. These limitations should be recognized by the user both in preparing input data for the programs and in the analysis of the results. The following items are worthy of mention:

1. Brake Fade - Although the technique used to account for brake fade in a single stop has been proved to be reliable on a macroscopic scale, care must be taken in the selection of the lining friction parameters, ULL, ULH, and FRAY.

2. Suspensions - It was pointed out that the model of the four spring suspension, as presently constituted, predicts excessive inter-axle load transfer; this factor must be taken into account in the analysis of the results.

3. Tires - Road test data is required to determine appropriate values for MUZERO and FA for the tire model, and some care must be taken in simulating vehicle performance on a wet, slippery surface to account for the wiping action of the wheels on the front and/or forward axles.

6.3 RECOMMENDATIONS FOR FURTHER WORK

The findings of the Phase I study have pointed up several areas in which additional work can be accomplished which would minimize the effort required to utilize the computer programs which have been generated and to extend their applicability to a wider range of vehicles and systems. These include the following:

1. Development of a digital computer-based method of predicting the moments of inertia and center of gravity locations along the principal axles for various truck, tractor, and trailer configurations.

2. Refinement of tandem suspension models already developed and formulation of models for three additional suspension types.

3. Determination of the longitudinal slip characteristics of truck tires.

4. Development of models for typical truck antilock systems to be used with Phase I (Braking Performance) and Phase II (Braking and Handling Performance) simulation programs.

5. Extension of the Phase I (Braking Performance) Program to include provision for simulating a doubles (tractor-semitrailer-full trailer) combination.

6. Development of more complete models of mechanical friction brakes, which will more accurately predict the decrease in brake effectiveness as a result of fade.

7. Development of a computer-based mathematical model for evaluating the acceleration and handling performance of trucks and tractor-trailer combinations.

8. Development of a computer-based mathematical method to study the dynamics of automotive air brake systems.

The above mentioned tasks have been incorporated into a follow-on program of study at HSRI, which is being funded by the Motor Vehicle Manufacturers Association.

APPENDIX A
List of Symbols

Preceding page blank

APPENDIX A
List of Symbols

The following list includes all the input parameters to the program, the parameters which are computed in the program, and the variables of motion. The dimensions of the input parameters are in [inch, pound, second]. These are converted to the [slug, foot, second] system immediately after they are read into the program subroutine INPUT. Thus, the equations of motion and all the auxiliary computations in subroutine FCT1 are written in terms of variables in the [slug, foot, second] system.

To avoid confusion, parameters which are read in are labelled with an (R), parameters which are calculated rather than input are labelled with a (C), and the variables of motion are labelled with a (V).

For the walking beam; straight truck or tractor...

- AA1 horizontal distance from walking beam pin to front tandem axle (in) (R)
- AA2 horizontal distance from walking beam pin to rear tandem axle (in) (R)
- AA3 horizontal distance from walking beam pin to walking beam mass center (ft) (C)
- AA4 vertical distance from axle to walking beam (in) (R)
- AA5 vertical distance from axle to torque rod (in) (R)
- AA6 horizontal distance from front tandem axle to walking beam mass center (ft) (C)
- AA7 horizontal distance from rear tandem axle to walking beam mass center (ft) (C)

For the 4 spring suspension; straight truck or tractor...

- AA1 horizontal distance from front leaf-frame contact to axle center (in) (R)
- AA2 horizontal distance from rear leaf-frame contact to axle center (in) (R)
- AA4 horizontal distance from front leaf contact to load leveler "pin" (in) (R)
- AA5 horizontal distance from rear leaf contact to load leveler "pin" (in) (R)
- AA6 vertical distance from axle down to torque rod (in) (R)
- AA7 angle between torque rod and horizontal (deg) (R)
- AA8 horizontal distance from axle center forward to torque rod (in) (R)
- ARM1 perpendicular distance from line of action of TR2 (TR3) to forward (rear) tandem axle center (ft) (C)
- ARM2 horizontal distance from sprung mass c.g. to forward tandem axle center (ft) (C)
- ARM3 horizontal distance from sprung mass c.g. to rear tandem axle center (ft) (C)

For walking beam; trailer...

- AA9 horizontal distance from walking beam pin to front tandem axle (in) (R)
- AA10 horizontal distance from walking beam pin to rear tandem axle (in) (R)
- AA11 horizontal distance from walking beam pin to walking beam mass center (ft) (C)
- AA12 vertical distance from axle to walking beam (in) (R)
- AA13 vertical distance from axle to torque rods (in) (R)
- AA14 horizontal distance from front tandem axle to walking beam mass center (ft) (C)

AA15 horizontal distance from rear tandem axle to walking beam mass center (ft) (C)

For the 4 spring suspension; trailer...

AA9 horizontal distance from front leaf-frame contact to axle center (in) (R)
AA10 horizontal distance from rear leaf-frame contact to axle center (in) (R)
AA12 horizontal distance from front leaf contact to load leveler "pin" (in) (R)
AA13 vertical distance from rear leaf contact to load leveler "pin" (in) (R)
AA14 vertical distance from axle down to torque rod (in) (R)
AA15 angle between torque rod and horizontal (deg) (R)
AA16 horizontal distance from axle center forward to torque rod (in) (R)
ARM4 perpendicular distance from line of action of TR4 (TR5) to forward (rear) tandem axle center (ft) (C)
ARM5 horizontal distance from sprung mass c.g. to forward tandem axle center (ft) (C)
ARM6 horizontal distance from sprung mass c.g. to rear tandem axle center (ft) (C)

For all vehicles...

A1 horizontal distance from truck (tractor) CG to center of truck (tractor) front suspension (in) (R)
A2 horizontal distance from truck (tractor) CG to center of truck (tractor) rear suspension (in) (R)
A3 horizontal distance from trailer CG to 5th wheel (in) (R)
A4 horizontal distance from trailer CG to center of trailer suspension (in) (R)
ALPHA1 static distance, truck (tractor) front axle to ground (in) (R)
ALPHA2 static distance, truck (tractor) rear axle to ground (in) (R)
ALPHA3 static distance, trailer axle(s) to ground (in) (R)
BB horizontal distance from 5th wheel to midpoint of tractor rear suspension (in) (R)
C1 viscous damping: jounce on truck (tractor) front suspension (lb-sec/in) (R)
C2 viscous damping: rebound on truck (tractor) front suspension (lb-sec/in) (R)
C3 viscous damping: jounce on truck (tractor) rear suspension (lb-sec/in) (R)
C4 viscous damping: rebound on truck (tractor) rear suspension (lb-sec/in) (R)
C5 viscous damping: jounce on trailer suspension (lb-sec/in) (R)
C6 viscous damping: rebound on trailer suspension (lb-sec/in) (R)
CF1 maximum coulomb friction, truck (tractor) front suspension (lb) (R)
CF2 maximum coulomb friction, truck (tractor) rear suspension (lb) (R)
CF3 maximum coulomb friction, trailer suspension (lb) (R)
CS(I) longitudinal stiffness, axle I (lbs) (R)
CT(I) tire-road interface vertical damping, axle I (lb-sec/ft) (C)

D vertical distance from 5th wheel to tractor CG (in) (R)
D1 vertical distance from 5th wheel to trailer CG (in) (R)
DELL-DEL3 coulomb friction "break points" (ft/sec) (C)
DELTA1 static vertical distance, truck (tractor) CG to truck
(tractor) front axle (in) (R)
DELTA2 static vertical distance, truck (tractor) CG to truck
(tractor) rear axle(s) (ft) (C)
DELTA3 static vertical distance, trailer CG to trailer rear
axle(s) (in) (R)
EBX array containing RPM points for RPM vs torque table
(see engine braking) (R)
EBY array containing TORQUE points for RPM vs torque ta-
ble (see engine braking) (R)
EMPTY(I) empty proportioning, axle I (R)
FA(I) tire/road friction reduction parameter, axle I (sec/ft)
(R)
GEARV(I) velocity at which driver shifts into Ith gear
(I=1, NOGEAR) (R)
GRAT(I) gear ratio (I=1, NOGEAR) (R)
GVW gross vehicle weight (lbs) (C)
H horizontal force on 5th wheel (lbs) (V)
ICOUNT engine braking and/or prop shaft braking and/or
auxiliary retarders key (R)
J truck (tractor) polar moment (in lb sec**2) (R)
J1 trailer polar moment of inertia (in lb sec**2) (R)
JS(I) polar moment of inertia, wheels at axle I (in lb sec
**2) (R)
K1 spring rate, truck (tractor) front suspension (lb/in)
(R)
K2 spring rate, truck (tractor) rear suspension (lb/in)
(R)
K3 spring rate, trailer suspension (lb/in) (R)
KAXLE number of axles on vehicle (C)
KEY truck axle key 0 for single axle
KEY(1) tractor axle key 1 for walking beam
KEY(2) trailer axle key 2 for four spring
suspension
KEYAR* auxiliary retarder key 1 for in use
KEYEB* engine braking key 0 for not in use
KF vertical spring rate of 5th wheel (lb/ft) (C)
KMAPB mechanical actuation of parking brakes key (R)
KPROP static load sensing brake key (R)
KPSB* prop shaft braking key 1 for in use
0 for not in use
KROAD road key (R)
KSAFB spring actuation of foundation brakes key (R)
KT(I) spring rate of tires, axle I (lb/in) (R)
L(I) horizontal force at suspension I (lb) (C)
MAPBX array containing time points for parking brake table
(see mechanical actuation of parking brakes) (R)
MAPBY array containing TORQUE points for parking brake
table (see mechanical actuation of parking brakes) (R)
MAXAX(I) maximum load, axle I (lbs) (R)
M1 sprung mass of truck (tractor) (slugs) (C)
M2 sprung mass of trailer (slugs) (C)
MS(I) mass of suspension axle and wheel, axle I (slugs) (C)
MUZERO(I) coefficient of friction, tires, axle I (R)
N(I) normal force on tire, axle I (lbs) (V)
NOGEAR number of gears on vehicle (R)

*Only used if ICOUNT = 1.

NOMAPB number of points in time vs TORQUE to rear (front tandem) wheels table (see mechanical actuation of parking brakes) (R)
 NS(I) total static load on tires, axle I (lbs) (C)
 NUMEB number of points in PRM vs TORQUE to drive wheels table (see engine braking) (R)
 OMEGAD(I) wheel angular acceleration (rad/sec^2) (V)
 ONTIME time at which spring brakes are applied (sec) (R)
 P1 truck (tractor) walking beam interaxle load transfer parameter (C)
 PERCNT percent effectiveness of truck torque rods (R)
 PERCNT(1) percent effectiveness of tractor torque rods (R)
 PERCNT(2) percent effectiveness of trailer torque rods (R)
 PJ polar moment of payload (in lb sec^2) (R)
 PM payload mass (slugs) (C)
 PROP(I) brake proportioning constant, axle I (R)
 PX horizontal distance from midpoint of truck rear (trailer) suspension to payload mass center (in) (R)
 PW weight of payload (lb) (R)
 PZ vertical distance from ground to payload mass center (in) (R)
 RISET time to reach 60% of TMAX (see spring actuation of foundation brakes) (sec) (R)
 ROADZ(I) vertical coordinate of road, axle I...up is positive (in) (R)
 RR(I) rolling radius, tires on axle I (ft) (C)
 S(I) extension of suspension at axle I (ft) (C)
 SD(I) velocity of suspension extension at axle I (ft/sec) (C)
 SF(I) total load minus static load in the suspension, axle I (tension is positive) (lbs) (V)
 SLIP(I) wheel slip, axle I (V)
 T(I) attempted brake torque, axle I (in lbs) (R)
 TIMEF maximum real time for simulation (sec) (R)
 TMAX(I) maximum torque to the wheels, axle I (see spring actuation foundation brakes) (in lbs) (R)
 TN1-TN4 contact force between tractor leaf springs and frame (lb) (V)
 TP1 trailer walking beam interaxle load transfer parameter (C)
 TQ(I,1) line pressure time lag, axle I (sec) (R)
 TQ(I,2) line pressure rise time characteristic, axle I (sec) (R)
 TRUCK exit key (R): TRUCK=1.0, another data set follows
 TRUCK=0.0, call exit
 TR2-TR5 tensile forces in torque rods at appropriate axle (lb) (C)
 TT(I) actual brake torque, axle I (ft lbs) (V)
 TTN1-TTN4 contact forces between trailer leaf spring and frame (lb) (V)
 TXX static load on trailer walking beam pin (lb) (C)
 V total vertical load on 5th wheel minus VS (lb) (V)
 VEL initial velocity (ft/sec) (R)
 VS static vertical load on 5th wheel (lb) (C)
 W1 sprung weight of truck (tractor) (lb) (R)
 W2 sprung weight of trailer (lb) (R)
 WS(I) weight of suspension, axle, and wheel; axle I (lb) (R)
 XDD vehicle acceleration (ft/sec^2) (V)
 XDOT vehicle velocity (ft/sec) (V)

XXX static load on tractor walking beam pin (lb) (C)
 YT(I) tire position, axle I (ft) (V)
 YTD(I) tire velocity, axle I (ft/sec) (V)
 Z1-Z3 static suspension deflection computed in look-up for
 nonlinear spring (ft) (C)

For brake module at axle I...

AB(I) distance from horizontal centerline of drum to parallel
 line through shoe contact (in) (R)
 AC(I) brake chamber area (sq. in) (R)
 ALPH1(I) acute angle between a diametrical line through a shoe
 pin and a diametrical line through the top (see figure
 2-31) drum/lining contact point of the same shoe (deg)
 ALPH3(I) $ALPHO(I) + 2*ALPH1(I)$ (deg) (R)
 ALPHO(I) lining contact angle (deg) (R)
 ALPHW(I) wedge angle (deg) (R)
 ALPRIM(I) radial distance from center of drum to shoe pin (in) (R)
 BETA(I) lining offset angle (deg) (R)
 C2(I) distance from horizontal centerline of drum to parallel
 line through point of actuating force (in) (R)
 EM(I) mechanical efficiency (R)
 FRAY brake fade coefficient (R)
 HB(I) distance from horizontal centerline through shoe pin
 to parallel line through connector contact point
 (in) (R)
 IBRT(I) brake type (R) 0 for no brakes
 1 for s-cam brake
 2 for 2-wedge brake
 3 for 1-wedge brake
 4 for DSSA
 5 for duplex brake
 6 for disc brake
 OH(I) distance from vertical centerline of drum to parallel
 line through shoe contact point (in) (R)
 PO(I) pushout pressure (psi) (R)
 RC(I) cam radius (in) (R)
 RD(I) drum radius (in) (R)
 SAL (I) slack adjuster length (in) (R)
 ULH(I) lining friction coefficient, high (R)
 ULL(I) lining friction coefficient, low (R)

For all vehicles...The following are the integration variables sent to subroutine HPCC

Y(1) Z (ft), vertical position of truck (tractor) mass center
 Y(2) $\frac{dz}{dt}$ (ft/sec)
 Y(3) θ (rad), truck (tractor) pitch angle
 Y(4) $\frac{d\theta}{dt}$ (rad/sec)
 Y(5) X (ft), truck (tractor) longitudinal position
 Y(6) $\frac{dX}{dt}$ (ft/sec)
 Y(7) ZS(1) (ft), vertical position, axle 1
 Y(8) $\frac{d}{dt}(ZS(1))$ (ft/sec)
 Y(9) ZS(2) (ft), vertical position, axle 2

Y(10) $\frac{d}{dt}(ZS(2))$ (ft/sec)
 For the walking beam; truck or tractor...
 Y(11) θT (rad), walking beam pitch angle
 Y(12) $\frac{d}{dt}(\theta T)$ (rad/sec)
 For the four spring suspension; truck or tractor...
 Y(11) ZS(3) (ft), vertical position, axle 3
 Y(12) $\frac{d}{dt}(ZS(3))$ (ft/sec)
 For the trailer...
 Y(13) Z1 (ft), vertical position of trailer mass center
 Y(14) $\frac{d}{dt}(Z1)$ (ft/sec)
 Y(15) $\theta 1$ (rad), trailer pitch angle
 Y(16) $\frac{d}{dt}(\theta 1)$ (rad/sec)
 Y(17) ZS(4) (ft), vertical position, axle 4
 Y(18) $\frac{d}{dt}(ZS(4))$ (ft/sec)
 For the walking beam trailer rear tandem...
 Y(19) $\theta 1$ (rad), walking beam pitch angle
 Y(20) $\frac{d}{dt}(\theta 1)$ (rad/sec)
 For the four spring suspension, trailer rear tandem...
 Y(19) ZS(5) (ft), vertical position, axle 5
 Y(20) $\frac{d}{dt}(ZS(5))$ (ft/sec)
 DERY(I) $\frac{d}{dt}(Y(I))$ (I=1, 20)

APPENDIX B
Equations on Motion

Preceding page blank

APPENDIX B

1. INTRODUCTION

The equations of motion of the articulated vehicle are given below. The straight truck equations may be derived by setting the kingpin forces V and H to zero in the tractor equations. The equations for the static loading, the mass center and inertia changes due to payload, and the brake forces were given in Section 2 and will not be repeated here.

Equations are given in the following order:

- a) Equations concerning the entire vehicle
- b) Tractor Equations
- c) Trailer Equations.

In sections (b) and (c) single axle equations are presented first, then those equations which change when a walking beam suspension is used, then those equations which change when a four spring suspension is used.

2. EQUATIONS CONCERNING BOTH THE TRACTOR AND TRAILER

Deceleration:

$$\frac{GVW}{32.2} XDD = \sum_{I=1}^{KAXLE} FX(I) \quad (B-1)$$

Kingpin Forces:

$$V = [Z1 - A3 \cdot \theta - Z - (A2 - BB) \theta] \quad (B-2)$$

$$H = \sum_{\substack{\text{Trailer} \\ \text{Axles}}} \{FX(I) - MS(I) \cdot XDD\} - M1 \cdot XDD \quad (B-3)$$

3. THE TRACTOR EQUATIONS - SINGLE AXLE

Suspension Deflection:

$$S(1) = -Z + A1 \cdot \theta + ZS(1) \quad (B-4)$$

$$S(2) = -Z - A2 \cdot \theta + ZS(2) \quad (B-5)$$

Suspension Velocity:

$$SD(1) = -\dot{Z} + A1 \cdot \dot{\theta} + \dot{ZS}(1) \quad (B-6)$$

$$SD(2) = -\dot{Z} - A2 \cdot \dot{\theta} + \dot{ZS}(2) \quad (B-7)$$

Axle Positions (I = 1,3):

$$YT(I) = ZS(I) \quad (B-8)$$

Axle Velocities (I = 1,3):

$$YTD(I) = ZSD(I) \quad (B-9)$$

Suspension Forces:

$$SF(1) = K(1) \cdot S(1) + CCCC \cdot SD(1) + CCl \quad (B-10)$$

where $CCCC = C(1), SD(1) \leq 0$

$CCCC = C(2), SD(1) > 0$

$CC1 = CF(1) \cdot SD(1)/DEL1, |SD(1)| \leq DEL1$

$CC1 = CF(1) \cdot SD(1)/|SD(1)|, |SD(1)| > DEL1$

$$SF(2) = K(2) \cdot S(2) + CCCC \cdot SD(2) + CC2 \quad (B-11)$$

where $CCCC = C(3), SD(2) \leq 0$

$CCCC = C(4), SD(2) > 0$

$CC2 = CF(2) \cdot SD(2)/DEL2, |SD(2)| \leq DEL2$

$CC2 = CF(2) \cdot SD(2)/|SD(2)|, |SD(2)| > DEL2$

Normal Forces on the Tires (I = 1,2):

$$N(I) = NS(I) + KT(I)(YT(I) + ROADZ(I)) + CT(I)(YTD(I)) \quad (B-12)$$

where $CT(I) = .04[KT(I) \cdot MS(I)]^{1/2}$

Unsprung Masses - Vertical Motion (I = 1,2)

$$MS(I) \ddot{ZS}(I) = -SF(I) + NS(I) - N(I) \quad (B-13)$$

Sprung Mass-Bounce:

$$M1(\ddot{Z}) = SF(1) + SF(2) + V \quad (B-14)$$

Sprung Mass - Pitch:

$$\begin{aligned} J(\ddot{\theta}) = & -SF(1)A1 + SF(2)A2 + V(A2-BB) - H \cdot D - TT(1) \\ & - TT(2) - L1(DELTA1) - L2(DELTA2) \end{aligned} \quad (B-15)$$

4. THE TRACTOR EQUATIONS - WALKING BEAM SUSPENSION

Axle Positions and Velocities:

$$YT(2) = ZS(2) - AA6 \cdot \theta T \quad (B-16)$$

$$YT(3) = ZS(2) + AA7 \cdot \theta T \quad (B-17)$$

$$YTD(2) = ZSD(2) - AA6 \cdot \dot{\theta T} \quad (B-18)$$

$$YTD(3) = ZSD(3) + AA7 \cdot \dot{\theta T} \quad (B-19)$$

Torque Rod Forces (I = 2,3):

$$TRI = \frac{TT(I) - AA4(MS(I) \cdot XDD-FX(I))}{AA4 + (1+P1)AA5} \quad (B-20)$$

Moment About the Axle Due to Vertical Forces (I = 2,3):

$$VAI = P1(TRI)AA5 \quad (B-21)$$

Rear Unsprung Masses - Vertical Motion:

$$(MS(2) + MS(3)) \ddot{ZS}(2) = -SF(2) + NS(2) - N(2) + NS(3) - N(3) \quad (B-22)$$

where in this case, ZS(2) locates the mass center of the tandem assembly.

Rear Unsprung Mass - Pitch:

$$AA8 \cdot \dot{\theta} = N(2)AA6 - N(3)AA7 - VA2 - VA3 + (SF2-XXX)AA3 \quad (B-23)$$

Sprung Mass - Pitch:

$$\begin{aligned} J\ddot{\theta} = & -SF(1) A1 + SF(2) A2 + DELTA(2) \cdot \\ & [FX(2) + FX(3) - (MS(2) + MS(3)) \cdot XDD] - TT(1) - TT(2) - TT(3) \\ & + VA2 + VA3 - L(1) DELTA(1) + V(A2-BB) - H \cdot D \quad (B-24) \end{aligned}$$

5. THE TRACTOR EQUATIONS - FOUR SPRING SUSPENSION Axle Positions and Velocities: (I = 2,3)

$$YT(I) = ZS(I) \quad (B-25)$$

$$YTD(I) = \dot{ZS}(I) \quad (B-26)$$

Suspension Position and Velocity:

$$S(2) = -Z + \frac{YT(2) + YT(3)}{2} - A2 \cdot \theta \quad (B-26)$$

$$SD(2) = -\dot{Z} + \frac{YTD(2) + YTD(3)}{2} - A2 \cdot \dot{\theta} \quad (B-27)$$

Torque Rod Forces (I = 2,3):

$$TRI = [MS(I) \cdot XDD - FX(I)] / \cos(AA7) \quad (B-28)$$

Leaf-Frame Contact Forces

$$TN1(AA1) - TN2(AA2) = JS(2) \cdot \dot{r}(2) + TR2 ARM(1) + FX(2) \cdot RR(2) \quad (B-29)$$

$$TN3(AA1) - TN4(AA2) = JS(3) \cdot \dot{r}(3) + TR3 ARM(1) + FX(3) \cdot RR(3) \quad (B-30)$$

$$TN2(AA4) - TN3(AA5) = 0 \quad (B-31)$$

$$TN1 + TN2 + TN3 + TN4 = -SF(2) + TN1S + TN2S + TN3S + TN4S \quad (B-32)$$

Rear Unsprung Masses - Vertical Motion:

$$MS(2) (\ddot{Z}\dot{S}(2)) = TN1 + TN2 + MS(2) g - N2 - TR2 \cdot \sin(AA7) \quad (B-33)$$

$$MS(3) (\ddot{Z}\dot{S}(3)) = TN3 + TN4 + MS(3) g - N3 - TR3 \cdot \sin(AA7) \quad (B-34)$$

Sprung Mass Pitch

$$\begin{aligned} J\ddot{\theta} = & (TN1S - TN1)(ARM(2) - AA1) + (TN2S - TN2)(ARM(2) + AA2) \\ & + (TN3S - TN3)(ARM(3) - AA1) + TN4S - TN4)(ARM(4) + AA2) \\ & - SF1(A1) - TT(1) - L(1) \cdot DELTA1 \\ & + \sin(AA7) [ARM(2) \cdot TR2 + ARM(3) \cdot TR3] - [\cos(AA7) \cdot DELTA2 + ARM(1)] \\ & (TR2 + TR3) + V(A2-BB) - H \cdot D \quad (B-35) \end{aligned}$$

6. THE TRAILER EQUATIONS - SINGLE AXLE:

Note axles four and five are discussed here, thus assuming tandem axles on the tractor. If the tractor has a single rear axle, the trailer axles will be axles three and four. No confusion should result in the suspension designation--the trailer suspension is always suspension three.

Suspension Deflection and Velocity:

$$S(3) = -Z1 - A4 \cdot \theta1 + ZS(4) \quad (B-36)$$

$$SD(3) = -\dot{Z}1 - A4 \cdot \dot{\theta}1 + ZSD(4) \quad (B-37)$$

Axle Position and Velocity

$$YT(4) = ZS(4) \quad (B-38)$$

$$YTD(4) = Z\dot{S}(4) \quad (B-39)$$

Suspension Force:

$$SF(3) = K(3) * S(3) + CCCC * SD(3) + CC(3) \quad (B-40)$$

where

$$CCCC = C(5), \quad SD(3) \leq 0$$

$$CCCC = C(6), \quad SD(3) > 0$$

$$CC(3) = CF(3) \cdot SD(3) / DEL3, \quad |SD(3)| \leq DEL3$$

$$CC(3) = CF(3) \cdot SD(3) / |SD(3)|, \quad |SD(3)| > DEL3$$

Normal Forces on the Tire:

$$N(4) = NS(4) + KT(4) * (YT(4) + ROAD(4)) + CT(4) * YTD(4) \quad (B-41)$$

where

$$CT(4) = .04 [KT(4) \cdot MS(4)]^{1/2}$$

Unsprung Mass - Vertical Motion

$$MS(4) \dot{ZS}(4) = -SF(3) + NS(4) - N(4) \quad (B-42)$$

Sprung Mass - Bounce

$$M2 \dot{Zi} = SF(3) - V \quad (B-43)$$

Sprung Mass - Pitch

$$J1 (\dot{\theta i}) = SF(3) A4 + V \cdot A3 - H \cdot D1 \quad (B-43)$$

7. THE TRAILER EQUATIONS - WALKING BEAM SUSPENSION

Axle Positions and Velocities:

$$YT(4) = ZS(3) - AA13 \cdot \theta T1 \quad (B-44)$$

$$YT(5) = ZS(3) + AA14 \cdot \theta T1 \quad (B-45)$$

$$YTD(4) = ZS(3) - AA13 \cdot \dot{\theta T1} \quad (B-46)$$

$$YTD(5) = ZS(3) + AA14 \cdot \dot{\theta T1} \quad (B-47)$$

Torque Rod Forces (I = 4,5):

$$TRI = \frac{TT(I) - AA12 (MS(I) \cdot XDD - FX(I))}{AA12 + (1 + TP1) AA13} \quad (B-47)$$

Moment About the Axle Due to Vertical Forces (I = 4,5):

$$VAI = TP1(TRI) AA13 \quad (B-48)$$

Unsprung Masses - Bounce:

$$(MS(4) + MS(5)) \dot{ZS}(3) = -SF(3) + NS(4) - N(4) + NS(5) - N(5) \quad (B-49)$$

where, in this case, ZS(3) locates the mass center of the tandem assembly.

Unsprung Masses - Pitch:

$$AA15 (\dot{\theta iT}) = N(4)AA14 - N(5)AA15 - VA4 - VA5 + (SF(3) - TXXX) AA10 \quad (B-50)$$

Sprung Mass - Pitch:

$$\begin{aligned} J1 (\dot{\theta i}) &= SF(3) A4 + V \cdot A3 - H \cdot D1 \\ &+ DELTA3 [FX(4) + FX(5) - (MS(4) + MS(5)) \cdot XDD] \\ &- TT(4) - TT(5) + VA4 + VA5 \end{aligned} \quad (B-51)$$

8. THE TRAILER EQUATIONS - FOUR SPRING SUSPENSION

Axle Positions and Velocities (I = 4,5):

$$YT(I) = ZS(I) \quad (B-52)$$

$$YTD(I) = Z\dot{S}(I) \quad (B-53)$$

Suspension Position and Velocity:

$$S(3) = -Z(1) + \frac{XT(4) + XT(5)}{2} - A4 \cdot \theta 1 \quad (B-54)$$

$$SD(3) = -\dot{Z}(1) + \frac{YTD(4) + YTD(5)}{2} - A4 \cdot \theta 1 \quad (B-55)$$

Torque Rod Forces (I = 4,5):

$$TRI = (MS(I) \cdot XDD - FX(I))/\cos(AA14) \quad (B-56)$$

Leaf Frame Contact Forces

$$\begin{aligned} TTN1(AA9) - TTN2(AA10) &= JS(4) \cdot \dot{r}(4) \\ &+ TR4 \cdot ARM(4) + FX(4) \cdot RR(4) \end{aligned} \quad (B-57)$$

$$\begin{aligned} TTN3(AA9) - TTN4(AA10) &= JS(5) \cdot \dot{r}(5) \\ &+ TR5 \cdot ARM(4) + FX(5) \cdot RR(5) \end{aligned} \quad (B-58)$$

$$TTN2(AA12) - TTN3(AA13) = 0 \quad (B-59)$$

$$TTN1 + TTN2 + TTN3 + TTN4 = -SF(3) + TTN1S + TTN2S + TTN3S + TTN4S \quad (B-60)$$

Rear Unsprung Masses Vertical Motion:

$$MS(4) \cdot \dot{Z}\dot{S}(4) = TTN1 + TTN2 - MS(4) g - N4 - TR4 \sin(AA14) \quad (B-61)$$

$$MS(5) \cdot \dot{Z}\dot{S}(5) = TTN3 + TTN4 - MS(5) g - N5 - TR5 \sin(AA14) \quad (B-62)$$

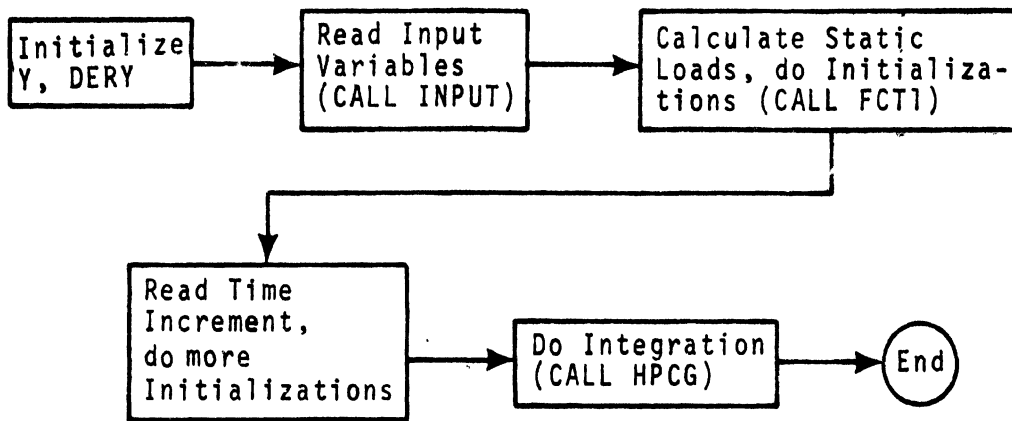
Sprung Mass Pitch:

$$\begin{aligned} J1 \cdot \dot{\theta}\dot{i} &= (TTN1S - TTN1)(ARM(4) - AA9) \\ &+ (TTN2S - TTN2)(ARM(4) + AA10) + (TTN3S - TTN3)(ARM(5) - AA9) \\ &+ (TTN4S - TTN4)(ARM(5) + AA10) \\ &+ \sin(AA14)[ARM(4) \cdot TR4 + ARM(5) \cdot TR5] \\ &- [\cos(AA15) \cdot DELTA2 + ARM(1)](TR2 + TR3) + V \cdot A3 - H \cdot D1 \end{aligned} \quad (B-63)$$

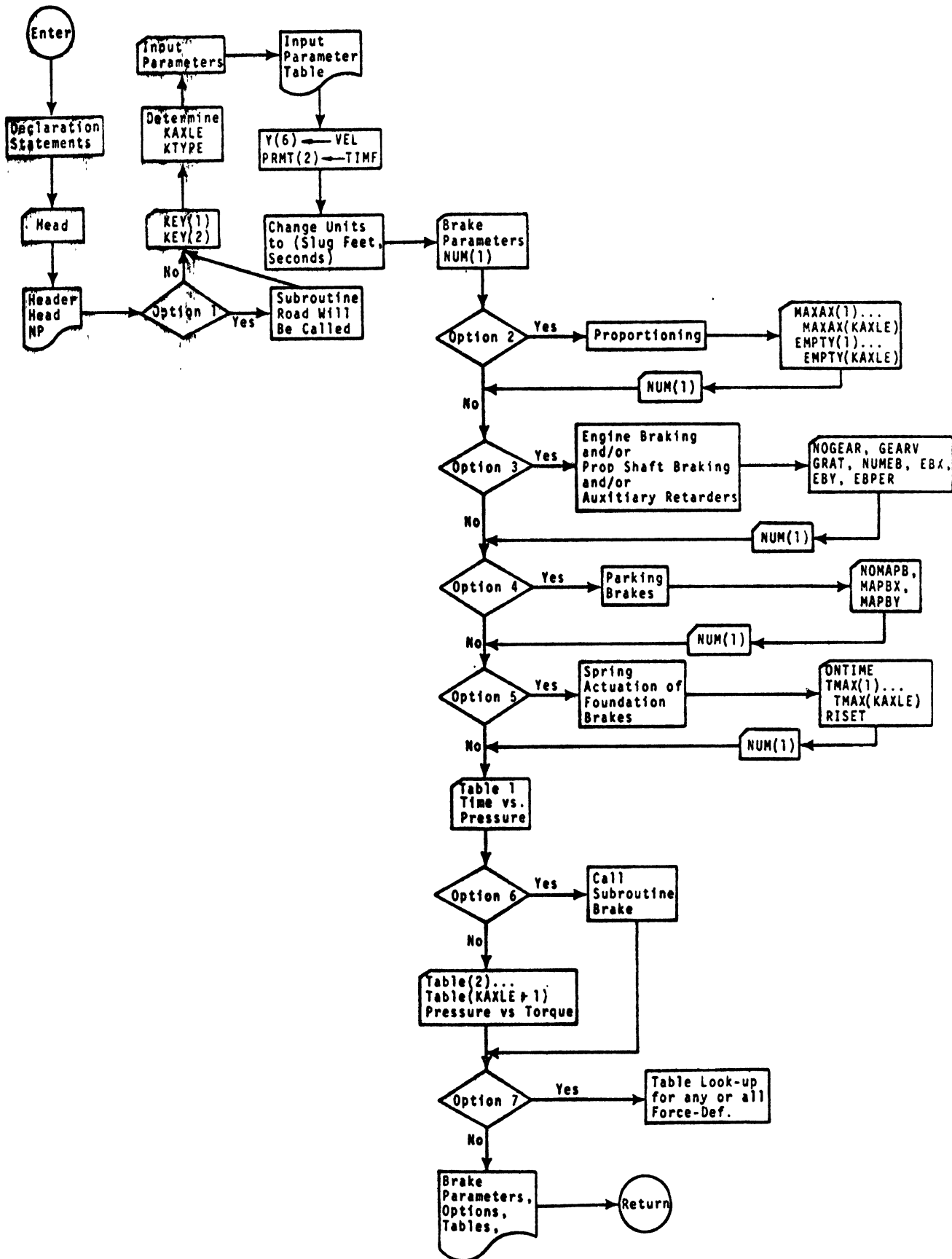
APPENDIX C
Flow Charts

Preceding page blank

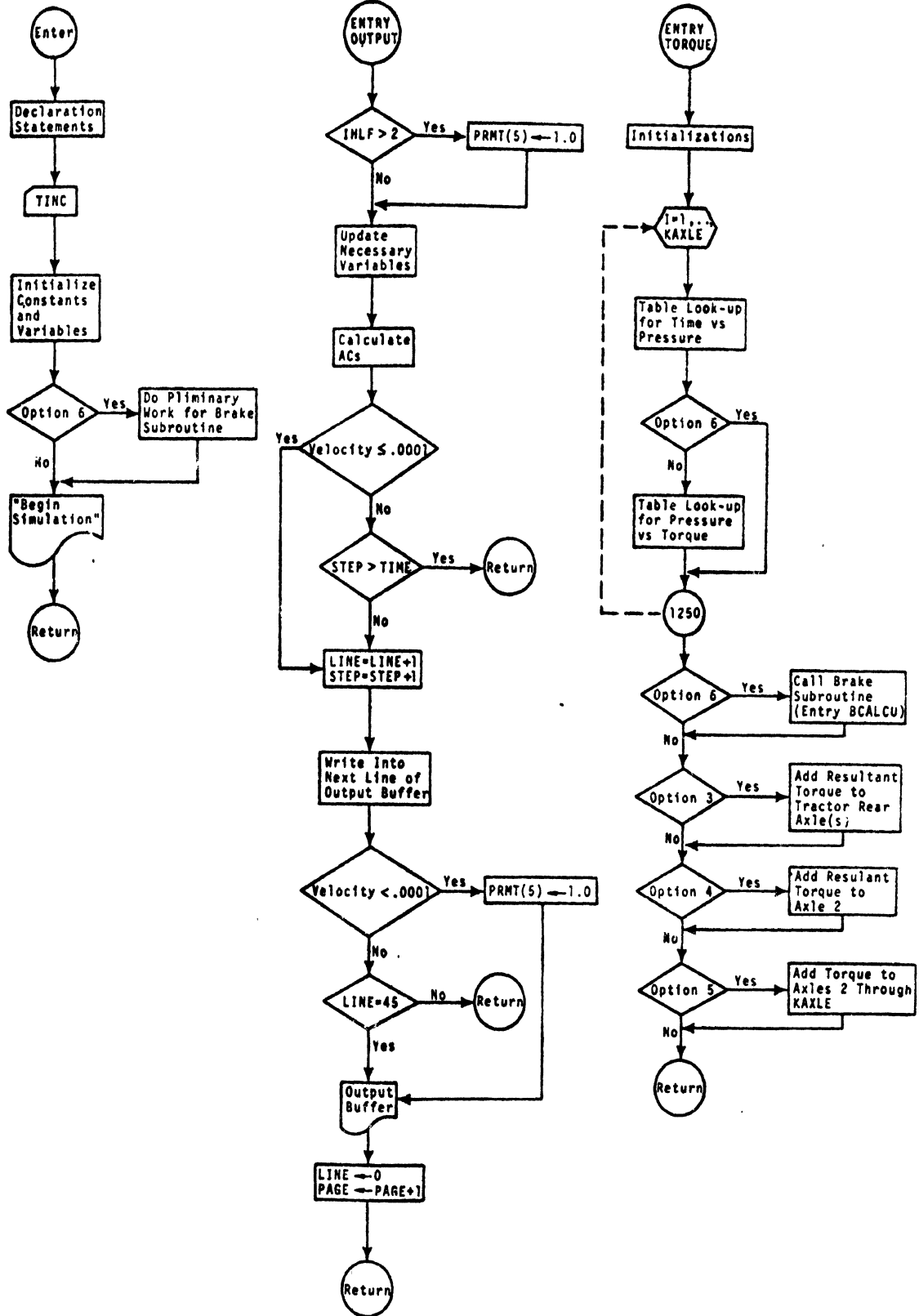
Main



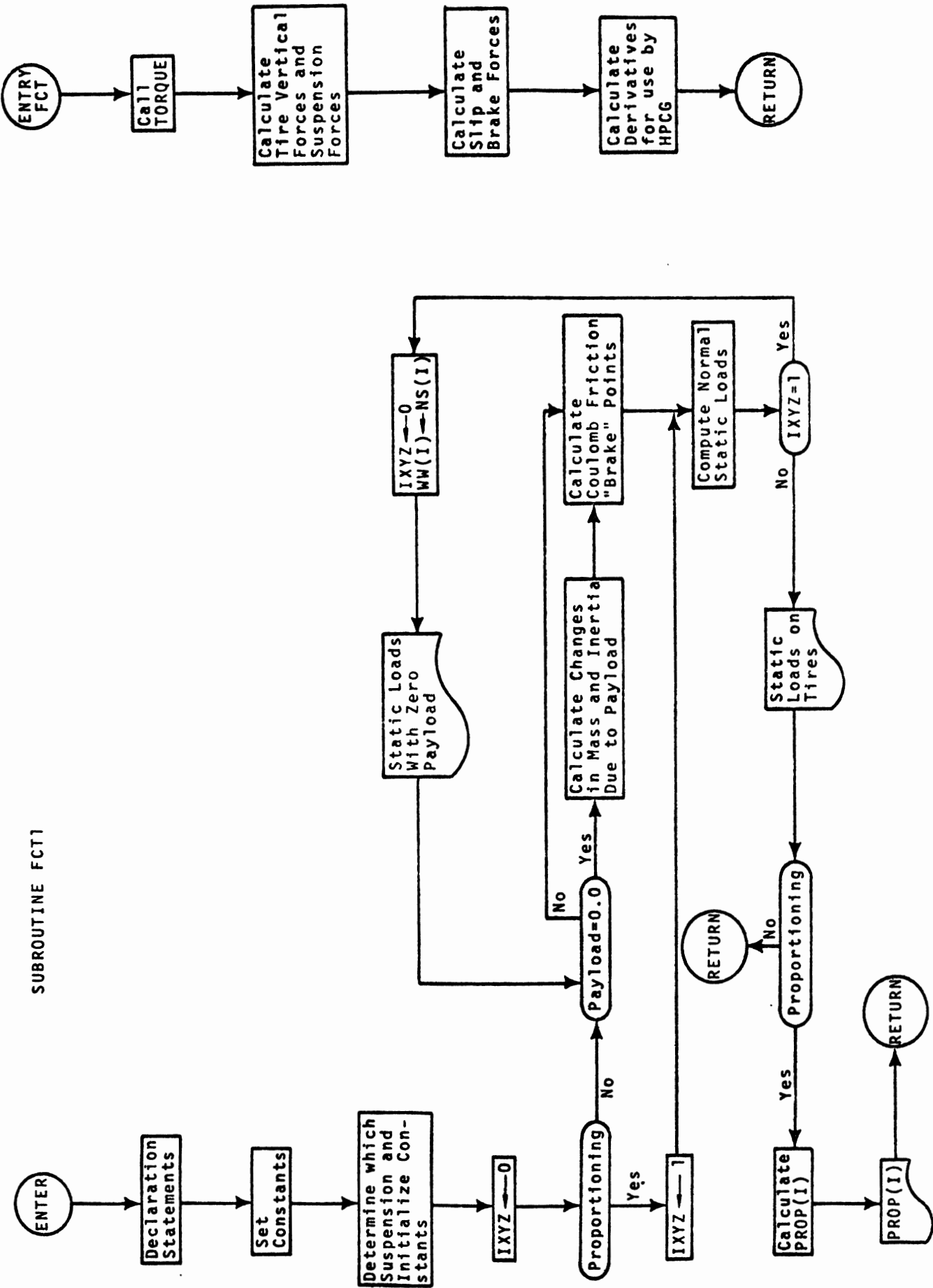
SUBROUTINE INPUT



SUBROUTINE OUTPUT



SUBROUTINE FCT1



APPENDIX D
Program Manipulation

Preceding page blank

APPENDIX D

1. INTRODUCTION

The purpose of this appendix is to facilitate user manipulation of the program. Initially, the most straightforward options are presented. Note there is one parameter per record except where a two coordinate relationship is appropriate; i.e., pressure-torque tables, etc. Integer variables are in I2 format. Real variables are in F15.3 format. Pairs of numbers are entered in 2F10.3 format.

2. INPUT INSTRUCTIONS FOR THE STRAIGHT TRUCK PROGRAM

In this section, the most straightforward options of the straight truck program are presented. Data List D-1 gives the order of data input for a single rear axle vehicle with dynamometer tables.

In the case of tandem rear axles, there will be several changes from the sequence in Data List D-1. Data List D-2 and D-3 give the order of the input data for the walking beam and the four spring tandem axles, respectively.

3. INPUT INSTRUCTIONS FOR THE ARTICULATED VEHICLE

In this section, the most straightforward options of the articulated vehicle are given. Data List D-4 gives the order of the input data for a three-axle vehicle.

In the case of tandem axles, there will be several changes from the sequence shown in Data List D-4. Data List D-5 gives the input sequence for a four spring tandem axle tractor with a four spring tandem axle trailer. The input sequence for the walking beam tandem axle tractor with a walking beam tandem axle trailer differs from Data List D-5 by the absence of AA6, AA7, AA8, AA14, AA15, and AA16. PERCNT(1) and PERCNT(2) are to be inserted after MUZERO(5).

4. THE BRAKE TABLES - INPUT INSTRUCTIONS

The brake tables allow user input time varying pressure at the foot valve and dynamometer curves for each axle. Table 1 is the time vs. pressure table. Tables 2 through KAXLE + 1 are the pressure vs. torque tables. (Note KAXLE is the total number of axles. Thus, there is one pressure vs. torque table for each axle.) Each table may contain up to 25 coordinate pairs entered in 2F10.3 format. The actual number of pairs in the a table is always the first entry for that table. The time vs. pressure table must always be entered. The pressure vs. torque tables must be entered unless the brake modules are to be used.

5. INPUT INSTRUCTIONS FOR VARIOUS OPTIONS

To use the following program options, special action by the user is required. Input instructions for the various options are explained below:

ROUGH ROAD

A data card containing a -1 (I2 format) must be inserted after the 80-character title data card and before KEY or KEY(1). This signals the program to call subroutine ROAD at the proper time and place. Subroutine ROAD contains a user input function or series of points for road height coordinate data. An examination of the subroutine ROAD list will clearly indicate how and where to insert the road profile.

PROPORTIONING - INPUT INSTRUCTIONS

The data cards for proportioning must immediately follow the last TQ data card. The first proportioning data card contains a -1 (I2 format) which signals the program to read the necessary data for the proportioning calculations. (See Data List D-6.)

BRAKE TORQUE APPLIED TO THE DRIVE SHAFT - INPUT INSTRUCTIONS

The data cards for this option, which will be referred to as the engine braking option, must follow the proportioning data cards, if proportioning is used, otherwise, they follow the last TQ data card. The first data card contains a -2 (I2 format) which signals the program to read the necessary data for engine braking calculations. (See Data List D-7.)

MECHANICAL ACTUATION OF PARKING BRAKES - INPUT INSTRUCTIONS

The data cards for the mechanical actuation of the parking brakes follow the last TQ data card, the proportioning data cards, if they exist, and the engine braking data cards, if they exist. The first data card contains a -3 (I2 format) which signals the program to read the necessary data for the mechanical actuation of parking brake calculations. (See Data List D-8.)

SPRING ACTUATION OF FOUNDATION BRAKES - INPUT INSTRUCTIONS

The data cards for foundation brakes follow the proportioning data cards, the engine braking cards, and the parking brake data cards, if any of these are used; otherwise, they follow the last TQ data card. The first data card contains a -4 (I2 format) which signals the program to read the necessary data for the spring actuation of foundation brake calculations. (See Data List D-9.)

THE BRAKE MODULES

To use the brake subroutine, insert a -1 (I2 format) where you would otherwise have put the number of points for the first pressure-torque table. This will cause a call to subroutine BRAKE. The parameters needed for the brake calculations will then be read. One brake type (described by the appropriate integer as given in Data List D-10) and its related parameters must be entered for each axle.

FORCE-DEFLECTION TABLE LOOKUP

The user sets the flag for force deflection table lookup by setting the appropriate K(I) to a negative value. (Note: this is not an option on the four spring suspension.) Each table of force deflection points may contain up to 25 coordinate pairs entered in 2F10.3 format. The first entry for one of these tables is always the actual number of pairs for that table.

The force-deflection tables are placed after the last pressure-torque table, or if the brake modules are used, after the end of the input for the brake modules.

DATA LIST D-1
SINGLE REAR AXLE VEHICLE

80 Character Title (20A4 format)

KEY (I2 format)

A1

A2

ALPHA 1

ALPHA 2

C1**

C2**

C3**

C4**

CF1**

CF2**

CS1***

CS2***

DELTA 1

FA1

FA2

J

JS1**

JS2**

K1**

K2**

KT1**

KT2**

MUZERO1

MUZERO2

PW

PJ*

PX*

PF*

TIME

VEL

W

WS1**

WS2**

TQ (1,1), TQ (1,2) (2F10.3 format)

TQ (2,1), TQ (2,2)

NUMBER OF PAIRS IN TIME VS. PRESSURE TABLE (I2 format)

TIME PRESSURE (UP TO 25 PAIRS IN 2F10.3 FORMAT)

.
. .
. .

NUMBER OF PAIRS IN PRESSURE VS. TOTAL TORQUE TO AXLE 1 (I2 format)

PRESSURE TORQUE (UP TO 25 PAIRS IN 2F10.3 FORMAT)

.
. .
. .

NUMBER OF PAIRS IN PRESSURE VS. TOTAL TORQUE TO AXLE 2 (I2 format)

PRESSURE TORQUE (UP TO 25 PAIRS IN 2F10.3 FORMAT)

.
. .
. .

TINC

TRUCK

*Omit if PW=0.0

**Sum of right and left side

***Value for one tire multiplied by number of tires on the axle.

DATA LIST D-2
WALKING BEAM SUSPENSION, STRAIGHT TRUCK

80 Character Title (20A4 format)

KEY (I2 format)

AA1
AA2
AA4
AA5
A1
A2
ALPHA 1
ALPHA 2
C1**
C2**
C3**
C4**
CF1**
CF2**
CS1***
CS2***
CS3***
DELTA 1
FA1
FA2
FA3
J
JS1**
JS2**
JS3**
K1**
K2**
KT1**
KT2**
KT3**
MUZERO1
MUZERO2
MUZERO3
PERCNT
PW
PJ*
PX*
PZ*
TIME
VEL
W
WS1**
WS2**
WS3**
TQ (1,1), TQ (1,2) (2F10.3 Format)
TQ (2,1), TQ (2,2)
TQ (3,1), TQ (3,2)
NUMBER OF PAIRS IN TIME VS. PRESSURE TABLE (I2 FORMAT)
TIME PRESSURE (UP TO 25 PAIRS IN 2F10.3 FORMAT)
.
.
.

* Omit if PW=0.0

**Sum of left and right side

***Value for one tire multiplied by number of tires on the axle.

DATA LIST D-2 (Continued)

NUMBER OF PAIRS IN PRESSURE VS. TOTAL TORQUE TO AXLE 1 (I2 FORMAT)
PRESSURE TORQUE (UP TO 25 PAIRS IN 2F10.3 FORMAT)

. .
. .
. .

NUMBER OF PAIRS IN PRESSURE VS. TOTAL TORQUE TO AXLE 2 (I2 FORMAT)
PRESSURE TORQUE (UP TO 25 PAIRS IN 2F10.3 FORMAT)

. .
. .
. .

NUMBER OF PAIRS IN PRESSURE VS. TOTAL TORQUE TO AXLE 3 (I2 FORMAT)
PRESSURE TORQUE (UP TO 25 PAIRS IN 2F10.3 FORMAT)

. .
. .
. .

TINC
TRUCK

DATA LIST D-3
FOUR SPRING

80 Character Title

KEY (I2 format)

AA1

AA2

AA4

AA5

AA6

AA7

AA8

A1

A2

ALPHA 1

ALPHA 2

C1**

C2**

C3**

C4**

CF1**

CF2**

CS1***

CS2***

CS3***

DELTA 1

FA1

FA2

FA3

J

JS1**

JS2**

JS3**

K1**

K2**

KT1**

KT2**

KT3**

MUZERO1

MUZERO2

MUZERO3

PW

PJ*

PX*

PZ*

TIMF

VEL

W

WS1**

WS2**

WS3**

TQ (1,1), TQ (1,2)

TQ (2,1), TQ (2,2)

TQ (3,1), TQ (3,2)

NUMBER OF PAIRS IN TIME VS. PRESSURE TABLE (I2 FORMAT)

TIME PRESSURE (UP TO 25 PAIRS IN 2F10.3 FORMAT)

:
:

*Omit if PW=0.0

**Sum of left and right side

***Value for one tire multiplied by number of tires on the axle

DATA LIST D-3 (Continued)

NUMBER OF PAIRS IN PRESSURE VS. TOTAL TORQUE AXLE 1 (I2 FORMAT)
PRESSURE TORQUE (UP TO 25 PAIRS IN 2F10.3 FORMAT)

.
.

NUMBER OF PAIRS IN PRESSURE VS. TOTAL TORQUE TO AXLE 2 (I2 FORMAT)
PRESSURE TORQUE (UP TO 25 PAIRS IN 2F10.3 FORMAT)

.
.

NUMBER OF PAIRS IN PRESSURE VS. TOTAL TORQUE TO AXLE 3 (I2 FORMAT)
PRESSURE TORQUE (UP to 25 PAIRS IN 2F10.3 FORMAT)

.
.

TINC
TRUCK

DATA LIST D-4
TRACTOR-TRAILER SINGLE-AXLE VEHICLE

80 Character Title (20A4 format)

KEY (1) (I2 format)

KEY (2) (I2 format)

A1

A2

A3

A4

ALPHA 1

ALPHA 2

ALPHA 3

BB

C1**

C2**

C3**

C4**

C5**

C6**

CF1**

CF2**

CF3**

CS1***

CS2***

CS3***

D

DELTA 1

DELTA 3

FA1

FA2

FA3

J

J1

JS1**

JS2**

JS3**

K1**

K2**

K3**

KT1**

KT2**

KT3**

MUZERO1

MUZERO2

MUZERO3

PW

PJ*

PX*

PZ*

TIMF

VEL

W1

W2

WS1**

WS2**

*Omit if PW=0.0

**Sum of left and right sides

***Value for one tire multiplied by number of tires on the axle

DATA LIST D-4 (Continued)

WS3**

TQ (1,1), TQ (1,2) (2F10.3 format)

TQ (2,1), TQ (2,2)

TQ (3,1), TQ (3,2)

NUMBER OF PAIRS IN TIME VS. PRESSURE TABLE (I2 FORMAT)

TIME PRESSURE (UP TO 25 PAIRS IN 2F10.3 FORMAT)

.
.

NUMBER OF PAIRS IN THE PRESSURE VS. TOTAL TORQUE TO AXLE 1 (I2 FORMAT)

PRESSURE TORQUE (UP TO 25 PAIRS IN 2F10.3 FORMAT)

.
.

NUMBER OF PAIRS IN THE PRESSURE VS. TOTAL TORQUE TO AXLE 2 (I2 FORMAT)

PRESSURE TORQUE (UP TO 25 PAIRS IN 2F10.3 FORMAT)

.
.

NUMBER OF PAIRS IN THE PRESSURE VS. TOTAL TORQUE TO AXLE 3 (I2 FORMAT)

PRESSURE TORQUE

.
.

TINC

TRUCK

**Sum of left and right sides

DATA LIST D-5
TRACTOR-TRAILER FOUR SPRING

80 Character Title (20A4 format)

KEY (1) (I2 format)

KEY (2)

AA1

AA2

AA4

AA5

AA6

AA7

AA8

AA9

AA10

AA12

AA13

AA14

AA15

AA16

A1

A2

A3

A4

ALPHA 1

ALPHA 2

ALPHA 3

BB

C1**

C2**

C3**

C4**

C5**

C6**

CF1**

CF2**

CF3**

CS1***

CS2***

CS3***

CS4***

CS5***

D

DELTA 1

DELTA 3

FA1

FA2

FA3

FA4

FA5

J

J1

JS1**

JS2**

JS3**

JS4**

**Sum of right and left side

***Value for one tire multiplied by number of tires on the axle.

DATA LIST D-5 (Continued)

JS5**
 K1**
 K2**
 K3**
 KT1**
 KT2**
 KT3**
 KT4**
 KT5**
 MUZERO1
 MUZERO2
 MUZERO3
 MUZERO4
 MUZERO5
 PW
 PJ*
 PX*
 PZ*
 TIME
 VEL
 W1
 W2
 WS1**
 WS2**
 WS3**
 WS4**
 WS5**
 TQ (1,1), TQ (1,2) (2F10.3 format)
 TQ (2,1), TQ (2,2)
 TQ (3,1), TQ (3,2)
 TQ (4,1), TQ (4,2)
 TQ (5,1), TQ (5,2)
 NUMBER OF PAIRS IN TIME VS. PRESSURE TABLE (I2 FORMAT)
 TIME PRESSURE (UP TO 25 PAIRS IN 2F10.3 FORMAT)
 . .
 . .
 NUMBER OF PAIRS IN PRESSURE VS. TOTAL TORQUE TO AXLE 1 (I2 FORMAT)
 PRESSURE TORQUE (UP TO 25 PAIRS IN 2F10.3 FORMAT)
 . .
 . .
 NUMBER OF PAIRS IN PRESSURE VS. TOTAL TORQUE TO AXLE 2 (I2 FORMAT)
 PRESSURE TORQUE (UP TO 25 PAIRS IN 2F10.3 FORMAT)
 . .
 . .
 NUMBER OF PAIRS IN PRESSURE VS. TOTAL TORQUE TO AXLE 3 (I2 FORMAT)
 PRESSURE TORQUE (UP TO 25 PAIRS IN 2F10.3 FORMAT)
 . .
 . .
 NUMBER OF PAIRS IN PRESSURE VS. TOTAL TORQUE TO AXLE 4 (I2 FORMAT)
 PRESSURE TORQUE (UP TO 25 PAIRS IN 2F10.3 FORMAT)
 . .
 . .
 NUMBER OF PAIRS IN PRESSURE VS. TOTAL TORQUE TO AXLE 5 (I2 FORMAT)

*Omit if PW=0.0

**Sum of right and left side

DATA LIST D-5 (Continued)

PRESSURE TORQUE (UP TO 25 PAIRS IN 2F10.3 FORMAT)

.
.
TINC
TRUCK

DATA LIST D-6
PROPORTIONING

-1 (I2 FORMAT)
MAXAX (1)
.
.
MAXAX (KAXLE)
EMPTY (1)
.
EMPTY (KAXLE)

DATA LIST D-7
BRAKE TORQUE APPLIED TO THE DRIVE SHAFT

-2 (I2 FORMAT)
YDYEB
KPSB
KEYAR
NOGEAR
GEARV (2)
.
.
.
GEARV (NOGEAR)
GRAT (1)
.
.
GRAT (NOGEAR)
NUMEB
EBX (1) EBY (1)
.
.
EBX (NOGEAR) EBX (NOGEAR)
EBPER }read only if KEY or KEY (1) is greater than zero

DATA LIST D-8
MECHANICAL ACTUATION OF PARKING BRAKES

-3 (I2 FORMAT)

NOMAPB

MAPBX(1)

.

.

.

MAPBX(NOMAPB)

MAPBY(1)

.

.

.

MAPBY(NOMAPB)

DATA LIST D-9
SPRING ACTUATION OF FOUNDATION BRAKES

-4 (I2 FORMAT)

ONTIME

TMAX(2)

.

.

.

TMAX(KAXLE)

RISET

DATA LIST D-10
BRAKE MODULES

0 NO BRAKES (I1 format)
1 S-CAM BRAKE (I1 format)
AC (AXLE)
EM (AXLE)
PO (AXLE)
RD
ULH
ULL
ALPH0
ALPH3
APRIM
HB
RC
SAL
2 2-WEDGE BRAKE (I1 format)
AC
EM
PO
RD
ULH
ULL
AB
ALPH0
ALPHW
BETA
C2
OH
3 1-WEDGE (I1 format)
AC
EM
PO
RD
ULH
ULL
ALPH0
ALPHW
ALPH3
APRIM
HB
4 DSSA (I1 format)
AC
EM
PO
RD
ULH
ULL
AB
ALPH0
ALPHW
ALPH3
APRIM
BETA
C2
HB
OH

DATA LIST D-10 (Continued)

5 DUPLEX BRAKES (I1 format)

AC
EM
PO
RD
ULH
ULL
AB
ALPH0
ALPHW
BETA
C2
OH

6 DISC BRAKES (I1 format)

AC
EM
PO
RD
ULH
ULL

APPENDIX E
A Short Algorithm for the Choice
of Tire Parameters

Preceding page blank

APPENDIX E
A SHORT ALGORITHM FOR THE CHOICE OF TIRE PARAMETERS

The μ -slip curve is given by equations 2-94, 2-95, and 2-96. The "high SLIP" range is of particular interest, since, in that range, the peak coefficient of friction μ_p , and the locked wheel coefficient of friction, μ_s , occur.

For λ less than 1, Equation 2-94 may be written

$$\mu = \left| \frac{F_x}{N} \right| = \mu_o (1 - FA \cdot XDOT \cdot SLIP) \cdot \left\{ 1 - \frac{\mu_o N (1 - FA \cdot XDOT \cdot SLIP) (1 - SLIP)}{4CS \cdot SLIP} \right\} \quad (E-1)$$

It is assumed that the following parameters are known:

- N ... normal force at the tire-road interface
- XDOT ... vehicle speed
- μ_p ... peak friction coefficient
- S_m ... SLIP for μ_p
- μ_s ... locked wheel friction coefficient

The following is an approximate method to find μ_o , CS, and FA. The vehicle speed XDOT is fixed in this analysis. Thus, with the substitution

$$A = FA \cdot XDOT \quad (E-2)$$

Equation E-1 may be written

$$\mu = \mu_o (1 - A \cdot SLIP) [1 - f(SLIP)] \quad (E-3a)$$

where

$$f(SLIP) = \frac{\mu_o N (1 - A \cdot SLIP) (1 - SLIP)}{4CS \cdot SLIP} \quad (E-3b)$$

Differentiation of μ with respect to slip yields

$$\mu' = -\mu_o A [1 - f(SLIP)] - \mu_o (1 - A \cdot SLIP) [f'(SLIP)] \quad (E-4)$$

where the prime denotes partial differentiation with respect to SLIP. But $f'(SLIP)$ may be shown to be

$$f'(SLIP) = \frac{\mu_o N}{4CS} \cdot \frac{(A \cdot SLIP^2 - 1)}{SLIP^2} \quad (E-5)$$

and Equation E-4 may then be written

$$\mu' = -\mu_o \left[A - \frac{\mu_o N}{4CS \cdot SLIP^2} (1 - 2A \cdot SLIP^2 - A^2 \cdot SLIP^2 + 2A^2 \cdot SLIP^3) \right] \quad (E-6)$$

For the range of friction reduction parameters normally encountered, A will be small ($A < .3$) and S_m will be small ($S_m < .3$).

Thus, an approximate solution to E-6 may be found at $SLIP = S_m$

(where $\mu' = 0$):

$$0 = -\mu_o \left[A - \frac{\mu_o N}{4CS \cdot S_m^2} + \frac{2A\mu_o N}{4CS} \right] \quad (E-7a)$$

$$A = \frac{\frac{\mu_o N}{4CS \cdot S_m^2}}{1 + \frac{2\mu_o N}{4CS}} \quad (E-7b)$$

The substitution of S_m in E-3 yields

$$\mu_p = \mu_o (1 - A \cdot S_m) \left[1 - \frac{\mu_o N (1 - AS_m) (1 - S_m)}{4CS \cdot S_m} \right] \quad (E-8a)$$

Noting from Equation E-7b that

$$\frac{\mu_o N}{4CS \cdot S_m} = A \cdot S_m \left(1 + \frac{2\mu_o N}{4CS} \right),$$

Equation E-8a may be written in the form

$$\mu_p = \mu_o (1 - A \cdot S_m) (1 - A \cdot \bar{S}_m \{ (1 - A \cdot S_m) (1 - S_m) \}) \quad (E-8b)$$

where

$$\bar{S}_m = S_m \left(1 + \frac{\mu_o N}{2CS} \right) \quad (E-8c)$$

Noting that we expect $\frac{\mu_o N}{2CS}$ to be small (say on the order of S_m), and again dropping small terms, we get from Equation E-8b

$$\mu_p = \mu_o (1 - 2A \cdot S_m + A \cdot S_m^2) \quad (E-9)$$

Equation E-3 also yields the locked wheel information

$$\mu_s = \mu_o (1 - A) \quad (E-10)$$

Thus, from Equations E-9 and E-10,

$$\frac{\mu_p}{\mu_s} = \frac{1 - 2A \cdot S_m + A \cdot S_m^2}{1 - A} \quad (E-11a)$$

$$A = \frac{\frac{\mu_p}{\mu_s} - 1}{\frac{\mu_p}{\mu_s} - 2S_m + S_m^2} \quad (E-11b)$$

Now we can systematically find the desired parameters in this order:

1. Use E-11b to find A,
2. Use E-10 to find μ_0 ,
3. Use E-7b to find CS,
4. Use E-2 to find FA.

Added locked wheel information may be used in an alternate method to determine tire parameters. If, for example, $\left| \frac{FX}{N} \right|$ is known for locked wheels at two values of XDOT, μ_0 and FA may easily be found. Note that higher values of XDOT should correspond to lower values of $\left| \frac{FX}{N} \right|$ at SLIP = 1

At SLIP = 1, equation E-1 becomes

$$\mu_{(SLIP=1)} = \mu_0 (1 - XDOT(FA)) \quad (E-12)$$

Given two values of $\mu_{(SLIP=1)}$ (μ_1 and μ_2) and two values of XDOT (XDOT1 and XDOT2)*,

$$\mu_0 (1 - (XDOT1)FA) = \mu_1 \quad (E-13a)$$

$$\mu_0 (1 - (XDOT2)FA) = \mu_2 \quad (E-13b)$$

Dividing E-13a by E-13b and carrying out the necessary algebra yields:

$$FA = \frac{1 - \frac{\mu_1}{\mu_2}}{XDOT1 - \frac{\mu_1}{\mu_2} XDOT2} \quad (E-14)$$

and it follows that

$$\mu_0 = 1 - \frac{\mu_1}{(XDOT1)FA} \quad (E-15)$$

Either μ_p , S_m , or CS may now be chosen. Assuming the user wishes to choose μ_p , the peak coefficient at velocity \overline{XDOT} , the following calculations are necessary:

A may be found from Equation E-2

$$A = \overline{XDOT} FA$$

Now Equation E-9 can then be solved to get S_m .

$$S_m = 1 - \left[1 - \frac{1}{A} \left(\frac{\mu_p}{\mu_0} - 1 \right) \right]^{1/2} \quad (E-16)$$

*Note if $XDOT1 > XDOT2$, $\mu_2 > \mu_1$

and from Equation E-7b,

$$CS = \frac{\mu_o N}{4S_m^2 A} - \frac{\mu_o N}{2} \quad (E-17)$$

Note that these calculations are meant to lead to peak coefficient μ_p occurring at vehicle velocity \overline{XDOT} at $SLIP = S_m$. Since there is no approximation in Equations E-15 through E-17, the locked wheel friction values μ_1 and μ_2 will be the exact result of the tire model equations at $XDOT1$ and $XDOT2$. The results from the tire model at S_m with velocity \overline{XDOT} will be approximately μ_p .

A short program has been written for each of the above methods of choosing tire parameters. These programs are included with the pitch plane simulation. Sample results follow:

#EXECUTION BEGINS

ENTER TIRE PARAMETERS IN F FORMAT

XDOT = 44.

MUPEAK = .75

MSLIDE = .6

SMAX = .12

N = 5000.

VEHICLE SPEED INPUT WAS 44.000
PEAK FRICTION COEFFICIENT INPUT WAS 0.750
LOCKED WHEEL COEFFICIENT INPUT WAS 0.600
SLIP AT PEAK FRICTION COEFFICIENT INPUT WAS 0.120
NORMAL FORCE INPUT WAS 5000.000

THE APPROPRIATE TIRE PARAMETERS AS CALCULATED ARE:

MUZERO = 0.79370

CS = 280329.875

FA = 0.00555

WITH THESE PARAMETERS, AT SLIP = 0.12000 THE TIRE MODEL
WILL CALCULATE 0.75104 FOR FX/N

ENTER A 1 IF YOU WANT A MU-SLIP CURVE

ENTER A ZERO TO CONTINUE

1

ENTER VELOCITY IN F FORMAT

XDOT = 44.

ENTER NORMAL LOAD IN F FORMAT

N = 5000.

WITH THESE PARAMETERS THE FOLLOWING VALUES
FOR FX/N AND SLIP ARE OBTAINED

S =	0.050	FX/N =	0.73194
S =	0.100	FX/N =	0.75027
S =	0.150	FX/N =	0.74987
S =	0.200	FX/N =	0.74479
S =	0.250	FX/N =	0.73784
S =	0.300	FX/N =	0.72996
S =	0.350	FX/N =	0.72154
S =	0.400	FX/N =	0.71279
S =	0.450	FX/N =	0.70381
S =	0.500	FX/N =	0.69468
S =	0.550	FX/N =	0.68544
S =	0.600	FX/N =	0.67512
S =	0.650	FX/N =	0.66672
S =	0.700	FX/N =	0.65728
S =	0.750	FX/N =	0.64780
S =	0.800	FX/N =	0.63829
S =	0.850	FX/N =	0.62874
S =	0.900	FX/N =	0.61918
S =	0.950	FX/N =	0.60960
S =	1.000	FX/N =	0.60000

TO CALCULATE ANOTHER CURVE, USING THE CALCULATED
PARAMETERS, ENTER A ONE (1), TO CALCULATE NEW VEHICLE
PARAMETERS, ENTER A TWO (2), TO TERMINATE ENTER A ZERO
0

** LOGICAL END OF PROGRAM **
** ENTER A 1 TO RESTART, 0 TO END **
0
#EXECUTION TERMINATED
#

#EXECUTION BEGINS

ENTER PARAMETERS IN F FORMAT

XDOT1 = 44.
XDOT2 = 66.
MU 1 = .75
MU 2 = .72

THE PARAMETERS ENTERED WERE:

XDOT1 = 44.000
XDOT2 = 66.000
MU1 = 0.750
MU2 = 0.720

THE APPROPRIATE CALCULATED PARAMETERS ARE:

FA = 0.0016834789
MUZERO = 0.809999

ENTER VEHICLE SPEED, NORMAL LOAD, AND MUPEAK
NOTE THAT MUPEAK MUST BE LESS THAN MUZERO

XDOT = 44.
MUPEAK = .75
N = 5000.

PARAMETERS ENTERED WERE :

XDOT = 44.000
MUPEAK = 0.750
N = 5000.000

THE TIRE MODEL CANNOT MEET THESE REQUIREMENTS...
YOU NEED A HIGHER MUPEAK VALUE.....

ENTER VEHICLE SPEED, NORMAL LOAD, AND MUPEAK
NOTE THAT MUPEAK MUST BE LESS THAN MUZERO

XDOT = 44.
MUPEAK = .79
N = 5000.

PARAMETERS ENTERED WERE :

XDOT = 44.000
MUPEAK = 0.790
N = 5000.000

AT VELOCITY 44.000 PEAK COEFFICIENT WILL BE APPROX. 0.790

AT LOGITUDINAL SLIP 0.183 WITH LOW SLIP SLOPE 403927.437 FOR CS

WITH THESE PARAMETER, AT SLIP = 0.18350 THE TIRE MODEL
WILL CALCULATE 0.79020 FOR FX/N

ENTER A 1 IF YOU WANT A MU-SLIP CURVE
ENTER A ZERO TO CONTINUE

1

ENTER VELOCITY IN F FORMAT
XDOT = 44.

ENTER NORMAL LOAD IN F FORMAT
N = 5000.

WITH THESE PARAMETERS THE FOLLOWING VALUES
FOR FX/N AND SLIP ARE OBTAINED

S = 0.050	FX/N =	0.76871
S = 0.100	FX/N =	0.78600
S = 0.150	FX/N =	0.78975
S = 0.200	FX/N =	0.79012
S = 0.250	FX/N =	0.78913
S = 0.300	FX/N =	0.78747
S = 0.350	FX/N =	0.78542
S = 0.400	FX/N =	0.78313
S = 0.450	FX/N =	0.78068
S = 0.500	FX/N =	0.77812
S = 0.550	FX/N =	0.77547
S = 0.600	FX/N =	0.77276
S = 0.650	FX/N =	0.77001
S = 0.700	FX/N =	0.76722
S = 0.750	FX/N =	0.76440
S = 0.800	FX/N =	0.76155
S = 0.850	FX/N =	0.75859
S = 0.900	FX/N =	0.75580
S = 0.950	FX/N =	0.75291
S = 1.000	FX/N =	0.75000

TO CALCULATE ANOTHER CURVE, USING THE CALCULATED
PARAMETERS, ENTER A ONE (1), TO CALCULATE NEW VEHICLE
PARAMETERS, ENTER A TWO (2), TO TERMINATE ENTER A ZERO
0

** LOGICAL END OF PROGRAM **
** ENTER A 1 TO RESTART, 0 TO END **

0
#EXECUTION TERMINATED
#

APPENDIX F
Validation Data

TABLE F-1
INPUT PARAMETERS, STRAIGHT TRUCK

<u>SYMBOL</u>	<u>DESCRIPTION</u>	<u>VALUE FOR ALL CONDITIONS</u>	<u>SPECIAL CONDITION</u>	<u>SPECIAL VALUE</u>
	*****Vehicle Parameters*****			
KEY	Axle Key: Set to 0 for Single Axle 1 for Walking Beam 2 for Elliptic Leaf	1		
KROAD	Road Key: 0 Implies a Smooth Road -1 Implies a Rough Road	0		
AA1	Horizontal Dist. From Walking Beam Pin to Front Axle (in)	24.00		
AA2	Horizontal Dist. From Walking Beam Pin to Rear Axle (in)	26.00		
AA4	Vertical Dist. From Axle to W.B. (in)	8.00		
AA5	Vertical Dist. From Axle to Torque Rod (in)	18.00		
A1	Horizontal Distance From CG to Midpoint of Front Suspension (in)*		Empty Loaded, Low C.G. Loaded, High C.G.	49.50 108.00 108.00
A2	Horizontal Distance From CG to Midpoint of Rear Suspension (in)*		Empty Loaded, Low C.G. Loaded, High C.G.	140.50 82.00 82.00
ALPHA1	Static Distance, Front Axle to Ground (in)		Empty Loaded, Low C.G. Loaded, High C.G.	19.95 19.55 19.10
ALPHA2	Static Distance, Rear Axle(s) to Ground (in)		Empty Loaded, Low C.G. Loaded, High C.G.	20.00 19.90 19.90
C1	Viscous Damping: Jounce on Front Axle (lb-sec/in)	8.33		
C2	Viscous Damping: Rebound on Front Axle (lb-sec/in)	16.67		
C3	Viscous Damping: Jounce on Rear Axle(s) (lb-sec/in)	0.0		
C4	Viscous Damping: Rebound on Rear Axle(s) (lb-sec/in)	0.0		
CF1	Max. Coulomb Friction, Front Suspension (lb)		Empty Loaded, Low C.G. Loaded, High C.G.	2200.00 3600.00 5200.00
CF2	Max. Coulomb Friction, Rear Suspension (lb)		Empty Loaded, Low C.G. Loaded, High C.G.	4400.00 4800.00 4800.00
CS1	Longitudinal Stiffness, Front Tires (lbs)		Empty Loaded, Low C.G. Loaded, High C.G.	120000.00 148000.00 148000.00
CS2	Longitudinal Stiffness, Front Tandem Tires (lbs)		Empty Loaded, Low C.G. Loaded, High C.G.	80000.00 115000.00 115000.00
CS3	Longitudinal Stiffness, Rear Tandem Tires (lbs)		Empty Loaded, Low C.G. Loaded, High C.G.	80000.00 115000.00 115000.00
DELTA1	Static Vertical Distance, Front Axle to Tractor CG (in)		Empty Loaded, Low C.G. Loaded, High C.G.	22.00 37.21 37.21
FA1	Friction Reduction Parameter on Front Tires		Dry Road Wet Road	0.0055 0.019
FA2	Friction Reduction Parameter on Front Tandem Tires		Dry Road Wet Road	0.0055 0.015
FA3	Friction Reduction Parameter on Rear Tandem Tires		Dry Road Wet Road	0.0055 0.010

*For empty vehicle, body was considered as payload. For loaded vehicles, body was considered as part of truck.

TABLE F-1 (Continued)

<u>SYMBOL</u>	<u>DESCRIPTION</u>	<u>VALUE FOR ALL CONDITIONS</u>	<u>SPECIAL CONDITION</u>	<u>SPECIAL VALUE</u>
J	Sprung Mass Polar Moment of Inertia (in-lb-sec**2)*		Empty Loaded, Low C.G. Loaded, High C.G.	103492. 385670. 385670.
JS1	Polar Moment of Front Wheels (in-lb-sec**2)	326.00		
JS2	Polar Moment of Front Tandem Wheels (in-lb-sec**2)	410.00		
JS3	Polar Moment of Rear Tandem Wheels (in-lb-sec**2)	410.00		
K1	Spring Rate, Front Suspension (lb/in)		Empty Loaded, Low C.G. Loaded, High C.G.	5600.00 5600.00 7200.00
K2	Spring Rate, Rear Suspension (lb/in)	30000.00		
KT1	Spring Rate, Front Tires (lb/in)	9400.00		
KT2	Spring Rate, Front Tandem Tires (lb/in)	18800.00		
KT3	Spring Rate, Rear Tandem Tires (lb/in)	18800.00		
MUZERO1	Coefficient of Friction, Front Wheels		Dry Road Wet Road	0.97 0.35
MUZERO2	Coefficient of Friction, Front Tandem Wheels		Dry Road Wet Road	0.97 0.55
MUZERO3	Coefficient of Friction, Rear Tandem Wheels		Dry Road Wet Road	0.97 0.60
PERCNT	Percent Effectiveness of Torque Rods	100.00		
PW	Weight of Payload (lbs)*		Empty Loaded, Low C.G. Loaded, High C.G.	7390.00 23820.00 29410.00
PJ	Polar Moment of Payload (in-lb-sec**2)*		Empty Loaded, Low C.G. Loaded, High C.G.	112051.00 170000.00 79137.00
PX	Horizontal Distance From Midpoint of Rear Suspension to Mass Center (in)*		Empty Loaded, Low C.G. Loaded, High C.G.	22.00 36.00 61.80
PZ	Vertical Distance From Ground to Paylaod Center of Mass (in)*		Empty Loaded, Low C.G. Loaded, High C.G.	72.00 64.50 93.00
TIMF	Max. Real Time for Simulation	**		
VEL	Initial Velocity (fps)		30 MPH Stops 50 MPH Stops	44.00 73.30
W1	Sprung Weight of Truck (lbs)*		Empty Loaded, Low C.G. Loaded, High C.G.	8190.00 15580.00 15580.00
WS1	Weight of Front Suspension (lbs)	1742.00		
WS2	Weight of Tandem Front (lbs)	2078.00		
WS3	Weight of Rear Tandem (lbs)	1972.00		
	*****Brake Parameters*****			
TQ(1,1)	Brake Timing Parameters	0.032		
TQ(1,2)		0.296		
TQ(2,1)		0.070		
TQ(2,2)		0.181		
TQ(3,1)		0.073		
TQ(3,2)		0.276		
FRAY	Brake Fade Coefficient		30 MPH Tests 50 MPH Tests	0.0045 0.0120
	Axle 1			
IBRT(1)	Brake Type	2-Wedge		
AC(1)	Brake Chamber Area (sq.in)	9.000		
EM(1)	Mechanical Efficiency	0.880		
PO(1)	Pushout Pressure (PSI)	8.000		
RD(1)	Drum Radius (in)	7.500		
ULH(1)	Mu Lining, High	0.500		
ULL(1)	Mu Lining, Low	0.350		

*For empty vehicle, body was considered as payload. For loaded vehicles, body was considered part of truck.

**Varies with expected duration of stop.

TABLE F-1 (Continued)

<u>SYMBOL</u>	<u>DESCRIPTION</u>	<u>VALUE FOR ALL CONDITIONS</u>	<u>SPECIAL CONDITION</u>	<u>SPECIAL VALUE</u>
AB(1)	Distance From Horizontal Centerline of Drum to Parallel Line Through Shoe Contact Point (in)	5.560		
ALPH0(1)	Lining Contact Angle (deg)	127.197		
ALPHW(1)	Wedge Angle (deg)	12.548		
BETA(1)	Lining Offset Angle (deg)	0.573		
C2(1)	Distance from Horizontal Centerline of Drum Parallel Line Through Point of Actuating Force (in)	5.310		
OH(1)	Distance From Vertical Centerline of Drum to Parallel Line Through Shoe Contact Point (in)	3.160		
	Axle 2			
IBRT(2)	Brake Type	2-Wedge		
AC(2)	Brake Chamber Area (sq in)	12.000		
EM(2)	Mechanical Efficiency	0.880		
PO(2)	Pushout Pressure (PSI)	7.500		
RD(2)	Drum Radius (in)	7.500		
ULH(2)	Mu Lining, High	0.540		
ULL(2)	Mu Lining, Low	0.370		
AB(2)	Distance From Horizontal Centerline of Drum to Parallel Line Through Shoe Contact Point (in)	5.310		
ALPH0(2)	Lining Contact Angle (deg)	126.051		
ALPHW(2)	Wedge Angle (deg)	12.548		
BETA(2)	Lining Offset Angle (deg)	0.573		
C2(2)	Distance From Horizontal Centerline of Drum Parallel Line Through Point of Actuating Force (in)	5.440		
OH(2)	Distance From Vertical Centerline of Drum to Parallel Line Through Shoe Contact Point (in)	3.050		
	Axle 3			
IBRT(3)	Brake Type	2-Wedge		
AC(3)	Brake Chamber Area (sq. in)	12.000		
EM(3)	Mechanical Efficiency	0.880		
PO(3)	Pushout Pressure (PSI)	7.500		
RD(3)	Drum Radius (in)	7.500		
ULH(3)	Mu Lining, High	0.540		
ULL(3)	Mu Lining, Low	0.370		
AB(3)	Distance From Horizontal Centerline of Drum to Parallel Line Through Shoe Contact Point (in)	5.310		
ALPH0(3)	Lining Contact Angle (deg)	126.051		
ALPHW(3)	Wedge Angle (deg)	12.548		
BETA(3)	Lining Offset Angle (deg)	0.573		
C2(3)	Distance From Horizontal Centerline of Drum Parallel Line Through Point of Actuating Force (in)	5.440		
OH(3)	Distance From Vertical Centerline of Drum to Parallel Line Through Shoe Contact Point (in)	3.050		

TABLE F-2
INPUT PARAMETERS, TRACTOR TRAILER

<u>SYMBOL</u>	<u>DESCRIPTION</u>	<u>VALUE FOR ALL CONDITIONS</u>	<u>SPECIAL CONDITION</u>	<u>SPECIAL VALUE</u>
	*****Vehicle Parameters*****			
KEY(1)	Tractor Axle Key: 0 for Single Axle 1 for Walking Beam 2 for 4 Elliptic Leaf			2
KEY(2)	Trailer Axle Key			2
KROAD	Road Key: 0 Implies a Smooth Road -1 Implies a Rough Road			0
AA1	Horizontal Distance From Tractor Front Leaf-Frame Contact to Axle Center (in)	21.60		
AA2	Horizontal Distance From Tractor Rear Leaf-Frame Contact to Axle Center (in)	19.25		
AA4	Horizontal Distance From Tractor Front Leaf-Frame Contact to Load Leveler Pin (in)	6.75		
AA5	Horizontal Distance From Tractor Rear Leaf-Frame Contact to Load Leveler Pin (in)	6.75		
AA6	Vertical Distance From Axle Down to Tractor Torque Rod (in)	7.00		
AA7	Angle Between Tractor Torque Rod and Horizontal (deg)	13.00		
AA8	Horizontal Distance From Axle Center Forward to Tractor Torque Rod (in)	-1.00		
AA9	Horizontal Distance From Trailer Front Leaf-Frame Contact to Axle Center (in)	18.50		
AA10	Horizontal Distance From Trailer Rear Leaf-Frame Contact to Axle Center (in)	18.50		
AA12	Horizontal Distance From Trailer Front Leaf-Frame Contact to Load Leveler Pin (in)	6.00		
AA13	Horizontal Distance From Trailer Rear Leaf-Frame Contact to Load Leveler Pin (in)	6.25		
AA14	Vertical Distance From Axle Down to Trailer Torque Rod (in)	7.00		
AA15	Angle Between Trailer Torque Rod and Horizontal (deg)	15.01		
AA16	Horizontal Distance From Axle Center Forward to Trailer Torque Rod (in)	5.50		
A1	Horizontal Distance From Tractor CG to Center of Tractor Front Suspension (in)	35.90		
A2	Horizontal Distance From Tractor CG to Center of Tractor Rear Suspension (in)	106.10		
A3	Horizontal Distance From Trailer CG to 5th Wheel (in)	222.00		
A4	Horizontal Distance From Trailer CG to Center of Trailer Suspension (in)	144.00		
ALPHA1	Static Distance, Tractor Front Axle to Ground (in)	19.20		
ALPHA2	Static Distance, Tractor Rear Axle(s) to Ground (in)	19.50		
ALPHA3	Static Distance, Trailer Axle(s) to Ground (in)	19.50		
BB	Horizontal Distance From 5th Wheel to Midpoint of Tractor Rear Suspension (in)	0.0		
C1	Viscous Damping: Jounce on Tractor Front Suspension (lb-sec/in)	8.33		
C2	Viscous Damping: Rebound on Tractor Front Suspension (lb-sec/in)	16.67		
C3	Viscous Damping: Jounce on Tractor Rear Suspension (lb-sec/in)	0.0		
C4	Viscous Damping: Rebound on Tractor Rear Suspension (lb-sec/in)	0.0		
C5	Viscous Damping: Jounce on Trailer Suspension (lb-sec/in)	0.0		
C6	Viscous Damping: Rebound on Trailer Suspension (lb-sec/in)	0.0		

TABLE F-2 (Continued)

<u>SYMBOL</u>	<u>DESCRIPTION</u>	<u>VALUE FOR ALL CONDITIONS</u>	<u>SPECIAL CONDITION</u>	<u>SPECIAL VALUE</u>
CF1	Maximum Coulomb Friction, Tractor Front Suspension (lb)	1800.00		
CF2	Maximum Coulomb Friction, Tractor Rear Suspension (lb)	8800.00		
CF3	Maximum Coulomb Friction, Trailer Suspension (lb)	7200.00		
CS1	Longitudinal Stiffness, Tractor Front Tires (lbs)	84000.00		
CS2	Longitudinal Stiffness, Tractor Front Tandem Tires (lbs)	40000.00		
CS3	Longitudinal Stiffness, Tractor Rear Tandem Tires (lbs)	52000.00		
CS4	Longitudinal Stiffness, Trailer Front Tandem Tires (lbs)	60000.00		
CS5	Longitudinal Stiffness, Trailer Rear Tandem Tires (lbs)	80000.00		
D	Vertical Distance From 5th Wheel Connection to Tractor CG (in)	-4.50		
DELTA1	Static Vertical Distance, Tractor CG to Tractor Front Axle (in)	33.30		
DELTA3	Static Vertical Distance, Trailer CG to Trailer Axle(s) (in)	49.50		
FA1	Friction Reduction Parameters for Tractor Front Tires		Dry Road	0.003
			Wet Road	0.014
FA2	Friction Reduction Parameter for Tractor Front Tandem Tires		Dry Road	0.003
			Wet Road	0.014
FA3	Friction Reduction Parameter for Tractor Rear Tandem Tires		Dry Road	0.003
			Wet Road	0.014
FA4	Friction Reduction Parameter for Trailer Front Tandem Tires		Dry Road	0.003
			Wet Road	0.014
FA5	Friction Reduction Parameters for Trailer Rear Tandem Tires		Dry Road	0.003
			Wet Road	0.014
J	Tractor Polar Moment (in-lb-sec**2)	53374.00		
J1	Trailer Moment of Inertia (in-lb-sec**2)	607200.00		
JS1	Polar Moment of Tractor Front Wheels (in-lb-sec**2)	206.00		
JS2	Polar Moment of Tractor Front Tandem Wheels (in-lb-sec**2)	462.00		
JS3	Polar Moment of Tractor Rear Tandem Wheels (in-lb-sec**2)	462.00		
JS4	Polar Moment of Trailer Front Tandem Wheels (in-lb-sec**2)	462.00		
JS5	Polar Moment of Trailer Rear Tandem Wheels (in-lb-sec**2)	462.00		
K1	Spring Rate, Tractor Front Suspension (lb/in)	2600.00		
K2	Spring Rate, Tractor Rear Suspension (lb/in)	20800.00		
K3	Spring Rate, Trailer Suspension (lb/in)	28000.00		
KT1	Spring Rate, Tractor Front Tires (lb/in)	9400.00		
KT2	Spring Rate, Tractor Front Tandem Tires (lb/in)	18000.00		
KT3	Spring Rate, Tractor Rear Tandem Tires (lb/in)	18000.00		
KT4	Spring Rate, Trailer Front Tandem Tires (lb/in)	18000.00		
KT5	Spring Rate, Trailer Rear Tandem Tires (lb/in)	18000.00		

TABLE F-2 (Continued)

<u>SYMBOL</u>	<u>DESCRIPTION</u>	<u>VALUE FOR ALL CONDITIONS</u>	<u>SPECIAL CONDITION</u>	<u>SPECIAL VALUE</u>
MUZERO1	Coefficient of Friction, Tractor Front Tires		Dry Road Wet Road	1.03 0.55
MUZERO2	Coefficient of Friction, Tractor Front Tandem Tires		Dry Road Wet Road	1.03 0.75
MUZERO3	Coefficient of Friction, Tractor Rear Tandem Tires		Dry Road Wet Road	1.03 0.75
MUZERO4	Coefficient of Friction, Trailer Front Tandem Tires		Dry Road Wet Road	1.03 0.75
MUZERO5	Coefficient of Friction, Trailer Rear Tandem Tires		Dry Road Wet Road	1.03 0.75
PW	Weight of Payload (lbs)		Empty Loaded	0.0 46800.00
PJ	Polar Moment of Paylaod		Empty Loaded	not entered 1420000.00
PX	Horizontal Distance From Midpoint of Rear Suspension to Payload Mass Center (in)		Empty Loaded	not entered 183.00
PZ	Vertical Distance From Ground to Payload Mass Center (in)		Empty Loaded	not entered 68.25
TIMF	Maximum Real Time for Simulation (sec)	*		
VEL	Initial Velocity (ft/sec)		30 MPH Tests 60 MPH Tests	44.00 88.00
W1	Sprung Weight of Tractor (lbs)	9245.00		
W2	Sprung Weight of Trailer (lbs)	8120.00		
WS1	Weight of Tractor Front Suspension (lbs)	1321.00		
WS2	Weight of Tractor Front Tandem Suspension (lbs)	2330.00		
WS3	Weight of Tractor Rear Tandem Suspension (lbs)	2074.00		
WS4	Weight of Trailer Front Tandem Suspension (lbs)	1520.00		
WS5	Weight of Trailer Rear Tandem Suspension (lbs)	1520.00		
	****Brake Parameters****			
TQ(1,1)	Brake Timing Parameter	0.050		
TQ(1,2)		0.270		
TQ(2,1)		0.075		
TQ(2,2)		0.245		
TQ(3,1)		0.075		
TQ(3,2)		0.245		
TQ(4,1)		0.175		
TQ(4,2)		0.303		
TQ(5,1)		0.175		
TQ(5,2)		0.303		
FRAY	Brake Fade Coefficient		30 MPH Tests 60 MPH Tests	0.0045 0.0080
	Axle 1			
IBRT(1)	Brake Type	2-Wedge		
AC(1)	Brake Chamber Area (sq. in)	12.000		
EM(1)	Mechanical Efficiency	0.800		
PO(1)	Pushout Pressure (PSI)	7.500		
RD(1)	Drum Radius (in)	7.500		
ULH(1)	Mu Lining, High	0.400		
ULL(1)	Mu Lining, Low	0.250		
AB(1)	Distance From Horizontal Centerline of Drum to Parallel Line Through Shoe Contact Point (in)	5.400		

*Varies with expected duration of run.

TABLE F-2 (Continued)

<u>SYMBOL</u>	<u>DESCRIPTION</u>	<u>VALUE FOR ALL CONDITIONS</u>	<u>SPECIAL CONDITION</u>	<u>SPECIAL VALUE</u>
ALPH0(1)	Lining Contact Angle (deg)	125.000		
ALPHW(1)	Wedge Angle (deg)	12.000		
BETA(1)	Lining Offset Angle (deg)	0.0		
C2(1)	Distance From Horizontal Centerline of Drum Parallel Line Through Point of Actuating Force (in)	5.400		
OH(1)	Distance From Vertical Centerline of Drum to Parallel Line Through Shoe Contact Point (in)	3.000		
	Axle 2			
IBRT(2)	Brake Type	2-Wedge		
AC(2)	Brake Chamber Area (sq. in)	12.000		
EM(2)	Mechanical Efficiency	0.800		
PO(2)	Pushout Pressure (PSI)	7.500		
RD(2)	Drum Radius (in)	7.500		
ULH(2)	Mu Lining, High	0.400		
ULL(2)	Mu Lining, Low	0.300		
AB(2)	Distance From Horizontal Centerline of Drum to Parallel Line Through Shoe Contact Point (in)	5.400		
ALPH0(2)	Lining Contact Angle (deg)	125.000		
ALPHW(2)	Wedge Angle (deg)	12.000		
BETA(2)	Lining Offset Angle (deg)	0.0		
C2(2)	Distance From Horizontal Centerline of Drum Parallel Line Through Point of Actuating Force (in)	5.400		
OH(2)	Distance From Vertical Centerline of Drum to Parallel Line Through Shoe Contact Point (in)	3.000		
	Axle 3			
IBRT(3)	Brake Type	2-Wedge		
AC(3)	Brake Chamber Area (sq. in)	12.000		
EM(3)	Mechanical Efficiency	0.800		
PO(3)	Pushout Pressure (PSI)	7.500		
RD(3)	Drum Radius (in)	7.500		
ULH(3)	Mu Lining, High	0.420		
ULL(3)	Mu Lining, Low	0.300		
AB(3)	Distance From Horizontal Centerline of Drum to Parallel Line Through Shoe Contact Point (in)	5.400		
ALPH0(3)	Lining Contact Angle (deg)	125.000		
ALPHW(3)	Wedge Angle (deg)	12.000		
BETA(3)	Lining Offset Angle (deg)	0.0		
C2(3)	Distance From Horizontal Centerline of Drum Parallel Line Through Point of Actuating Force (in)	5.400		
OH(3)	Distance From Vertical Centerline of Drum to Parallel Line Through Shoe Contact Point (in)	3.000		
	Axle 4			
IBRT(4)	Brake Type	S-Cam		
AC(4)	Brake Chamber Area (sq. in)	30.000		
EM(4)	Mechanical Efficiency	0.700		
PO(4)	Pushout Pressure (PSI)	2.500		
RD(4)	Drum Radius (in)	8.250		
ULH(4)	Mu Lining, High	0.280		
ULL(4)	Mu Lining, Low	0.150		
ALPH0(4)	Lining Contact Angle (deg)	111.000		
ALPH3(4)	ALPH0(4) + 2*ALPH1(4) (deg)	207.000		
APRIM(4)	Radial Distance From Center of Drum to Shoe Pin (in)	6.900		
HB(4)	Distance From Horizontal Centerline Through Shoe Pin to Parallel Line Through Connector Contact Point (in)	12.600		
RC(4)	Cam Radius (in)	0.500		
SAL(4)	Slack Adjuster Length (in)	6.000		

TABLE F-2 (Continued)

<u>SYMBOL</u>	<u>DESCRIPTION</u>	<u>VALUE FOR ALL CONDITIONS</u>	<u>SPECIAL CONDITION</u>	<u>SPECIAL VALUE</u>
	Axle 5			
IBRT(5)	Brake Type		S-Cam	
AC(5)	Brake Chamber Area (sq. in)	30.000		
EM(5)	Mechanical Efficiency	0.700		
PO(5)	Pushout Pressure (PSI)	2.500		
RD(5)	Drum Radius (in)	8.250		
ULH(5)	Mu Lining, High	0.280		
ULL(5)	Mu Lining, Low	0.150		
ALPH0(5)	Lining Contact Angle (deg)	111.000		
ALPH3(5)	ALPH0(5) + 2*ALPH1(5) (deg)	207.000		
APRIM(5)	Radial Distance From Center of Drum to Shoe Pin (in)	6.900		
HB(5)	Distance From Horizontal Centerline Through Shoe Pin to Parallel Line Through Connector Contact Point (in)	12.600		
RC(5)	Cam Radius (in)	0.500		
SAL(5)	Slack Adjuster Length (in)	8.000		

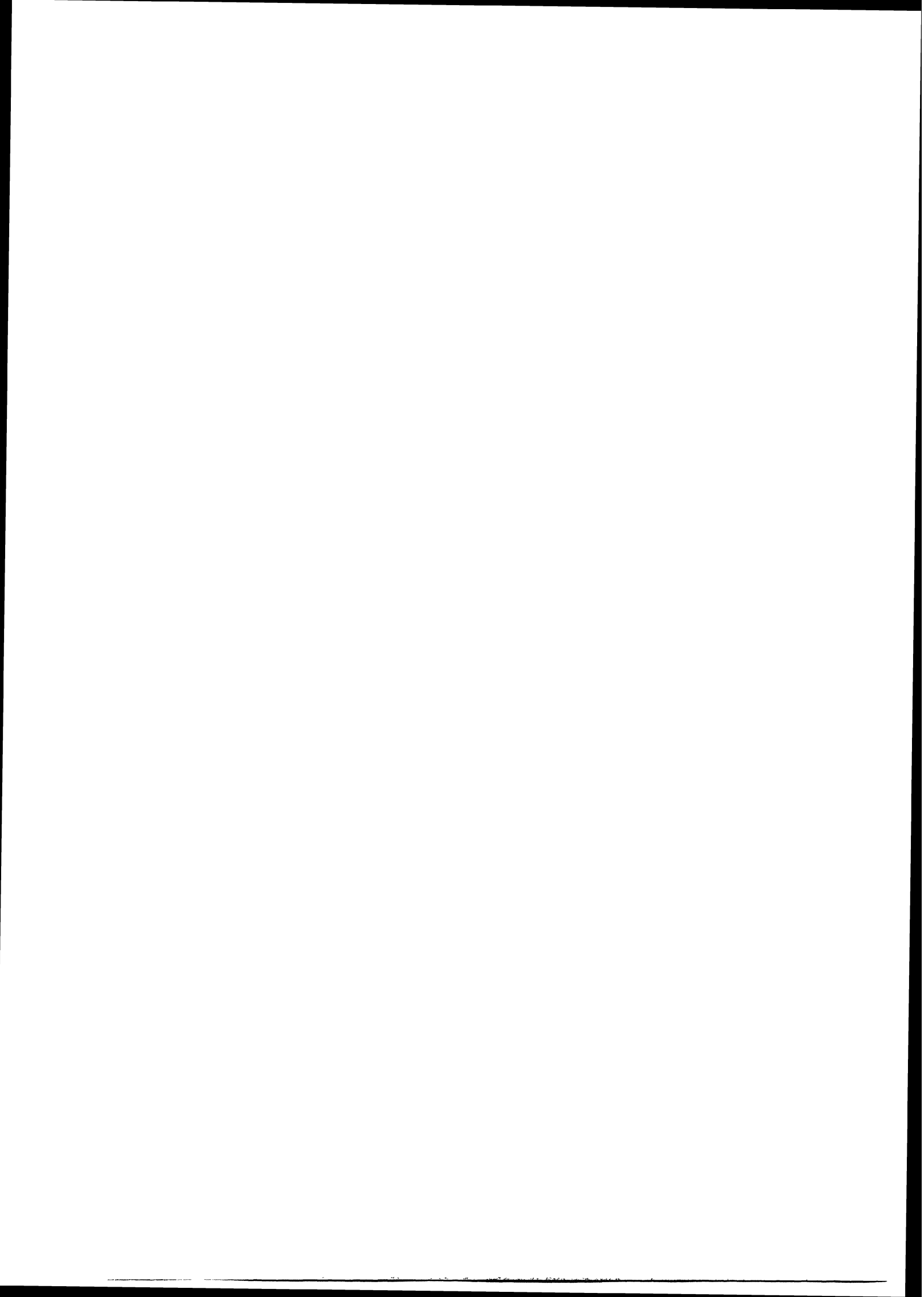
REFERENCES

1. Dugoff, H., and Murphy, R.W., "The Dynamic Performance of Highway Vehicles - A Review of the State of the Art," SAE Paper 710223, January 1971.
2. Ellis, J.R., "The Dynamics of Vehicles During Braking," Symposium Control of Vehicles, Automobile Division, London:Inst. Mech. Engrs.(1963), pp. 20-29.
3. Bode, O., and G6rge, W., "Mathematical Investigation of the Braking Performance of Articulated Vehicles," Deutsche Kraftfahrtforschung, No. 49(1961).
4. Limpert, R., "An Investigation of the Brake Force Distribution of Tractor-Semitrailer Combinations," SAE Paper 710044, January 1971.
5. North, M.R., and Oliver, S.J., "Transient Load Transfer in an Articulated Vehicle Under Braking Conditions," M.I.R.A. Report No. 1967/7, June 1967.
6. Mikulcik, E.C., "The Dynamics of Tractor-Semitrailer Vehicles: The Jackknifing Problem," Ph.D. Thesis, Cornell University, Ithaca, N.Y., June 1968.
7. Leucht, P.M., "The Directional Dynamics of the Commercial Tractor-Semitrailer Vehicle During Braking," 1970 International Automobile Safety Conference Compendium, SAE, 1970.
8. Rasmussen, R. E., and Cortese, A.D., "Dynamic Spring Rate Performance of Rolling Tires," SAE Transactions, Vol. 77 (1968), paper 680408.
9. Dugoff, H., Fancher, P. S., and Segel, L., Tire Performance Characteristics Affecting Vehicle Response to Steering and Braking Control Inputs, Final Report for Period May 1968 - August 1969 for Contract CST-460, Office of Vehicle Systems Research, National Bureau of Standards, Washington, D.C. August 1969.
10. Cripe, R. A., "Making a Road Simulator Simulate," SAE Paper 720095, 1972.
11. Murphy, R. W., Limpert, R., and Segel, L., Bus, Truck and Tractor-Trailer Braking System Performance, final report for Contract FH-111-7290, National Highway Traffic Safety Administration, Department of Transportation, March 1971.
12. Strien, H., "Computation and Testing of Automotive Brakes," dissertation, Technical University, Braunschweig, Germany, 1949.
13. Alfred Teves K.G., Ate Brake Handbook, Frankfurt-Main, Germany, 1960, pp. 131-135.
14. Stroh, G. B., Lawrence, M. H., and Deibal, W. T., Effects of Shoe Force Geometry on Heavy Duty Internal Shoe Brake Performance, SAE Paper No. 680432, Society of Automotive Engineers, May 1968.

Preceding page blank

15. Ralston, A., and Wilk, H., Mathematical Methods for Digital Computers, Wiley, Inc., New York, 1960.
16. Mabie, H. H. , and Ocvirk, F.W., Mechanisms and Dynamics of Machinery, Wiley, Inc., New York, 1957
17. Dugoff, H., and Brown, B. J., "Measurement of Tire Shear Forces," SAE Paper 700092, January 1970.

THE FOLLOWING PAGES ARE DUPLICATES OF
ILLUSTRATIONS APPEARING ELSEWHERE IN THIS
REPORT. THEY HAVE BEEN REPRODUCED HERE BY
A DIFFERENT METHOD TO PROVIDE BETTER DETAIL.



This page is reproduced at the back of the report by a different reproduction method to provide better detail.

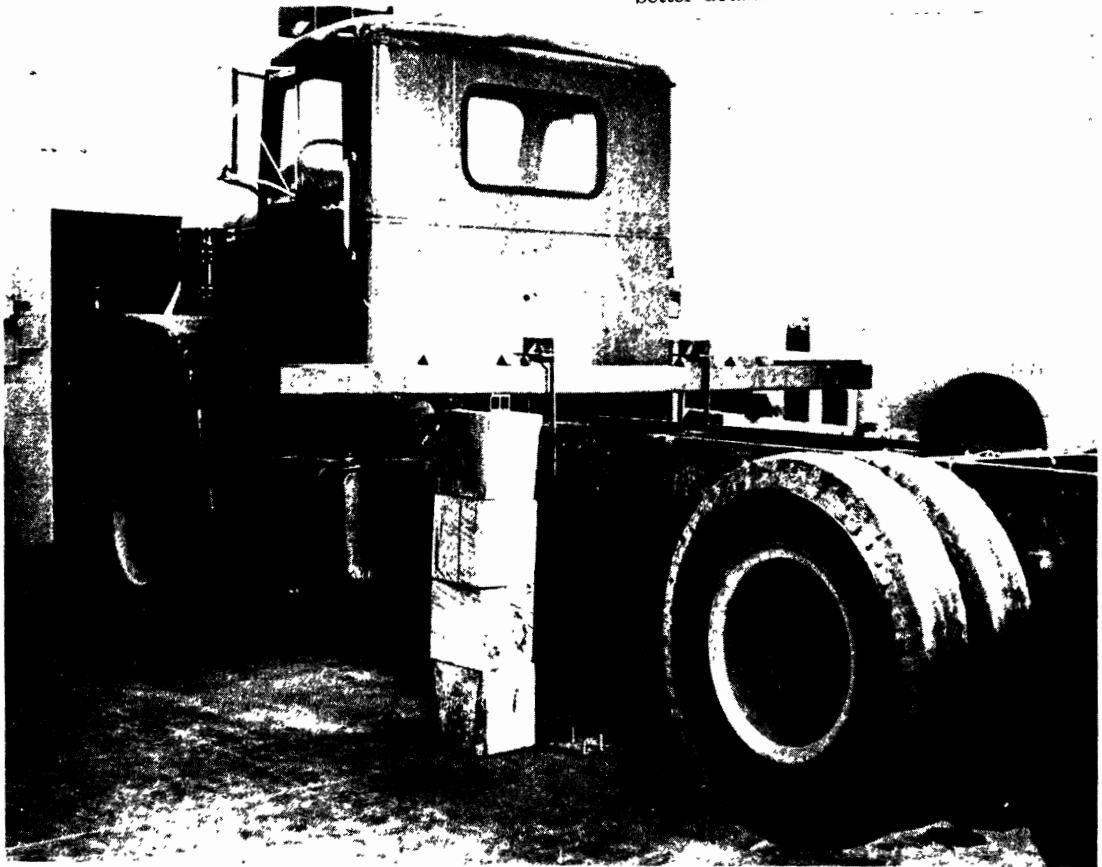
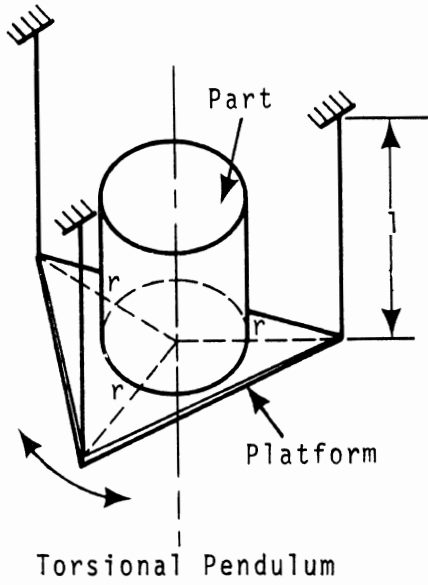


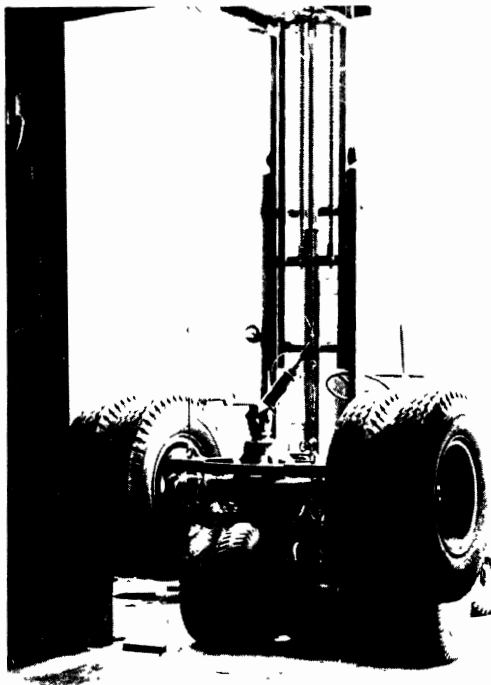
Figure 4-25. Pitch moment of inertia measurement.



This page is reproduced at the back of the report by a different reproduction method to provide better detail.



Torsional Pendulum Platform With Tire, Wheel, & Brake Drum Assembly



Pendulum Suspended by Means of Lift Truck

Figure 4-26. Apparatus for measuring polar moment of inertia of wheels and rotating assemblies.

This page is reproduced at the back of the report by a different reproduction method to provide better detail.



Figure 5-1. Test vehicle, straight truck

This page is reproduced at the back of the report by a different reproduction method to provide better detail.

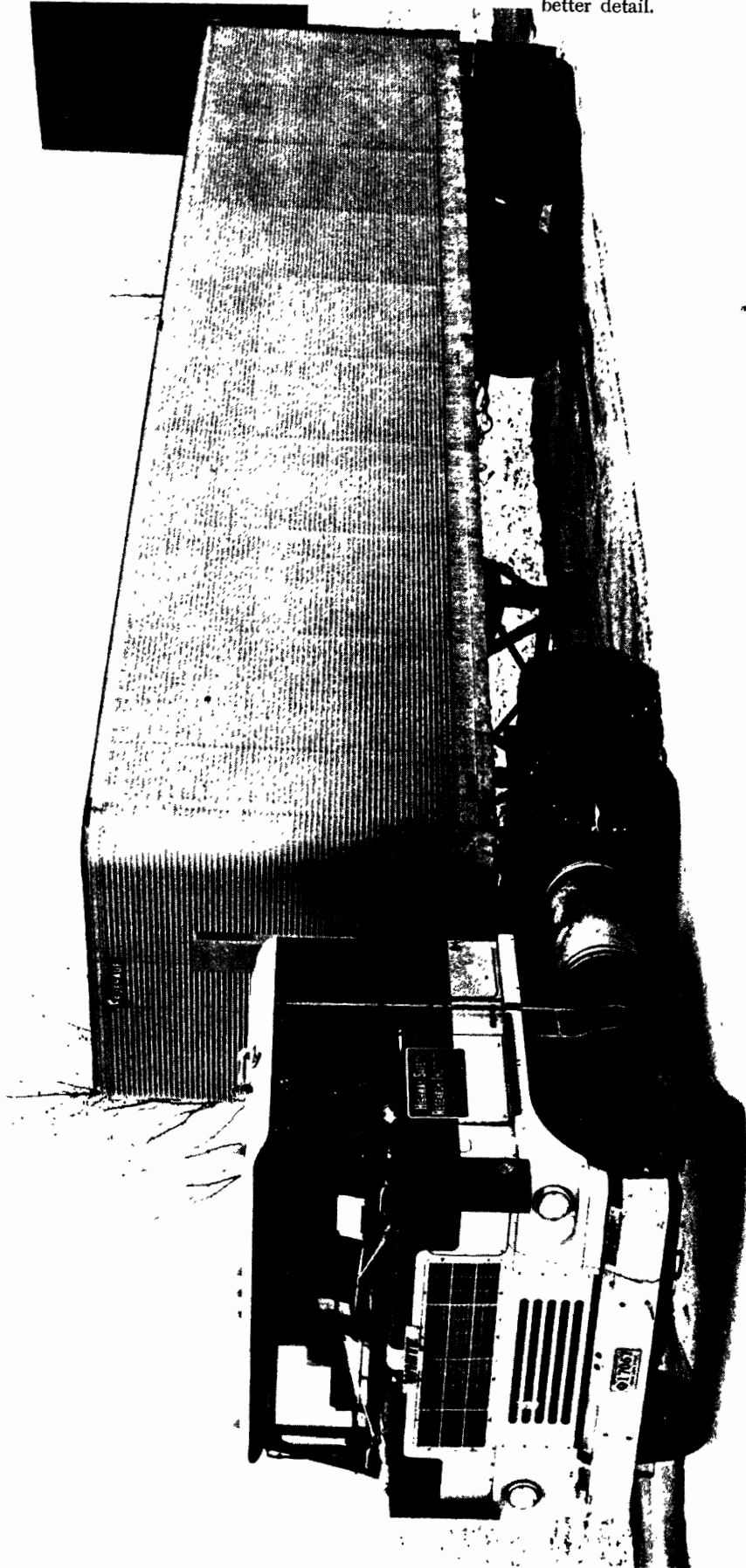


Figure 5-2. Test vehicle, tractor-trailer



Figure 5-3. High c.g. load configuration

This page is reproduced at the back of the report by a different reproduction method to provide better detail.



Figure 5-4. Articulation angle limiter

This page is reproduced at the back of the report by a different reproduction method to provide better detail.

This page is reproduced at the back of the report by a different reproduction method to provide better detail.

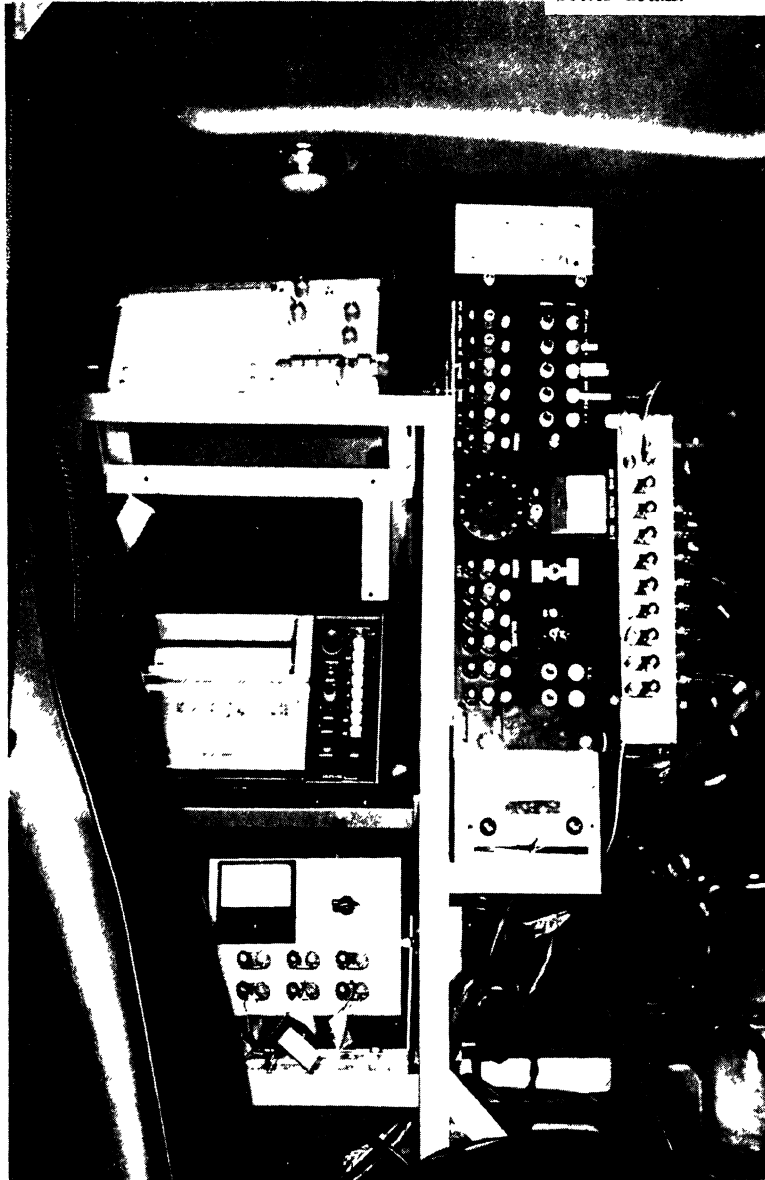


Figure 5-6. Signal processing equipment installed in truck

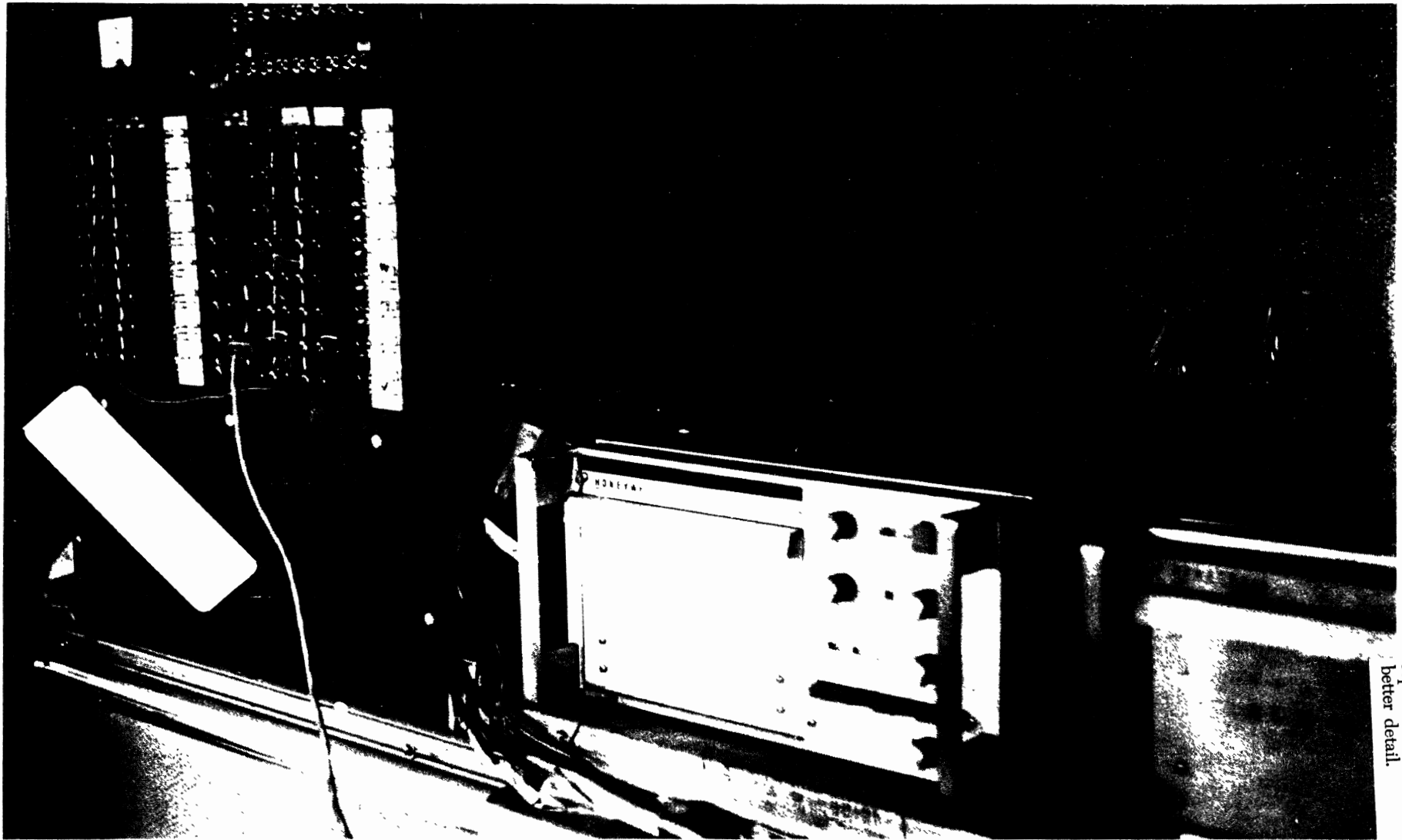


Figure 5-7. Signal processing equipment installed in tractor cab

This page is reproduced at the back of the report by a different reproduction method to provide better detail.

This page is reproduced at the back of the report by a different reproduction method to provide better detail.

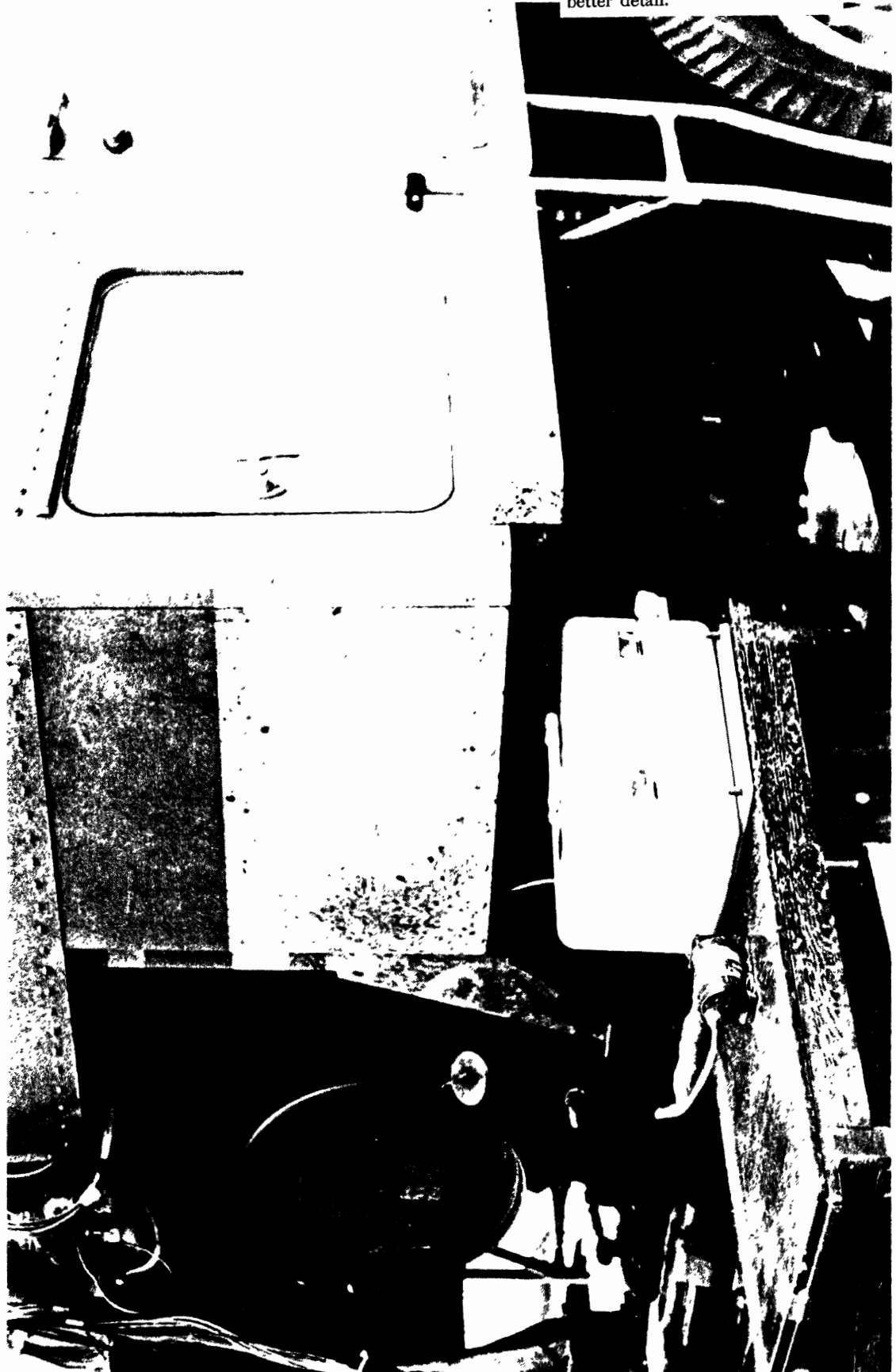


Figure 5-8. Stabilized platform unit mounted on tractor frame

Highway Safety
Research Institute